Vol. 43 (Supplement 1) 2025 ISSN 2630-0559 (Online)

PRINCE OF SONGKLA UNIVERSITY

FACULTY OF MEDICINE

JHSMR
Journal of Health Science and Medical Research

AHR-iCON 2025

ABSTRACT AND PROCEEDING BOOK

The 4th Annual Health Research International Conference

AHR-iCON 2025

Shaping the Future: Innovation, Health and Well-being

OCTOBER 9-10TH, 2025

FACULTY OF MEDICINE,
PRINCE OF SONGKLA UNIVERSITY

Content

Welcome Message

Asst. Prof. Kittipong Riabroi, M.D., M.Sc.

Dean, Faculty of Medicine, Prince of Songkla University

It is with great pleasure that I welcome all participants to the Annual Health Research International Conference of 2025 (AHR-iCON 2025), being held at the Medical Research, Innovation, and Technology Transfer Building, Faculty of Medicine, Prince of Songkla University.

This year marks the 4th edition of the AHR-iCON conference, which is being held under the theme: "Shaping the Future: Innovation, Health, and Well-being." This theme highlights the vital role of research and innovation in driving the future of healthcare systems and enhancing the quality of life for all. The conference will take place from October 9–10, 2025.

The primary objective of this conference is to provide an international academic platform for presenting research and innovations in health, medical sciences as well as relevant interdisciplinary fields. Additionally, it aims to foster the exchange of knowledge, experiences, and new ideas among researchers, academics, healthcare professionals, and students both from Thailand and around the world. Furthermore, the event serves as a foundation for building and expanding international academic and research collaborations.

The conference features keynote speeches by leading experts, oral and poster presentations by participants, and discussion sessions that bring together researchers, physicians, policymakers, and students to explore solutions to both current and emerging challenges within healthcare systems.

The organizing committee places strong emphasis on empowering medical students as future leaders by encouraging their participation in presenting research—an important first step toward becoming academically and scientifically grounded physicians.

The ultimate goal of AHR-iCON 2025 is to ignite interdisciplinary collaboration, promote innovation, and collectively shape a sustainable healthcare system. It is our belief that the shared knowledge and dedication of all participants from this conference will mark the beginning of a new direction; wherein health research and innovation serve as cornerstones for societal progress and well-being.

We would like to express our sincere gratitude to the International Scientific Committee, keynote and invited speakers, and expert reviewers for their invaluable contributions to the success of this conference.

Finally, I sincerely hope to have the opportunity to welcome you all once again at the next AHR-iCON conference in the coming year.

Asst. Prof. Kittipong Riabroi, M.D., M.Sc.
Dean of Faculty of Medicine, Prince of Songkla University

Preface

Prof. Sarunyou Chusri, M.D., Ph.D.

Vice Dean for Research and Innovation Affairs, Faculty of Medicine, Prince of Songkla University Chair of AHR-iCON 2025

The Faculty of Medicine, Prince of Songkla University, in collaboration with the Research Support and Administration Unit, the Department of Biomedical Sciences, Biomedical Engineering, and other relevant academic units, have jointly organized the: 4th Annual Health Research International Conference (AHR-iCON 2025), under the theme: "Shaping the Future: Innovation, Health, and Well-being." This will be held on October 9–10, 2025, at the Research, Innovation, and Medical Technology Transfer Building (RI-MeT), Faculty of Medicine, Prince of Songkla University.

The AHR-iCON International Health Research Conference serves as a significant platform for the exchange of knowledge, research findings, and innovations in the fields of health sciences and medicine. It is held continuously to both promote and advance research in response to emerging challenges as well as opportunities in present and future societies. This conference offers opportunities for faculty members researchers, experts and students; from both domestic and international communities, to meet, share experiences and collaboratively develop research approaches and innovations that address local and global health needs.

Under the theme: "Shaping the Future: Innovation, Health, and Well-being," this year's conference focuses on fostering interdisciplinary collaboration and integrating knowledge to create sustainable medical and health innovations. It covers a wide range of disciplines; including biomedical sciences, biomedical engineering, pharmacy, clinical and health sciences, data science, and medical technology along with special activities. This including: academic forums and hackathons, which are aimed at promoting idea exchange and networking among researchers, entrepreneurs as well as various stakeholders.

This conference not only serves as a venue for knowledge exchange but also encourages constructive dialogue; including the development of research projects, with the potential for practical application in the healthcare system. Hence, contributing to the sustainable improvement of people's quality of life—a key objective of health research today.

The Faculty of Medicine, Prince of Songkla University, takes great pride in hosting this event and expresses sincere gratitude to all faculty members, researchers, experts, students, supporters and all participating organizations whom have contributed to the advancement of health research and innovation for a better future for humanity.

We sincerely hope that this conference will be the beginning of strong and continuous academic collaboration, innovation and will drive progress in health science and medical technology; effectively meeting society's future needs.

Prof. Sarunyou Chusri, M.D., Ph.D.
Vice Dean of Research Affairs, Faculty of Medicine, Prince of Songkla University
Chair of AHR-iCON 2025

International Scientific Committee

Name	Affiliation
1. Prof. Jos Vander Sloten, Ph.D.	Biomedical Engineering, Faculty of Engineering Science, KU Leuven, Belgium
2. Prof. Duško Kozić, M.D.	Radiology, Oncology Institute of Vojvodina, Center for Imaging Diagnostics, Faculty of Medicine, University of Novi Sad, Serbia
3. Prof. Espen Bjertness, Ph.D.	Department of Community Medicine and Global Health, Institute of Health and Society Faculty of Medicine, University of Oslo, Oslo, Norway
4. Prof. Tippawan Liabsuetrakul, MD, Ph.D.	Department of Epidemiology, Faculty of Medicine, Prince of Songkla University, Thailand
5. Prof. Kittisak Sawanyawisuth, M.D., Ph.D.	Department of Medicine, Faculty of Medicine, Khon Kaen University, Thailand
6. Prof. Prasit Palittapongarnpim, M.D., Ph.D.	Department of Microbiology, Faculty of Science, Mahidol University, Thailand
7. Prof. Sakda Daduang, Ph.D.	Faculty of Pharmaceutical Sciences, Khon Kaen University, Thailand
8. Prof. Surasak Sangkathat, M.D., Ph.D.	Bumrungrad International Hospital, Thailand
9. Prof. Dumnoensun Pruksakorn. M.D., Ph.D.	Department of Orthopaedics, Faculty of Medicine, Chiang Mai University, Thailand
10. Prof. Po-Liang Lu, M.D., Ph.D	Kaohsiung Medical University, Taiwan
11. Prof. Suthat Liangpunsakul, M.D., MPH.	Division of Gastroenterology and Hepatology, Indiana University School of Medicine (IUSM), USA
12. Prof. Chatchalit Rattarasarn, M.D.	Faculty of Medicine Ramathibodi Hospital, Mahidol University, Thailand
13. Assoc. Prof. Desmond Chong, Ph.D.	Engineering Cluster, Singapore Institute of Technology, Singapore
14. Assoc. Prof. Luelak Lomlim, Ph.D.	Department of Pharmaceutical Chemistry, Faculty of Pharmaceutical Sciences, Prince of Songkla University, Thailand
15. Assoc. Prof. Sarawut Kumphune, Ph.D.	Biomedical Engineering Institute, Chiang Mai University, Thailand
16. Assoc. Prof. Surapong Chatpun, Ph.D.	Department of Biomedical Sciences and Biomedical Engineering, Faculty of Medicine, Prince of Songkla University, Thailand
17. Assoc. Prof. Santad Wichienchot, M.D.	Faculty of Agro-Industry, Prince of Songkla University, Thailand
18. Assoc. Prof. Apichai Tuanyok, M.D., Ph.D.	Department of Infectious Diseases and Immunology, College of Veterinary Medicine, University of Florida, USA
19. Assoc. Prof. Kosin Wirasorn, M.D.	Head of the Cancer Excellence Center, Srinagarind Hospital, Faculty of Medicine, Khon Kaen University, Thailand
20. Assoc. Prof. Varomyalin Tipmanee, Ph.D.	Department of Biomedical Sciences and Biomedical Engineering, Faculty of Medicine, Prince of Songkla University, Thailand

Working Committee

Honorary Chair

Asst. Prof. Kittipong Riabroi, M.D., M.Sc.

Conference Chair

Prof. Sarunyou Chusri, M.D., Ph.D.

Program Chair

Assoc. Prof. Nawamin Pinpathomrat, M.D., DPhil

Executive Committee

Prof. Varah Yuenyongviwat, M.D.
Assoc. Prof. Wit Wichaidit, Ph.D.
Assoc. Prof. Weerawat Kiddee, M.D.
Assoc. Prof. Thitiworn Choosong, Ph.D.
Assoc. Prof. Surapong Chatpun, Ph.D.
Assoc. Prof. Sumittra Pratep, M.D.
Assoc. Prof. Pritsana Raugrut, Ph.D.
Assoc. Prof. Polathep Vichitkunakorn, M.D., Ph.D.
Assoc. Prof. Pittayapon Pitathawatchai, M.D.,Ph.D.
Assoc. Prof. Osaree Akaraborworn, M.D, Ph.D
Assoc. Prof. Ninlapa Pruksanusak, M.D
Assoc. Prof. Nawamin Pinpathomrat M.D., DPhil
Assoc. Prof. Arunee Dechaphunkul, M.D.
Assoc. Prof. Sarayut Lucien Geater, M.D., Ph.D.
Asst. Prof. Thammasin Ingviya, M.D., M.H.S., Ph.D.
Asst. Prof. Pasarat Khongkow, Ph.D.
Asst. Prof. Jatuporn Pakpirom, M.D.

Organizing Committee

Assoc. Prof. Nawamin Pinpathomrat, M.D., DPhil
Dr. Jermphiphut Jaruenpunyasak, Ph.D.
Assoc.Prof. Sumittra Pratep, M.D.
Dr. Theerawat Dobutr, Ph.D.
Dr. Ampapan naknaen, Ph.D.
Assoc.Prof. Surapong Chatpun, Ph.D.
Dr. Somyot Chirasatitsin, Ph.D.
Assoc. Prof. Potchanapond Graidist, Ph.D.
Asst. Prof. Pasarat Khongkow, Ph.D.
Asst. Prof. Kamonnut Singkhamanan, Ph.D.
Assoc. Prof. Kanyanatt Kanokwiroon, Ph.D.
Dr. Pemikar Srifa, Ph.D.

Secretary

Mrs. Thanatta Nuntadusit

Secretary assistant

Miss Punika Saikaew
Miss Mayuree Boonrach
Miss Yaowanee Chookum

Academic Editor

Assoc. Prof. Dr. Potchanapond Graidist, Ph.D.

Academic Section Editor List

Precision Medicine/Clinical Medicine

Section editor: Assoc. Prof. Dr. Raphatphorn Navakanitworakul, Ph.D.

Vice-section editor: Asst. Prof. Dr. Kittinun Leetanaporn, M.D., Ph.D.

Dr. Rassanee Bissanum, Ph.D.

Data Science/Digital Health

Section editor: Assoc. Prof. Dr. Raphatphorn Navakanitworakul, Ph.D.

Vice-section editor: Asst. Prof. Dr. Kittinun Leetanaporn, M.D., Ph.D.

Dr. Rassanee Bissanum, Ph.D.

Medical Innovation

Section editor: Assoc. Prof. Dr. Tonghathai Phairatana, Ph.D.

Vice-section editor: Asst. Prof. Dr. Wanwara Thuptimdang, Ph.D.

Emerging Infectious Disease

Section editor: Asst. Prof. Dr. Kamonnut Singkhamanan, Ph.D.

Vice-section editor: Dr. Theerawat Dobutr, Ph.D.

Dr. Ampapan Naknaen, Ph.D.

Health System & Policy/Global Health

Section editor: Prof. Dr. Tippawan Liabsuetrakul, M.D., Ph.D.

Climate Change

Section editor: Asst. Prof. Dr. Thammasin Ingviya, M.D., Ph.D.

Healthy Aging

Section editor: Assoc. Prof. Dr. Potchanapond Graidist, Ph.D.

Vice-section editor: Assoc. Prof. Dr. Varomyalin Tipmanee, Ph.D.

Assoc. Prof.Dr.Krit Charupanit, Ph.D.

Asst. Prof. Dr. Kantida Juncheed, Ph.D.

JHSMR Staff List

Editor-in-Chief

Prof. Sarunyou Chusri, M.D., Ph.D.

Manager

Mrs. Kamolthip Suwanthavee

Assistant Manager

Miss Sarinthra Khunisri

Miss Supanich Lertjettanakul

Miss Nutchada Binlateh

Mr. Tarathep Boonpipat

International Hybrid Conference

The 4rd Annual Health Research International Conference 2025 (AHR-iCON 2025)

"Shaping the Future: Innovation, Health and Well-being"

Background

The Faculty of Medicine, Prince of Songkla University, in collaboration with the Research Support and Administration Unit, the Department of Biomedical Sciences, Biomedical Engineering and other academic departments, is pleased to announce the 4th Annual Health Research International Conference 2025 (AHR-iCON 2025); under the theme: "Shaping the Future: Innovation, Health and Well-being." The event will be held on October 9–10, 2025, at the Research Innovation and Medical Technology Transfer Building (RI-MeT), Faculty of Medicine, Prince of Songkla University.

This international conference serves as a platform for the exchange of knowledge, research, and innovation in the fields of health and medical sciences. It brings together researchers, academics, professionals as well as students from both Thailand and abroad, with the aim of advancing interdisciplinary collaboration and driving progress in health and well-being.

The event encourages meaningful dialogue across sectors and institutions—supporting the development of impactful research and innovations that contribute to better health outcomes. By fostering academic networking and partnership-building, the conference seeks to transform research into real-world solutions for communities at the local, national and international levels.

Ultimately, AHR-iCON 2025 aims to catalyze the translation of research into practice—enhancing healthcare delivery in ways that are effective, sustainable and responsive to societal needs.

Aims

1. To organize an international academic forum for the presentation of research and innovations in health and medical sciences.
2. To promote the exchange of knowledge, experiences and new ideas among researchers, academics, healthcare professionals and students, at both national and international levels.
3. To establish and expand academic and research collaboration networks among educational institutions, research organizations as well as various sectors at both national and international levels.

Duration and Venue

Date: October 9–10, 2025

Time: 08:30 AM–04:30 PM

Venue: Research, Innovation and Medical Technology Transfer Building, Faculty of Medicine, Prince of Songkla University

Organizing Units

- Research Support and Management Unit, Faculty of Medicine, Prince of Songkla University
- Department of Biomedical Sciences and Biomedical Engineering, Faculty of Medicine, Prince of Songkla University

Important Date

Abstract and Full paper submissions: May 20– July 20, 2025

Abstract and Full paper acceptance notifications: September 1, 2025

Registration: May 20–September 30, 2025

Early Bird Registration: May 20–July 31, 2025

Activities

1. Keynote Lecture
2. Invited Lecture
3. Oral Presentation
4. Poster Presentation

Topics

1. Healthy Aging
2. Emerging Infectious/Diseases
3. Medical Innovation
4. Data Science/Digital Health
5. Precision Medicine/Clinical Medicine
6. Food Sciences
7. Health Policy/Global Health
8. Climate Change

Conference Program

Day 1: Thursday, October 9, 2025	
08.30 – 09.00 ROOM: Auditorium	**Registration**
08.30 – 10.40 ROOM: Auditorium	**MC: Miss Satita Rongrodjanarug, Postdoc** Department of Epidemiology, Faculty of Medicine, Prince of Songkla University
09.00 – 09.10 10 minutes ROOM: Auditorium	**Open Speech** **Prof. Sarunyou Chusri, M.D., Ph.D.** Vice Dean for Research and Innovation Affairs **Asst. Prof. Kittipong Riabroi, M.D., M.Sc.** Dean, Faculty of Medicine, Prince of Songkla University
09.10 – 09.55 45 minutes include Q&A ROOM: Auditorium	**Keynote 1:** Climate Change -> Air Pollution -> Health Effects **Prof. Perapong Tekasakul, Ph.D.** Department of Mechanical and Mechatronics Engineering, Faculty of Engineering, Prince of Songkla University
09.55 – 10.40 45 minutes include Q&A ROOM: Auditorium	**Keynote 2:** Dengue Pathology and Management of Patients with Warning Signs **Dr. Chun-Yu Lin, Ph.D.** Director of Infectious Diseases, Kaohsiung Medical University Hospital **Prof. Kamolwish Laoprasopwattana, M.D.** Head of Department of Pediatric, Faculty of Medicine, Prince of Songkla University **Chair: Prof. Tippawan Liabsuetrakul, M.D., Ph.D.** Head of Department of Epidemiology, Faculty of Medicine, Prince of Songkla University
10.40 – 11.30 50 minutes include Q&A	**Coffee Break and Poster Presentation Session A & B (Precision Medicine/Clinical Medicine)**

	Session A	Session B	
10:40 – 10:45	**P001** The Association Between Bell's Palsy and Subsequent Diabetes Mellitus: A Retrospective Cohort Study / **Mr. Suppanut Siriseth**	**P009** Retrospective Cohort Study on Clinical Outcomes in Endogenous Cushing's Syndrome in Songklanagarind hospital (Pilot study prepared for A Multi-Center in Thailand) / **Mr. Tawan Limamornrat**	
10:45 – 10:50	**P002** The Impact of Invasive Coronary Angiography during admission in the Elderly with NSTE-ACS / **Miss Hattaya Chutiphimon**	**P010** Adrenal Tumor Spectrum and Surgical Indications: A 10-Year Retrospective Study from Southern Thailand / **Mr. Auttawut Chalermwuttanon**	
10:50 – 10:55	**P003** The Effect of Schroth Method Exercise on preoperative Flexibility in AIS Surgical Candidates: A Randomized Controlled Trial / **Miss Yanin Tangjaroenpaisan**	**P011** Predictors of Unfavorable Outcomes of In-Hospital Acute Ischemic Stroke: A Retrospective Case-control Study / **Mr. Natthapong Chuaipitak**	
10:55 – 11:00	**P004** Association of Inhospital Guideline-directed Medical Treatment Scores and Mortality in Post-myocardial Infarction Patients with LV Dysfunction; A Single Center Retrospective Study / **Mr. Knokpit Wattanapaiboon**	**P012** Heart failure prognostication from guideline-directed medical therapy / **Mr. Chonlanat Puetpaiboon**	
11:00 – 11:05	**P005** Glucocorticoid-Induced Hyperglycemia in Hospitalized Non-Diabetic Patients: A Retrospective Cohort Study / **Miss Ruamporn Kansawai**	**P013** Prevalence and Risk Factors of Acute Pancreatitis in Childhood Acute Leukemia / **Miss Kamonluk Thepuatrakul**	
11:05 – 11:10	**P006** Hematopoietic Stem Cell-derived Natural Killer Cells: A Potential Alternative Cell Source for Cancer immunotherapy / **Miss Suppanut Komjakraphan**	**P014** Associations of Weight Reduction with Respiratory Function and Gas Exchange in Obesity Hypoventilation Syndrome: A Retrospective Study / **Mr. Tawatchai Piathong**	

11:10 – 11:15	**P007** Normal Reference Range of Skeletal Muscle in Healthy Thai Population / **Miss Samittha Fueangfupong**	**P015** Prognostic Implications of Circulating Cell-free DNA Concentration and Somatic Mutation Profiling in Advanced Prostate Cancer / **Mr. Sarawut Chamnina**	
11:15 – 11:20	**P008** Lung Injury and Subclinical Respiratory Symptoms among Young Chinese Vapers: Evidence from Symptom Screening and Pulmonary Function Tests / **Miss Chunxia He**		
11.30 – 13.45	**MC: Mr. Prem Kumar Neopanay, M.Sc. Candidate** Department of Epidemiology, Faculty of Medicine, Prince of Songkla University		
11.30 – 12.05 35 minutes include Q&A	**Invited Speaker 1:** The role of WGS in the control of hospital-acquired bacterial infections **Prof. Prasit Palittapongarnpim, M.D., Ph.D.** Department of Microbiology, Faculty of Science, Mahidol University		
12.05 – 13.00	**Lunch**		
13.00 – 13.45 45 minutes, include Q&A ROOM: Auditorium	**Keynote 3:** Food Sciences & Healthy Aging **Prof. Emilie Combet Aspray, Ph.D.** Professor of Human Nutrition (Medicine) School of Medicine, Dentistry & Nursing, Human Nutrition University of Glasgow		
13.45 – 14.45 include Q&A	**Oral Presentation Session 1**		
	ROOM 1: Precision Medicine/Clinical Medicine **Chair:** Assoc. Prof. Dr. Pritsana Raungrut **Co-chair:** Asst. Prof. Dr. Pasarat Khongkow **Committee:** 1. Dr. Padiporn Limumpornpetch, M.D. 2. Assoc. Prof. Dr. Raphatphorn Navakanitworakul	**ROOM 2: Data Science/Digital Health** **Chair:** Asst. Prof. Dr. Chanon Kongkamol, M.D. **Co-chair:** Asst. Prof. Dr. Kittinun Leetanaporn, M.D. **Committee:** 1. Assoc. Prof. Dr. Sarayut Lucien Geater, M.D. 2. Dr. Rassanee Bissanum	**ROOM 3: Health System & Policy/Global Health** **Chair:** Prof. Kamolwish Laoprasopwattana, M.D. **Co-chair:** Assoc. Prof. Phoomjai Sornsenee, M.D. **Committee:** 1. Asst. Prof. Teerapat Teetharatkul, M.D. 2. Asst. Prof. Ponlagrit Kumwichar, M.D.

13:45 – 14:00	**O001** Knowledge, Attitudes, and Practices of Enhanced Recovery After Surgery Among Registered Nurses in a University Hospital: A Cross-sectional Study / **Miss Surangkana Ongsakul**	**O005** Skin-Sight: AI-Enhanced Early Detection and Classification of Skin Cancer, Using Image-Based Deep Learning Models / **Mr. Punyapat Sengdonprai**	**O008** Prevalence of Cannabis use, Health Consequences and Harm to others from Cannabis use Among Undergraduate Students One Year after Medical Cannabis Legalization / **Miss Chutinan Sukkua**
14:00 – 14:15	**O002** Risk of Peroneal Nerve Injury in All-inside Lateral Meniscal Repair through the Popliteus Tendon using Five Different Needle Designs: A Cadaveric Study / **Miss Panpaporn Asavanapakas**	**O006** Fusion of Thermal and Multispectral Diabetic Foot Ulcer Imaging with AI, for Non-Invasive Healthcare Monitoring / **Mr. Chakrin Techaboonsermsak**	**O010** Assessing the Relationships between Diet, Sports and Anthropometric Indicators of Elementary School Students in Vietnam using Structural Equation Modeling / **Mr. Lê Bá Giang**
14:15 – 14:30	**O003** Real-World Effectiveness of Once-Weekly Semaglutide Injections in Type 2 Diabetes: A Retrospective Study / **Mr. Supanut Sereeaphinan**		**O011** Rubella Vaccination Acceptance in Bangladesh: Exploring Young Female Adults' Willingness for Self and Child as Policy Guidance / **Mr. Md. Nuruzzaman**
14:30 – 14:45	**O004** Identification of Prognostic Markers for Predicting Recurrence and Progression of Non-muscle Invasive Urothelial Carcinoma, via Bioinformatic Analysis / **Miss Thitawan Chimpalee**		**O012** Stakeholder Perspective on the Barriers of Interventions for Childhood Vaccination in Urban Slums of Bangladesh: A Qualitative Study / **Mr. Kazi Salahin**
14.45 – 15.35	**Coffee Break and Poster Presentation Session B (Data Science/Digital Health & Medical Innovation)**		
14:45 – 14:50	**P016** Survival Outcomes in Advanced Stage Cancer Patients: A Retrospective Study on the Impact of Consultation Approaches in Palliative Care / **Miss Tanyalak Sanphiboon**	**P019** Personalized and General Knowledge-Based Cognitive Engagement for Alzheimer's Patients Using AI-Generated Image and Word Prompts / **Miss Thitirat Boriboonsri**	
14:50 – 14:55	**P017** Applying Large Language Models (LLMs) to Automatically Generate Hospital Discharge Summaries / **Mr. Detphop Tanasanchonnakul**	**P020** A Pilot Evaluation of a Culturally Tailored Virtual Reality Exposure Therapy Program for Social Anxiety in Thailand / **Assoc. Prof. Warut Aunjitsakul**	

14:55 – 15:00	**P018** Correlation between the National Early Warning Score and Acute Kidney Injury and Outcomes in Songklanagarind hospital / **Mr. Jutinun Kittivarapong**	**P021** AI-Based Multi-Classification of B12 Deficiency Using Deep Learning on Photographic Eye Images / **Mr. Pannatat Wongbangpo**	
15:00 – 15:05		**P022** Deep Learning AI Detection of Skin Rashes, via Image Analysis / **Miss Nutwaree Chanthavijaikul**	
15:05 – 15:10		**P024** A Microfluidic Biosensing Platform for Neutrophil Gelatinase-associated Lipocalin Detection in Acute Kidney Injury / **Miss Kewarin Phonklam**	
15:10 – 15:15		**P025** Modeling Nutrient and Oxygen Diffusion in 3D Cancer on-a-chip Platform, using COMSOL Simulation / **Mr. Kadbodee Pliphon**	
15:15 – 15:20		**P026** Development of a Troponin I Based Biosensor, for Acute Myocardial Infarction Diagnosis / **Miss Suwali Wichian**	
15.35 – 16.35 include Q&A	**Oral Presentation Session 2**		
	ROOM 1: Precision Medicine/Clinical Medicine **Chair:** Assoc. Prof. Dr. Pritsana Raungrut **Co-chair:** Asst. Prof. Dr. Pasarat Khongkow **Committee:** Dr. Rassanee Bissanum	**ROOM 2: Medical Innovation** **Chair:** Asst. Prof. Dr. Wanwara Thuptimdang **Co-chair:** Assoc. Prof. Dr. Tonghathai Phairatana **Committee:** 1. Prof. Dr. Pornchai Phukpattaranont 2. Dr. Jermphiphut Jaruenpunyasak	**ROOM 3: Climate Change** **Chair:** Suebsai Varopichetsan, M.D., M.Sc. **Co-chair:** Assoc. Prof. Dr. Racha Dejchanchaiwong **Committee:** 1. Dr. Thanathip Limna 2. Assoc. Prof. Dr. Apiradee Saelim

15:35 – 15:50	**O013** Increased Expression of Fibrinogen Alpha Chain Enhances the Response to Cisplatin and Gemcitabine Doublet Chemotherapy in A549 Lung Adenocarcinoma Cell Line / **Miss Wirawan Worakit**	**O018** Silk Fibroin Incorporated with Disaccharide to Organize Morphological Construction of Wound Dressing; Fabrication, Characterization, Physical Performance / **Mr. Nitikorn Phattanee**	**O021** Correlation between Exposure to PM2.5 and Incidence of Acute Exacerbation for Chronic Obstructive Pulmonary Disease in Health Region 12, Thailand: A Retrospective Study with Time Series Analysis / **Miss Proudpisooth Wongprakornkul**
15:50 – 16:05	**O014** Regional and Subphase Gait Analysis for Foot Loading Characteristics of Post-stroke Patients and Healthy Participants / **Miss Prangnapas Kongneam**	**O020** Virtual Reality Intervention During Hysteroscopy: A Novel Approach to Enhancing Parasympathetic Responses / **Miss Preyahathai Aroonvanichporn**	**O022** Effects of Air Pollution on Natural Deaths in Southern Thailand; A Case-Crossover Study / **Miss Natthaya Bunplod**
16:05 – 16:20	**O015** Evaluation of the Radioprotective Effects of Curcumin Derivatives on Ionizing Radiation-Induced Damage in Normal Human Breast Epithelial Cells / **Miss Pimlapas Suravee**	**O028** Transforming Leftover Skin Specimens into an Ex Vivo Skin Culture Platform for Medical Innovation Development / **Miss Phetploy Rungkamoltip**	**O023** Impact of Meteorological Factors and Air Quality Index on COVID-19 Incidence in Pekanbaru, Indonesia: A Three-Year Data Analysis (2020–2023) / **Mr. Suyanto Suyanto**
16:20 – 16:35	**O016** Genetic Architecture of Pubertal Disorders Revealed by Whole-exome Sequencing / **Mr. Natthapon Khongcharoen**		
18.00 – 20.00	**Welcome Dinner**		

Day 2: Friday, October 10, 2025			
08.30 – 09.00 ROOM: Auditorium	**Registration**		
09.00 – 10.20	**MC: Ms. Khin Oo Mon, M.Sc. Candidate** Department of Epidemiology, Faculty of Medicine, Prince of Songkla University		
09.00 – 09.45 45 minutes, include Q&A ROOM: Auditorium	**Plenary session:** The Chemical and cellular basis of drug hypersensitivity reactions **Prof. Dean Naisbitt, Ph.D.** Institute of Systems, Molecular & Integrative Biology, Faculty of Health and Life Sciences, University of Liverpool **Moderator:** Asst. Prof. Kanoot Jaruthamsophon, M.D.		
09.45 – 10.20 35 minutes, include Q&A ROOM: Auditorium	**Invited Speaker 2:** Nucleic Acid–Based In Vitro Diagnostics: Research and Development at K-MEDI Hub **Dr. Jeewoong Park, Ph.D.** Daegu-Gyeongbuk Medical Innovation Foundation (KMEDIhub)		
10.20 – 11.10	**Coffee Break**		
11.10 – 11.40 include Q&A	**Oral Presentation Session 3**		
	ROOM 1: Emerging Infectious Disease **Chair:** Asst. Prof. Dr. Kamonnut Singkhamanan **Co-chair:** Dr. Ampapan Naknaen **Committee:** 1. Asst. Prof. Dr. Mingkwan Yingkajorn 2. Asst. Prof. Dr. Rachanida Praparatana	**ROOM 2: Healthy Aging** **Chair:** Assoc. Prof. Dr. Varomyalin Tipmanee **Co-chair:** Dr. Theerawat Dobutr **Committee:** 1. Asst. Prof. Dr. Kasemsiri Chandarajoti 2. Assoc. Prof. Thareerat Ananchaisarp, M.D.	
11:10 – 11:25	**O024** *In silico* Analysis of Apigenin and Luteolin as Dual Inhibitors of Dengue Virus Serotype 2 NS2B/NS3 Protease and Host C-type Lectin Receptor / **Miss Siriwan Aroonrungreang**	**O026** Phloretin Inhibits Glucose Uptake in HepG2 Cells: *In Vitro* and Docking Insights / **Miss Worarat Boonpech**	

11:25 – 11:40	**O025** One-year Humoral Immunogenicity of the SARS-CoV-2 mRNA Vaccine Booster in Patients with Autoimmune Rheumatic Disease Receiving Immunosuppressants / **Mr. Wuttirote Sangchayoswat**	**O027** Factors Predicting Ambulatory Status at Hospital Discharge After Fragility Hip Fracture Surgery: A Retrospective Cohort Study / **Miss Thitirut Jongutchariya**	
12.00-13.00.	**Lunch**		
13.00 – 14.30 ROOM: Auditorium	**MC: Mr. Songyos Rajborirug, Lecturer** Department of Epidemiology, Faculty of Medicine, Prince of Songkla University		
	Closing Remarks and certificate presentation **Prof. Sarunyou Chusri, M.D., Ph.D.** Vice Dean for Research and Innovation Affairs **Asst. Prof. Kittipong Riabroi, M.D., M.Sc.** Dean, Faculty of Medicine, Prince of Songkla University		

KEYNOTE SPEAKER

9 October 2025 Morning

Climate Change -> Air Pollution -> Health Effects

Prof. Perapong Tekasakul, Ph.D.
Department of Mechanical and Mechatronics Engineering,
Faculty of Engineering; Prince of Songkla University

Dengue Pathology and Management of Patients with Warning Signs

Dr. Chun-Yu Lin, Ph.D.
Director of Infectious Diseases
Kaohsiung Medical University Hospital

9 October 2025 Afternoon

Food Sciences & Healthy Aging

Prof. Emilie Combet Aspray, Ph.D.
Professor of Human Nutrition (Medicine)
School of Medicine, Dentistry & Nursing, Human Nutrition
University of Glasgow

10 October 2025 Morning

The Chemical and Cellular Basis of Drug Hypersensitivity Reactions

Prof. Dean Naisbitt, Ph.D.
Institute of Systems, Molecular & Integrative Biology
Faculty of Health and Life Sciences
University of Liverpool

Keynote Speaker 1

Prof. Perapong Tekasakul, Ph.D.
Department of Mechanical and Mechatronics Engineering,
Faculty of Engineering; Prince of Songkla University

Perapong Tekasakul is a professor in Mechanical and Mechatronics Engineering at Prince of Songkla University (PSU). He also serves as a director of Air Pollution and Health Effect Research Center leading a team of researchers from several disciplines to work on an integral approach aiming at the discovery of air pollution sources and forecasting, impact on human heath, and development of instrument. His current research interests encompass aerosol mechanics, atmospheric environment, and computational fluid dynamics. Prof. Tekasakul has published extensively in these areas, with his work cited more than 2,000 times on SCOPUS, reflecting his substantial impact on the fields. Prof. Tekasakul actively engages in international research collaborations. He has worked with institutions such as National Yangming Chiao Tung University in Taiwan, Kanazawa University in Japan, and Universiti Kebangsaan Malaysia among many others. He also collaborates with many institutions in Thailand. In addition to his academic pursuits, he has served as a member of the Commission of Higher Education, Ministry of Higher Education, Science, Research and Innovation (MHESI), and chair of a sub-committee to reinvent Thai universities.

Topic: Climate Change -> Air Pollution -> Health Effects
Date: Thursday, October 9, 2025
Time: 09.10-09.55 a.m.

Keynote Speaker 2

Dr. Chun-Yu Lin, Ph.D.
Director of Infectious Diseases
Kaohsiung Medical University Hospital

Dr. Chun-Yu Lin is a Ph.D. candidate in Psychology at the University of Arizona, specializing in cognition and neuroimaging under the supervision of Dr. Lee Ryan. He holds an M.S. in Applied Psychology from Fu Jen Catholic University, Taiwan, and a B.S. in Psychology from National Taiwan University. His research focuses on memory, unconscious processes and brain imaging, with publications in NeuroImage, Journal of Neuroscience Methods, and Magnetic Resonance in Medicine.

Dr. Lin has received multiple fellowships and awards; including the SBSRI Dissertation Research Grant, Cognitive Science Graduate Research Fellowship in addition to several international travel awards. He has presented his work at leading conferences; such as the Society for Neuroscience, Human Brain Mapping, and the Cognitive Neuroscience Society.

His professional experience includes: research assistantships in neuroimaging and electrophysiology, teaching courses on human memory and neuroimaging techniques and service as a psychological counselor in the Taiwanese Army. Moreover, he has contributed as a reviewer for academic awards and conferences. Also having served as webmaster for the Cognition and Neuroimaging Lab at the University of Arizona.

Topic: Dengue Pathology and Management of Patients with Warning Signs
Date: Thursday, October 9, 2025
Time: 09.55–10.40 a.m.

Keynote Speaker 3

Prof. Emilie Combet Aspray, Ph.D.
Professor of Human Nutrition (Medicine)
School of Medicine, Dentistry & Nursing, Human Nutrition
University of Glasgow

Emilie Combet is a professor of human nutrition at the University of Glasgow, where she leads a research team investigating the impact of diet on health and disease. Her research focuses on the nutritional and environmental quality of foods and their impact on human health, with a particular interest in obesity and weight management, and how diet and dietary choices influence health-spans.

Prof Combet is also interested in exploring how the food industry can contribute to reducing the risk of chronic diseases through food reformulation. In addition to her research, she is actively involved in teaching and supervising students at both undergraduate and postgraduate levels.

Combet is a member of several scientific societies and serves as a trustee of the Association for the Study of Obesity in addition to being the director of the European Nutrition Leadership Platform. She is passionate about translating research findings into recommendations and products; with colleagues across Scotland. Currently, she is exploring how trans-disciplinary research can address the complex challenges faced by our food system through the newly established Scottish Alliance for Food; which she leads

Topic: Food Sciences & Healthy Aging
Date: Thursday, October 9, 2025
Time: 13.00-13.45 p.m.

Keynote Speaker 4

Prof. Dean Naisbitt, Ph.D.

Institute of Systems, Molecular & Integrative Biology

Faculty of Health and Life Sciences

University of Liverpool

Professor Dean Naisbitt is a Professor of Pharmacology & Therapeutics at the University of Liverpool, specializing in the chemical and cellular basis of immunological drug reactions. His research integrates genetics, cell biology, and chemistry to study mechanisms of drug hypersensitivity, with direct impact on clinical practice and safe drug development. He has published over 200 peer-reviewed papers; including in leading journals; such as the Journal of Allergy and Clinical Immunology and Hepatology.

He has led major international research programs funded by the MRC, EU, and industry partners, and established collaborations with more than 40 clinical centers worldwide. His work has received prestigious awards; including the American Chemical Society Young Investigator Award and the British Pharmacological Society Novartis Prize. Professor Naisbitt has supervised 45 PhD students and plays an active role in editorial boards and professional societies in pharmacology, toxicology and allergy research

Topic: The Chemical and Cellular Basis of Drug Hypersensitivity Reactions
Date: Friday, October 10, 2025
Time: 09.00-09.45 a.m.

INVITED SPEAKER

9 October 2025

The Role of WGS in the Control of Hospital-Acquired Bacterial Infections

Prof. Prasit Palittapongarnpim, M.D., Ph.D.
Department of Microbiology, Faculty of Science, Mahidol University

Room : Auditoriam
11.30-12.05 p.m.

10 October 2025

Nucleic Acid–Based in Vitro Diagnostics: Research and Development at K-MEDI Hub

Dr. Jee-Woong Park, Ph.D.
Daegu-Gyeongbuk Medical Innovation Foundation (KMEDIhub)

Room : Auditoriam
09.45-10.20 a.m.

Invited Speaker 1

Prof. Prasit Palittapongarnpim, M.D., Ph.D.
Department of Microbiology, Faculty of Science,
Mahidol University

Professor Prasit Palittapongarnpim is a Professor of Microbiology; at the Faculty of Science, Mahidol University. He obtained his M.D. with first-class honors from Ramathibodi Hospital, Mahidol University, and completed postdoctoral training in molecular genetics at the University of Alberta, Canada. He is a founding member of the Pornchai Matangkasombut Center for Microbial Genomics, and serves on the University Councils of Prince of Songkla University and Taksin University. He also plays advisory and leadership roles as Chairman of the Steering Committee for the Faculty of Medical Technology, Prince of Songkla University in addition to being a committee member for the Faculty of Medicine, Chiang Mai University.

Nationally, Professor Prasit has served on the National Vaccine Committee, the National Committee for Emerging Infectious Diseases Preparedness, and the Academic Committee of the National Vaccine Institute. Wherein, he contributes significantly to policy and research strategies for infectious disease prevention in Thailand. Regionally, he has participated in the Asia and Pacific Rim Research Integrity Network and serves on editorial boards of: Scientific Reports (Nature Publishing Group) and the Malaysian Journal of Microbiology. Professor Prasit's research focuses on microbial genomics, tuberculosis, and infectious diseases, with particular emphasis on molecular epidemiology, pathogen genomics, and host–pathogen interactions. He has published over 100 peer-reviewed papers (with more than 2,650 citations and an h-index of 25) in leading journals; such as Scientific Reports, Virulence, BMC Infectious Diseases, and Microbial Genomics. His research has advanced understanding of Mycobacterium tuberculosis lineages, drug resistance, and genomic epidemiology in Southeast Asia. Moreover, he has collaborated extensively with regional and international partners.

In addition to his research, he holds several patents related to innovative diagnostics and therapeutics for tuberculosis and other infectious diseases. He has also co-authored book chapters and review articles that highlight Thailand's role in global infectious disease research. His contributions have positioned him as one of Thailand's foremost microbiologists, bridging basic science, clinical application and policy development in infectious diseases and public health.

Topic: The Role of WGS in the Control of Hospital-Acquired Bacterial Infections
Date: Thursday, October 9, 2025
Time: 11.30–12.05 p.m.

Invited Speaker 2

Dr. Jee-Woong Park, Ph.D.

Daegu-Gyeongbuk Medical Innovation Foundation (KMEDIhub)

Dr. Jee-Woong Park is a Senior Researcher at the Medical Device Development Center, Daegu-Gyeongbuk Medical Innovation Foundation, where he has served since 2019. He earned his B.S. in Bioscience and Technology (2006) and completed an integrated M.S./Ph.D. program in Life Sciences and Biotechnology at Korea University (2012), with his doctoral thesis focusing on developing an immobilization-free DNA aptamer screening method using graphene oxide.

Throughout his career, Dr. Park has pursued advanced research across several leading institutions worldwide. He has worked as a Research Assistant at the Korea Institute of Science and Technology, a Postdoctoral Fellow at Lund University in Sweden and the University of Tokyo, and later as Project Assistant Professor at the University of Tokyo's Institute of Medical Science. His research has covered diverse areas, including DNA nanomaterials for siRNA delivery, acoustophoresis-based SELEX, microfluidic chip applications, and aptamer-CRISPR diagnostic platforms. In addition, he served as a project manager for a molecular diagnostics start-up, contributing to technology transfer and commercialization.

Dr. Park's research interests lie in diagnostic technologies such as loop-mediated isothermal amplification (LAMP) and CRISPR-based diagnosis, aptamer development, acoustophoretic microfluidics, and the biomedical application of nanomaterials. As Principal Investigator, he has led several competitive projects funded by the National Research Foundation of Korea and international programs, focusing on biosensing platforms, point-of-care testing systems, and integrated nano-biosensors.

He has authored numerous high-impact publications and is the corresponding author of several works on aptamer selection, biosensors, and diagnostic devices. His innovative research has also resulted in multiple patents on molecular diagnostic devices, biosensors, and microfluidic technologies. In recognition of his contributions, he has received multiple research awards, including honors from Korea University, the Society for Chemistry and Micro-Nano Systems in Japan, and the Ministry of Food and Drug Safety of Korea.

With extensive expertise in biotechnology, nanotechnology, and biomedical engineering, Dr. Park has established himself as a leading scientist in developing next-generation diagnostic platforms and innovative biosensing solutions for healthcare and infectious disease detection.

Topic: Nucleic Acid–Based in Vitro Diagnostics: Research and Development at K-MEDI Hub

Date: Friday, October 10, 2025

Time: 09.45–10.20 a.m.

Abstract of Oral and Poster Presentation

The 4th Annual Health Research International Conference

Shaping the Future: Innovation, Health and Well-being

Abstract of Oral Presentation

R1-O-024	**In Silico Analysis of Apigenin and Luteolin as Dual Inhibitors of Dengue Virus Serotype 2 NS2B/NS3 Protease and Host C-Type Lectin Receptor** *Siriwan Aroonrungreang[1], Benjaporn Noppradit, Ph.D.[2], Panupong Puttarak, Ph.D.[2], Smonrapat Surasombatpattana, Ph.D.[3], Nawamin Pinpathomrat, M.D., Ph.D.[1], Theerawat Dobutr, Ph.D.[1]** [1]Department of Biomedical Sciences and Biomedical Engineering, Faculty of Medicine, Prince of Songkla University, Hat Yai, Songkhla 90110, Thailand. [2]Department of Pharmacognosy and Pharmaceutical Botany, Faculty of Pharmaceutical Sciences, Prince of Songkla University, Hat Yai, Songkhla 90110, Thailand. [3]Division of Virology and Serology, Department of Pathology, Faculty of Medicine, Prince of Songkla University, Hat Yai, Songkhla 90110, Thailand.	p 44
R1-O-025	**One-Year Humoral Immunogenicity of the SARS-CoV-2 mRNA Vaccine Booster in Patients with Autoimmune Rheumatic Disease Receiving Immunosuppressants** *Wuttirote Sangchayoswat, Siriporn Juthong, Porntip Intapiboon* Department of Internal Medicine, Faculty of Medicine, Prince of Songkla University, Hat Yai, Songkhla 90110, Thailand.	p 45
R2-O-027	**Factors Predicting Ambulatory Status at Hospital Discharge After Fragility Hip Fracture Surgery: A Retrospective Cohort Study** *Thitirut Jongutchariya[1], Jittima Saengsuwan[2], Palanthorn Loomcharoen[1], Saowaluck Settheekul[3]* [1]Department of Rehabilitation, Hatyai Hospital, Hat Yai, Songkhla 90110, Thailand. [2]Department of Rehabilitation Medicine, Faculty of Medicine, Khon Kean University, Khon Kean 40002, Thailand. [3]Independent Researcher, Chiang Mai 50300, Thailand.	p 46
R2-O-028	**Transforming Leftover Skin Specimens into an Ex Vivo Skin Culture Platform for Medical Innovation Development** *Phetploy Rungkamoltip[1], Laliphat Kongpanichakul[2], Orawan Chansanti[2], Pasarat Khongkow[1,3]* [1]Department of Biomedical Sciences and Biomedical Engineering, Faculty of Medicine, Prince of Songkla University, Hat Yai, Songkhla 90110, Thailand. [2]Division of Plastic Surgery, Department of Surgery, Faculty of Medicine, Prince of Songkla University, Hat Yai, Songkhla 90110, Thailand. [3]Translational Medicine Research Center, Faculty of Medicine, Prince of Songkla University, Hat Yai, Songkhla 90110, Thailand.	p 47

Abstract of Poster Presentation

P-024	**A Microfluidic Biosensing Platform for Neutrophil Gelatinase-Associated Lipocalin Detection in Acute Kidney Injury** *Kewarin Phonklam[1], Tonghathai Phairatana[1,2]* [1]Department of Biomedical Sciences and Biomedical Engineering, Faculty of Medicine, Prince of Songkla University, Hat Yai, Songkhla 90110, Thailand. [2]Institute of Biomedical Engineering, Faculty of Medicine, Prince of Songkla University, Hat Yai, Songkhla 90110, Thailand.	p 71
P-025	**Modeling Nutrient and Oxygen Diffusion in 3D Cancer-On-A-Chip Platform, using COMSOL Simulation** *Kadbodee Pliphon[1], Siwattra Pruksasri[1], Sunisa Saengchan[1], Mooktapa Plikomol[1], Tonghathai Phairatana[1], Pasarat Khongkow[1,2]* [1]Department of Biomedical Sciences and Biomedical Engineering, Faculty of Medicine, Prince of Songkla University, Hat Yai, Songkhla 90110, Thailand. [2]Translational Medicine Research Center, Faculty of Medicine, Prince of Songkla University, Hat Yai, Songkhla 90110, Thailand.	p 72
P-026	**Development of a Troponin I Based Biosensor, for Acute Myocardial Infarction Diagnosis** *Suwali Wichian[1], Kewarin Phonklama[1], Tonghathai Phairatana[1,2]* [1]Department of Biomedical Sciences and Biomedical Engineering, Faculty of Medicine, Prince of Songkla University, Hat Yai, Songkhla 90110, Thailand. [2]Institute of Biomedical Engineering, Faculty of Medicine, Prince of Songkla University, Hat Yai, Songkhla 90110, Thailand.	p 73

Real-World Effectiveness of Once-Weekly Semaglutide Injections in Type 2 Diabetes: A Retrospective Study

Supanut Sereeaphinan, M.D.[1], Noppadol Kietsiriroge, M.D., Ph.D.[2], Chaitong Churuangsuk, M.D., Ph.D.[3]*

[1]Department of Internal Medicine, Faculty of Medicine, Prince of Songkla University, Hat Yai, Songkhla 90110, Thailand.
[2]Endocrinology and Metabolism Unit, Department of Internal Medicine, Faculty of Medicine, Prince of Songkla University, Hat Yai, Songkhla 90110, Thailand.
[3]Clinical Nutrition and Obesity Medicine Unit, Department of Internal Medicine, Faculty of Medicine, Prince of Songkla University, Hat Yai, Songkhla 90110, Thailand.

Abstract:

Background: Although, Semaglutide, a once-weekly GLP-1 receptor agonist, has demonstrated significant glycemic and weight reduction in clinical trials, its real-world effectiveness in Thai patients remains unexplored.

Objective: To assess the glycemic and weight-lowering effects of Semaglutide in patients with type 2 diabetes (T2D) in a real-world clinical setting.

Material and Methods: We conducted a retrospective study in adult patients with T2D receiving subcutaneous Semaglutide at Songklanagarind Hospital; from 01/2021 until 06/2025. Data was collected from electronic medical records. Study outcomes were: HbA1c and body weight at 3 and 6 months after semaglutide commencement. Adverse events were also reported.

Results: A total of 146 patients were analyzed (50% females: mean age 56.5±12.7 years). Baseline HbA1c was 8.0±1.6%, with a diabetes duration of 8.2±6.7 years. Mean body weight was 85.2±21.2 kg. Semaglutide dose average was 0.64±0.30 mg/week and 0.69±0.35 mg/week at 3 and 6 months, consecutively. There was significant reductions in HbA1c by –0.87% (95% confidence interval [CI] –1.06 to –0.68; p-value<0.001) at 3 months, and by –1.05% (95% CI –1.27 to –0.83; p-value<0.001) at 6 months, with the greatest reduction in patients having higher baselines: HbA1c ≥9% (-2.12%; 95% CI -2.76 to -1.48; p-value<0.001). Similarly, body weight reduced from baseline by –2.65% (95% CI –3.28 to –2.03; p-value<0.001) at 3 months, with a further reduction by –3.86% (95% CI –4.59 to –5.83; p-value<0.001) at 6 months. One-third of patients reported mild gastrointestinal symptoms. Half of the patients (n=73/146) could tolerate up to a 1 mg/week dose, while 43.8% (n=64/146) received a 0.25-0.75 mg/week dose. Only 6.2% received a 1.5-2.0 mg/week dose.

Conclusion: Semaglutide demonstrated significant improvements in glycemic control and body weight in a real-world Thai T2D cohort, with nearly half achieving clinical benefits with doses <1 mg/week, compared to standard clinical trial protocols. Such lower doses combined with lifestyle modification may provide optimal therapeutic outcomes, while minimizing adverse effects and offering potential cost-effectiveness advantages.

Keywords: HbA1c, real-world data, Semaglutide, type 2 diabetes, weight reduction

Identification of Prognostic Markers for Predicting Recurrence and Progression of Non-Muscle Invasive Urothelial Carcinoma, via Bioinformatic Analysis

Paramee Thongsuksai[1]*, Worapat Attawettayanon[2], Thitawan Chimpalee[1]

[1]Department of Pathology, Faculty of Medicine, Prince of Songkla University, Hat Yai, Songkhla 90110, Thailand.
[2]Department of Surgery, Faculty of Medicine, Prince of Songkla University, Hat Yai, Songkhla 90110, Thailand.

Abstract:

Background: Non-muscle invasive bladder cancer (NMIBC), which accounts for approximately 75% of all bladder cancer cases, is characterized by high recurrence rates and potential progression to muscle-invasive bladder cancer (MIBC). Early cystectomy is often considered for patients at very high risk of progression and recurrence. Current risk stratification systems rely on clinicopathological data; however, they demonstrate only moderate predictive accuracy.

Objective: This study aimed to develop a prognostic prediction model for recurrence-free survival and progression-free survival in NMIBC using transcriptomic analysis.

Material and Methods: Gene expression data from 375 NMIBC and 203 MIBC samples were obtained from the GEO database (datasets: GSE32894, GSE32548 and GSE48075). Significant differentially expressed genes (DEGs) were identified, based on |log2 fold changel ≥1.5, and adjusted p-value<0.05. Candidate DEGs were further refined using LASSO regression analysis, with an independent dataset (GSE163209: n=217 NMIBC). The final prognostic model incorporated both clinical parameters and gene expression data. Model performance was assessed by the area under the curve (AUC) and concordance index (C-index). Internal validation was performed using bootstrapping.

Results: A total of 33 significant DEGs were identified. LASSO regression selected four genes (CTHRC1, BTBD16, FAM3B and CYP3A5) as independent predictors of disease progression. The model, based on clinical parameters (age and stage), achieved an AUC of 0.77 (95% confidence interval [CI], 0.65–0.87) and a C-index of 0.79. Incorporating the four-gene signature improved predictive performance yielded an AUC of 0.87 (95% CI, 0.75–0.96) and a C-index of 0.86. The calibration curve demonstrated an acceptable model fit.

Conclusion: Integration of gene expression data with clinical parameters enhances predictive accuracy for NMIBC prognosis. The developed model demonstrated strong internal validity; however, further external validation using immunohistochemistry in clinical cohorts is warranted.

Keywords: bioinformatic analysis, differentially expressed gene, non-muscle invasive bladder cancer, prognostic prediction model, urothelial carcinoma

Assessing the Relationships between Diet, Sports and Anthropometric Indicators of Elementary School Students in Vietnam using Structural Equation Modeling

Giang Le Ba, M.Sc[1,2], Rassamee Chotipanvithayakul, M.D., Ph.D.[1], Virasakdi Chongsuvivatwong, M.D., Ph.D.[1]*

[1]Department of Epidemiology, Faculty of Medicine, Prince of Songkla University, Hat Yai, Songkhla 90110, Thailand.
[2]Department of Medical Ethics – Law and Behavioral Science, Faculty of Public Health, Pham Ngoc Thach University of Medicine, Ho Chi Minh City 700000, Vietnam.

Abstract:

Background: Good nutrition and physical activity are essential for children's development and growth. The complex relationships among diet, sports, and socio-demographic factors influencing children's growth require specific analytical techniques, not only linear regression, but also structural equation modeling (SEM).

Objective: This study aimed to describe the relationship of anthropometric indices among elementary school students, with socioeconomic factors, diet factors, and sports.

Material and Methods: We analyzed a data set of primary school children's weight and height, together with a self-administered questionnaire on their socioeconomic variables. The anthropometric indices z-BMI and z-Height were age-standardized and were computed using the WHO Anthro software V.1.0.4.

Results: The z-BMI of male students was higher than that of female students (β=0.48, p-value<0.001). Children whose mothers were workers, housewives, businesswomen and government employees had higher z-BMI than children whose mothers were farmers, with respective effect sizes of 0.79, 0.64, 0.82, and 0.83. The z-Height of students whose fathers were workers and civil servants was 0.82 and 0.86 times lower than that of students whose fathers were farmers, respectively. According to SEM, diet affected on z-BMI was 0.19, while sport affected z-BMI directly and overall by β=0.47, β=0.46, respectively. Diet and sports, however, show no significant effect on z-Height (with Sport being β=0.04, p-value=0.66; with diet being β=0.13, p-value=0.09).

Conclusion: Improvement of diet and sports in primary school children would be useful to reduce wasting, but the benefits on height could not be observed in this study.

Keywords: diet, sports, anthropometric indicators, elementary school, students, Vietnam

Rubella Vaccination Acceptance in Bangladesh: Exploring Young Female Adults' Willingness for Self and Child as Policy Guidance

Md Nuruzzaman, MPH, Wit Wichaidit, Ph.D., Quazi Monirul Islam, MBBS, MPH, FRCOG, Tippawan Liabsuetrakul, M.D., Ph.D.*

Department of Epidemiology, Faculty of Medicine, Prince of Songkla University, Hat Yai, Songkhla 90110, Thailand.

Abstract:

Background: Rubella vaccination is critical for preventing congenital rubella syndrome (CRS). However, vaccine acceptance remains a challenge in many low- and middle-income countries; including Bangladesh. Understanding women's willingness to receive the vaccine for themselves and their children is essential to inform effective policy.

Objective: This study aimed to explore young female adults' willingness to accept the rubella vaccination for themselves and their children as well as to assess the level of agreement between the two decisions to inform policy guidance.

Material and Methods: A cross-sectional study was conducted among 580, young female adult, garment factory workers; aged 18–24 years, in Bangladesh. Participants were surveyed regarding their willingness to accept the rubella vaccination for themselves and for a child. Agreement between women's willingness to accept rubella vaccination for themselves and for their children was assessed using Cohen's Kappa (κ), Prevalence-Adjusted Bias-Adjusted Kappa (PABAK), and McNemar's test.

Results: Among the participants, 86.2% expressed willingness to accept rubella vaccination for themselves, while 89.5% were willing for a child. Cohen's Kappa showed substantial agreement (κ=0.69; 95% CI: 0.59–0.78) and PABAK, yielding a stronger agreement estimate (PABAK=0.87; 95% CI: 0.83–0.91). McNemar's test indicated a statistically significant asymmetry in paired responses (p-value=0.002).

Conclusion: This asymmetry highlights a policy-relevant gap in awareness and perceived risk related to vaccination in reproductive aged women. While child health is prioritized, women may not fully recognize the importance of their own immunity in preventing CRS. Addressing this disparity through age- and gender-sensitive vaccine communication strategies could help inform the development of more equitable and gender-responsive immunization policies.

Keywords: Bangladesh, Rubella, young adults, vaccination programs, willingness to vaccinate

Stakeholder Perspective on the Barriers of Interventions for Childhood Vaccination in Urban Slums of Bangladesh: A Qualitative Study

Kazi Fayzus Salahin, M.Sc., MBA[1,2], Wit Wichaidit, Ph.D.[1],
Quazi Monirul Islam, MBBS, MPH, FRCOG[1], Tippawan Liabsuetrakul, M.D., Ph.D.[1]*

[1]Department of Epidemiology, Faculty of Medicine, Prince of Songkla University, Hat Yai, Songkhla 90110, Thailand.
[2]Department of Data Management and Analytic, Eminence Associates for Social Development, Dhaka 1206, Bangladesh.

Abstract:

Background: Childhood vaccination is a cornerstone of global public health, saving millions of children's lives worldwide. However, equitable coverage remains a persistent global health challenge; especially in urban slum areas. In Bangladesh, similar settings face compounded challenges; including fragmented health systems, socio-economic vulnerability, mistrust and limited services, which hinder access to and uptake of childhood vaccination. Stakeholders' perspectives are essential to identify the health system and community level barriers in these vulnerable populations.

Objective: This study aimed to explore the barriers of implementing potential interventions for improving the vaccine uptake from the both demand- and supply-side stakeholders.

Material and Methods: This cross-sectional qualitative study was conducted from 30 November 2023 to 7 January 2024. It involved 102 participants; including 67 demand-side stakeholders (49 parents and 18 grandparents) and 35 supply-side stakeholders. Each interview took approximately one hour, while focus groups lasted around 90 minutes. Data was collected in six slum areas in Dhaka, where half of the informal settlements of the city are located. It used focus group discussions, in-depth interviews, and key informant interviews. The data were analyzed using thematic analysis for vaccination barriers and intervention priority.

Results: Demand-side stakeholders revealed the informal costs, lost wages, inconvenient service hours, fear of vaccine side effects and irregular clinics as major barriers. Supply-side stakeholders raised the issues of staffing shortages, supply interruptions, lack of multi-sectoral alignment and community disengagement.

Conclusion: This study highlights the insights of each stakeholder group, which requires common ground of felt needs and possible pathways for context-specific interventions. This is to overcome economic and access to care constraints, and feasible models of service delivery for both groups of stakeholders, with respect to social realities and to increase trust. Integrating stakeholder-endorsed interventions into routine service designs may improve childhood vaccination equity across urban slum populations.

Keywords: Bangladesh, childhood vaccination, slum, stakeholder perspective, urban health system, vaccination equity

Regional and Subphase Gait Analysis for Foot Loading Characteristics of Post-Stroke Patients and Healthy Participants

Prangnapas Kongneam[1], Thanita Sanghan, Ph.D.[2], Surapong Chatpun, Ph.D.[2]*

[1]Faculty of Medicine, Prince of Songkla University, Hat Yai, Songkhla 90110, Thailand.
[2]Department of Biomedical Sciences and Biomedical Engineering, Faculty of Medicine, Prince of Songkla University, Hat Yai, Songkhla 90110, Thailand.

Abstract:

Objective: This study aimed to determine the differences of foot loading characteristics and gait asymmetry index between hemiplegic patients and healthy participants; focusing on specific foot regions during subphases of the gait cycle.

Material and Methods: The plantar pressure data, using Pedar® system, were obtained from 15 hemiplegic patients and 15 healthy participants. Key foot regions; such as medial and lateral of the forefoot, midfoot and rearfoot, were analyzed across stance subphases. The difference of foot loading parameters was analyzed with a linear mixed model, using R program; adjusting for confounding variables and presenting as Estimated marginal means (Emmeans) pressure (kPa). Gait asymmetry index was determined for each region across all subphases.

Results: Hemiplegic patients showed significant asymmetries in plantar pressure between paretic and non-paretic sides, with notable differences compared to healthy participants. During double support 1, Emmeans pressure was significantly decreased on the paretic side of the medial and lateral rearfoot, and medial midfoot. In single support, Emmeans pressure was significantly decreased in the medial and lateral forefoot, and medial midfoot. In double support 2, Emmeans pressure was significantly decreased in the lateral and medial forefoot. Additionally, the medial midfoot in the hemiplegic group showed the highest asymmetry index across all subphases compared to other foot regions.

Conclusion: Hemiplegic patients exhibit significant gait asymmetries in the lateral forefoot and medial midfoot across all subphases. These findings can lead to targeted rehabilitation strategies and monitoring devices to improve post-stroke gait.

Keywords: foot region, gait training, hemiplegic gait, plantar pressure, stroke

Genetic Architecture of Pubertal Disorders Revealed by Whole-Exome Sequencing

Natthapon Khongcharoen, M.D.[1,2], Surasak Sangkhathat, M.D., Ph.D.[3], Tansit Saengkaew, M.D, Ph.D.[2,4]*

[1]Department of Biomedical Sciences and Biomedical Engineering, Faculty of Medicine, Prince of Songkla University, Hat Yai, Songkhla 90110, Thailand.
[2]Translational Medicine Research Center, Faculty of Medicine, Prince of Songkla University, Hat Yai, Songkhla 90110, Thailand.
[3]Department of Surgery, Faculty of Medicine, Siriraj Hospital, Bangkok 10700, Thailand.
[4]Endocrinology Unit, Department of Pediatrics, Faculty of Medicine, Prince of Songkla University, Hat Yai, Songkhla 90110, Thailand.

Abstract:

Background: Pubertal timing is strongly influenced by genetics, and causative variants have been described in congenital hypogonadotropic hypogonadism (CHH).

Objective: To evaluate the clinical, hormonal, and molecular spectrum of pubertal disorders, and to explore the contribution of oligogenic inheritance.

Material and Methods: We performed whole-exome sequencing (WES) in 29 patients with CHH (8 Kallmann syndrome; 21 normosmic CHH) and analyzed the data. Variants were interpreted with ACMG/AMP criteria within curated gene panels (122 CHH genes), and by interrogating additional genes involved in GnRH biology to identify novel candidates. Oligogenic inheritance, defined as ≥2 rare variants in pubertal-disorder-related genes, was also assessed.

Results: In CHH, WES identified 30 rare variants in 18/29 patients (62.1%). Pathogenic/likely pathogenic variants were detected in 10/29 (34.5%), most frequently in CHD7 (n=3) and PROKR2 (n=2); single cases involved: ANOS1, FGFR1, TCF12, PNPLA6 and SEMA7A. Eight additional patients carried variants of uncertain significance (VUS), predicted to be deleterious *in silico*. Oligogenic inheritance was observed in 9/29 (31.0%).

Conclusion: WES achieves a high diagnostic yield in CHH and often uncovers oligogenic inheritance. These findings support WES as a first-line genetic test for CHH.

Keywords: congenital hypogonadotropic hypogonadism, delayed puberty, genetic defects, whole-exome sequencing

Correlation between Exposure to PM2.5 and Incidence of Acute Exacerbation for Chronic Obstructive Pulmonary Disease in Health Region 12, Thailand: A Retrospective Study with Time Series Analysis

Thammasin Ingviya, M.D., MHS, Ph.D.[1]*, Kittitat Chitmanee[2], Jiramet Sotatwi[2], Chiyakarn Piboonjirachart[2], Nantat Rakchum[2], Mukmanee Rattanakosom[2], Proudpisooth Wongprakornkul[2], Wirinda Onchulee[2], Siriphat Sombatkultana[2], Natthaya Bunplod, M.Sc.[1,3]

[1]Department of Clinical Research and Medical Data Science, Faculty of Medicine, Prince of Songkla University, Hat Yai, Songkhla 90110, Thailand.
[2]Medical Student, Faculty of Medicine, Prince of Songkla University, Hat Yai, Songkhla 90110, Thailand.
[3]Air pollution and Health Effect Research Center, Prince of Songkla University, Hat Yai, Songkhla 90110, Thailand.

Abstract:

Background: Seasonal transboundary haze is a known trigger for respiratory morbidity; particularly among clinically vulnerable individuals with pre-existing conditions. However, while the effects on diseases like asthma are better documented, there is a scarcity of research quantifying the specific burden on patients with chronic obstructive pulmonary disease (COPD) in Southern Thailand.

Objective: This study quantified the association between $PM_{2.5}$ exposure from transboundary haze and the incidence of acute exacerbations for chronic obstructive pulmonary disease (AECOPD) across Thailand's seven southernmost provinces.

Material and Methods: We obtained two primary datasets from the period of 1 January 2015 until 31 December 2019: daily air pollution data ($PM_{2.5}$) of the seven provinces from the pollution control department, and records of 700,321 AECOPD incidence in Health Region 12 from the National Health Security Office. Missing $PM_{2.5}$ data were imputed using multiple imputation by chained equations and inverse distance weighting. 'Haze days' were defined as days with $PM_{2.5}$ concentrations exceeding the 95th percentile, with sources confirmed via backward trajectory simulation. Poisson regression models were used to estimate unadjusted and adjusted incidence rate ratios (IRR) for said association.

Results: The mean daily $PM_{2.5}$ concentration during the study period was 18.3 $\mu g/m^3$, with a maximum of 87.9 $\mu g/m^3$. A 10 $\mu g/m^3$ increase in $PM_{2.5}$ was significantly associated with an increased incidence of AECOPD across multiple lags (lag 0-5 day). Furthermore, 'haze days' were associated with a 9.5% increase in AECOPD incidence (IRR=1.095; 95% confidence interval: 1.093-1.097). An effect observed across all age and gender subgroups.

Conclusion: Exposure to $PM_{2.5}$ from transboundary haze is a significant risk factor for AECOPD in Southern Thailand. These results justify the development of early warning systems for vulnerable populations and emphasize the needs for cross-border cooperations and legislations to manage major pollution sources.

Keywords: acute exacerbation of COPD, Air pollution, $PM_{2.5}$, transboundary haze, time-series analysis

Effects of Air Pollution on Natural Deaths in Southern Thailand: A Case-Crossover Study

Natthaya Bunplod[1,2], Thammasin Ingviya, M.D., M.HS., Ph.D.[1,2]*

[1]Department of Clinical Research and Medical Data Science, Faculty of Medicine, Prince of Songkla University, Hat Yai, Songkhla 90110, Thailand.

[2]Air Pollution and Health Effect Research Center, Prince of Songkla University, Hat Yai, Songkhla 90110, Thailand.

Abstract:

Background: Air pollution poses a significant threat to public health worldwide, yet its impact in Southern Thailand remains understudied.

Objective: This study investigated the association between ambient air pollutants ($PM_{2.5}$, PM_{10}, NO_2, CO, O_3 and SO_2) and natural deaths in Southern Thailand.

Material and Methods: A case-crossover design was employed, using daily average concentrations of air pollutants and individual mortality data from 14 southern provinces of Thailand: spanning from January 1, 2015, to December 31, 2023. Conditional logistic regression was applied to assess the associations, adjusting for ambient temperature, relative humidity, and public holidays. To examine the lagged associations between air pollution exposure and natural-cause mortality, lag structures were analyzed over a 6-day period (lag 0 to lag 5), using both single lag and moving average lag models. These models were used to capture both acute and cumulative effects over time, within a distributed lag non-linear modeling framework.

Results: The average mortality rate among the study population was 595.3 per 100,000 population, with a mean age of death at 69 years. The daily average concentrations of air pollutants were: $PM_{2.5}$ (14.6 $\mu g/m^3$), PM_{10} (30.0 $\mu g/m^3$), NO_2 (5.6 ppb), SO_2 (1.1 ppb), O_3 (19.0 ppb), and CO (0.4 ppm). Despite these low levels, significantly positive associations were found between all pollutants and mortality. For single-day exposures, the highest mortality risk for $PM_{2.5}$, PM_{10} and O_3 occurred at a 3-day lag. For cumulative exposures, the largest risk estimates were observed across different windows: Lag 0–5 for O_3 and CO, Lag 2–4 for $PM_{2.5}$, Lag 3–4 for PM_{10}, Lag 4–5 for SO_2; and Lag 0–1 for NO_2.

Conclusion: Unique to this region, this study investigated the association between air pollutants; notably transboundary haze, and natural deaths, and it found a significant association even at concentrations lower than World Health Organization recommendations. These findings emphasize the need to control or minimize these transboundary pollutants.

Keywords: air pollution, case-crossover study, natural death

Impact of Meteorological Factors and Air Quality Index on COVID-19 Incidence in Pekanbaru, Indonesia: A Three-Year Data Analysis (2020–2023)

Suyanto Suyanto, Ph.D.[1]*, Agrina Agrina, Ph.D.[2], Arya Marganda Simanjuntak, M.D.[1], Zulharman Zulharman, M.Sc.[1], Nerissa Isfa, M.Sc.[3], Nanda Safira, M.Sc.[4], Satiti Palupi Purwanto, Ph.D.[5], Novi Reandy Sasmita, M.Sc.[6]

[1]Faculty of Medicine, Universitas Riau, Pekanbaru 28000, Indonesia.
[2]Faculty of Nursing, Universitas Riau, Pekanbaru 28000, Indonesia.
[3]Faculty of Medicine, Universitas Prima Nusantara, Bukittinggi 26136, Indonesia.
[4]Department of Epidemiology, Faculty of Medicine, Prince of Songkla University, Hat Yai, Songkhla 90110, Thailand.
[5]Department of Communicable Disease, East Java Provincial Health Office, Surabaya 60271, Indonesia.
[6]Department of Statistics, Faculty of Mathematics and Natural Sciences, Universitas Syiah Kuala, Banda Aceh 23111, Indonesia.

Abstract:

Background: As a major city in Indonesia, Pekanbaru experienced significant fluctuations in COVID-19 incidence during the pandemic period. Meteorological factors and air quality are hypothesized to influence the transmission dynamics of the virus, yet empirical evidence from tropical, urban settings remains limited.

Objective: This study aimed to examine the impact of temperature, humidity, and the air quality index (AQI) on COVID-19 transmission in Pekanbaru; from 2020 to 2023, and to assess their potential role in shaping public health strategies.

Material and Methods: Daily data on confirmed COVID-19 cases, meteorological parameters, and AQI were obtained from official health and meteorological sources. Distributed Lag Non-Linear Models, with Quasi-Poisson regression were applied to evaluate temporal associations between these environmental factors and COVID-19 incidence.

Results: Pekanbaru exhibited a relatively stable tropical climate during the study period, with an average temperature of 33 °C and relative humidity of 82%. The analysis indicated that extreme temperatures at the 1st percentile (24 °C) were associated with an increased transmission risk (RR: 2.81; 95% CI: 0.67–11.8), while at the 99th percentile (29 °C), the risk was moderately elevated (RR: 1.85; 95% CI: 0.51–6.69). Humidity variations showed no meaningful effect: with RR of 1.12 (95% CI: 0.58–2.15) at the 1st percentile (70%) and 0.48 (95% CI: 0.14–1.72) at the 99th percentile (95%). In contrast, elevated AQI levels at the 99th percentile (127)—particularly during the dry season—were consistently associated with higher COVID-19 transmission (RR: 1.50; 95% CI: 0.90–2.52).

Conclusion: Although these estimates did not reach statistical significance, the observed trends suggest that air pollution, more than meteorological variability, may play a substantial role in COVID-19 spread in tropical, urban environments. Understanding these environmental influences provides valuable insights for anticipating disease surges and for designing targeted interventions. Pollution control measures should therefore be prioritized as an integral component of infectious disease mitigation strategies in cities like Pekanbaru.

Keywords: air quality index, COVID-19, meteorological factors, Pekanbaru, tropical urban

In Silico Analysis of Apigenin and Luteolin as Dual Inhibitors of Dengue Virus Serotype 2 NS2B/NS3 Protease and Host C-Type Lectin Receptor

Siriwan Aroonrungreang[1], Benjaporn Noppradit, Ph.D.[2], Panupong Puttarak, Ph.D.[2], Smonrapat Surasombatpattana, Ph.D.[3], Nawamin Pinpathomrat, M.D., Ph.D.[1], Theerawat Dobutr, Ph.D.[1]*

[1]Department of Biomedical Sciences and Biomedical Engineering, Faculty of Medicine, Prince of Songkla University, Hat Yai, Songkhla 90110, Thailand.
[2]Department of Pharmacognosy and Pharmaceutical Botany, Faculty of Pharmaceutical Sciences, Prince of Songkla University, Hat Yai, Songkhla 90110, Thailand.
[3]Division of Virology and Serology, Department of Pathology, Faculty of Medicine, Prince of Songkla University, Hat Yai, Songkhla 90110, Thailand.

Abstract:

Objective: This study aimed to investigate the pharmacokinetic characteristics and molecular binding affinities of apigenin and luteolin toward both structural and non-structural proteins of dengue virus serotype 2, as well as selected host cell receptors implicated in viral attachment and entry.

Material and Methods: Molecular docking simulations were performed, using the SeamDock web server, to assess the binding affinity of the compounds with dengue viral proteins. The biological activities of the compounds were predicted using PASS Online. Pharmacokinetic properties; such as gastrointestinal absorption, skin permeation, blood–brain barrier penetration, cytochrome P450 interactions, bioavailability score and drug-likeness, using SwissADME. Additionally, toxicity predictions; including LD_{50} and organ-specific toxicity, were assessed using ProTox 3.0.

Results: Luteolin and apigenin exhibited strong antioxidants and anti-inflammatory properties, favorable pharmacokinetics and low predicted toxicity. Molecular docking showed that luteolin binds the DENV NS2B-NS3 protease with slightly stronger affinity (–7.74 kcal/mol) than apigenin (–7.67 kcal/mol), engaging allosteric sites. Additionally, both compounds demonstrated notable binding to the host C-type lectin receptor.

Conclusion: Apigenin and luteolin show strong potential as anti-dengue agents by targeting both the viral protease and host entry receptor. Their effective binding, along with favorable pharmacokinetics and low toxicity, supports further development as dual-action therapeutics.

Keywords: Apigenin, anti-dengue, Dengue serotype-2, Dengue virus, Flavonoids, Luteolin

One-Year Humoral Immunogenicity of the SARS-CoV-2 mRNA Vaccine Booster in Patients with Autoimmune Rheumatic Disease Receiving Immunosuppressants

Wuttirote Sangchayoswat, M.D., Siriporn Juthong M.D., Porntip Intapiboon M.D.*

[1]Department of Internal Medicine, Faculty of Medicine, Prince of Songkla University, Hat Yai, Songkhla 90110, Thailand.

Abstract:

Background: Patients with autoimmune rheumatic diseases (ARDs) receiving immunosuppressive therapy are a recognised high-risk group for severe COVID-19, and may show reduced responses to vaccination.

Objective: To evaluate the one-year humoral immunogenicity after a SARS-CoV-2 mRNA booster in immunosuppressed ARD patients, and to identify factors associated with non-responsiveness.

Material and Methods: In this prospective cross-sectional study, adult ARD patients at Songklanagarind Hospital having received a SARS-CoV-2 mRNA booster were evaluated for anti-RBD IgG levels one year post-vaccination, using a chemiluminescent immunoassay. The response was defined as: anti-RBD IgG ≥182 BAU/mL. Predictors of non-response were assessed using univariate and multivariate analyses.

Results: Among 51 patients, 68.6% were classified as responders, with significantly higher median anti-RBD IgG levels compared to non-responders (546.1 vs. 74.1 BAU/mL, p-value<0.001). Baseline characteristics and immunosuppressive regimens were generally comparable between groups. Non-responders more frequently received corticosteroids and azathioprine; whereas, the use of methotrexate was lower (15.4% vs. 48.4%, p-value=0.04). Methotrexate use was associated with a higher rate of vaccine response in univariate analysis (odds ratios [OR] 0.19, p-value=0.024), but not in multivariate analysis (OR 0.27, p-value=0.15).

Conclusion: Within one year after SARS-CoV-2 mRNA booster vaccination, some immunosuppressed ARD patients fail to achieve or maintain an adequate antibody response. Given their heightened vulnerability to severe COVID-19, routine booster vaccination remains an important consideration.

Keywords: immunogenicity, mRNA vaccine, booster, autoimmune rheumatic diseases, immunosuppressive therapy

Factors Predicting Ambulatory Status at Hospital Discharge After Fragility Hip Fracture Surgery: A Retrospective Cohort Study

Thitirut Jongutchariya, M.D.[1]*, Jittima Saengsuwan, M.D., Ph.D.[2], Palanthorn Loomcharoen, M.D.[1], Saowaluck Settheekul, R.N., Ph.D.[3]

[1]Department of Rehabilitation, Hatyai Hospital, Hat Yai, Songkhla 90110, Thailand.
[2]Department of Rehabilitation Medicine, Faculty of Medicine, Khon Kean University, Khon Kean 40002, Thailand.
[3]Independent Researcher, Chiang Mai 50300, Thailand.

Abstract:

Background: Hip fractures from low-energy trauma in older adults increase disability, mortality, and reduce quality of life. Discharge ambulation reflects early rehabilitation progress, underscoring the need to identify predictors of recovery.

Objective: To determine independent predictors of ambulation at hospital discharge, for patients undergoing hip fracture surgery.

Material and Methods: A retrospective review was conducted in patients aged ≥50 years, having undergone low-energy hip fracture surgery at Hatyai Hospital; from October 2018 until September 2023. Discharge ambulation was classified as: ambulatory (independent, with a gait aid) or non-ambulatory (bedridden or wheelchair-dependent). Preoperative, intraoperative, and postoperative variables; including process-of-care factors, were compared using Student's t-tests and Chi-square tests. Variables with more than 50.0% missing data were excluded. Univariable and multivariable regression analyses were performed to identify independent predictors of discharge ambulation.

Results: Among 532 patients (72.7% women, mean age 76.8±9.7 years), 314 (59.0%) were ambulatory at discharge. Positive predictors included: rehabilitation reaching ambulation-training level (mRR, 24.1; 95% confidence interval [CI], 9.14–63.6, p-value<0.001) and hip arthroplasty (mRR, 1.17, 95% CI, 1.07–1.29, p-value<0.001). Negative predictors were: history of stroke (mRR, 0.70, 95% CI, 0.53–0.91, p-value=0.007) and delayed rehabilitation beyond 72 hours postoperatively (mRR, 0.84, 95% CI, 0.73–0.97, p-value=0.014).

Conclusion: Early, ambulation-level rehabilitation and hip arthroplasty improved discharge mobility; whereas, stroke history and delayed rehabilitation reduced it. These findings emphasize the importance of timely, targeted rehabilitation to optimize functional recovery. Limitations of this study included: the retrospective, single-center design, reliance on EMRs, and unmeasured factors; such as nutrition, social support, and patient motivation. Outcomes were restricted to discharge ambulation, rather than long-term function. Future multi-center studies, with extended follow-up, using validated functional assessments are needed to better identify predictors of recovery after hip fracture surgery.

Keywords: ambulatory ability, hip fracture, predictive factors, older adults, surgery, walking

Transforming Leftover Skin Specimens into an Ex Vivo Skin Culture Platform for Medical Innovation Development

Phetploy Rungkamoltip, M.Sc.[1], Laliphat Kongpanichakul, M.D.[2], Orawan Chansanti, M.D.[2], Pasarat Khongkow, Ph.D.[1,3]*

[1]Department of Biomedical Sciences and Biomedical Engineering, Faculty of Medicine, Prince of Songkla University, Hat Yai, Songkhla 90110, Thailand.
[2]Division of Plastic Surgery, Department of Surgery, Faculty of Medicine, Prince of Songkla University, Hat Yai, Songkhla 90110, Thailand.
[3]Translational Medicine Research Center, Faculty of Medicine, Prince of Songkla University, Hat Yai, Songkhla 90110, Thailand.

Abstract:

Background: Skin irritation is a critical endpoint in the safety assessment of chemical and medical products prior to market release. While the OECD 439 epidermal reconstruction model is widely used for irritation testing, it lacks key physiological components that affect human absorption and real-life skin responses. To address this limitation, we propose an *ex vivo* skin culture model utilizing leftover human skin specimens, offering a more physiologically relevant platform.
Objective: This study aimed to develop and validate an *ex vivo* human skin culture platform to bridge the gap between conventional *in vitro* assays and *in vivo* applications, enhancing translational relevance in medical product testing.
Material and Methods: Leftover skin specimens from surgical procedures were cultured under optimized conditions. Skin viability and integrity were confirmed prior to testing. Topical applications of standard irritants were performed, followed by assessments of tissue viability, histological alterations, and cytokine secretion to evaluate post-treatment effects. The formulation was applied to both *ex vivo* and *in vivo* skin models to compare outcomes.
Results: The *ex vivo* skin tissues maintained structural integrity and cellular viability for up to 7 days in culture. According to the standard irritation performed, the model demonstrated damage consistent with GHS classification, which was validated by viability assays, histopathology, and pro-inflammatory cytokine expression. The *ex vivo* skin irritation results aligned with findings from the clinical single patch test, supporting the model's relevance for skin irritation assessment.
Conclusion: Leftover skin specimens from abdominoplasty provide a valuable, human-relevant platform for evaluating the safety of medical innovations. The *ex vivo* skin model showed strong correlation with clinical results and offers a cost-effective alternative to imported, reconstructed skin models. This approach adds value to surgical waste, while supporting localized, sustainable product testing.

Keywords: *ex vivo* skin model, leftover skin specimens, medical innovation, skin irritation, safety testing

The Association Between Bell's Palsy and Subsequent Diabetes Mellitus : A Retrospective Cohort Study

Suppanut Siriseth, M.D., Thammasin Ingviya, Ph.D, M.D., Pornchai Sathirapanya, M.D.*

Department of Internal Medicine, Faculty of Medicine, Prince of Songkla University, Hat Yai, Songkhla 90110, Thailand.

Abstract:

Background: Bell's palsy possibly associates with diabetes mellitus (DM). We investigated time to progression to diabetes (TTPD) among patients presenting solely with Bell's palsy.

Material and Methods: Non-diabetes patients presenting with Bell's palsy; from January 2007 to December 2017, were 1:1 age, gender, and presentation-date, were matched with the controls. We collected the results of HbA1C, fasting blood sugar (FBS), low-density lipoprotein (LDL) tested within one year as well as systolic/diastolic blood pressures (SBP/DBP), and body mass index (BMI) recorded within 3 months of the presentation. Time to progression to diabetes (TTPD) after the onset of Bell's palsy was estimated by Kaplan–Meier curves (log-rank test), and stratified Cox proportional-hazards were used with adjusting all the studied metabolic variables.

Results: A total of 351 patients presenting with Bell's palsy: 47% being male, were enrolled. The overall mean age was 53.9±12.1 years. Baseline HbA1C was 5.80±0.88% vs. 6.07±0.45%, p-value=0.090, and FBS was 97.3±10.1 vs. 95.3±9.0 mg/dL, p-value=0.056. Unadjusted cox analysis showed Bell's palsy shortened TTPD (HR 2.63; 95% confidence interval [CI] 1.59–4.35; p-value<0.001). Over the 19-year follow-ups, 5-, 10-, and 15-year diabetes incidences were: 6.4%, 16.8%, and 25.6% vs. 2.6%, 6.9%, and 10.7%, respectively (log-rank p-value<0.001). Bell's palsy patients with obesity (BMI >25 kg/m^2) had a significant shorter TTPD in the adjusted model (log-rank p-value<0.01).

Conclusion: Patients presenting with Bell's palsy had a significant shorter TTPD, independent of baseline cardiometabolic parameters. Long-term and regular surveillance of DM following the presentation of Bell's palsy is suggested.

Keywords: Bell's palsy, cardiometabolic risks, diabetes mellitus, progression

Impact of Invasive Coronary Angiography during Admission in the Elderly with NSTE-ACS

Hattaya Chutiphimon, M.D., Ply Chichareon, M.D, Ph.D.*

Department of Internal Medicine, Faculty of Medicine, Prince of Songkla University, Hat Yai, Songkhla 90110, Thailand.

Abstract:

Background: Whether an invasive treatment strategy (coronary angiography, with revascularization plus medical therapy) or a conservative strategy of medical therapy alone is more beneficial in elderly patients, with non–ST elevation acute coronary syndrome (NSTE-ACS), remains uncertain. Elderly patients often present with frailty and multiple comorbidities and are frequently excluded from clinical trials, leaving the benefits of invasive therapy unclear.

Objective: To assess the impact of invasive coronary angiography during admission in the elderly versus non-elderly patients with NSTE-ACS.

Material and Methods: This single-center retrospective observational cohort study included: patients diagnosed with NSTE-ACS at Songklanagarind Hospital; from January 1, 2010, until December 31, 2020. Patients were identified using ICD-10 codes and principal diagnoses. Exclusion criteria were: other types of myocardial infarction, in-hospital onset of NSTE-ACS and referral for angiography. Elderly patients were defined as aged ≥75 years, consistent with prior ACS trials. The primary outcome was 12-month all-cause mortality, analyzed using the Kaplan–Meier method and Cox regression. A two-sided p-value<0.05 was considered statistically significant. A total of 377 patients were included. Patients were categorized into four groups, based on age (<75 or ≥75 years) and treatment strategy (conservative or invasive): non-elderly–conservative (n=90), elderly–conservative (n=40), non-elderly–invasive (n=167) and elderly–invasive (n=71).

Results: Median ages were 64.4, 81.7, 62.8, and 81.4 years, respectively; 60.5% were male. 12-month all-cause mortality occurred in 63, 34, 54, and 139 patients, respectively. Compared with the non-elderly–conservative group, hazard ratios (HRs) were elderly–conservative: HR 1.36 (95% CI: 0.69–2.69, p-value=0.377); non-elderly–invasive: HR 0.32 (95% CI: 0.16–0.65; p-value=0.001); and elderly–invasive: HR 0.59 (95% CI: 0.28–1.27; p-value=0.180). Survival analysis demonstrated significant differences across groups (Peto–Peto test, p-value=0.0002). Composite secondary outcomes; including myocardial infarction, stroke, readmission and clinically significant bleeding, did not differ significantly among groups.

Conclusion: Invasive coronary angiography during admission was associated with reduced 12-month all-cause mortality in both elderly and non-elderly patients with NSTE-ACS, without a significant increase in major bleeding.

Keywords: elderly, invasive coronary angiography, NSTE-ACS

The Effect of Schroth Method Exercise on Preoperative Flexibility in AIS Surgical Candidates: A Randomized Controlled Trial

Yanin Tangjaroenpaisan, M.D.[1], Jitsupa Kittarakul, MPT[2], Weera Chaiyamongkol, M.D.[1]*

[1]Department of Orthopedics, Faculty of Medicine, Prince of Songkla University, Hat Yai, Songkhla 90110, Thailand.
[2]Department of Physical Therapy, Faculty of Medicine, Prince of Songkla University, Hat Yai, Songkhla 90110, Thailand.

Abstract:

Background: Adolescent idiopathic scoliosis (AIS) surgical candidates are characterized by a spinal curvature of 30–40 degrees or more. Patients typically face wait times of 6 months to 2 years for surgery, during which maintaining spinal flexibility is crucial for better surgical outcomes. Physiotherapeutic Scoliosis Specific Exercises (PSSE), utilizing the Schroth method, being a well-researched technique, has shown effectiveness in improving spinal flexibility; however, limited research remains on the effects of these exercises for more severe curvatures.

Objective: This study aimed to compare the curve flexibility after the Schroth method exercise and traditional exercise in AIS surgical candidates.

Material and Methods: A randomized controlled trial was conducted; involving 21 AIS patients having a Cobb angle of 40 degrees or greater. Patients were randomly allocated into two groups: Schroth method exercise group and control group. The Schroth method exercise group received supervised training and individualized home programs, with 2–3 in-hospital sessions per month and home exercises 3–5 days a week. The control group engaged in traditional exercise training; including stretching and core muscle training, with at least one in-hospital session in the first month and subsequent home exercises 3–5 days a week. Main curve flexibility index was assessed along with Cobb angle, ATR and quality of life, using Thai SRS-22 questionnaire at 3 and 6 months.

Results: In total, 21 patients were included in the study (11 in the Schroth method exercise group: 10 in the control group). The Schroth method exercise group maintained a stable main curve flexibility index from the beginning of the study (51.60±14.13) to 6 months post intervention (53.54±18.46). On the contrary, the control group demonstrated a significant decline in main curve flexibility index: from 43.87±20.34 to 36.09±16.88 (p-value 0.032). The Schroth method exercise group also showed an improvement in quality of life, based on the SRS-22 scores (from 3.757±0.395 to 3.843±0.393: p-value 0.023), while no significant change was observed for the control group (p-value 0.529). No significant change in Cobb angle and trunk rotation was observed throughout the study for both groups.

Conclusion: In this randomized controlled trial, the Schroth method exercise was superior to traditional exercise regimens in its ability to preserve spinal mobility in AIS surgical candidates, and led to significant improvements in SRS-22 scores.

Keywords: adolescent idiopathic scoliosis, ais, physiotherapeutic scoliosis specific exercise, schroth method exercise

Association of in Hospital Guideline-Directed Medical Treatment Scores and Mortality in Post-Myocardial Infarction Patients with LV Dysfunction: A Single-Center Retrospective Study

Knokpit Wattanapaiboon[1], Thammarak Songsangjinda[2], Ply Chicharoen[2]*

[1]Department of Internal Medicine, Faculty of Medicine, Prince of Songkla University, Hat Yai, Songkhla 90110, Thailand.
[2]Cardiology unit, Department of Internal Medicine, Faculty of Medicine, Prince of Songkla University, Hat Yai, Songkhla 90110, Thailand.

Abstract:

Background: Myocardial infarction (MI) remains a leading cause of heart failure, with reduced ejection fraction (HFrEF). Guideline-directed medical therapy (GDMT) is proven effective in such populations and increasingly being applied early in post-MI care. A GDMT scoring method has been proposed for guiding the initiation of GDMTs in HFrEF. However, the application of this score has not been tested in post-MI populations.

Objective: To evaluate the prognostic impact of GDMT scores before discharge in MI patients with left ventricular dysfunction.

Material and Methods: A single-center, retrospective study was conducted; from April 2016 to December 2024. Patients with acute myocardial infarction treated with percutaneous coronary intervention (PCI) and having initial left ventricular ejection fraction (LVEF<40%), without in-hospital mortality, were included. GDMT scores were calculated based on the dosage of four medication classes at the time of discharge from index PCI admission: ranging from 0-9. The higher scores indicated more usage of GDMT. Mortality data was reviewed using electronic medical records. The associations between GDMT score and all-cause mortality were evaluated using time-to-event analysis.

Results: From 602 MI patients screened, 225 met inclusion criteria. The mean age was 60.8±12.6 years and 84% were males. The majority of the patients (65%) were classified into Killip class I. The average LVEF was 31.9±7.4%. Patients that received at least one GDMT class accounted for 85.8%. The median GDMT score was 1 (interquartile range 1-2). Total GDMT score was not associated with all-cause mortality (Hazard ratio [HR] 0.84, 95% confidence interval [CI] 0.65-1.09). However, the initiation of angiotensin converting enzyme inhibitor/angiotensin receptor blockers or beta blockers was independently associated with lower mortality (HR 0.52, 95% CI 0.31-0.89; and HR 0.56, 95% CI 0.33-0.95) after being adjusted for age: LVEF, creatinine, and Killip class.

Conclusion: GDMT score at the time of discharge was not associated with all-cause mortality in post MI patient with LV dysfunction. However, in-hospital implementation of ACEI/ARB and BB remains beneficial. The results of this study support the benefit of some GDMT classes over emphasizing the need for a more tailored score in this specific population.

Keywords: guideline directed medical therapy score, left ventricular dysfunction, myocardial infarction

Glucocorticoid-Induced Hyperglycemia in Hospitalized Non-Diabetic Patients: A Retrospective Cohort Study

Ruamporn Kansawai M.D., Padiporn Limumpornpetch M.D., Ph.D., Siriporn Juthong M.D.*

Department of Internal Medicine, Faculty of Medicine, Prince of Songkla University, Hat Yai, Songkhla 90110, Thailand.

Abstract:

Background: The impact of systemic glucocorticoid therapy on blood glucose fluctuations in hospitalized patients without preexisting diabetes remains unclear.

Objective: To explore the trend of blood glucose elevation above 180 mg/dL, following the first dose of systemic glucocorticoids in adult non-diabetic inpatients.

Material and Methods: This retrospective cohort study included: adult patients (≥18 years) without a prior diagnosis of diabetes mellitus having newly started glucocorticoid therapy during hospital admission. Clinical and potential factors were investigated; including glucocorticoid dose (prednisolone-equivalent: <30 mg, 30-60, 60–125 mg, 125–320 mg, >320 mg), glucocorticoid type and underlying disease indication for treatment. The primary outcome was factor associated with time to occurrence of blood glucose (DTX) >180 mg/dL (hyperglycemia) following first dose of glucocorticoid administration.

Results: A total of 1,400 patients were included. The median time for first hyperglycemia was 3.48 days. The most common indication for glucocorticoid therapy were: infections (305 patients, 22%), inflammatory diseases (293 patients, 21%) and cancer (202 patients, 14%). From multivariable Cox regression analysis, compared to dexamethasone; methylprednisolone was significantly associated with higher rates of hyperglycemia, with a HR of 1.54 (1.13–2.09). Prednisolone and hydrocortisone showed no significant effect (p-value=0.4 and 0.9, respectively). A dose-dependent response of glucocorticoid was also observed, with HR of 1.60, 2.06, 2.49 and 2.92 for doses over 30, 60, 125 and a 320 mg of prednisolone equivalent dose, respectively.

Conclusion: Systemic glucocorticoids are commonly administered in hospitalized patients and frequently lead to hyperglycemia. Within four days of initiation, blood glucose levels frequently exceed 180 mg/dL, with a clear dose-dependent effect. Awareness of this risk is crucial for early glucose monitoring and management in non-diabetic inpatients receiving glucocorticoids.

Keywords: glucocorticoids, glucocorticoid-induced hyperglycemia

Hematopoietic Stem Cell-Derived Natural Killer Cells: A Potential Alternative Cell Source for Cancer Immunotherapy

Suppanut Komjakraphan[1], Poonnattha Anantasaeree[1], Kajornkiat Maneechai[2,3], Panarat Noiperm[1,2,3], Watsamon Uraiwan[1,2,3], Jakrawadee Julamanee[1,2,3]*

[1]Hematology Unit, Department of Internal Medicine, Faculty of Medicine, Prince of Songkla University, Hat Yai, Songkhla 90110, Thailand.

[2]Stem Cell Transplantation and Cellular Therapy Excellence Center, Songklanagarind Hospital, Prince of Songkla University, Hat Yai, Songkhla 90110, Thailand.

[3]Thailand Hub of Talents in Cancer Immunotherapy (TTCI), Pathumwan, Bangkok 10330, Thailand.

Abstract:

Background: Adoptive cell therapies, particularly CD19CAR-T cells, have demonstrated significant efficacy in the treatment of B-cell hematologic malignancies. However, broader use is limited by T-cell exhaustion, immune dysfunction and insufficient functional T cells for manufacturing. Natural killer (NK) cells have gained attention due to their ability to mediate cytotoxicity independent of MHC recognition, and their favorable safety profile. Despite these advantages, the clinical translation of peripheral blood-derived NK (PB-NK) cells has been limited by inconsistent expansion potential and functional variability. In contrast, hematopoietic stem cell-derived NK (HSC-NK) cells offer a more uniform and scalable source for NK cell production.

Objective: To develop a protocol for HSC-NK generation and evaluate their phenotypic and functional characteristics compared to PB-NK.

Material and Methods: Leftover peripheral blood stem cells (PBSCs), from transplant donors, were used to isolate $CD34^+$ HSCs and $CD56^+$ PB-NK cells. $CD34^+$ cells underwent a 28-day two-step differentiation protocol (StemSpan™) to generate HSC-NK cells. PB-NK cells were frozen down for later downstream experiments. Both NK populations were then further expanded for seven days with IL-12, IL-15, IL-18, and γ-irradiated EBV-LCL feeder cells. NK cell phenotypes and functions were assessed.

Results: $CD34^+$ and $CD56^+$ cells were purified from HSCs at 92.12% and 83.49%, respectively. HSC-NKs were successfully generated with an expansion fold of 432 by day 28. CD56 expression was similar in both groups, while CD16 and CD94 were higher in PB-NKs. HSC-NKs exhibited higher activating receptor, NKp44, and lower inhibitory receptors; such as NKG2A and KIR2DL, compared to PB-NKs. Moreover, CD62L-differentiation and TRAIL-mediated signaling markers were more prominent on HSC-NKs. Functionally, HSC-NKs showed increased CD69 activation and comparable CD107a, granzyme B, and TNF-α expression. Cytotoxicity assays suggested enhanced anti-tumor activity in HSC-NKs.

Conclusion: HSC-NKs can be efficiently generated and expanded, with preserved functional activity and favorable phenotypes, supporting the potential off-the-shelf cancer immunotherapy.

Keywords: adoptive immunotherapy, HSC-NK cells, NK cell expansion

Normal Reference Range of Skeletal Muscles in a Healthy Thai Population

Samittha Fueangfupong, M.D.[1], Kittithat Taemkaew M.D.[2]*

[1]Department of Internal Medicine, Faculty of Medicine, Prince of Songkla University, Hat Yai, Songkhla 90110, Thailand.
[2]Division of Clinical Nutrition and Obesity Medicine, Department of Internal Medicine, Prince of Songkla University, Hat Yai, Songkhla 90110, Thailand.

Abstract:

Background: Skeletal muscle mass (SMM) is critical for mobility, metabolic function, and quality of life. Despite its clinical relevance, reference values for skeletal muscle mass in the Thai population are not well established.

Objective: To determine normative values for skeletal muscle mass in healthy Thai adults and identify factors associated with low SMM.

Material and Methods: This retrospective observational study analyzed 561 eligible subjects, aged 20–60 years, having undergone body composition assessment via bioelectrical impedance analysis (BIA); between June 2022 and June 2023, at Songklanagarind Hospital. Data were extracted from 5,720 records, of which 1,647 met initial inclusion criteria. After removing 1,085 duplicate or inconsistent entries, 561 records were used for analysis. Baseline characteristics and Skeletal Muscle Index (SMI) were compared by gender. Multivariate logistic regression identified predictors of low SMM.

Results: Participants had a median age of 46 years for males and 49 years for females (p-value=0.002). Median SMI was significantly higher in males [10.3 kg/m^2 (IQR: 9.7–10.9)] than in females [8.2 kg/m^2 (IQR: 7.7–8.8), p-value<0.001]. Multivariate analysis identified BMI and fat-free mass as independent predictors of SMI (p-value<0.001). Gender and age group also showed significant differences in muscle distribution.

Conclusion: This study provides the first BIA-based reference values for skeletal muscle mass in healthy Thai adults. These findings will support sarcopenia screening and inform population-specific clinical guidelines for muscle health in Thailand.

Keywords: bioelectrical impedance analysis, muscle, reference values, sarcopenia, skeletal

Lung Injury and Subclinical Respiratory Symptoms among Young Chinese Vapers: Evidence from Symptom Screening and Pulmonary Function Tests

Chunxia He[1], Rassamee Chotipanvithayakul[1]*, Yongxia Li[2], Virasakdi Chongsuvivatwong[1]

[1]Department of Epidemiology, Faculty of Medicine, Prince of Songkla University, Hat Yai, Songkhla 90110, Thailand.
[2]Department of Respiratory Medicine, Hospital of Kunming Medical University, Yunnan 650101, China.

Abstract:

Background: Electronic cigarettes contain nicotine and other toxic substances. There has been an increase in vaping from 68 million in 2020 to 82 million in 2021, worldwide: especially among the young population. The industries claimed vaping is less harmful than smoking; however, some health consequences may be underreported.

Objective: This study examined the effects of vaping and smoking on respiratory symptoms and lung function.

Material and Methods: This study recruited healthy volunteers, aged 18–44 years, whom were free from underlying diseases. The American Thoracic Society Questions (ATSQ) were used to screen for respiratory symptoms. Subsequently, a lung function test (LFT) was performed. ATSQ scores were analyzed by one-way ANOVA. Principal component analysis (PCA) was used to classify lung function parameters, and a linear regression was used to assess the effects of vaping on lung function.

Results: A total of 83 volunteers (36 females, 47 males; mean age 29.1±6.0 years) were recruited and classified as never smoking or vaping (n=27) as a control group, smoking only (n=24), vaping only (n=12), and dual users (n=20). The dual groups reported higher average scores for shortness of breath while walking (2.0) and overall ATSQ scores (16.2) compared to the control group (1.3 and 12.4). The PCA revealed two primary components of LFT: labeled as large and small airway obstructions. Linear regression showed that the vaping-only group had significantly lower function of the small airway than the control group (β=-0.83, 95% confidence interval: -1.56 to -0.10, p-value=0.026).

Conclusion: Our study highlights hidden lung injury among vapers, although they reported lower symptoms than cigarette smokers and dual smokers. This subclinical manifestation should be assessed and addressed among electronic cigarette vapers, health personnel and policymakers.

Keywords: cigarette, electronic cigarette, lung function test, respiratory symptoms

Retrospective Cohort Study on Clinical Outcomes in Endogenous Cushing's Syndrome in Songklanagarind Hospital (Pilot Study Prepared for A Multi-Center in Thailand)

Tawan Limamornrat, M.D., Padiporn Limumpornpetch, M.D.*

Department of Internal Medicine, Faculty of Medicine, Prince of Songkla University, Hat Yai, Songkhla 90110, Thailand.

Abstract:

Background: Endogenous Cushing's syndrome (CS) is a rare but serious endocrine disorder, associated with substantial morbidity and mortality. Global studies have reported elevated standardized mortality ratios (SMRs) and identified cardiovascular disease as the leading cause of death in CS. However, data from Southeast Asian populations; particularly in Thailand, remains limited. Given potential differences in genetics, healthcare systems, infectious ecology and environmental factors, region-specific investigations are warranted.

Objective: This study aimed to evaluate standardized mortality ratio (SMR) and all-cause mortality in patients with CS and its subtypes treated at Songklanagarind Hospital; from 2005 until 2024.

Material and Methods: Demographic data, comorbidities, and CS subtypes were retrospectively collected. A total of 89 patients diagnosed with CS were included in the survival analysis. The median follow-up period was 16.1 years. Survival outcomes across CS subtypes were evaluated using Kaplan–Meier analysis. Multivariable Cox regression was performed, with pituitary-dependent CS as the reference group to assess relative risks of mortality.

Results: Among the 89 patients, 16 deaths occurred during follow-up. Kaplan–Meier analysis revealed significant differences in survival among CS subtypes. Patients with pituitary-dependent CS demonstrated the most favorable prognosis, with no deaths recorded during follow-up. In contrast, patients with adrenocortical carcinoma-associated CS (ACC-CS) exhibited the poorest outcomes, showing a steep decline in survival probability within the first two years. Cox regression analysis confirmed that ACC-CS carried a significantly higher risk of death compared with pituitary CS (Hazard Ratio [HR] 28.69; 95% CI: 6.95–118.40; p-value<0.001).

Conclusion: Survival outcomes in CS vary substantially by subtype. Pituitary-dependent CS demonstrated an excellent long-term prognosis, with no observed mortality; whereas, ACC-CS and ectopic/other ACTH-dependent CS were associated with markedly reduced survival: especially within the first two years after diagnosis. These findings highlight the importance of early recognition, subtype-specific management, and region-specific data to improve outcomes in Southeast Asian populations.

Keywords: cause of death, Cushing's syndrome, mortality, standardized mortality ratio

Adrenal Tumor Spectrum and Surgical Indications: A 10-Year Retrospective Study from Southern Thailand

Auttawut Chalermwuttanon, M.D.[1], Supamai Soonthornpun, M.D.[1], Pramot Thanutit, M.D.[2], Teeravut Tabtawee, M.D.[2], Srila Samphao, M.D.[3], Wongsakorn Chaochankit, M.D.[3], Pattira Boonsri, M.D.[2], Seechad Noonpradej, M.D.[3], Sarayut Lucirn Geater, M.D.[1], Somrit Mahattanobon, M.D.[3], Onnicha Suntornlohanakul, M.D.[1], Padiporn Limumpornpetch, M.D., Ph.D.[1]*

[1]Division of Internal Medicine, Faculty of Medicine, Prince of Songkla University, Hat Yai, Songkhla 90110, Thailand.
[2]Division of Radiology, Faculty of Medicine, Prince of Songkla University, Hat Yai, Songkhla 90110, Thailand.
[3]Division of Surgery, Faculty of Medicine, Prince of Songkla University, Hat Yai, Songkhla 90110, Thailand.

Abstract:

Background: Adrenal tumors encompass a broad range of clinical entities; including benign non-functioning adenomas, hormonally active lesions and malignant tumors. With improved access to imaging, adrenal incidentalomas (AIs) are being increasingly detected; often in asymptomatic patients. Despite advances in endocrine diagnostics, challenges remain in clinical decision-making regarding which adrenal tumors warrant surgical intervention.

Objective: This study aimed to review the clinical, demographic, and histopathological characteristics of patients having undergone tissue biopsies or adrenalectomy at a tertiary academic center over the past decade.

Material and Methods: A retrospective review was conducted at Prince of Songkla University Hospital; including adult patients aged 18 years and older having undergone adrenalectomy; from 2014 until 2023. Data collected included: age, gender, body mass index (BMI), hormonal function, presenting symptoms, imaging reports and histopathological diagnosis;

Results: A total of 355 adrenalectomy cases were included. The mean age was 52.2 years (range 18–89), with a female predominance (62%). The average BMI was 24.8 kg/m^2. Primary aldosteronism was the most common indication for surgery (41.1%), followed by adrenal incidentaloma (27.6%), Cushing's syndrome (13.2%) and pheochromocytoma (11.0%). Histopathologic findings included: benign cortical adenomas (59.4%), pheochromocytomas (13.5%), myelolipomas (4.5%), adrenocortical carcinomas (3.9%) and metastatic lesions (2.5%).

Conclusion: This 10-year review provides an updated landscape of adrenal pathology in Southern Thailand. The predominance of benign lesions and functional tumors highlights the need for accurate clinical stratification. Future studies should focus on predictive models, molecular profiling and long-term outcomes, so as to improve risk-based surgical decision-making and personalised management of adrenal tumors.

Keywords: adrenalectomy, adrenal tumor, adrenal incidentaloma, endocrine surgery, pathology, retrospective study

Predictors of Unfavorable Outcomes of In-Hospital Acute Ischemic Stroke: A Retrospective Case-Control Study

Natthapong Chuaipitak, M.D.[1], Pornchai Sathirapanya, M.D.[2], Chanon Kongkamol M.D., Ph.D.[3]*

[1]Division of Internal Medicine, Faculty of Medicine, Prince of Songkla University, Hat Yai, Songkhla 90110, Thailand.
[2]Neurology Unit, Division of Internal Medicine, Faculty of Medicine, Prince of Songkla University, Hat Yai, Songkhla 90110, Thailand.
[3]Department of Family Medicine and Preventive Medicine, Faculty of Medicine, Prince of Songkla University, Hat Yai, Songkhla 90110, Thailand.

Abstract:

Background: In-hospital stroke (IHS) is associated with higher morbidity and mortality than community-onset stroke (COS). Validated predictors of the outcomes of HIS remain limited.

Objective: We aimed to evaluate the potential predictors for unfavorable outcomes in in-hospital acute ischemic stroke (IHAIS).

Material and Methods: This retrospective case-control study included: patients with IHAIS in Songklanagarind Hospital, a tertiary care university hospital in Thailand; from January 2011 and December 2024. The diagnosis of IHAIS was confirmed by clinical evaluation and neuroimaging (CT or MRI). Patients associated with cardiovascular peri-operative strokes, hemorrhagic strokes, or advanced malignancy were excluded. Clinical data extracted from the electronic medical records system were: demographics, cause of hospitalization, comorbidities, stroke severity scores (NIHSS), Glasgow coma scale (GCS), time of diagnosis; brain imaging, neurovascular interventions (NVIs) and stroke etiology and complications. The IHAIS outcome, evaluated at 30 days after stroke onset or discharge, was considered unfavorable if the modified Rankin Scale score (mRS) was 3–6. Univariate and multivariate Cox regression analyses were performed to identify independent predictors, adjusting for age, gender and pre-stroke mRS.

Results: Among 376 IHS patients initially enrolled, 110 IHAIS patients (71 with unfavorable outcomes) were analyzed. Baseline characteristics, comorbidities, and vascular risk factors were similar between groups. The significant predictors for unfavorable outcomes were: older age (HR=1.0, 95% confidence interval [CI] 1.0–1.0, p-value=0.005), higher initial NIHSS score (HR=0.91, 95% CI 0.88–0.95, p-value<0.001), stroke of other determined etiology (SOD) (HR=2.9, 95% CI 1.4–6.2, p-value=0.006) and receiving NVIs (HR=16, 95% CI 5.7–43, p-value<0.001).

Conclusion: Higher NIHSS, older age, SOD and receiving NVIs were significant predictors of unfavorable outcome in IHAIS. Targeted strategies are needed to improve the outcomes of these high-risk patients.

Keywords: acute ischemic stroke, in-hospital stroke, predictors, prognosis outcomes

Heart Failure Prognostication from Guideline-Directed Medical Therapy

Chonlanat Puetpaiboon, M.D., Thanapon Nilmoje, M.D.*

Department of Internal Medicine, Faculty of Medicine, Prince of Songkla University, Hat Yai, Songkhla 90110, Thailand.

Abstract:

Background: Heart failure, with reduced ejection fraction (HFrEF), is a prevalent syndrome in Southeast Asia, Currently, guideline-directed medical therapy (GDMT) remains the cornerstone of treatment to reduce mortality and morbidity. However, the implementation of GDMT in real-world practice is often suboptimal, due to patient-related factors, clinician concerns and systemic barriers. The GDMT score, developed to quantify the adequacy of medication prescription, may serve as a prognostic marker in HFrEF; though its predictive value is underexplored.

Objective: This study aimed to evaluate whether the GDMT score at hospital discharge predicts 1-year all-cause mortality and worsening heart failure events in patients with HFrEF.

Material and Methods: A retrospective cohort study was conducted at Songklanagarind Hospital; from 2015 and 2023. Adults with left ventricular ejection fraction (LVEF) <40% discharged alive were eligible. Patients with in-hospital death, active malignancy, CKD stage V refusing renal replacement therapy, cirrhosis Child-Pugh C, or incomplete follow-up were excluded. Demographics, comorbidities, and GDMT prescriptions at discharge were collected. The primary outcome was a composite of 1-year all-cause mortality and worsening heart failure events. Associations between GDMT score and outcomes were analyzed using multivariable logistic regression and Cox proportional hazards models; adjusted for confounders.

Results: Deom 1,024 screened patients, 216 met inclusion criteria. During 1-year follow-up, 79 patients (36%) experienced the composite outcome; including 18 deaths (8.3%). Higher GDMT scores were significantly associated with reduced risk of adverse outcomes (HR 0.76, 95% confidence interval [CI]: 0.66–0.87, p-value<0.001). Predictive performance was modest, with an area under the curve (AUC) of 0.665.

Conclusion: The GDMT score at hospital discharge is independently associated with reduced 1-year mortality and heart failure worsening events in patients with HFrEF. These findings support its potential role in risk stratification and therapeutic goal setting, highlighting the importance of optimizing GDMT in routine clinical practice.

Keywords: heart failure with reduced ejection fraction, guideline-directed medical therapy, GDMT score

Prevalence and Risk Factors of Acute Pancreatitis in Childhood Acute Leukemia

Kamonluk Thepuatrakul, M.D.[1], Atchariya Chanpong, M.D., Ph.D.[2], Natsaruth Songthawee, M.D.[3], Pornpun Sripornsawan, M.D.[3], Sirinthip Kittivisuit, M.D.[1], Hansa Sriphongphankul, M.D.[2], Thirachit Chotsampancharoen, M.D.[3]*

[1]Department of Pediatrics, Faculty of Medicine, Prince of Songkla University, Hat Yai, Songkhla 90110, Thailand.
[2]Division of Gastroenterology and Hepatology, Department of Pediatrics, Faculty of Medicine, Prince of Songkla University, Hat Yai, Songkhla 90110, Thailand.
[3]Division of Hematology and Oncology, Department of Pediatrics, Faculty of Medicine, Prince of Songkla University, Hat Yai, Songkhla 90110, Thailand.

Abstract:

Background: Acute pancreatitis (AP) is an uncommon but serious complication in children undergoing treatment for acute leukemia. Determining its prevalence, associated risk factors, and its impact on treatment outcomes is essential for timely diagnosis and optimal management.

Objective: To determine the prevalence of AP in pediatric patients with acute leukemia, identify associated risk factors, and assess its effect on treatment outcomes and overall survival.

Material and Methods: We retrospectively reviewed medical records of children under 15 with acute leukemia, presenting with abdominal pain suggestive of AP at Songklanagarind Hospital; from 2004 to 2024. Demographic data; including leukemia subtypes, treatment protocols and clinical outcomes, were compared between patients with and without AP. Statistical analyses were performed using R program.

Results: Among 560 leukemia patients, 49 presented with abdominal pain; 11 were diagnosed with AP (prevalence 1.9%). Baseline age and gender were significantly different between the groups. AP occurred more often in patients with T-cell ALL (27.3% vs. 13.2%; p-value=0.09), and in those receiving high-intensity protocols (81.8% vs. 31.8%; p-value=0.04). Logistic regression suggested decreased risk in B-cell ALL (OR 0.56; 95% CI 0.10–3.21). AP patients had shorter pain duration before diagnosis (median 1 vs. 2 days; p-value=0.029) and more frequent imaging (100% vs. 55.3%; p-value=0.009). They required prolonged fasting periods (median 5 vs. 0 days; p-value<0.001) and greater intravenous fluid volumes within 48 hours (median 5541 vs. 3249 mL; p-value=0.028). Mortality was markedly higher in the AP group (80% vs. 13%; risk ratio 2.9; 95% CI 1.09–7.62).

Conclusion: Although the prevalence of AP among pediatric leukemia patients is low, it is strongly associated with increased mortality. High- and very-high-risk protocols are associated with AP. A trend toward higher risk was observed among patients with T-cell ALL. Larger studies are warranted to refine risk stratification and guide preventive strategies.

Keywords: children, leukemia, pancreatitis

Associations of Weight Reduction with Respiratory Function and Gas Exchange in Obesity Hypoventilation Syndrome: A Retrospective Study

Tawatchai Piathong, M.D.[1], Chaitong Churuangsuk, M.D., Ph.D.[2], Pattaraporn Panyarath, M.D.[3] , Sarayut Lucien Geater, M.D., Ph.D.[3]*

[1]Department of Internal Medicine, Faculty of Medicine, Prince of Songkla University, Hat Yai, Songkhla 90110, Thailand.
[2]Clinical Nutrition and Obesity Medicine Unit, Department of Internal Medicine, Faculty of Medicine, Prince of Songkla University, Hat Yai, Songkhla 90110, Thailand.
[3]Respiratory and Respiratory Critical Care Unit, Department of Internal Medicine, Faculty of Medicine, Prince of Songkla University, Hat Yai, Songkhla 90110, Thailand.

Abstract:

Background: Obesity hypoventilation syndrome (OHS) is characterized by obesity and chronic daytime hypercapnia, leading to impaired gas exchange and increased morbidity. While weight reduction is a recommended intervention, evidence in real-world clinical settings remains limited; particularly among the Thai population, as is the improvement in weight reduction intensity for achieve respiratory effect.

Objective: To assess the impact of weight reduction on arterial blood gas parameters in patients with OHS over a one-year period.

Material and Methods: This retrospective study analyzed 30 eligible subjects that met the inclusion criteria: adult patients with OHS treated at Songklanagarind Hospital; from 2010 to 2024. Pre- and post-weight reduction data were extracted from electronic records. Variables included: BMI, body weight, $PaCO_2$, PaO_2, pH, HCO_3^-, and SpO_2. Paired t-tests and Wilcoxon signed-rank tests were used as appropriate.

Results: Thirty patients (mean age 56.7±17.3 years; baseline weight 117.4±31.1 kg and BMI 47.7±9.8) were analyzed. At baseline, mean SpO_2 was 85.4±8.3%, $PaCO_2$ 55.4±10.0 mmHg, PaO_2 55.8±11.8 mmHg and pH 7.40±0.10 . After one year of weight reduction (mean weight loss 15.9±5 kg, p-value<0.05), $PaCO_2$ decreased by 10.87 (mmHg) (p-value<0.05); PaO_2 increased by 10.08 (mmHg) (p-value<0.05); pH remained stable (0.01); and SaO_2 improved by 4.99% (p-value<0.05).

Conclusion: Weight reduction in patients with OHS was significantly associated with improvements in gas exchange; including lower $PaCO_2$ and higher PaO_2 and SpO_2, as well as reduced bicarbonate retention. These findings support structured weight loss as a cornerstone therapy in OHS management, and suggests potential for improved respiratory physiology with modest weight reduction.

Keywords: gas exchange, obesity hypoventilation syndrome, retrospective study, weight reduction

Prognostic Implications of Circulating Cell-Free DNA Concentration and Somatic Mutation Profiling in Advanced Prostate Cancer

Sarawut Chamnina[1], Natakorn Nokchan[1,2], Tanan Bejrananda[3], Sarayuth Boonchai[3], Wichien Sirithanaphol[4], Apinya Jusakul[5], Akara Amantakul[6], Thiraphat Saengmearnuparp[6], Jarin Chindaprasirt[7], Pongsakorn Choochuen[1,2], Rassanee Bissanum[1,2], Pasarat Khongkow[1,2]

[1]Department of Biomedical Sciences and Biomedical Engineering, Faculty of Medicine, Prince of Songkla University, Hat Yai, Songkhla 90110, Thailand.
[2]Translational Medicine Research Center, Faculty of Medicine, Prince of Songkla University, Hat Yai, Songkhla 90110, Thailand.
[3]Urology Unit, Department of Surgery, Faculty of Medicine, Prince of Songkla University, Hat Yai, Songkhla 90110, Thailand.
[4]Division of Urology, Department of Surgery, Faculty of Medicine, Khon Kaen University, Khon Kaen 40002, Thailand.
[5]Department of Clinical Immunology and Transfusion Sciences, Faculty of Associated Medical Sciences, Khon Kaen University, Khon Kaen 40002, Thailand.
[6]Division of Urology, Department of Surgery, Faculty of Medicine, Chiang Mai University, Chiang Mai 50200, Thailand.
[7]Division of Oncology, Department of Medicine, Faculty of Medicine, Khon Kaen University, Khon Kaen 40002, Thailand.

Abstract:

Background: Prostate cancer remains one of the most prevalent malignancies worldwide. Advanced prostate cancer (APC) poses two major clinical challenges: repeated tissue biopsies are often unsuitable, and prostate-specific antigens (PSA) lack disease specificity and prognostic accuracy. These limitations highlight the need for reliable and minimally invasive biomarkers to improve disease stratification. Circulating cell-free DNA (cfDNA), released into the bloodstream by apoptotic or necrotic cells, represents a promising tool for prognostic assessment.

Objective: This study investigated the prognostic utility of cfDNA through two approaches: (1) quantification of cfDNA concentration and (2) somatic mutation profiling.

Material and Methods: A total of 69 plasma samples were analyzed; including non-tumor individuals (NT), castration-sensitive prostate cancer (CSPC), and castration-resistant prostate cancer (CRPC). Total cfDNA concentration was quantified using a TapeStation-based electrophoresis assay. Logistic regression and receiver operating characteristic (ROC) analyses were performed to evaluate associations between cfDNA levels and disease status. Additionally, targeted next-generation sequencing (NGS) was conducted on cfDNA from 25 APC patients to identify recurrent somatic mutations.

Results: Total cfDNA concentration was significantly higher in CRPC compared with NT, although differences among other groups were not statistically significant. Logistic regression revealed increased odds of CRPC with rising cfDNA concentration. ROC analysis demonstrated robust predictive capability, with an area under the curve (AUC) exceeding 0.80. Targeted sequencing identified recurrent mutations in DNA repair genes (BRCA2, ATM) and members of the lysine methyltransferase family, which regulate chromatin structure. These alterations are consistent with prior studies linking them to treatment resistance, poor prognosis and aggressive disease behavior.

Conclusion: Both cfDNA concentration and somatic mutation analysis provide complementary prognostic insights in APC. Elevated cfDNA levels distinguish CRPC from non-tumor individuals, while NGS-based mutation profiling highlights clinically relevant genomic alterations. Together, these approaches establish a translational framework for cfDNA-based molecular stratification and biomarker development in advanced prostate cancer.

Keywords: advanced prostate cancer, circulating cell-free DNA, prognostic biomarker, somatic mutation

Survival Outcomes in Advanced Stage Cancer Patients: A Retrospective Study on the Impact of Consultation Approaches in Palliative Care

Tanyalak Sanphiboon, M.D.[1], Orapan Fumaneeshoat, M.D.[1], Thammasin Ingviya, M.D., Ph.D.[2]*

[1]Department of Family Medicine and Preventive Medicine, Faculty of Medicine, Prince of Songkla University, Hat Yai, Songkhla 90110, Thailand.

[2]Department of Clinical Research and Medical Data Sciences, Faculty of Medicine, Prince of Songkla University, Hat Yai, Songkhla 90110, Thailand.

Abstract:

Background: The rising global cancer burden has increased the need for palliative care to manage symptoms and quality of life. Previous studies have shown that integrating palliative care may prolong survival through uncertain mechanisms. Although integration has demonstrated positive outcomes, access remains limited in many low- and middle-income countries; including Thailand. To address workforce shortages, both physician-led and nurse-led consultation models are used.

Objective: To compare overall survival between physician-led and nurse-led palliative care teams, and evaluate pain control in advanced-stage cancer patients.

Material and Methods: This retrospective cohort included adults with advanced-stage cancer treated at a tertiary hospital; from 2020 to 2024. Kaplan–Meier estimates and Cox regression assessed survival. pain scores were analyzed using linear mixed-effects models. Propensity score matching reduced baseline imbalances.

Results: From 26,779 patients, 281 consulted patients were matched to 1,343 non-consulted patients, with balanced characteristics. Five-year overall survival was significantly longer in the non-consultation group (median 28.4 vs. 13.2 months; HR 0.58, 95% confidence interval [CI]: 0.51–0.66; p-value<0.001). Among those having received palliative care, survival did not differ significantly between physician-led and nurse-led teams when measured from diagnosis (HR 0.98, 95% CI: 0.68–1.40) or from consultation (HR 0.92, 95% CI: 0.65–1.30). Subgroup analysis showed no difference in early or late consultation, though late referrals had better survival with physician-led teams (HR 0.79, 95% CI: 0.51–1.23, p-value=0.296). Pain scores stayed low and stable, with no significant difference between teams.

Conclusion: Shorter survival in the consultation group likely reflects more advanced disease at referral. Physician-led teams may benefit from complex, late referrals, while nurse-led teams could manage less complex cases; especially where specialists are scarce.

Keywords: cancer, nurse-led care, palliative care, physician-led care, survival

Applying Large Language Models (LLMs) to Automatically Generate Hospital Discharge Summaries

Detphop Tanasanchonnakul, M.D.[1], Thammasin Ingviya, M.D., Ph.D.[1], Sitthichok Chaichulee, Ph.D.[2]*

[1]Department of Clinical Research and Medical Data Science, Faculty of Medicine, Prince of Songkla University, Hat Yai, Songkhla 90110, Thailand.
[2]Department of Biomedical Sciences and Biomedical Engineering, Faculty of Medicine, Prince of Songkla University, Hat Yai, Songkhla 90110, Thailand.

Abstract:

Background: Large Language Models (LLM) have influenced professional sectors; including healthcare. A hospital discharge summary is a critical medical document that summarizes the details of a patient's hospital admission for communication between healthcare professionals. The manual process of drafting the summaries is often a time-consuming task for physicians. Although, previous studies explored the use of LLM in summarizing medical records, few studies have utilized a real-world dataset that reflects real-world variability.

Objective: To develop and evaluate a large language model capable of automatically generating accurate, coherent, contextually relevant, and multilingual hospital discharge summaries from medical records.

Material and Methods: We extracted medical records and hospital discharge summaries of patients that were admitted to internal medicine wards; between January 1, 2004, and December 31, 2024, from the Hospital Information System (HIS) of Songklanagarind Hospital. The dataset was split into training, validation, and test sets, with a ratio of 80:10:10. The training and validation sets were used for fine-tune LLMs. The performance of the fine-tuned LLMs was measured using multiple evaluation metrics to benchmark the model-generated discharge summaries against reference discharge summaries in the test set.

Results: A total of 14,228 patient records were included in the analysis. The average age of the patients was 59.60 years, with 56.4% being male. The average length of hospital stay was 8.93 days. The best model achieved an overall score (an average score among all the scores) of 0.584. The individual automated evaluation scores were as follows: BLEU-4: 0.378, ROUGE-1: 0.640, ROUGE-2: 0.520, ROUGE-L: 0.545, BERTScore: 0.784, METEOR: 0.573, AlignScore: 0.598 and MEDCON: 0.635.

Conclusion: LLM shows potential in generating a discharge summary from medical records during a hospital stay. However, manual verification by physicians remains crucial to ensure the accuracy of generated summaries. Integrating LLMs alongside humans may reduce the workload for physicians.

Keywords: bilingual text summarization, hospital discharge summary, large language model, text summarization

Correlation between the National Early Warning Score and Acute Kidney Injury and Outcomes in Songklanagarind Hospital

Jutinun Kittivarapong, M.D.[1], Ussanee Boonsrirat, M.D.[2], Suntornwit Praditu-krit, M.D.[2]*

[1]Department of Internal Medicine, Faculty of Medicine, Prince of Songkla University, Hat Yai, Songkhla 90110, Thailand.
[2]Division of Nephrology, Department of Internal Medicine, Faculty of Medicine, Prince of Songkla University, Hat Yai, Songkhla 90110, Thailand.

Abstract:

Background: Acute kidney injury (AKI) significantly impacts patient morbidity and mortality; particularly among critically ill patients. Early recognition of AKI risk factors is crucial for timely intervention. The National Early Warning Score (NEWS), a system used to identify patients at risk of clinical deterioration, could potentially serve as a predictive tool for AKIj.

Objective: To investigate the correlation between NEWS and the incidence and outcomes of AKI in patients admitted to the Medical Intensive Care Unit (MICU) at Songklanagarind Hospital.

Material and Methods: This retrospective cohort study analyzed data from 3,198 patients admitted or transferred to the MICU; from January 2019 until May 2024. Patients with pre-existing advanced chronic kidney disease, those on renal replacement therapy, transplant recipients, palliative cases, advanced malignancy, or missing NEWS data were excluded. Demographic characteristics, NEWS data, and clinical outcomes were assessed. Logistic regression analyses were performed to evaluate NEWS as a predictor for AKI and its outcomes.

Results: From 3,198 patients, 636 (19%) developed AKI. The mean patient age was 63.2±17.4 years. The median age of AKI patients was significantly lower (64.8 years, IQR: 53.7–76) compared to non-AKI patients (67.5 years, IQR: 55.4–77.7; p-value=0.018). Logistic regression analysis indicated a significant correlation between NEWS scores and AKI incidence (adjusted OR=1.16; 95% confidence interval [CI]: 1.13–1.19, p-value<0.001). NEWS scores ≥5 significantly predicted AKI occurrence (OR=5.11, 95% CI: 3.35–7.78, p-value<0.001), and scores ≥7 were associated with an even higher risk (OR=2.89, 95% CI: 2.31–3.61, p-value<0.001). However, NEWS demonstrated modest predictive accuracy for AKI (AUC=0.66).

Conclusion: The NEWS system significantly correlates with AKI incidence in critically ill patients. Higher NEWS thresholds (≥5 and ≥7) effectively identify patients at elevated AKI risk, suggesting that integrating NEWS into clinical protocols may improve early AKI recognition and management, although predictive accuracy remains moderate.

Keywords: acute kidney injury, national early warning score, predictive models, intensive care unit

Personalized and General Knowledge-Based Cognitive Engagement for Alzheimer's Patients, Using AI-Generated Image and Word Prompts

Thitirat Boriboonsri[1]*, Aueaphum Aueawatthanaphisut[2]

[1]High School Student, Ruamrudee International School, Bangkok 10510, Thailand.
[2]Sirindhorn International Institute of Technology, Thammasat University, Pathum Thani 12120, Thailand.

Abstract:

Background: The global rise in Alzheimer's disease (AD) has created a demand for accessible and effective cognitive engagement tools. While combined cognitive training shows efficacy in slowing disease progression, its high costs and reliance on specialized facilities limit accessibility; particularly for home-bound patients.

Objective: This study presents an AI-driven serious game system, designed to deliver personalized, home-accessible cognitive stimulation for individuals with early-stage AD.

Material and Methods: The system integrates a dynamic question generation pipeline using large language models (LLMs). Multi-format quizzes (images, words, multiple-choice and short-answers) are generated from both personalized life history data (family, events, places and objects) and general knowledge domains. Patient-facing interfaces are optimized for usability, featuring large text, voice interaction (ASR) and skipping mechanisms. Emotional well-being is prioritized by omitting performance scores, while a secure caregiver dashboard provides real-time metrics for clinical review.

Results: A 2D mobile-based prototype demonstrated feasibility for home-based deployment, offering user-friendly interactions and remote monitoring capabilities. The dual-structured cognitive tasks with combine emotional familiarity with general training—are designed to reinforce memory recall, language fluency and executive function, while minimizing patient distress.

Conclusion: This AI-driven serious game represents a scalable, accessible, and personalized approach to cognitive engagement in AD. By blending personalized content with gamified delivery, it addresses barriers to conventional interventions and supports both patient dignity and caregiver oversight. Future integration with LLM-driven feedback loops and adaptive memory reinforcement is anticipated to further enhance individualized cognitive trajectories.

Keywords: Alzheimer's disease, assistive technology, cognitive engagement, large language models, personalization, remote monitoring, serious games

A Pilot Evaluation of a Culturally Tailored Virtual Reality Exposure Therapy Program for Social Anxiety in Thailand

Warut Aunjitsakul, M.D., Ph.D.[1]*, Kanthee Anantapong, M.D., Ph.D.[1], Pakawat Wiwattanaworaset, M.D.[1], Aimorn Jiraphan, M.D.[1], Teerapat Teetharatkul, M.D.[1], Katti Sathaporn, M.D.[1], Kreuwan Jongbowonwiwat, B.Sc.[1], Sitthichok Chaichulee, Ph.D.[2]

[1]Department of Psychiatry, Faculty of Medicine, Prince of Songkla University, Hat Yai, Songkhla 90110, Thailand.
[2]Department of Biomedical Sciences and Biomedical Engineering, Faculty of Medicine, Prince of Songkla University, Hat Yai, Songkhla 90110, Thailand.

Abstract:

Background: Social anxiety disorder (SAD) significantly impacts an individual's social functioning. Virtual reality exposure therapy (VRET) presents a promising treatment approach, by offering a controlled and adaptable environment for exposure exercises.

Objective: This pilot investigation aimed to develop and evaluate the effectiveness and user interaction of a VRET program.

Material and Methods: This preliminary study involved the creation of a VRET program tested in two phases: initially with the general population (Phase I) and subsequently with individuals diagnosed with SAD (Phase II), at a university hospital in Thailand. Measures of social anxiety, depression, anxiety, and stress were obtained using the Social Interaction Anxiety Scale (SIAS) and the Depression Anxiety and Stress Scale (DASS-21); at three time points: before VRET, immediately after, and two weeks post-VRET. The Virtual Reality Neuroscience Questionnaire (VRNQ) was used to assess various aspects of user experiences; including game mechanics, in-game assistance and VR-induced symptoms. The VRET program incorporated gradual exposure techniques and simulated diverse social situations pertinent to the local cultural context.

Results: Both participant groups demonstrated significant reductions in their social anxiety levels following VRET sessions when compared to their pre-VRET scores (ps<0.01). However, individuals with SAD reported an increase in social anxiety at the two-week follow-up, while the general population maintained their improvement. The virtual reality software was rated as satisfactory regarding its usability, safety, and overall acceptability.

Conclusion: In conclusion, the VRET program showed promise in alleviating social anxiety and delivered a satisfactory virtual reality experience, indicating its practicality for individuals with SAD within a developing country setting. Further research with larger participant groups and repeated sessions is necessary to enhance its effectiveness and ensure sustained benefits. Comprehensive treatment protocols; including tutorials, relaxation techniques and stress monitoring, are recommended for optimal outcomes.

Keywords: developing countries, mental health, pilot projects, social phobia, user-computer interface, virtual reality exposure therapy

AI-Based Multi-Classification of B12 Deficiency Using Deep Learning on Photographic Eye Images

Pannatat Wongbangpo*, Nattawat Moleeset

Ekamai International School, Watthana, Bangkok 10110, Thailand.

Abstract:

Background: Vitamin B12 deficiency is a widespread yet frequently overlooked condition, particularly in early stages where clinical symptoms are subtle. Among the visual signs associated with this deficiency, eye discoloration (such as scleral yellowing) can serve as non-invasive indicator, but it is often difficult to assess accurately without clinical training. Traditional diagnosis typically relies on blood testing, which can be invasive, costly and less accessible in remote or under-resourced areas.

Objective: This study addresses the need for an accessible, image-based screening tool by developing a deep learning model capable of classifying B12 deficiency using only photographic eye images focused on discoloration.

Material and Methods: A total dataset of 156 curated images was labeled into having or not having discoloration by a standardized visual test. The dataset was divided into 3 categories: train-valid-test, with a picture distribution of 15%-70%-15%, respectively. Images were cropped to highlight the scleral and augmented using techniques; such as rescale, rotation, horizontal flipping, shear, height shift, weight shift and fill mode, to reduce overfitting. Four convolutional neural network (CNN) architectures: Xception, VGG16, ResNet50 and EfficientNetB0 were trained on Google Colab using Python, with categorical cross-entropy loss and the Adam optimizer over 50 epochs.

Results: The VGG16 model achieved the highest test accuracy of 100%, outperforming Xception (95.83%), ResNet50 (83.33%) and EfficientNetB0 (50%). Confusion matrix analysis showed accurate predictions in distinguishing discoloration and non-discoloration, with the exception of the EfficientNetB0 model.

Conclusion: These findings demonstrate the potential of AI-assisted eye image analysis as a non-invasive, cost-effective screening tool for early B12 deficiency detection. Future studies should expand the dataset; especially through other parts of the body; such as the tongue or palm, and incorporate advanced techniques; such as attention mechanisms, to further improve model performance. Ultimately, this chosen model should be adapted into a mobile application to improve accessibility for both clinicians and the public.

Keywords: vitamin B12 deficiency, eye discoloration, deep learning, CNN, image classification, non-invasive screening

Deep Learning AI Detection of Skin Rashes, via Image Analysis

Nayaporn Wisaruttanun[1], Nutwaree Chanthavijaikul[2]*

[1]Anglo Singapore International School, Bangkok 10260, Thailand.
[2]Ekamai International School, Bangkok 10110, Thailand.

Abstract:

Background: Accurate identification of skin rashes is essential for effective treatment. However, many conditions share visual characteristics; despite differing underlying causes. To overcome this obstacle, artificial intelligence (AI) was used to analyze images, differentiating types of rashes.

Objective: Our goal was to compare the performance of four convolutional neural network (CNN) models in classifying dermatological images, so as to identify the model with the highest potential for future clinical application.

Material and Methods: The data was divided into three subsets: training, validation, and testing. Each image within these subsets was classified into one of four categories: bacterial rashes (BA), viral rashes (VI), fungal rashes (FU) or normal skin. The development of the AI models was carried out using Python on Google Colab. There was a total of 330 images used through all three subsets, by incorporating data augmentation techniques; such as rotation, zooming, flipping and rescaling. These augmentations are widely recognized for enhancing model generalization and mitigating overfitting in convolutional neural networks. The CNN architectures used were: VGG16, Xception, ResNet50 and EfficientNetB0. Additionally, 30 epochs were conducted for all models.

Results: The results of the accuracy of these models suggest that Xception, with an accuracy of 91.62%, performed the best; followed by VGG16 (88.06%), ResNet50 (45.47%), and EfficientNetB0 (40.30%). The confusion matrix results for Xception revealed the test accuracy of normal skin at 92.59%, and the following with BA 90%, FU 93.75% and VI 85.71%. This indicates a high accuracy with normal skin and a certain amount of misclassification between the other types of rashes.

Conclusion: These findings suggest the potential of a multi-condition AI models to serve as a beneficial screening aid for general practitioners and the future of healthcare. Going forward, the implications are clear; the model Xception was the most successful and should be developed for further use.

Keywords: artificial intelligence, bacterial, deep learning, rash, fungal, viral

A Microfluidic Biosensing Platform for Neutrophil Gelatinase-Associated Lipocalin Detection in Acute Kidney Injury

Kewarin Phonklam, M.Sc.[1], Tonghathai Phairatana, Ph.D.[1,2]*

[1]Department of Biomedical Sciences and Biomedical Engineering, Faculty of Medicine, Prince of Songkla University, Hat Yai, Songkhla 90110, Thailand.
[2]Institute of Biomedical Engineering, Faculty of Medicine, Prince of Songkla University, Hat Yai, Songkhla 90110, Thailand.

Abstract:

Background: Acute kidney injury (AKI) is marked by a sudden decline in renal excretory function, often leading to serious complications and increased morbidity and mortality. Neutrophil gelatinase-associated lipocalin (NGAL) is a key biomarker for the early detection of acute kidney injury. Accurate and timely diagnosis is essential for effective clinical management, which makes the development of rapid, sensitive, and user-friendly detection platforms a critical need.

Objective: This study aimed to develop a self-powered, finger-driven microfluidic biosensor, by integrating a custom-designed microfluidic system; with a label-free electrochemical immunosensor for point-of-care detection of NGAL.

Material and Methods: The finger-driven microfluidic chip was fabricated by casting polydimethylsiloxane (PDMS) onto a 3D-printed mold, using soft lithography. A label-free electrochemical immunosensor for NGAL detection was developed, using gold nanoparticles (AuNPs) and Prussian blue (PB), on a gold electrode embedded polypropylene substrate. This sensing component was then integrated into the finger-driven microfluidic platform. The sensor performance was evaluated using differential pulse voltammetry.

Results: The developed sensing device demonstrated efficient fluid handling, achieving a mixing efficiency of 96±1.4%, using microliter-scale sample volumes. The AuNPs–PB-based electrochemical immunosensor enabled NGAL detection through a decrease in PB oxidation current upon NGAL binding. It exhibited a linear detection range of 0.10–1.5 ng mL^{-1}, with a limit of detection of 0.099 ng mL^{-1}. Recovery from spiked urine samples ranged from 88% to 107%, confirming its accuracy.

Conclusion: This finger-driven microfluidic biosensing platform offers a rapid, sensitive, and user-friendly approach for NGAL detection, demonstrating high potential for point-of-care diagnostics in acute kidney injury.

Keywords: neutrophil gelatinase-associated lipocalin, acute kidney injury, finger-driven microfluidic chip, electrochemical biosensor, point of care testing

Modeling Nutrient and Oxygen Diffusion in 3D Cancer-On-A-Chip Platform, using COMSOL Simulation

Kadbodee Pliphon, M.Sc.[1], Siwattra Pruksasri, M.Sc.[1], Sunisa Saengchan, M.Sc.[1], Mooktapa Plikomol, M.Sc.[1], Tonghathai Phairatana, Ph.D.[1], Pasarat Khongkow, Ph.D.[1,2]*

[1]Department of Biomedical Sciences and Biomedical Engineering, Faculty of Medicine, Prince of Songkla University, Hat Yai, Songkhla 90110, Thailand.
[2]Translational Medicine Research Center, Faculty of Medicine, Prince of Songkla University, Hat Yai, Songkhla 90110, Thailand.

Abstract:

Background: 3D cancer-on-chip platforms are widely used to mimic *in vivo* conditions for cancer research and anti-cancer drug screening. These platforms effectively grow three-dimensional (3D) tumor spheroids, which more closely mimic tumor physiology than traditional 2D cultures. A major challenge in designing 3D cancer-on-chip devices is ensuring that oxygen and nutrients can sufficiently diffuse to the core of tumor spheroids; especially under continuous flow.

Objective: This study aimed to evaluate whether the designed PDMS-based microfluidic chip for 3D cell culture provides sufficient oxygen and glucose delivery under different flow conditions using computational simulation.

Material and Methods: A two-dimensional cross-section of the developed design was modeled in COMSOL Multiphysics software, using the Transport of Diluted Species module. The simulations were performed at two different flow rates: 10 µL/min and 100 µL/min, representing low and high perfusion.

Results: The results showed that both flow rates enabled oxygen and glucose to diffuse efficiently into the microwells, reaching over 90% of the main channel concentration at the bottom within 30–60 minutes. At 100 µL/min, flow velocity increased to a level higher than that of physiological interstitial flow, while at 10 µL/min it remained within the range. Shear stress values in both conditions were low, and within the *in vivo* range for maintaining spheroid structure. These findings indicate that our designed chip could support effective nutrient delivery without generating harmful mechanical forces, even under higher flow.

Conclusion: Altogether, integrating COMSOL simulation during design phase provides valuable insights into flow behaviors and microenvironment stability, facilitating the development of reliable and reproducible cancer-on-a-chip platforms for drug testing.

Keywords: anti-cancer drug screening, cancer-on-a-chip, COMSOL simulation

Development of a Troponin I Based Biosensor, for Acute Myocardial Infarction Diagnosis

Suwali Wichian, B.Sc.[1], Kewarin Phonklama, M.Sc.[1], Tonghathai Phairatana, Ph.D.[1,2]*

[1]Department of Biomedical Sciences and Biomedical Engineering, Faculty of Medicine, Prince of Songkla University, Hat Yai, Songkhla 90110, Thailand.
[2]Institute of Biomedical Engineering, Faculty of Medicine, Prince of Songkla University, Hat Yai, Songkhla 90110, Thailand.

Abstract:

Background: Acute myocardial infarction (AMI) is a major global health concern, requiring rapid, accurate, and minimally invasive diagnostics with small blood volumes. Cardiac Troponin I (cTnI) is a clinically validated AMI biomarker, but standard methods; like ECLIA, are time-consuming and require skilled personnel and centralized laboratories, making them unsuitable for point-of-care and emergency applications.

Objective: This study aimed to develop a portable, label-free electrochemical biosensor; based on a screen-printed electrode. It was designed for the quantitative detection of cTnI to enable efficient point-of-care testing (POCT) in both clinical and resource-limited settings.

Material and Methods: The cTnI biosensor was conducted using screen-printed carbon electrodes (SPCEs) modified with conductive polyaniline (PANI) and methylene blue (MB). PANI was electrodeposited onto the SPCE surface to enhance the electrode's conductivity and the specific surface area, while MB was applied as a redox mediator. Anti-cTnI antibodies were immobilized via glutaraldehyde cross-linking. Electrochemical detections were performed using differential pulse voltammetry (DPV), focusing on the MB reduction peak. The surface morphology was examined using a scanning electron microscope.

Results: SEM analysis showed a porous surface structure that promoted effective antibody immobilization and improved sensitivity. A clear concentration-dependent response to cTnI was observed. The DPV measurements revealed a concentration-dependent decrease in the reduction current as cTnI levels increased. This response is attributed to the formation of antigen–antibody complexes that obstruct electron transfer at the electrode surface; thus, reducing the availability of redox-active sites and enabling reliable quantification of cTnI.

Conclusion: A portable, label-free electrochemical biosensor for cTnI detection was developed using a PANI/MB-modified screen-printed electrode. The DPV signal decreased with increasing cTnI concentration. This low-cost POCT device enables rapid AMI diagnosis in emergency or resource-limited settings, supporting timely treatment and reducing mortality.

Keywords: acute myocardial infarction, electrochemical biosensor, point-of-care testing, troponin I

FULL PAPER

The 4th Annual Health Research International Conference

Shaping the Future: Innovation, Health and Well-being

Full Paper

Knowledge, Attitudes, and Practices of Enhanced Recovery after Surgery among Registered Nurses in a University Hospital: A Cross-Sectional Study

Khomapak Maneewat, R.N., Ph.D.[1], Sirinapa Kongsak, R.N.[2],
Surangkana Ongsakul, R.N.[2], Srila Samphao, M.D.[3],
Worapat Attawettayanon, M.D, Ph.D.[3], Duangsuda Siripituphum, R.N., Ph.D.[1]*

[1]Surgical Nursing Department, Faculty of Nursing, Prince of Songkla University, Hat Yai, Songkhla 90110, Thailand.
[2]Songklanagarind Hospital, Faculty of Medicine, Prince of Songkla University, Hat Yai, Songkhla 90110, Thailand.
[3]Department of Surgery, Faculty of Medicine, Prince of Songkla University, Hat Yai, Songkhla 90110, Thailand.

Abstract:

Objective: This study aimed to determine registered nurses' knowledge, attitudes, and practices regarding Enhanced recovery after surgery (ERAS), and their relationships as a guide to develop ERAS educational programs for registered nurses.

Material and Methods: A descriptive cross-sectional survey was conducted with Thai registered nurses. An anonymous 90-question self-report questionnaire was developed to collect the data. The questionnaire addressed 3 domains of knowledge, attitudes and practices towards ERAS. Purposive sampling was employed to recruit the samples according to the study criteria. Descriptive statistics were used to describe the basic characteristics of the study participants. Spearman correlation coefficient was used to test the relationships between the KAP variables.

Results: The results revealed that the mean percentage scores (MPS) of the knowledge towards ERAS was 66.67 (M=20.00, S.D=3.13). The MPS of the attitudes on ERAS was 70.55 (M=105.83, S.D=7.61). The MPS of the practices on ERAS was 60.15 (M=90.22, S.D=10.78). Spearman correlation coefficient analysis significantly revealed weak positive correlations between knowledge and attitudes (r=0.38, p-value<0.01), knowledge and practices (r=0.28, p-value<0.01) as well as attitudes and practices (r=0.33, p-value<0.01) of nurses towards ERAS. These results indicated a moderate level of attitudes as well as low levels of knowledge and practices of the registered nurses regarding ERAS. There is still room for improvement regarding the nurses' knowledge, attitudes, and practices towards ERAS in a Thai hospital context.

Conclusion: These results indicated low levels of knowledge, moderate level of attitudes, and very low level of practices among the registered nurses regarding ERAS. Hence, there is still room for improvement regarding the nurses' knowledge, attitudes, and practices towards ERAS in a Thai hospital context.

Corresponding author: Duangsuda Siripituphum
Department of Surgical Nursing, Faculty of Nursing, Prince of Songkla University, Hatyai, Songkhla 90110, Thailand.
E-mail: duangsuda.wo@psu.ac.th

Keywords: Enhanced recovery after surgery; Nurses' knowledge; Nurses' attitudes; Nurses' practices

Introduction

Enhanced recovery after surgery (ERAS) is a patient-centered, multidisciplinary and an evidence-based surgical care pathway to standardize surgical care pathways. It reduces the surgical stress response of patients, facilitates recovery, and improves surgical outcomes in patients[1-2]. Implementation of the ERAS multimodal models of care in a variety of surgical procedures has been evidenced to significantly reduce postoperative length of hospital stay (LOHS), postoperative complications as well as postoperative care costs[3-6]. The use of ERAS multimodal models of care has been advocated in Western societies; however, there is no evidence of successful implementation of this model in Southeast Asia: with the exception of Singapore[7].

A key component required for the successful implementation of ERAS is the development of a multidisciplinary team comprised at a minimum of: a surgeon, an anesthesiologist and a nurse. Nurses play a central role in increasing multidisciplinary team adherence towards ERAS, which is associated with improved surgical outcomes[8]. A hospital in Thailand as well as in the Veterans Administration Medical Center – St. Louis, implementation of the ERAS multimodal models of care was commenced prior to allocate formal ERAS education to direct-care registered nurses and a major stakeholder group[2]. In congruence with a recent study from Australia, fewer nurses used ERAS in the care of patients undergoing surgery, and perceived lower levels of knowledge and agreement. In the same study, the nurse participants perceived themselves as having a lack of information as the greatest barrier to knowledge on ERAS[9].

Due to inadequate ERAS knowledge, registered nurses involved in the implementation of ERAS protocols perceived themselves as not prepared and as having a lack in confidence[2]. The successful application of the ERAS care pathway to enhance recovery of patients undergoing surgery should not only be based on the evidence of outcome improvement, which has been developed within the Western context, but also on the capabilities of Thai nurses, the methods of facilitation, and on the context of healthcare in Thailand[3,10-11]. The first step to optimize the efficacy of ERAS implementation is therefore to understand the current capability of the nurses involved in the care of patients undergoing surgery[12].

A previous study conducted to investigate knowledge, attitudes, and practices regarding ERAS among pediatric surgical nurses in China revealed a lower level of postoperative recovery knowledge, with appropriate attitudes and moderate levels of practice[13]. Previous studies conducted to investigate this issue also revealed that most nurses displayed a lack of knowledge and education regarding ERAS[7,14-15]. Compared to other groups of healthcare providers involved in the ERAS team, staff nurses reported the lowest level of knowledge, attitudes, and practices regarding ERAS[16]. Another previous study revealed the level of knowledge and confidence among nurses regarding ERAS was significantly increased after attending an ERAS education program[2]. Inadequate ERAS knowledge, attitudes, and practices on ERAS encountered in the implementation failure of ERAS programs[2].

To date, no previous research in Thailand has examined knowledge, attitudes, and practices regarding the ERAS pathway among registered nurses. Such an assessment would be useful to determine whether additional training and education are needed.

Material and Methods

Materials

A cross-sectional survey design was employed to examine the current knowledge, attitudes, and practices of

registered nurses regarding the ERAS multimodal model of care. This design describes the status, frequency, and characteristics of an interesting issue at a certain point in time[17]. This approach is best suitable for answering the question of this study. Purposive sampling was employed to determine the research participants; between May 1st, 2024 and June 30th, 2024.

The sample size estimation of the complete study was calculated using the power analysis to represent the whole population. A G*power calculation was performed, using a level of significance of α=0.05 and the power of statistical test (1–β)=0.80[18]. The effect size 0.20 was taken from a previous study entitled: knowledge, attitude, and application towards fast-track surgery among operating room paramedics[19]. The sample size calculation yielded 153 samples. The inclusion criteria were: registered nurses with at least 6 months of clinical experience in providing direct care for adult surgical patients undergoing surgery, whom were willing and voluntarily participated in this study. Whilst the registered nurses that did not provide direct care for patients or were not in nursing roles and currently work under supervision were excluded from this study. A total of 218 registered nurses that provided care for patients undergoing surgery were eligible and participated in this study.

A knowledge self-report questionnaire towards attitudes, and practices regarding enhanced recovery after surgery was developed by the researchers, using a systematic process of a literature review and an expert consensus validation. It consisted of four parts encompassing: (1) basic characteristics of the nurse participants; (2) knowledge; (3) attitudes, and (4) practice of ERAS. The part of knowledge was used to asses what participants knew about theory, concept, and body of knowledge regarding ERAS throughout the preoperative and postoperative phases. The part of attitudes was used to evaluate what beliefs and feelings they hold as well as how they view ERAS. The practice part was used to measure what actions they take that reflect their knowledge and attitudes regarding ERAS.

Prior to analysis, the scores of the elements with negative statements were reversed. The mean scores of the knowledge, attitudes, and practices of ERAS were analyzed and converted into mean percentage scores (MPS) for interpretation. Knowledge, attitudes, and practices towards ERAS was classified into five levels according to the MPS: (1) very low (MPS<60.0); (2) low (MPS=60.0–69.9); (3) moderate (MPS=70.0–79.9); (4) high (MPS=80.0–89.9); and (5) very high (MPS>90.0).

The content validity of the questionnaire was established by five experts. The scale content validity index (S-CVI) of the knowledge and the attitudes questionnaire were 0.98 and the S-CVI of the practice questionnaire was 1. The internal consistency reliability was measured by 29 register nurses, and yielded Cronbach alpha coefficients (α) of knowledge, attitudes, and practices questionnaire 0.76, 0.77 and 0.76, respectively.

Data was collected using the self-reported questionnaire. The registered nurses that indicated a willingness to participate in the study and complete the questionnaire were recruited. The researchers clearly informed and discussed with the participants as to the study details, the involvement of participants, and gave each participant an information sheet. The questionnaires with a cover letter were distributed to 301 registered nurses through hard-copy method by the unit coordinators. The participants were asked to complete the questionnaire, the researchers informed the participants of the time frame to complete the questionnaire as well as the method of returning the questionnaire. In total, 223 registered nurses returned the questionnaire, giving an overall response rate of 74.09. Out of the 223, 5 registered nurses provided incomplete survey responses. 218 registered nurses completed the questionnaires and were included in the final data analysis.

Frequency, percentage, mean, and standard deviation (S.D.) were used to describe the basic characteristics of the

nurse participants. The knowledge, attitudes, and practices scores were manipulated and converted the mean scores into MPSs. The levels of knowledge, attitudes, and practices regarding ERAS were analyzed using the MPS. A high score represented a higher level of knowledge, attitudes, and practices regarding ERAS. Spearman correlation coefficient was used to test the relationships between the KAP variables.

Results

In total, 218 registered nurses participated and were included in the final analysis. Table 1 presents the basic characteristics of the nurse participants. As shown, most of the participants were female (n=214, 98.2%), had a bachelor level in nursing education (n=206, 94.5%), with an average age of 34.07 years. The average amount of clinical experience of the participants as a registered nurse

Table 1 Basic characteristics of nurse participants (*N*=218)

Variable	Mean	S.D.	Frequency (%)
Age (years)	34.07	8.74	
Gender			
Male			4 (1.8)
Female			214 (98.2)
Educational attainment			
Bachelor			206 (94.5)
Master			12(5.5)
Clinical experience as registered nurse (years)	11.27	9.05	
Area of specialty			
General surgery			146 (66.9)
Orthopedic surgery			27 (12.4)
Gynecological surgery			22 (10.1)
Cardio-thoracic surgery			23 (10.6)
Professional title			
Practitioner level			185 (84.9)
Professional level			32 (14.7)
Senior professional level			1(0.5)
Experiences of ERAS			
Yes			97 (44.7)
No			73 (33.6)
Not sure			47 (21.7)
ERAS training/ workshop experience			
Yes			32 (14.7)
No			185 (85.3)
Interest/ need in attending ERAS educational program			
No			6 (2.8)
Indifferent			47 (21.6)
Yes			165 (75.7)
Interest/ need in adapting of the ERAS nursing care protocol			
No			5 (2.3)
Indifferent			38 (17.4)
Yes			175 (80.3)

was 11.27 years. Most worked at practitioner level (n=185, 84.9%); additionally, most had been providing care for patients undergoing general surgery (n=146, 66.9%).

Almost half of the had experienced in using the ERAS program (n=97, 44.7%). Only 32 had prior ERAS training (14.7%), and the majority had no prior ERAS training (n=185, 85.3%). Most demonstrated their interest in attending an ERAS educational program (n=165, 75.7%). Furthermore, almost all demonstrated their interests in adapting to the ERAS nursing care protocol (n=175, 80.3%).

The knowledge, attitudes, and practices (KAP) towards ERAS of the nurse participants

Table 2 displays the mean percentage score (MPS) of each element (KAP) and the overall elements on ERAS. As seen in Table 2, the overall MPS of the nurse participants' knowledge, attitudes, and practices on ERAS was 65.47 (M=216.04, S.D.=16.90).

The overall mean percentage scores (MPS) of the knowledge towards ERAS was 66.67 (M=20.00, S.D.=3.13). The highest MPS of correct answer was 98.62, which existed in items: 15 (planning for discharge for patient's self-management at home), followed by MPS 97.71 of items: 1 (practice-based evidence), 2 (multidisciplinary team collaboration), 14 (pain assessment and pain management plan after surgery), and 16 (assessment and prevention of postoperative nausea and vomiting). The lowest MPS of the correct answer was 5.05 (M=0.05, S.D.=0.22), from items: 10 (preoperative mechanical bowel preparation to reduce anastomosis leakage and infection), followed by 6.88 (M=0.07, S.D.=0.25), 17 (give opioids only for pain during the first 24 to 48 hours after surgery), 11.98 (M=0.12, S.D.=0.33), 30 (removed all surgical drains), 12.44 (M=0.12, S.D.=0.33), 11 (no food or drink after midnight), and 20.74 (M=0.21, S.D.=0.41) item 9 (preoperative counseling and education the day before surgery), respectively.

The overall mean percentage scores (MPS) of the attitudes towards ERAS was 70.55 (M=105.83, S.D.=7.61). The highest MPS positive attitude was 90.46 (M=4.52, S.D.=0.60), which existed item 15 (planning for discharge for patient's self-management at home), followed by 89.59 (M=4.48, S.D.=0.63), 14 (pain assessment and pain management plan after surgery), 89.27 (M=4.46, S.D.=0.60), 29 (no postoperative surgical complications that required hospitalization), 88.26 (M=4.41, S.D.=0.61), 3 (optimize postoperative outcomes), and 87.98 (M=4.40, S.D.=0.61) item 16 (assessment and prevention of postoperative nausea and vomiting).

The lowest MPS positive attitudes was 33.24 (M=1.66, S.D.=0.66) from item 10 (preoperative mechanical bowel preparation to reduce anastomosis leakage and infection), followed by 34.13 (M=1.71, S.D.=0.70), 30 (removed all surgical drains), 34.50 (M=1.72, S.D.=0.75), 17 (give opioids only for pain during the first 24 to 48 hours after surgery), 35.50 (M=1.78, S.D.=0.75),11 (no food or drink after midnight), and 38.99 (M=1.95, S.D.=0.92) item 9 (preoperative educational counseling 1 day prior to surgery), respectively.

The overall mean percentage scores (MPS) of the practices towards ERAS was 60.15 (M= 90.22,

Table 2 The participants' level of knowledge, attitudes, and practices on ERAS (N=218)

Components of ERAS	Mean	S.D.	MPS	Level
Knowledge	20.00	3.13	66.67	Low
Attitudes	105.83	7.61	70.55	Moderate
Practices	90.22	10.78	60.15	Low
Overall	216.04	16.90	65.47	Low

S.D.=10.78). The highest MPSs was 86.79 (M=4.34, S.D.=1.04), which existed in item 16 (assessment and prevention of postoperative nausea and vomiting), followed by 85.60 (M=4.28, S.D.=1.21), 14 (pain assessment and pain management plan after surgery), 84.98, 17 (M=4.25, S.D.=1.05) (give opioids with Paracetamol and/or NSAID's for pain management after surgery), 29 (M=4.25, S.D.=1.12) (no postoperative surgical complications that required hospitalization), and 82.95 (M=4.15, S.D.=1.10) item 27 (Pain can be controlled with oral analgesics).

The lowest MPS towards ERAS-related practices was 29.72 (M =1.49, S.D.=1.01) item 13 (drink carbohydrate 2 hours before surgery), followed by 36.04 (M=1.80, S.D.=1.26), 11 (no food or drink after midnight), 39.63 (M=1.98, S.D.=1.30), 12 (drink clear liquids until 2 hours before surgery), 39.91 (M=2.00, S.D.=1.23), 30 (removed all surgical drains), and 41.66 (M=2.08, S.D.=1.38) item 9 (preoperative educational counseling 1 day prior to surgery), respectively.

Sub-group analysis of basic characteristics of nurse participants and KAP towards ERAS

Additional analysis was conducted to compare knowledge towards ERAS between participants with different general, basic characteristics. However, no statistically significant correlations were observed between: educational attainment (*r=0.04*), professional title (*r=0.05*), experiences of ERAS (*r=0.08*) and ERAS training/ workshops (*r=0.14*) and knowledge levels of nurses regarding ERAS. This indicated minimal influence of these demographic characteristics on knowledge towards ERAS practices, with no correlation coefficients of 0.05 (p-value<0.05) (Table 3).

Correlation analysis of knowledge, attitudes and practices of nurses toward ERAS

Spearman correlation coefficient analysis revealed a weak positive correlation between knowledge and attitudes (*r*=0.38), knowledge and practices (*r*=0.28), and attitudes and practices (*r*=0.33) of nurses toward ERAS, with correlation coefficients of .01 (p-value<0.01) (Table 4).

Table 3 Relationships between nurses' knowledge and basic characteristics on ERAS (*N*=218)

Variables	Knowledge
Knowledge	1.000
Educational attainment	0.04
Professional title	0.05
Experiences of ERAS	0.08
ERAS training/ workshop	0.14

*p-value<0.05

Table 4 Relationships between nurses' knowledge, attitudes and practices on ERAS (*N*=218)

Variables	Knowledge	Attitudes	Practices
Knowledge	1.000		
Attitudes	0.38**	1.000	
Practices	0.28**	0.33**	1.000

**p-value<0.01

Discussion

The results of this descriptive cross-sectional study, regarding knowledge, attitudes, and practices on ERAS multimodal model of care, revealed inadequate knowledge, and practices; with moderate levels of attitudes among the registered nurses. It is also important to note that, as of this time, published literature and research evidence on registered nurses' knowledge, attitudes, and practices on ERAS has rarely been explored or studied nor reported globally. These study findings are directly in line with previous findings among registered nurses[2,7,9,14-15,20]. The study results are also important to support and highlight the limitation of evidence-based ERAS protocol adoption and implementation within this setting. Although, ERAS programs have been widely and internationally popularized as well as applied in the management of patients undergoing surgery since 1990s, the limitation, difficulty, and barriers in adoption

and implementation of ERAS are currently evidenced in Asia and in developed countries[9-10,13,20-24]. Despite ERAS programs having been disseminated worldwide, the implementation of ERAS in some countries has been slow[25].

Inadequate knowledge, attitudes, and practices regarding ERAS may be due to insufficient participation in ERAS education and training within the current sample. Like the previous study, the ERAS protocols were implemented at the setting hospital prior to providing formal education or preparation of direct-care registered nurses. ERAS education programs increase the level of knowledge and confidence among nurses towards ERAS[2]. As aforementioned, the majority had no prior ERAS training as a result this creates a non-supportive and non-encouraging atmosphere to ERAS implementation[26]. ERAS protocols are therefore secondary to traditional care knowledge, attitudes, and practices; having little or no emphasis on evidence-based care. Traditional practices for patients undergoing surgery have not been supported by said evidence[27-28].

The questionnaire used in this study was developed from high quality evidence in ERAS as well as ERAS nursing programs with acceptable levels of validity and reliability. However, the daily practices of patients undergoing surgery in this context is underpinned by tradition, rather than empirical evidence and formal training. Conflicting approaches to patient care after surgery between their day-to-day clinical practices and the evidence-based practice; such as fasting patients before surgery, could be developed. Despite the numerous ERAS evidence and research findings available to inform best practice for patients undergoing surgery, it is not applied into their day-to-day practice. Currently, as noted earlier, there is no policy that clearly distinguishes the roles and responsibilities of nurses in an ERAS team and no ERAS clinical practice guidelines for the management of patients undergoing surgery in this setting.

Consequently, they might perceive their real-world day-to-day practices as correct or appropriate and gave answers accordingly. This study's results indicated that the participants in this study selected their answers according to their real-world knowledge, attitudes and practices. For instance, preoperative mechanical bowel preparation was mostly viewed by the study participants as correct, appropriate and routine. So, the statements measured in the questionnaire possibly generated response bias and impacted the inadequate level of their knowledge, attitudes and practices regarding the application of ERAS programs.

ERAS components are inconsistently used in their clinical practice, so replacing traditional practices with evidence-based practices for patients undergoing surgery is challenging. This requires nurses to share expertise, knowledge, and skills with the interdisciplinary ERAS team across the entire pathway[3]. Successful implementation of ERAS in the Thai hospital context, ERAS preparation, education and training programs is required for nurses and clinical staff involved in the care of patients receiving ERAS pathways[2,26].

The inadequate level of knowledge, attitudes, and practices regarding ERAS among the registered nurse participants raises some concerns about the optimal outcomes of patients undergoing surgery. It is important to overcome traditional knowledge, attitudes, and practices for patients undergoing surgery through ongoing ERAS education and training.

In this present study, there was a statistically significant relationship between nurses' knowledge, attitudes, and practices towards ERAS. This finding is consistent with the findings of previous studies[19]. Nurses' knowledge and understanding[19,22,28] as well as their awareness[29] towards ERAS were predictors of nurses' practices towards ERAS. This study's results support a significant correlation between knowledge, attitudes, and practices according to the KAP framework. Sufficient knowledge and awareness; including appropriate attitudes stand as pivotal influences in addressing practice and behaviors. Adequate knowledge often leads to positive attitudes and proper practices.

Development and improvement of nurses' knowledge and attitude are considered in increasing the health outcomes of patients[23]. Intentions to perform actual behaviors are determined by attitude toward the behavior, subjective norm, work norms, and perceived behavioral control influence behavioral intention[25]. Beyond nurses' knowledge, attitudes, and practices towards ERAS, successful ERAS implementation requires engagement, collaborative, and a supportive environment in the context of practice [10,22,25].

Conclusion

These present findings provide important evidence for inadequate knowledge, attitudes, and practices of nurses towards ERAS in the hospital context. The results are broadly consistent with previous studies in other contexts. To our knowledge, this is the first report of knowledge, attitudes, and practices regarding ERAS among registered nurses in Thailand. There is still room for improvement regarding ERAS knowledge, attitudes, and practices of registered nurses. To incorporate ERAS pathways into the nursing care of patients undergoing surgery, future research is needed to develop a comprehensive ERAS education and training program in the hospital context.

Acknowledgments

The results of this study are part of a master thesis. We highly appreciate and are grateful to the registered nurse participants for their participation and encouragement. We would like to acknowledge our gratefulness to the Prince of Songkla University for providing the grant to support this study. Also, we would like to add abundant thanks to our research team for their compassion and support.

Conflicts of interest

There are no potential conflicts of interest to declare.

References

1. American association of nurse anesthesiology. Enhanced recovery after surgery overview 2023 [homepage on the Internet]. Illinois: American association of nurse anesthesiology; 2023. [cited 2024 June 3]. Available from: https://www.aana.com/practice/clinical-practice/clinical-practice-resources/enhanced-recovery-after-surgery.
2. Brooks L. Evaluation of educating registered nurses prior to implementing new evidence-based protocol: enhanced recovery after surgery (ERAS) [homepage on the Internet]. St. Louis: University of Missouri; 2018. [cited 2024 June 3]. Available from: https://irl.umsl.edu/cgi/viewcontent.cgi?article=1790&context=dissertation.
3. Achrekar MS. Enhanced recovery after surgery (ERAS) nursing programme. Asia Pac J Oncol Nurs 2022;9:100041.
4. Lannes F, Walz J, Maubon T, Rybikowski S, Fakhfakh S, Picini M, et al. Enhanced recovery after surgery for radical cystectomy decreases postoperative complications at different times. Urol Int 2022;106:171-9.
5. Lee HH, Kwon HM, Lee WS, Yang IH, Choi YS, Park KK. Effectiveness of ERAS (Enhanced Recovery after Surgery) Protocol via Peripheral Nerve Block for Total Knee Arthroplasty. J Clin Med 2022;11.
6. Zhou Y, Li R, Liu Z, Qi W, Lv G, Zhong M, et al. The effect of the enhanced recovery after surgery program on radical cystectomy: a meta-analysis and systematic review. Front Surg 2023;10:1101098.
7. Ongün P, Seyhan ak E. Examination of Knowledge Levels of Nurses Working in Surgical Clinics About ERAS Protocol. Bakirkoy Tip Dergisi / Medical Journal of Bakirkoy. 2020;16:287-94.
8. Nelson G. Nursing role central to successful implementation of enhanced recovery after surgery. Asia Pac J Oncol Nurs 2022;9.
9. Lovegrove J, Tobiano G, Chaboyer W, Carlini J, Liang R, Addy K, et al. Clinicians' perceptions of "enhanced recovery after surgery" (ERAS) protocols to improve patient safety in surgery: a national survey from Australia. Patient Saf Surg 2024;18:18.
10. Balfour A, Amery J, Burch J, Smid-Nanninga H. Enhanced recovery after surgery (ERAS®): Barriers and solutions for nurses. Asia Pac J Oncol Nurs. 2022;9:100040.
11. Jensen BT, Retinger NL, Lauridsen SV. From fast-track to enhanced recovery after surgery in radical cystectomy pathways: A nursing perspective. Asia Pac J Oncol Nurs. 2022;9:100048.

12. Norman A, Mahoney K, Ballah E, Pridham J, Smith C, Parfrey P. Sustainability of an enhanced recovery after surgery initiative for elective colorectal resections in a community hospital. Can J Surg 2020;63:e292–8.
13. Liu B, Liu S, Zheng T, Lu D, Chen L, Ma T, et al. Neurosurgical enhanced recovery after surgery ERAS for geriatric patients undergoing elective craniotomy: a review. Medicine (Baltimore) 2022;101:e30043.
14. Alemneh Y. Assessment of knowledge and attitude towards enhanced recovery after surgery among health professionals in university of Gondar hospital Northwest Ethiopia [monograph on the Internet]. Gongar: University of Gondar; 2017. [cited 2024 June 3]. Available from: https://core.ac.uk/download/pdf/199937881.pdf.
15. Centin T, Yagcan H. The enhanced recovery after surgery protocol implementation status of the health staff working in the gynecology-obstetric clinics. Izmir Democr Univ health Sci J 2023;6:131–48.
16. Ashagrie G. A study on assessment of knowledge attitude and practice of enhanced recovery after surgery on health care professionals at Tikur Anbessa Specialized Hospital, Addis Ababa, Ethiopia in 2021 [monograph on internet]. Addis Ababa: Addis Ababa University; 2021. [cited 2024 June 3]. Available from: http://etd.aau.edu.et/bitstream/handle/123456789/29745/Getu%20Ashagrie.pdf?sequence=1&isAllowed=y.
17. Aggarwal R, Ranganathan P. Study designs: part 2 – descriptive studies. Perspect Clin Res 2019;10:34–36.
18. Polit DF, Beck CT. Nursing Research (11th ed). Alphen aan den Rijn, Netherlands: Wolters Kluwer; 2021.
19. Huang T, Wang J, Chen Y, Ye Z, Fang Y, Xia Y. Knowledge, attitude and application towards fast track surgery among operating room paramedics: a cross-sectional study. BMC Health Serv Res 2022;22:1401.
20. Stavropoulou A, Stroubouki T. Evaluation of educational programmes-the contribution of history to modern evaluation thinking. Health Sci J 2014;8:193–204.
21. Clet A, Guy M, Muir JF, Cuvelier A, Gravier FE, Bonnevie T. Enhanced Recovery after Surgery (ERAS) Implementation and barriers among healthcare providers in France: a cross-sectional study. Healthcare (Basel) 2024;12.
22. Cohen R, Gooberman-Hill R. Staff experiences of enhanced recovery after surgery: systematic review of qualitative studies. BMJ Open 2019;9:e022259.
23. Goldblatt JG, Bibo L, Crawford L. Does Enhanced Recovery After Surgery Protocols Reduce Complications and Length of Stay After Thoracic Surgery: A Systematic Review of the Literature. Cureus 2024;16:e59918.
24. Pache B, Hübner M, Martin D, Addor V, Ljungqvist O, Demartines N, et al. Requirements for a successful Enhanced Recovery After Surgery (ERAS) program: a multicenter international survey among ERAS nurses. Eur Surg 2021;53:246–50.
25. Wang D, Liu Z, Zhou J, Yang J, Chen X, Chang C, et al. Barriers to implementation of enhanced recovery after surgery (ERAS) by a multidisciplinary team in China: a multicentre qualitative study. BMJ Open 2022;12:e053687.
26. Herbert G, Sutton E, Burden S, Lewis S, Thomas S, Ness A, et al. Healthcare professionals' views of the enhanced recovery after surgery programme: a qualitative investigation. BMC Health Serv Res 2017;17:617.
27. Mohamed RA, Alhujaily M, Ahmed FA, Nouh WG, Almowafy AA. Nurses' experiences and perspectives regarding evidence-based practice implementation in healthcare context: A qualitative study. Nurs Open 2024;11:e2080.
28. Yeheyis T, Hoyiso D, Borie YA, Tagesse N. Implementation of evidence-based clinical practice and its associated factors among health care workers at public hospitals in Sidama regional state, southern Ethiopia. PLoS One 2024;19:e0299452.
29. Xu P, Li D, Li J, Zhang C. Knowledge, attitude, and practice towards enhanced recovery after surgery among colorectal cancer patients. Sci Rep 2024;14:9034.

Risk of Peroneal Nerve Injury in All-inside Lateral Meniscal Repair through the Popliteus Tendon Using Five Different Needle Designs: A Cadaveric Study

Panpaporn Asavanapakas, M.D.*, Tanarat Boonriong, M.D.,
Wachiraphan Parinyakhup, M.D., Chaiwat Chuychoosakoon, M.D.

Department of Orthopedic Surgery, Faculty of Medicine, Prince of Songkla University, Hat Yai, Songkhla 90110, Thailand.

Abstract:

Objectives: All-inside meniscal repair through the popliteus tendon (PT) has been proposed to enhance fixation of posterior horn tears of the lateral meniscus. However, the proximity of the common peroneal nerve (PN) raises concerns regarding potential iatrogenic injury during suture placement. This study aimed to assess the risk of PN injury, and to evaluate the effectiveness of different needle curvatures and lengths in safely achieving capsular penetration during all-inside lateral meniscal repair through the PT.

Material and Methods: Twenty-six knees from 13 cadaveric specimens underwent simulated arthroscopic meniscal repair using TrueSpan devices, with five needle curvatures (straight, 12°-curved, 24°-curved, 12°-reverse-curved and 24°-reverse-curved) and three lengths (14 mm, 18 mm and 20 mm). Suture deployment was performed at both the upper and lower thirds of the lateral meniscus. Key outcomes included: incidence of PN injury, incidence of capsular under-penetration, distances from the needle tip to the PN and excess needle lengths beyond the capsule.

Results: No PN injury was observed in any of the repair attempts. Needle tip distances to the PN were not significantly different among all the devices. The 20-mm straight needle achieved 100% capsular penetration at the upper third of the meniscus, while the other needle types showed variable degrees of under-penetration.

Conclusion: All-inside lateral meniscal repair through the PT appeared safe, with no risk of PN injury in the cadaveric specimens. A 20-mm straight needle offered the most reliable capsular penetration at the upper third of the meniscus.

Keywords: all-inside repair, Lateral meniscus tear, Meniscal repair, Popliteus tendon

Corresponding author: Panpaporn Asavanapakas, M.D.
Department of Orthopedic Surgery, Faculty of Medicine, Prince of Songkla University, Hat Yai, Songkhla 90110, Thailand.
E-mail: panpaporn.a@psu.ac.th

Introduction

All-inside meniscal repair has been recognized as the gold standard treatment for tears of posterior horn of meniscus. This is due to its ability to provide sufficient reduction and stability to the tears, without having to make additional incisions for suture retrieval and knot tying; as opposed to the conventional inside-out method [1,2]. However, with lesions at the lateral meniscus, this repair technique can not be performed without concerns, as implant failure rates between 14% and 23% have been reported in previous studies[3-5]. The reasons explaining implant failure in all-inside lateral meniscal repair are because of the thin posterior knee capsule and the presence of a small gap between the meniscus and the knee capsule, lowering the stability of the implant anchroage[6-8].

To reduce the implant failure rate, the surgical technique of anchoring the suture to the capsule through the popliteus tendon (PT) has been proposed, and has been reported to result in good clinical outcomes[6,8,9]. However, suturing through the PT has caused concerns regarding common peroneal nerve (PN) injury due to its proximity to the posterolateral joint line. Cadaveric and magnetic resonance imaging (MRI) studies have been conducted to evaluate the risk of injury to the posterolateral neurovascular structures; including the PN[7,10-21]. The risk of PN injury during all-inside lateral meniscal repair with PT augmentation to the suture anchorage has been specifically examined in one MRI study[21]. Despite their study methodology, which took the actual operative conditions into account, the plane of the axial cuts of the MRI images used for analysis might not be parallel to the joint line in all of the cases. For this reason, these MRI cuts can not represent the actual positions of each specific structure in intra-operative situations.

This present study was undertaken[1] to evaluate the risk of PN injury during arthroscopic all-inside repair of the posterior horn of the lateral meniscus through the PT, using meniscal repair devices of different needle curvatures (straight, 12°-curve, 24°-curve, 12°-reverse-curved and 24°-reverse-curved) and lengths (14 mm, 18 mm and 20 mm). In addition to determine the ideal needle curvature and length for this repair technique, by conducting simulated repairs in knees of full cadaveric bodies.

Material and Methods

This prospective study was approved by the Institutional Review Board of the Faculty of Medicine of Prince of Songkla University [approval nos. 66-11-1-2-345]. Twenty-six knees from 13 cadaveric bodies (9 males and 4 females) of Asian descent were included in this study. The exclusion criteria were any cadaveric bodies with history of knee surgery; soft tissue and/or bony pathologies of the knee; such as tumors, fractures or deformities; meniscal pathologies, rheumatoid arthritis or patellar dislocation.

All of the recruited cadaveric bodies were placed in a supine position on a tilt table, with a side leg support attached to the side rail on the same side as the leg intended to be used in the repair. The knee was flexed to 90 degrees. A posterolateral (Henderson) incision was created for subsequent collection of data. The insertion of the lateral head of the biceps femoris was released to gain sufficient visualization of the posterolateral aspect of the joint capsule (Figure 1). An anterolateral (AL) portal was created, with a 1-cm stab incision 1 cm lateral to the lateral border of the patellar tendon, with the superior end of the incision ending at the level of the inferior pole of the patella. Intra-articular pressure was maintained at 30 mmHg, with a continuous fluid in-flow via an infusion pump. Arthroscopic examination for any knee pathologies was performed through the AL portal. All the eligible knees proceeded with the simulated repair steps.

To perform the simulated repair, an anteromedial (AM) portal was created 1 cm medial to the medial border of the patellar tendon at the level of the joint line, and used as a working portal. The knee was placed in a figure-of-four position (hip in 30° and knee in 90° flexion), with a varus force applied to the knee. This replicated the standard arthroscopic position for all-inside lateral meniscal repair (Figure 2). The locations for suture placement were identified

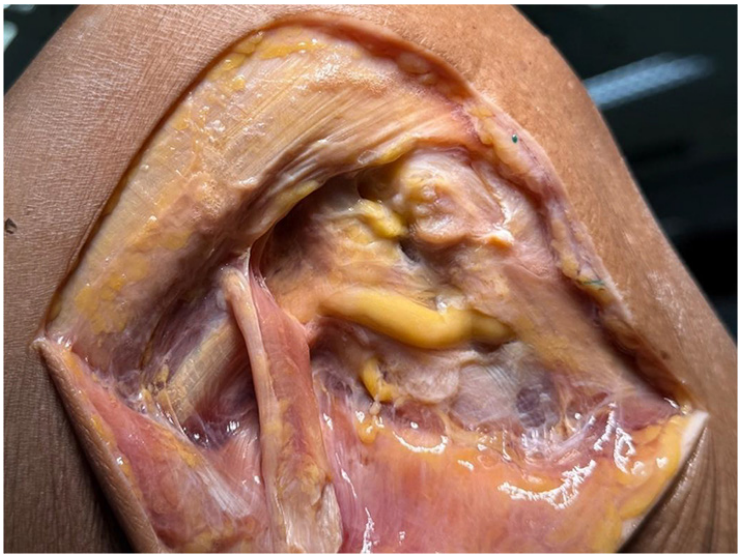

Figure 1 Posterolateral knee (Henderson) approach. The insertion of the biceps femoris was released to gain sufficient visualization of the posterolateral aspect of the joint capsule.

Figure 2 The knee was placed in a figure-of-four position (hip in 30° f and knee in 90° flexion), with varus force applied to the knee: replicating the standard arthroscopic position for all-inside lateral meniscal repair.

at the midpoints of the superior and inferior thirds of the lateral meniscus between the medial and lateral borders of the PT, and marked with an electrocautery. The sequences of the needle length (14 mm,18 mm and 20 mm) and curvature (straight, 12°-curved, 24°-curved, 12°-reverse-curved and 24°-reverse-curved) of the TrueSpan meniscal repair devices (DePuy Mitek, Raynham, MA) used in the simulated repair were randomized. The needle of the TrueSpan device, with randomaized curvature and length, was advanced through the superior third of the meniscus.

The knees were then put in a 90° flexion position, and the results were recorded through the previously created Henderson skin window.

Through direct visualization, via the Henderson skin window, any incidence of puncture injury of the PN or capsule underpenetration was recorded as numbers of events. In case of successful capsule penetration without PN injury, the closest distances from the needle tip to the PN and the excess needle lengths (Figure 3) were measured with a digital caliper three times. On the other hand, if there was PN injury or capsule underpenetration, these distances would be recorded as not assessed. The steps of simulated repair were repeated with all the needle combinations. Randomization of the needle combination sequence was performed and followed for the simulated repairs at the inferior third of the meniscus in the same manner as the superior third. The simulated repairs and measurements were performed by an experienced sports medicine orthopedic surgeon.

Statistical analysis

Statistical analysis was carried out using the R program and epicalc package (version 3.4.3, R Foundation for Statistical Computing). Averages of the three measurements of the distances from the needle tips of the 14-mm, 18-mm and 20-mm having different curvatures to the PN, with the excess needle lengths being reported as mean values. As these data were not normally distributed through the analysis of Shapiro-Wilk normality test, statistical significance among data was evaluated with Kruskal-Wallis test, and subsequently analyzed with Dunn's test with Bonferroni correction to minimize type I error: p-value being set at $p\text{-value}<0.05$.

The incidences of needle underpenetration and PN injury were expressed as percentages of the events of interest out of the number of repair attempts. The required sample size was calculated using the one-way ANOVA [effect size=0.25 (medium effect size), alpha (α)=0.05, power ($1-\beta$)=0.8, number of groups=15 (needles of 5 different

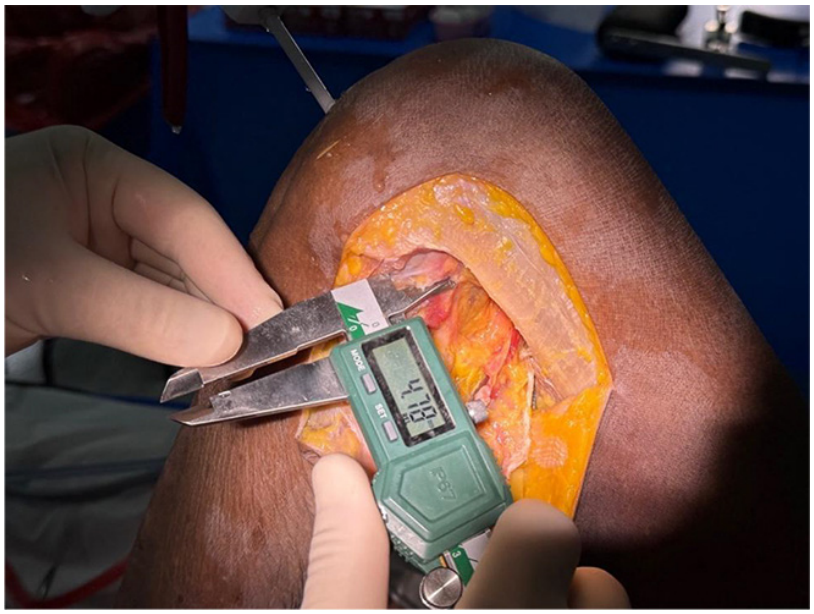

Figure 3 The excess needle length of a meniscal repair device was measured with a digital Caliper, via the posterolateral skin window.

curvatures and 3 different lengths)]. A 10% addition was added to the calculated sample size in case of missing data: a minimum of 24 knees was required.

Results

Twenty-six knees from 13 cadaveric bodies (9 males and 4 females) of Asian descent were included in the studyand the results are ahown below.

Risk of PN injury during repairs from the AM portal with straight, 12°-curved, 24°-curved, 12°-reverse-curved and 24°-reverse-curved needles, at 14 mm, 18 mm and 20 mm lengths

The incidence rate of PN injury during the simulated arthroscopic lateral meniscal repairs through the PT was 0%, with all the needle lengths and curvatures. The lowest average distance from the needle tip to the PN occurred with suture placement at the lower third of the meniscus made, with the 20-mm 24°-reverse-curved needle (Table 1). Nonetheless, there was no statistical significance (p-value>0.05) among all the average distance differences.

Rate of capsule underpenetration during repairs from the AM portal, with straight, 12°-curved, 24°-curved, 12°-reverse-curved and 24°-reverse-curved needles, at 14 mm, 18 mm and 20 mm lengths

During the repairs, there was 0% of unsuccessful capsule penetration when the 20-mm straight needles were used (Table 2). The remaining needle combination options posed risks of capsule underpenetration at varying degrees; ranging from 3.9% to 96.2%.

Distances from the needle tip to the PN and excess needle lengths in repairs made with straight, 12°-curved, 24°-curved, 12°-reverse-curved and 24°-reverse-curved needles, at 14 mm, 18 mm and 20 mm lengths

There was no statistical significance among the mean differences of the distances from the needle tip to the PN and the excess needle lengths.

Discussion

The most important finding of this current study was that suture placement through the PT during posterior horn of lateral meniscus repair resulted in 0% risk of PN injury, with all of the needle curvatures and lengths.

The safety of the PN in lateral meniscus repair, with the PT being augmented to the point of anchorage, has also been confirmed in an MRI study by Asavanapakas et al[21]. In that study, axial MRI cuts of knees in figure-of-four position were used in their analysis. Although, many factors have been controlled to make the results applicable to the actual operative settings, single axial sections of MRI images might not represent the orientation of the structures in the true joint line plane. Hence, whole cadaveric bodies were deemed an appropriate option to minimize this error.

From a biomechanical perspective, PT has been proposed as a reliable structure to be included in the anchorage point of an suture anchor. This is due to its high durability against tensile loads and static nature of the intra-articular portion[8,22,23]. Clinically, repairing tears of the posterior horn of the lateral meniscus through the PT resulted in good clinical outcomes among 200 patients over 45 months of follow-up period: as reported by Ouanezar et al.[6]. Nonetheless, 3.5% of the study population experienced failure of suture repair. The reasons for this failure rate has not been clearly explained in this previous study; however, high risk of improper anchor placement in this suture technique were reported to be at 77.5%, with a 14-mm needle and 100% with an 18-mm needle in a cadaveric study by Uchida et al.[7].

Despite its durability and the static nature of the PT, joint capsule is the preferred location for suture anchorage to reduce the risk of anchor migration. At the upper third of the lateral meniscus, the 20-mm straight needle was the only needle type that resulted in 0% joint underpenetration.

Table 1 The average distances from the needle tips of different curvatures and lengths to the PN (mm ± S.D.)

Curvatures	Straight			12°-curved			24°-curved			12°-reverse-curved			24°-reverse-curved		
Lengths (mm)	14	18	20	14	18	20	14	18	20	14	18	20	14	18	20
Upper 1/3	26.8 (±8.3)	25.6 (±8.1)	24.7 (±7.8)	31.6 (NA)*	29.1 (±6.9)	29.0 (±6.5)	27.0 (±4.9)	28.2 (±4.9)	31.3 (±8.6)	29.7 (±5.7)	25.0 (±7.9)	23.4 (±8.5)	23.9 (±6.4)	22.0 (±5.8)	22.7 (±9.3)
Lower 1/3	27.1 (±6.8)	25.3 (±7.6)	23.2 (±7.6)	36.7 (±20.0)	25.6 (±7.4)	26.5 (±6.8)	27.4 (±6.1)	28.9 (±9.1)	28.7 (±7.6)	29.7 (±11.1)	24.2 (±8.7)	23.6 (±8.4)	27.6 (±6.5)	23.0 (±8.2)	19.4 (±7.0)

*The S.D. was not assessable, as there was only one event of successful capsule penetration without PN injury.

Table 2 The percentages (%) of capsule underpenetration, with repairs made with different needle curvatures and lengths

Curvatures	Straight			12°-curved			24°-curved			12°-reverse-curved			24°-reverse-curved		
Lengths (mm)	14	18	20	14	18	20	14	18	20	14	18	20	14	18	20
Upper 1/3	50.0	3.9	0	96.2	61.5	38.5	84.6	57.7	42.3	61.5	23.1	3.85	65.4	30.8	11.5
Lower 1/3	65.4	19.2	19.2	88.5	61.5	19.2	73.1	46.2	11.5	76.9	53.9	19.2	80.8	57.7	38.5

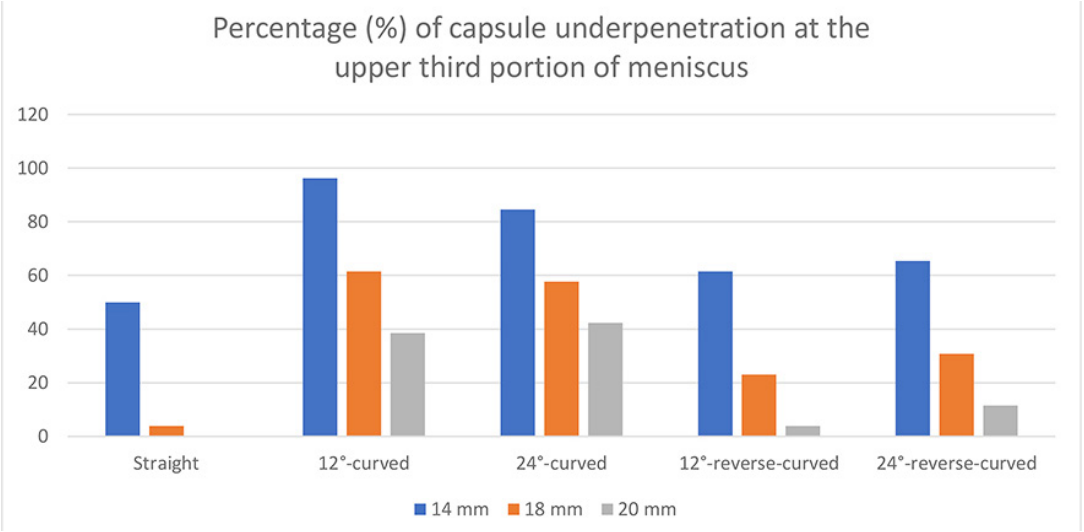

Figure 4 The percentages (%) of capsule underpenetration at the upper third portion of the lateral meniscus

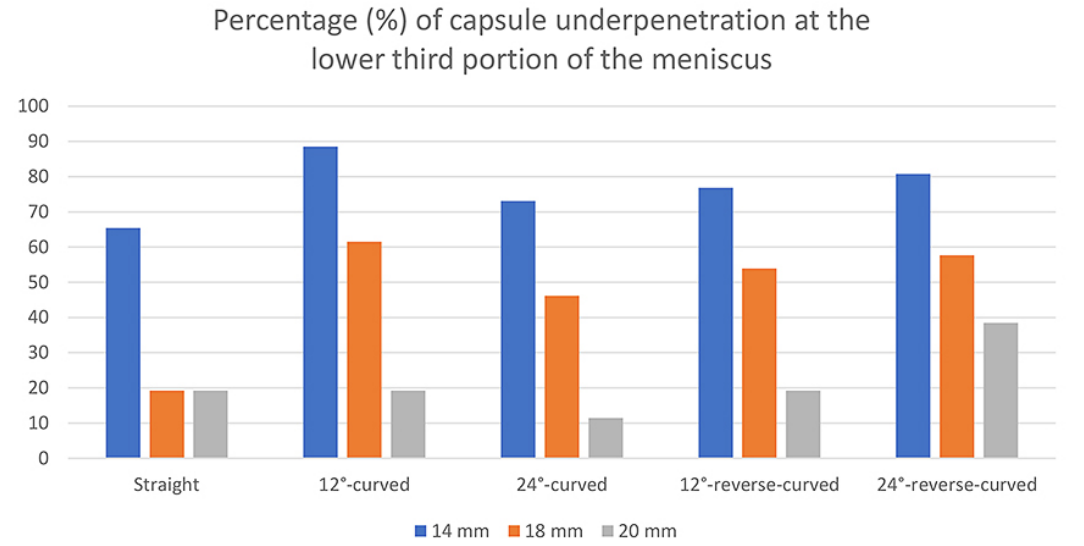

Figure 5 The percentages (%) of capsule underpenetration at the lower third portion of the lateral meniscus

Therefore, the recommended needle type for suture placement at this upper portion of the lateral meniscus is a 20–mm straight needle. On the other hand, at the lower third of the lateral meniscus, all the needle curvatures and lengths were not sufficient to achieve 100% successful knee capsule penetration. Therefore, suture placement at this location should be performed with caution, as implant failure may be persued.

There were a few limitations to this study. First, the proportion of the male cadavers was much higher than the female cadavers. Hence, the presented results might not represent the actual risk of PN injury or capsule

underpenetration in the female population. Second, the biceps femoris was released to expose the posterolateral aspect of the knee capsule. The release of the muscle might affect the soft tissue tension around the knee capsule, resulting in inaccurate results of the data. Third, the position of the knees needed to be changed from the figure-of-four position to a 90°-flexion position for data collection, via the window created with the Henderson approach. Although, the position of the repair devices and the angle of the knee flexion were kept the same throughout the change of position, random errors from this practice might arise. For future improvement, a more reliable method; such as, using a specifically designed tilt table that would allow data collection without having to change the knee position should be utilized.

In terms of the strengths, the methodology of the study was designed to simulate the actual operation. First, whole body cadavers instead of knee specimens were used. As the majority of the soft tissues were kept intact, the intra-articular and extra-articular structures were relatively unchanged. Second, the simulated repairs were performed through an arthroscopic approach, with actual meniscal repair devices instead of indirect methods; e.g. MRI image evaluation; wherein, orientation of the anatomic structures at the joint level may be inaccurate. Third, the curvatures and lengths of the repair needles experimented were extensive, allowing comprehensive understanding of a less studied surgical technique to be examined.

Conclusion

Simulated arthroscopic all-inside lateral meniscal repair including suture placement through the PT with meniscal repair devices of different needle curvatures, 14 mm, 18 mm and 20 mm, lengths resulted in no incidence of PN injury. For proper needle selection, to allow successful capsule penetration, recommendations provided in this study can be followed.

Acknowledgement

I would like to express my gratitude to my research advisor: Assoc. Prof. Tanarat Boonriong, M.D. for his guidance throughout the process of this research, and Asst. Prof. Wachiraphan Parinyakhup for his contribution in the data collection process.

Conflict of interest

There are no potential conflicts of interest to declare.

References

1. Becker R, Kopf S, Seil R, Hirschmann MT, Beaufils P, Karlsson J. From meniscal resection to meniscal repair: a journey of the last decade. Knee Surg Sports Traumatol Arthrosc 2020;28:3401–4.
2. Borque KA, Jones M, Cohen M, Johnson D, Williams A. Evidence-based rationale for treatment of meniscal lesions in athletes. Knee Surg Sports Traumatol Arthrosc 2022;30:1511–9. doi: 10.1007/s00167-021-06694-6.
3. Schweizer C, Hanreich C, Tscholl PM, Ristl R, Apprich S, Windhager R, et al. Nineteen percent of meniscus repairs are being revised and failures frequently occur after the second postoperative year: a systematic review and meta-analysis with a minimum follow-up of 5 years. Knee Surg Sports Traumatol Arthrosc 2022;30:2267–76.
4. Westermann RW, Wright RW, Spindler KP, Huston LJ, Wolf BR, Cox CL, et al. Meniscal repair with concurrent anterior cruciate ligament reconstruction. Am J Sports Med 2014;42:2184–92.
5. Paxton ES, Stock MV, Brophy RH. Meniscal repair versus partial meniscectomy: a systematic review comparing reoperation rates and clinical outcomes. Arthroscopy 2011;27:1275-88
6. Ouanezar H, Blakeney WG, Latrobe C, Saithna A, Fernandes LR, Delaloye JR, et al. The popliteus tendon provides a safe and reliable location for all-inside meniscal repair device placement. Knee Surg Sports Traumatol Arthrosc 2018;26:3611–9.
7. Uchida R, Mae T, Hiramatsu K, Iuchi R, Kinugasa K, Shino K, et al. Effects of suture site or penetration depth on anchor location in all-inside meniscal repair. Knee 2016;23:1024–8.
8. Mhaskar VA, Agrahari H, Maheshwari J. True all inside meniscus repair using the popliteus tendon. Eur J Orthop Surg Traumatol 2022;33:2151–7.

9. Ahn JH, Lee SH, Kim K Il, Nam J. Arthroscopic meniscus repair for recurrent subluxation of the lateral meniscus. Knee Surg Sports Traumatol Arthrosc 2018;26:787–92.
10. Shea KG, Dingel AB, Styhl A, Richmond CG, Cannamela PC, Anderson AF, et al. The position of the popliteal artery and peroneal nerve relative to the menisci in children: a cadaveric Study. Orthop J Sports Med 2019;7.
11. Rizzo MG, Seiter MN, Martin AR, Greif DN, Levi AD, Jose J, et al. A rare case of peroneal nerve palsy following inside-out lateral meniscus repair in a healthy collegiate-level football player. Interdiscip Neurosurg 2020;19:100619.
12. Oehler N, Foerg A, Haenle M, Blanke F, Vogt S. Assessment of popliteal neurovascular safety during all-inside suturing of the posterior horn of the lateral meniscus using Upright MRIs of the knee joint. Knee 2021;33:234–42.
13. Massey P, Parker D, Feibel B, Ogden A, Robinson J, Barton RS. Proximity of the neurovascular bundle during posterior-lateral meniscal repair: a comparison of the transpatellar, anteromedial, and anterolateral portals. Arthroscopy 2019;35:1557-64.
14. Mao DW, Upadhyay U, Thalanki S, Lee DYH. All-inside lateral meniscal repair via anterolateral portal increases risk of vascular injury: a cadaveric study. Arthroscopy 2020;36:225–32.
15. Leland DP, Pareek A, Therrien E, Wilbur RR, Stuart MJ, Krych AJ, et al. Neurological complications following arthroscopic and related sports surgery: prevention, work-up, and treatment. Sports Med Arthrosc Rev 2022;30:e1–8.
16. Laible C, Stein DA, Kiridly DN. Meniscal Repair. Journal of the American Academy of Orthopaedic Surgeons 2013;21:204–13.
17. Chuaychoosakoon C, Wuttimanop W, Tangjatsakow P, Charoenrattanawat S, Parinyakhup W, Boonriong T, et al. The danger zone for iatrogenic neurovascular injury in all-inside lateral meniscal repair in relation to the popliteal tendon: an MRI study. Orthop J Sports Med 2021;9.
18. Chuaychoosakoon C, Boonsri P, Tanutit P, Laohawiriyakamol T, Boonriong T, Parinyakhup W. The risk of iatrogenic peroneal nerve injury in lateral meniscal repair and safe zone to minimize the risk based on actual arthroscopic position: an MRI study. Am J Sports Med 2022;50:1858–66.
19. Abouheif MM, Shibuya H, Niimoto T, Kongcharoensombat W, Deie M, Adachi N, et al. Determination of the safe penetration depth during all-inside meniscal repair of the posterior part of the lateral meniscus using the FasT-Fix suture repair system. Knee Surg Sports Traumatol Arthrosc 2011;19:1868–75.
20. Yen YM, Fabricant PD, Richmond CG, Dingel AB, Milewski MD, Ellis HB, et al. Proximity of the neurovascular structures during all-inside lateral meniscal repair in children: a cadaveric study. J Exp Orthop 2018;5:50.
21. Asavanapakas P, Boonsri P, Parinyakhup W, Boonriong T, Chuaychoosakoon C. No risk of iatrogenic peroneal nerve injury in all-inside lateral meniscal repair with either 14- or 18-mm needles through the popliteus tendon in the standard arthroscopic knee conditions. Knee Surg Sports Traumatol Arthrosc 2023;31:2331–7.
22. Kaplan E. Surgical approach to the lateral (peroneal) side of the knee joint. Surg Gynecol Obsetet 1957: p.346–56.
23. LaPrade RF, Bollom TS, Wentorf FA, Wills NJ, Meister K. Mechanical properties of the posterolateral structures of the knee. Am J Sports Med 2005;33:1386–91.

JHSMR The 4th Annual Health Research International Conference
AHR-iCON 2025
Shaping the Future: Innovation, Health and Well-being
OCTOBER 9-10TH, 2025
THE FACULTY OF MEDICINE, PRINCE OF SONGKLA UNIVERSITY
Data Science/ Digital Health
R2-O-005

Skin-Sight: AI-Enhanced Early Detection and Classification of Skin Cancer, Using Image-Based Deep Learning Models

Punyapat Sengdonprai[1], Aueaphum Aueawatthanaphisut[2]*

[1]Srinakharinwirot University Prasarnmit Demonstration School, Bangkok 10110, Thailand.
[2]School of Information, Computer, and Communication Technology, Sirindhorn International Institute of Technology, Thammasat University, Pathum Thani, 12120, Thailand.

Abstract:

Objective: Both early and accurate diagnosis of skin cancer, particularly melanoma, basal cell carcinoma (BCC), and squamous cell carcinoma (SCC), remains a significant public health challenge; especially in underserved regions with limited access to dermatologists. This study proposes an AI-enhanced diagnostic framework, leveraging deep convolutional neural networks (CNNs) to facilitate automated skin cancer detection and classification from dermatoscopic and smartphone-acquired images.

Material and Methods: A total of 9,885 dermatoscopic images from the ISIC 2019 and 2020 Challenge datasets were utilized. The proposed framework comprised of a two-stage pipeline: (1) lesion segmentation, using a U-Net architecture to isolate the region of interest (ROI), and (2) classification via fine-tuned CNN models; including ResNet50, DenseNet121, MobileNetV2 and VGG-19. All models were initialized with ImageNet-pretrained weights and trained using transfer learning. Evaluation was performed using accuracy, precision, recall and F1-score. Classification was conducted on both multi-class (BCC, MEL, SCC) and binary (malignant vs. benign) tasks.

Results: Among the tested models, ResNet50 with U-Net-based segmentation achieved the highest accuracy of 96.6% in the three-class classification task. DenseNet121 and MobileNetV2 followed with accuracies of 94.1% and 91.4%; respectively. The VGG-19 model, applied to the binary classification task, reached an accuracy of 97.3%. Confusion matrix analyses confirmed high class-specific sensitivity and specificity; particularly for BCC and MEL. Incorporating lesion-focused segmentation markedly improved model discriminability and clinical relevance.

Conclusion: This study demonstrates that deep learning models, particularly when coupled with lesion segmentation, offer a scalable and reliable solution for early skin cancer detection. The cascaded framework enhances diagnostic performance, while maintaining computational feasibility, making it suitable for deployment in teledermatology and primary care settings. Its integration into clinical workflows may significantly reduce diagnostic delays and improve patient outcomes.

Keywords: convolutional neural networks, deep learning, melanoma, dermatoscopy, ResNet50, skin cancer detection, transfer learning, U-Net segmentation

Corresponding author: Aueaphum Aueawatthanaphisut
School of Information, Computer, and Communication Technology, Sirindhorn International Institute of Technology, Thammasat University, Pathum Thani, 12120, Thailand.
E-mail: m6622040662@g.siit.tu.ac.th

Introduction

Skin cancer is one of the most common malignancies worldwide, with three major histological types of clinical concern: basal cell carcinoma (BCC), squamous cell carcinoma (SCC), and melanoma (MEL). BCC, while rarely meta-static, can cause significant local tissue destruction (Figure 1). SCC carries a higher metastatic risk, while melanoma is the most aggressive; having rapid progression and high mortality if undetected early[1,2].

Accurate diagnosis is essential, yet traditional methods; such as visual inspection and dermatoscopy, are highly dependent on clinical expertise and often unavailable in rural or underserved settings. This underscores the need for scalable diagnostic tools that can support early detection.

Recent advances in deep learning (DL), particularly convolutional neural networks (CNNs), have demonstrated expert-level performance in medical image classification; including dermatology. Models; such as ResNet50, DenseNet121, and MobileNetV2—especially when combined with U-Net-based lesion segmentation—, have shown promising results on benchmark datasets like ISIC. Prior studies[3-6] have validated the effectiveness of cascaded pipelines that integrate segmentation and classification modules.

Building upon these developments, this study introduces Skin-Sight AI, a cascaded deep learning system combining U-Net segmentation with multiple CNN classifiers, so as to detect and classify skin cancer lesions from dermatoscopic images. The framework was evaluated via a curated dataset of 9,885 images, aiming to deliver accurate, interpretable and scalable solutions for dermatological diagnosis in resource-limited settings.

Material and Methods

Materials

This study employed publicly available dermatoscopic image datasets from the International Skin Imaging Collaboration (ISIC); specifically the ISIC 2019 and ISIC 2020 Challenge datasets. These datasets consist of expert-annotated, high-resolution images representing a diverse range of benign and malignant skin lesions, and are widely recognized as benchmarks for AI research in dermatology[3,4,6].

A total of 9,885 images were curated for this study. Among them, three malignant lesion types were prioritized due to their clinical relevance:

-BCC–4,448 images (45.0%)

-MEL–3,460 images (35.0%)

-SCC–1,977 images (20.0%)

This stratification reflects global incidence patterns and metastatic risks[1,2]. These three categories were the focus of both segmentation and multi-class classification tasks.

Figure 1 Representative visual appearances of the three major histological types of skin cancer.

To standardize inputs for deep CNNs, all images were resized to 224x224 pixels, converted to RGB colour space, and normalized to a range to ensure consistency and facilitate convergence in training[2,4]. Augmentation strategies—including horizontal/vertical flips, rotations (±15°) and contrast adjustments—were applied to increase variability and robustness; mimicking real-world acquisition conditions[2,3].

In addition to the nine-class dataset, a binary classification subset was created, regrouping images into:

-Malignant: Melanoma, BCC, SCC.

-Benign: Nevus, Seborrheic Keratosis, Pigmented Benign Keratosis, etc.

This binary partition supports clinical screening use cases, where quick malignant/benign triage is critical. VGG-19, known for its performance on limited class separability tasks[4], was used exclusively for this binary task.

All data were split into 70% training, 15% validation, and 15% external test sets, using stratified sampling. The external test set (1,200 images, sourced from ISIC 2018) was withheld entirely during model training and hyperparameter tuning to ensure unbiased evaluation. To further confirm reliability, a 5×2 nested cross-validation strategy was also employed within the training and validation sets[1,3,6].

This pre-processed dataset served as the foundation for a cascaded AI pipeline, comprising lesion segmentation via U-Net and classification via multiple CNN architectures, in accordance with current best practices in interpretable medical AI systems[3,6].

Methods

1. Overview of the AI pipeline

A cascaded artificial intelligence (AI) pipeline was designed to perform automated skin cancer detection, using a two-stage architecture comprising of lesion segmentation and lesion classification. This pipeline was developed to enhance the diagnostic accuracy and clinical reliability of deep learning systems applied to dermatoscopic images, where irrelevant background skin features and inter-patient variability often introduce noise into direct classification approaches.

In the first stage, lesion segmentation was performed using the U-Net architecture; a fully convolutional neural network (FCN) widely used in medical image segmentation tasks. The objective of this step was to generate a binary mask that accurately delineates the region of interest (ROI), i.e., the skin lesion. The ROI was then used to extract a cropped version of the original image; thereby, eliminating surrounding non-lesional regions that might introduce irrelevant features. This segmentation-enhanced preprocessing has been shown to improve downstream classification by enforcing the model's attention toward lesion-specific morphological cues[3].

In the second stage, the segmented ROI is provided in parallel to four CNN heads. ResNet50, DenseNet121, and MobileNetV2 address the multi-class task (BCC/MEL/SCC), with a 3-way softmax. Separately, VGG-19 addresses the binary triage task (malignant vs benign), with a sigmoid output. No CNN is chained after another; each head receives the same ROI and is trained/evaluated independently. This prevents serial information coupling and enables fair, task-matched comparisons[6].

The overall pipeline was inspired by the cascaded design strategy proposed in prior studies[3], wherein segmentation and classification are treated as distinct but interdependent modules. Such modularization not only improves performance but also allows for explainable intermediate outputs (i.e., lesion masks), which are valuable for clinical verification and trust.

Final prediction tasks and outputs. From the U-Net–segmented lesion ROI we formulated two independent tasks: (i) multi-class lesion subtype classification—basal cell carcinoma (BCC), melanoma (MEL), and squamous cell carcinoma (SCC); and **(ii) binary malignant-vs-benign triage. The ROI is fed in parallel to three multi-class CNN heads (ResNet50, DenseNet121, MobileNetV2), each

terminating in a 3-way softmax, and to a separate binary head (VGG-19), with a 1-node sigmoid (Figure 2). No CNN is chained after another; heads are trained and evaluated independently to ensure task-matched, fair comparisons.

Decision rules and metrics. For the multi-class task, the final prediction is the argmax of softmax probabilities (with per-class results and macro-averaged metrics). For the binary task, a single operating threshold τ is selected on the validation set by Youden's J, and then frozen for the external test set. We report accuracy, AUROC (one-vs-rest macro for multi-class; standard AUROC for binary), macro-F1, per-class F1, and 95% CIs. When reported, an optional probability-averaging ensemble over the three multi-class heads is computed by averaging class logits/probabilities, and is compared against each single model on a like-for-like basis.

2. Lesion segmentation using U-Net

To isolate the lesion region from the surrounding skin with high precision, semantic segmentation was performed using the U-Net architecture. This is a widely adopted standard in biomedical image analysis due to its encoder–decoder topology and strong spatial feature retention. The model accepted 224×224 RGB dermatoscopic images as input and generated binary segmentation masks indicating pixel-wise lesion probabilities. The contracting path consisted of repeated 3×3 convolutions with ReLU activation, followed by 2×2 max pooling, progressively reducing spatial dimensions while expanding feature depth to capture high-level semantic context. At the network's center, the bottleneck layer encoded deep lesion representations with high filter capacity. The expansive path mirrored the encoder, using 2×2 transposed convolutions

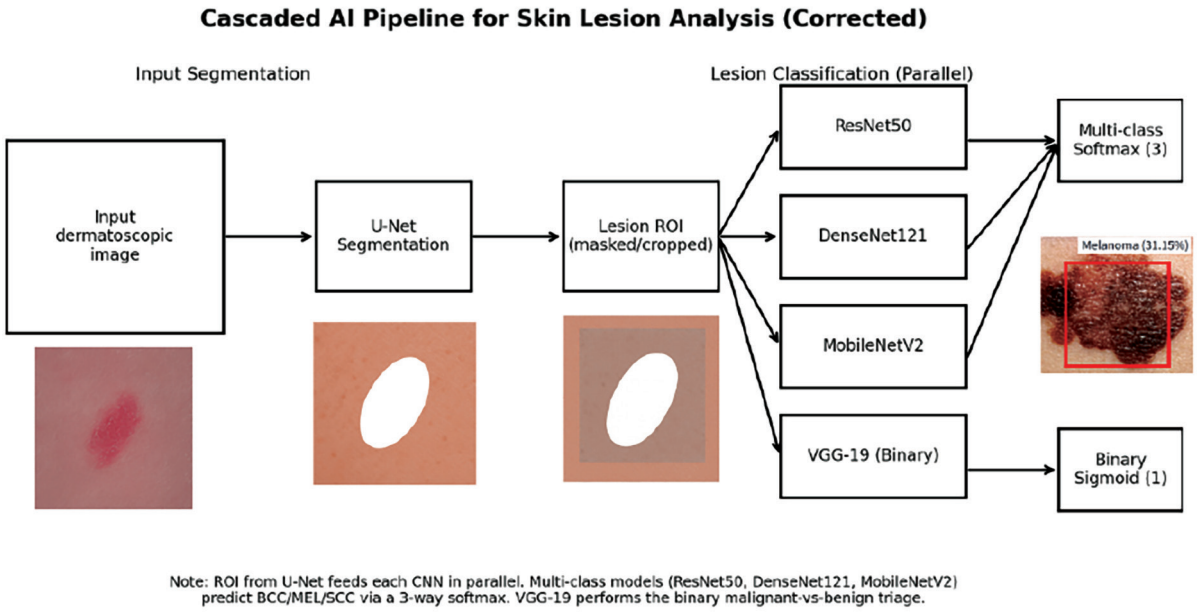

Figure 2 U-Net first segments the lesion and yields a masked/cropped ROI. The ROI is then fed in parallel to three multi-class classifiers (ResNet50, DenseNet121, MobileNetV2), each predicting BCC/MEL/SCC via a 3-way softmax. A separate VGG-19 head performs the binary malignant-vs-benign triage via a 1-node sigmoid. This design prevents inadvertent serial dependencies among CNNs, and aligns all comparisons under matched input/output conditions.

for up sampling. Crucially, skip connections concatenated encoder features with corresponding decoder layers, allowing fine-grained localization to be retained: essential for segmenting heterogeneous lesion borders. The final output was produced via a 1×1 convolution, followed by a sigmoid activation, generating a binary mask with lesion probability per pixel. Binary cross-entropy was used as the primary loss function, and the Dice coefficient was monitored to account for foreground–background imbalance during training. These binary masks were then applied to crop the ROI from the original images, which were subsequently resized to 224×224, and passed to downstream CNN classifiers. This segmentation-first approach helped eliminate irrelevant background noise, enabling the classifiers to focus on lesion-specific features; thereby, improving diagnostic performance and model interpretability. This strategy aligns with prior studies[3,6], demonstrating that incorporating U-Net-based lesion segmentation into classification pipelines enhances accuracy and clinical reliability in skin lesion analysis (Figure 3).

3. Deep CNN-based lesion classification

Following lesion segmentation, the extracted ROI was used as input for classification using four different deep CNN architectures. Each model was selected based on its unique structural advantages in addition to its suitability for either multi-class or binary skin cancer classification. All models were implemented using Keras with TensorFlow backend and initialized with ImageNet pre-trained weights, followed by fine-tuning on the ISIC dataset.

Results

1. Classification performance

Table 1 summarizes the classification performance of the four models evaluated in this study. The ResNet50 model, combined with U-Net-based lesion segmentation, achieved the highest performance in multi-class classification.

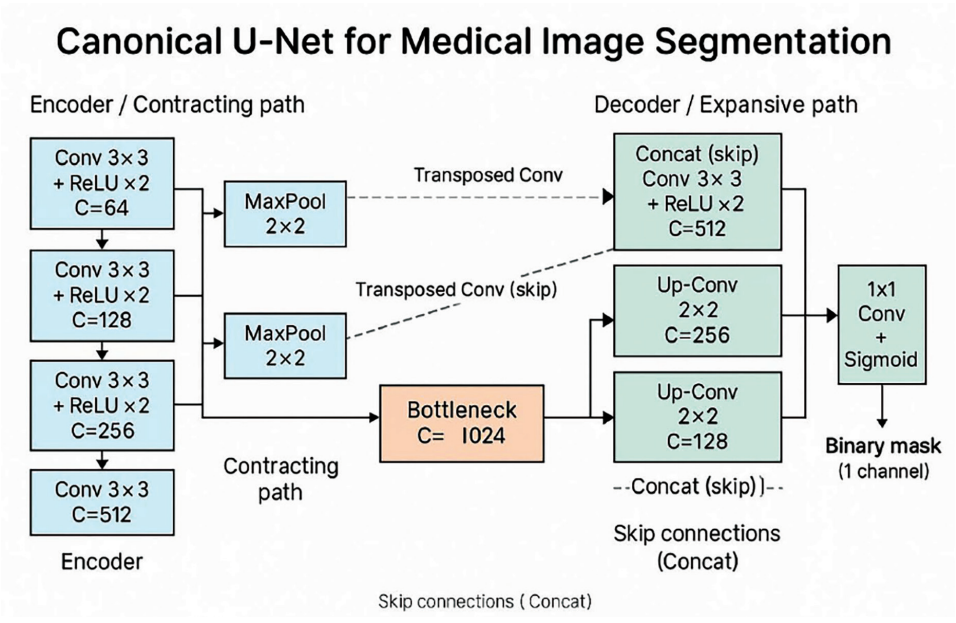

Figure 3 U-Net architecture for lesion segmentation. The model features an encoder–decoder structure with skip connections. The contracting path extracts contextual features, the bottleneck encodes semantic information, and the expansive path restores spatial resolution. The output is a binary mask delineating the lesion region.

It had an accuracy of 96.6%, precision of 0.95, recall of 0.94, and an F1-score of 0.95. This result highlights the effectiveness of the cascaded pipeline; wherein. lesion-focused ROIs improve model discriminability by reducing background noise and irrelevant features (Table 2).

The VGG-19 model, which was applied for binary classification (malignant vs. benign), achieved the highest accuracy overall at 97.3%, along with strong precision (0.96) and recall (0.95) values. This outcome reflects the model's suitability for binary tasks, where the decision space is less complex compared to multi-class classification (Table 3).

Among the remaining models, DenseNet121 outperformed MobileNetV2 in all metrics, which is consistent with its architecture that promotes dense feature propagation and reuse. MobileNetV2, while computationally lightweight, delivered competitive results and may serve as a viable option in resource-constrained applications; such as mobile diagnostic platforms.

2. Evaluation metrics

To comprehensively assess the classification models, four key performance metrics were employed.

-Accuracy: The proportion of correct predictions over the total number of predictions. It is a general measure of model correctness; however, it may be skewed by class imbalance.

-Precision: The ratio of true positives to all predicted positives. It reflects the model's ability to avoid false positives, and is particularly important in clinical settings where overdiagnosis may lead to unnecessary biopsies.

-Recall (Sensitivity): The ratio of true positives to all actual positives. It measures how well the model captures all true cancer cases, which is crucial in minimizing false negatives in skin cancer screening.

-F1-Score: The harmonic means of precision and recall. It balances the trade-off between false positives and false negatives, and is especially suitable for imbalanced datasets.

All metrics were macro-averaged across classes to ensure fair comparison in the multi-class setting. Macro-averaging treats each class equally, making it suitable when class distribution is uneven: a common characteristic in dermatoscopic datasets where certain cancer types (e.g., melanoma) are underrepresented.

Table 1 Deep CNN-based lesion classification

Model	Task	Input type	Output layer	Loss function	Remarks
ResNet50	Multi-class (3 classes: BCC, MEL, SCC)	224×224 segmented ROI	Softmax (3 outputs)	Categorical Crossentropy	Strong baseline; residual learning; benefits from U-Net ROI
DenseNet121	Multi-class (3 classes: BCC, MEL, SCC)	224×224 ROI or full image	Softmax (3 outputs)	Categorical Crossentropy	Dense connectivity; effective for subtle pattern recognition
MobileNetV2	Multi-class (3 classes: BCC, MEL, SCC)	224×224 segmented ROI	Softmax (3 outputs)	Categorical Crossentropy	Lightweight; optimized for mobile/edge deployment
VGG-19	Binary (Malignant vs Benign)	224×224 ROI or full image	Sigmoid (1 output)	Binary Crossentropy	Simple deep stack; suitable for binary triage applications

Table 2 Classification performance

Model	Task	Input type	Output units	Activation	Loss function	Remarks
ResNet50	Multi-class (3 classes: BCC, MEL, SCC)	224×224 lesion ROI (masked/ cropped)	3 (p[BCC], p[MEL], p[SCC])	Softmax	Categorical cross-entropy	Parallel head; same ROI as others
DenseNet121	Multi-class (3 classes: BCC, MEL, SCC)	224×224 lesion ROI (masked/ cropped)	3 (p[BCC], p[MEL], p[SCC])	Softmax	Categorical cross-entropy	Dense connectivity
MobileNetV2	Multi-class (3 classes: BCC, MEL, SCC)	224×224 lesion ROI (masked/ cropped)	3 (p[BCC], p[MEL], p[SCC])	Softmax	Categorical cross-entropy	Lightweight backbone
VGG-19	Binary (Malignant vs Benign)	224×224 lesion ROI (masked/ cropped)	1 (p[malignant])	Sigmoid	Binary cross-entropy	Separate binary head

Table 3 Model performance

Model	Accuracy (%)	Precision	Recall	F1-score
ResNet50 + U-Net	96.6	0.95	0.94	0.95
DenseNet121	94.1	0.92	0.91	0.92
MobileNetV2	91.4	0.88	0.87	0.88
VGG-19 (Binary)	97.3	0.96	0.95	0.96

In this context, the F1-score was emphasized as the primary metric for model comparison, due to its robustness in handling class imbalance and its clinical relevance in balancing sensitivity and specificity.

3. Confusion matrix analysis

To supplement the quantitative evaluation, confusion matrices were constructed for all four models to visualize classification performance across lesion types (Figure 4). These matrices highlight the models' class-specific strengths and limitations; particularly in distinguishing the three malignant types—BCC, MEL, and SCC as well as in the binary classification task using VGG-19.

ResNet50 + U-Net demonstrated the most favorable performance, with strong diagonal dominance. BCC, being the most distinct and abundant class, showed minimal misclassification. MEL, despite its visual similarity to other lesions, was accurately identified in over 96% of cases, underscoring the effectiveness of lesion-focused ROI segmentation in enhancing feature learning.

DenseNet121 also performed well, but showed slightly more confusion between MEL and SCC. This was likely due to texture overlap and its inherent dense connectivity, which may amplify shared visual patterns across classes.

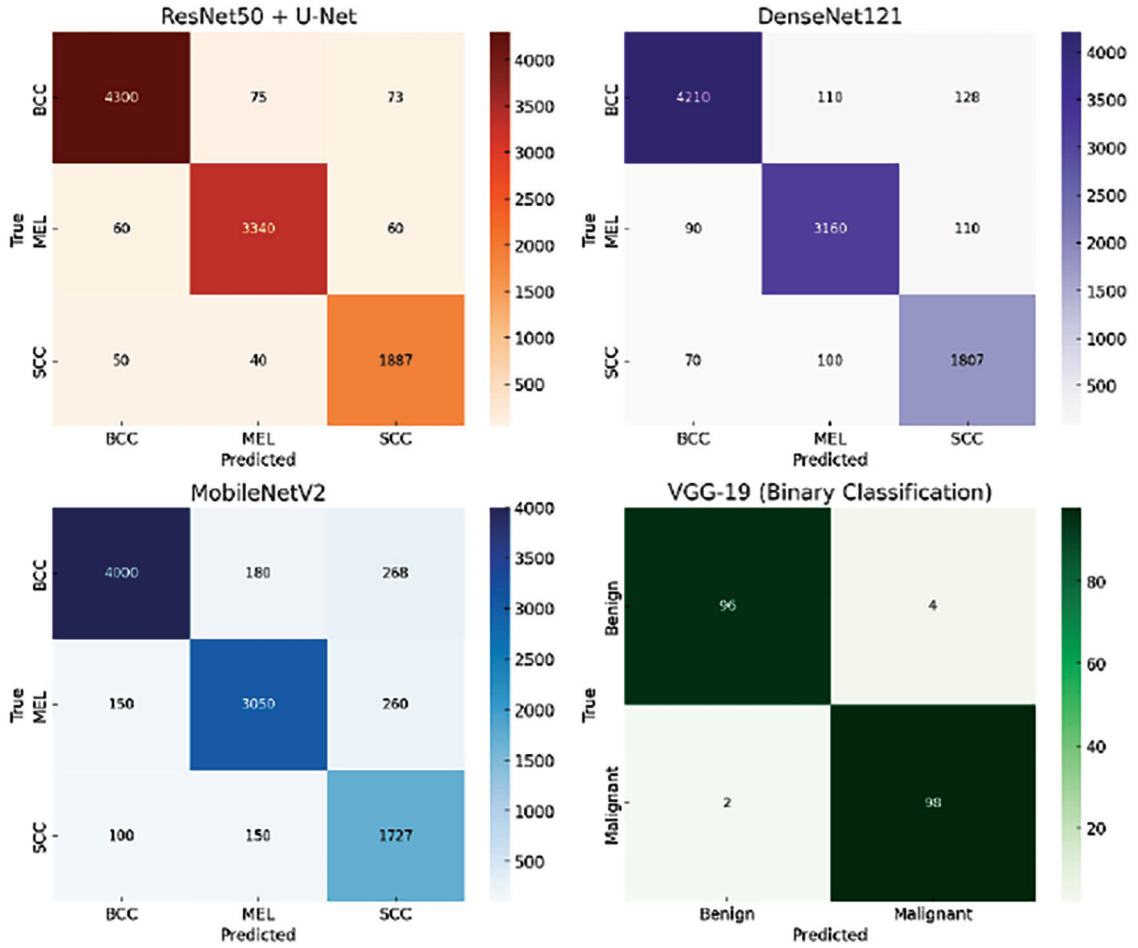

Figure 4 Comparative confusion matrices across models

MobileNetV2, designed for computational efficiency, showed the highest rate of misclassifications among multi-class models. Notably, BCC was more frequently confused with other classes, suggesting that model compactness may come at the cost of representational capacity. However, the model remains suitable for resource-constrained scenarios.

In contrast, VGG-19, applied to binary classification, achieved near-perfect separation between malignant and benign lesions. Both false positives and false negatives were minimal, reinforcing the model's suitability for initial screening applications.

Overall, the confusion matrices validate the role of segmentation in improving classification accuracy and reveal how architectural complexity influences both precision and generalizability. These insights offer critical guidance for selecting models in deployment scenarios and for refining future AI diagnostic systems.

4. External test set evaluation

To validate model generalizability, an independent external test set (ISIC 2018, n=1,200) was employed. Figure 5 presents ROC curves, where ResNet50+U-Net achieved the highest AUROC (0.971), followed by DenseNet121 (0.955) and MobileNetV2 (0.932). VGG-19, applied to the

binary malignant vs. benign task, achieved an AUROC of 0.968.

Figure 6 shows precision–recall curves, further highlighting the superior discriminability of ResNet50+U-Net, with high precision maintained across a broad recall range. MobileNetV2 demonstrated modestly lower PR performance, consistent with its lightweight architecture.

Figure 7 depicts confusion matrices. For multi-class classification, ResNet50+U-Net showed strong diagonal dominance with minimal confusion; particularly between melanoma and SCC. For the binary task, VGG-19 demonstrated near-perfect separation of malignant and benign lesions.

Collectively, these external test results confirm the robustness of the cascaded framework, while reflecting slightly lower but more realistic performance compared to validation; thereby, mitigating concerns of evaluation bias.

Discussion

This study validates the effectiveness of deep learning-based methods for early skin cancer detection using dermatoscopic imagery. Among the evaluated models, the cascaded ResNet50 + U-Net pipeline achieved the best multi-class classification performance; having an accuracy of 96.6% and balanced precision, recall, and F1-score. These results underscore the importance of lesion-focused segmentation in enhancing classifier attention and suppressing irrelevant background information. The associated confusion matrix confirmed minimal misclassification; particularly between melanoma and morphologically similar classes.

DenseNet121 also showed strong performance, benefitting from its densely connected layers that facilitate feature reuse and effective gradient flow. Although, it trailed ResNet50 slightly, its robustness in handling intra-class variation makes it a reliable alternative.

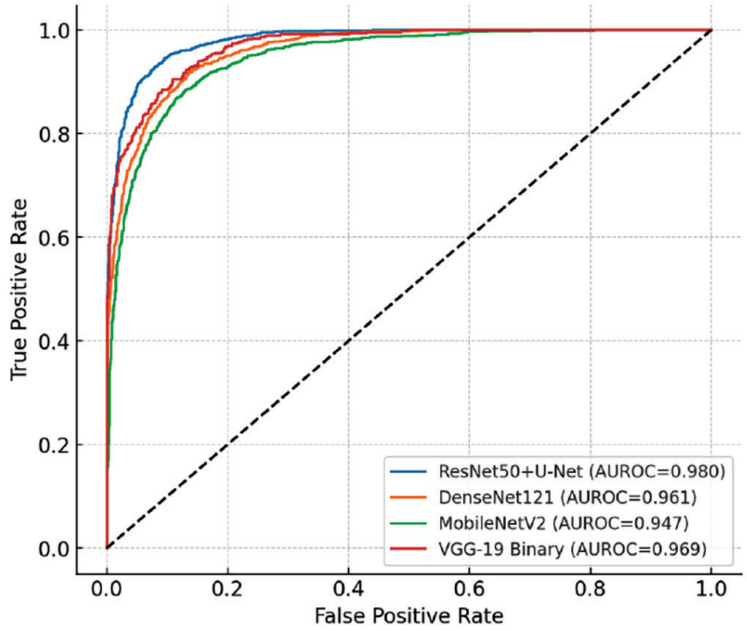

Figure 5 ROC curves on external test set

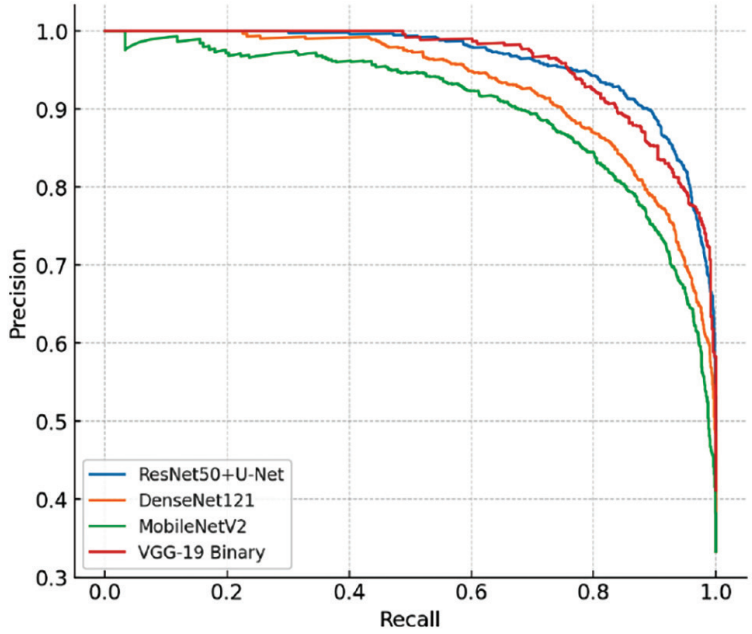

Figure 6 Precision–recall curves on external test

MobileNetV2, designed for efficiency in edge environments, demonstrated a moderate trade-off in performance (F1-score: 0.88). Its reduced representational depth likely contributed to a higher misclassification rate, though its compact design supports real-time use in mobile or remote healthcare settings.

In the binary classification task, VGG-19 achieved the highest overall accuracy (97.3%), reflecting its suitability for simplified decision boundaries. Its effectiveness reinforces the value of using lightweight, interpretable models for initial triage between malignant and benign lesions; especially in clinical screening workflows.

Furthermore, model interpretability was enhanced through XAI tools like Grad-CAM and SHAP, enabling visual explanation of predictions and improving clinician trust. Expert feedback affirmed the system's utility in diagnostic support; particularly in low-resource settings where specialist access is limited.

Nonetheless, while the addition of an independent, external test set improved methodological rigor, we recognize that broader multi-center validation remains necessary. Future research should incorporate larger, heterogeneous datasets across hospitals to ensure generalizability and robustness under domain shift, and the class imbalance—especially underrepresentation of SCC—could influence real-world deployment performance. Future research should focus on multi-center validation, real-time testing via smartphone-based apps, and clinical integration to assess usability in diverse environments.

Conclusion

This study presents Skin-Sight AI, a cascaded deep learning framework, integrating U-Net-based segmentation with state-of-the-art CNN classifiers for early detection and classification of skin cancer from dermatoscopic images. The system achieved high diagnostic performance across both multi-class and binary classification tasks, with ResNet50 + U-Net and VGG-19 emerging as the most effective models for multi-class and binary tasks, respectively.

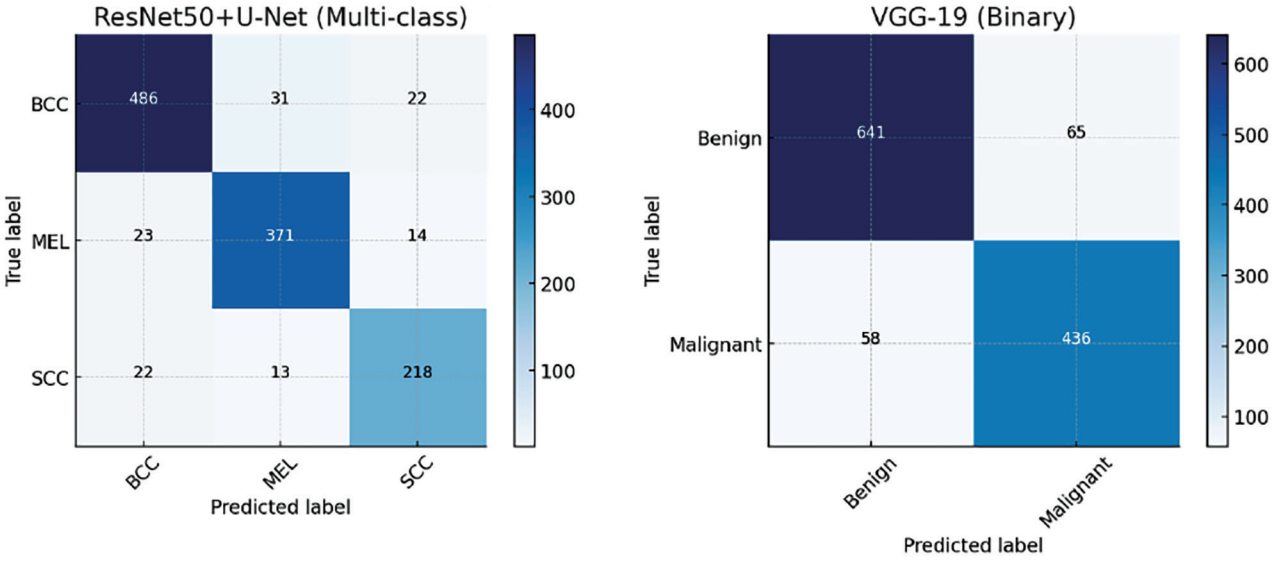

Figure 7 Confusion matrices on external test set

By leveraging lesion-focused segmentation, transfer learning and rigorous model evaluation, the proposed system demonstrates considerable potential as a scalable, interpretable and clinically applicable diagnostic support tool. It is particularly well-suited for deployment in underserved and remote areas where access to dermatological expertise is limited, yet early cancer detection remains critical.

Future directions include: extending the framework to support additional lesion types, integrating ensemble learning strategies and deploying the model in real-world telemedicine platforms. The inclusion of explainability and user-friendly interfaces further strengthens the case for integrating AI-based tools like Skin-Sight into routine dermatological workflows. It has the overarching goal of reducing diagnostic delay, improving early intervention rates and ultimately enhancing patient outcomes.

Acknowledgement

The authors gratefully acknowledge the support of the ISIC Archive for providing publicly accessible dermatological image datasets. Special thanks to the dermatologists that provided valuable clinical insights and feedback on the interface usability and diagnostic relevance.

Conflict of interest

The authors declare that there are no known financial or non-financial competing interests that could have appeared to influence the work reported in this paper.

References

1. Riyadi MA, Ayuningtias A, Isnanto RR. Detection and classification of skin cancer using YOLOv8n, 2024 11th International Conference on Electrical Engineering, Computer Science and Informatics (EECSI), Yogyakarta, Indonesia. 2024;p.9-15.
2. Abir MIH, Hossain A, Salam T. Using ImageNet Xception model to identify skin cancer and non-skin cancer image classification, 2024 IEEE International Conference on Computing, Applications and Systems (COMPAS), Cox's Bazar, Bangladesh. 2024;p.1-6.
3. Pattanaik A, Das L, Banerjee S. Cascaded approach for image segmentation and classification for skin cancer detection, 2024 5th International Conference for Emerging Technology (INCET), Belgaum, India. 2024;p.1-5.

4. Barbadekar A, Ashtekar V, Chaudhari A. Skin cancer classification and detection using VGG-19 and DesNet, 2023 International Conference on Computational Intelligence, Networks and Security (ICCINS), Mylavaram, India. 2023;p.1-6.
5. Lau HT, Al-Jumaily A. Automatically early detection of skin cancer: study based on nueral netwok classification, 2009 International Conference of Soft Computing and Pattern Recognition, Malacca, Malaysia. 2009;p.375-80.
6. Khan HC, Kim MAI, Mozumder R, Islam Sumon TP, Armand T, Omair M. Skin cancer detection using transfer learning models and ensemble approach to enhanced diagnostic accuracy, 2025 27th International Conference on Advanced Communications Technology (ICACT), Pyeong Chang, Republic of Korea. 2025; p.131-5.

JHSMR The 4th Annual Health Research International Conference
AHR-iCON 2025
Shaping the Future: Innovation, Health and Well-being
OCTOBER 9-10TH, 2025
THE FACULTY OF MEDICINE, PRINCE OF SONGKLA UNIVERSITY
Data Science/ Digital Health
R2-O-006

Fusion of Thermal and Multispectral Diabetic Foot Ulcer Imaging with AI, for Non-Invasive Healthcare Monitoring

Chakrin Techaboonsermsak[1], Aueaphum Aueawatthanaphisut[2]*

[1]Ramkhamhaeng Advent International School, Huamark, Bang Kapi, Bangkok 10240, Thailand.
[2]School of Information, Computer, and Communication Technology, Sirindhorn International Institute of Technology, Thammasat University, Pathum Thani 12120, Thailand.

Abstract:

Objective: Diabetic Foot Ulcer (DFU) is one of the most common and severe complications in diabetic patients, often leading to infection, necrosis and in extreme cases amputation. Early detection is critical for effective intervention. This study proposes a beta-version Artificial Intelligence (AI) system for non-invasive monitoring and assessment of early-stage DFU. By fusing data from thermal RGB and multispectral imaging, the system aims to detect subclinical changes associated with ulcer formation, enabling unbiased evaluation and minimizing direct wound contact.

Material and Methods: The AI model was trained using publicly available datasets consisting of thermal and multispectral foot images categorized according to ulcer severity. We employed the University of Texas Wound Classification System to assess ulcer depth, presence of infection, and ischemia. Furthermore, anatomical localization was enhanced using the Medial Plantar Area (MPA) and Lateral Plantar Area (LPA) coding, adapted from Alshayeji (2022), to ensure consistency in labeling. A multimodal deep learning pipeline was developed, integrating segmentation and classification tasks to analyze lesion risk and progression.

Results: The proposed system achieved an overall classification accuracy of 97.8%, with an F1-score of 0.94. Segmentation of the lesion area reached an Intersection over Union (IoU) score of 0.91 on the test set. The fusion of thermal and multispectral modalities significantly outperformed single-modality models, with a 9.3% improvement in sensitivity for early-stage detection.

Conclusion: This multimodal AI framework demonstrates strong potential as a non-invasive tool for continuous DFU monitoring, early intervention and personalized wound care. It lays the groundwork for future integration into diabetic healthcare systems and wearable telemedicine solutions. In this study, we report results on a dataset comprising of 1,236 images across thermal, multispectral, and RGB modalities from 198 patients, with clear class distribution following the University of Texas Wound Classification System (Grades 0/I/II). The proposed multimodal fusion framework demonstrates strong performance and practical potential for integration into telemedicine platforms as well as future wearable deployments for continuous at-home monitoring.

Corresponding author: Aueaphum Aueawatthanaphisut
School of Information, Computer, and Communication Technology, Sirindhorn International Institute of Technology, Thammasat University, Pathum Thani, 12120, Thailand.
E-mail: m6622040662@g.siit.tu.ac.th

Keywords: artificial intelligence, diabetic foot ulcer, early detection, multispectral imaging, multimodal fusion, non–invasive monitoring, segmentation, thermal imaging

Introduction

Diabetic Foot Ulcer (DFU) is a serious and common complication in individuals with diabetes mellitus; particularly with those having poorly managed blood glucose levels. It is estimated that 15–25% of diabetic patients will develop a foot ulcer during their lifetime, with a high risk of infection, hospitalization, and even amputation if left untreated.

Early detection and continuous monitoring of DFUs are essential to reduce the clinical burden and improve patient outcomes. Traditional diagnostic methods often involve visual inspection, manual palpation, or invasive techniques, which are limited in detecting early or subclinical signs; such as ischemia or neuropathy. Moreover, excessive contact with the wound can increase the risk of infection.

In recent years, non–invasive imaging modalities; including thermal imaging and multispectral imaging, have shown promise in detecting underlying physiological changes associated with DFUs before visible tissue breakdown occurs.

To provide a clear understanding of the potential and necessity for multimodal imaging in the early detection and monitoring of Diabetic Foot Ulcers (DFUs), Figure 1 illustrates four key perspectives obtained from different imaging modalities:

(a) RGB clinical image

This is the conventional visual observation method used by healthcare professionals during physical examination. The DFU appears as a visible open wound located on the plantar surface of the foot. Although, RGB images can capture surface–level visual signs; such as skin breakage, discoloration or dryness, they lack physiological insight into tissue perfusion or subclinical inflammation.

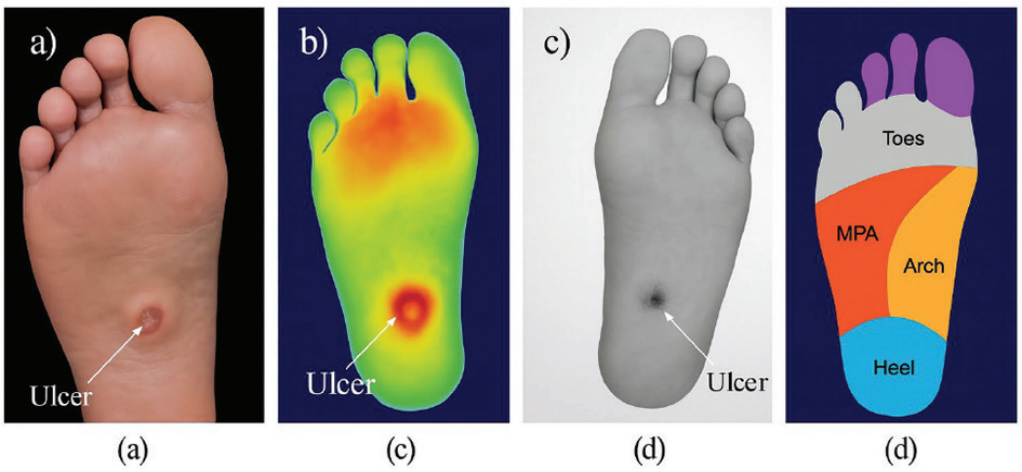

Figure 1 Multimodal imaging perspectives for diabetic foot ulcer (DFU) assessment.
(a) RGB clinical image showing visible ulceration on the plantar surface.
(b) Thermal image indicating heat asymmetry and inflammation at the ulcer site.
(c) Multispectral image revealing perfusion deficit and tissue damage.
(d) Anatomical zone map of the plantar foot; including toes, MPA (Medial Plantar Area), arch and heel, used for standardized ulcer localization.

The dependency on clinician expertise also introduces subjectivity in diagnosis and assessment.

(b) Thermal imaging

This modality provides insight into temperature distribution across the foot surface. In this figure, the ulcerated region exhibits a distinct hot zone (shown in red and yellow), indicating abnormal heat concentration, which may result from inflammation, infection or impaired blood flow regulation due to autonomic neuropathy. Thermal asymmetry between the affected and healthy regions has been widely recognized as an early indicator of DFU progression. This makes thermal imaging a valuable non-contact modality for early-stage detection, even before visible ulceration occurs[1].

(c) Multispectral imaging

The multispectral image captures subtle variations in tissue reflectance across different wavelengths, revealing physiological properties such as oxygen saturation (StO_2), blood perfusion, and tissue health. In this image, the ulcer appears as a darker region, indicating reduced perfusion or ischemia. Compared to RGB and thermal modalities, multispectral imaging offers deeper insight into tissue viability and wound severity. It can help classify ulcers into ischemic, neuropathic or neuroischemic types with higher precision[1].

(d) Anatomical zoning map

This schematic diagram divides the plantar surface into clinically relevant zones:

-Toes (distal digits),

-Medial Plantar Area (MPA),

-Lateral Plantar Area (LPA) (not shown separately here, but often grouped in MPA),

-Arch (non-weight-bearing area), and

-Heel (major weight-bearing area).

Such zonal classification is vital for standardizing data labeling and ensuring anatomical consistency during model training. This structured zoning enhances the spatial interpretability of AI predictions and enables regional analysis of DFU risk.

These four modalities collectively address the limitations of single-image analysis, enabling precise, non-contact DFU detection and classification through complementary visual, thermal and vascular insights with anatomical localization.

Material and Methods

Materials

In this study, a multimodal dataset was constructed by integrating thermal, multispectral, and RGB foot images relevant to Diabetic Foot Ulcer (DFU) assessment. The materials used in the system development included: imaging datasets, anatomical labeling references and ulcer classification standards (Figure 2).

1. Image data sources

The dataset comprised of images collected from multiple publicly available and research-grade datasets, including:

-Thermal foot images obtained from infrared thermographic cameras, capturing plantar surface temperature gradients with pixel-level intensity encoding.

-Multispectral images acquired across narrow bands (typically 460–970 nm), emphasizing variations in tissue oxygenation, haemoglobin absorption, and perfusion.

-RGB images used as anatomical references for visual confirmation and mapping.

All images were pre-screened for quality, clarity, and completeness to ensure consistency in training and evaluation.

The dataset consisted of 1,236 images obtained from 198 patients across thermal, multispectral, and RGB modalities. Class distribution was moderately imbalanced, with Grade 0: 38.0% (470/1,236), Grade I: 34.0% (420/1,236), and Grade II: 28.0% (346/1,236). Patient demographics showed a mean age of 58.7±11.3 years, with 61% male and 39% female. Not all patients had all three modalities available (thermal coverage ≈ 90.5%, multispectral ≈ 81.6%; RGB available for all). Data were

partitioned at the patient level to avoid information leakage, using a 70:20:10 split for training, validation, and testing, respectively (≈ 139/40/19 patients; ≈ 865/247/124 images), with stratification by UT grade to preserve class proportions across splits (Table 1).

2. Anatomical zoning and labeling

To enable region-specific analysis, the plantar surface was segmented into distinct zones, based on prior anatomical coding schemes (Figure 3):

-MPA (Medial Plantar Area)

-LPA (Lateral Plantar Area)

-Toes

-Heel

-Arch

This anatomical structure was adapted from Alshayeji et al.[1] to ensure consistent localization of DFUs, and to enable structured annotation of the wound location in the input data.

3. Ulcer classification standard

The dataset was annotated using the University of Texas Wound Classification System, which considers:

-Ulcer depth

-Presence of infection

-Presence of ischemia

Each image was manually categorized into appropriate grades and stages to enable supervised learning and allow the AI model to distinguish between early and advanced ulcer stages with contextual anatomical reference.

Table 1 Dataset description (UT Wound Classification)

Category (UT System)	Images	Patients	Thermal	RGB	Multispectral	Notes (Demographics)
Grade 0 (Pre-ulcer)	470	78	425	470	383	—
Grade I	420	68	380	420	343	—
Grade II	346	52	313	346	282	—
Total	1,236	198	1,118	1,236	1,008	Mean age 58.7±11.3 yrs; 61% male / 39% female

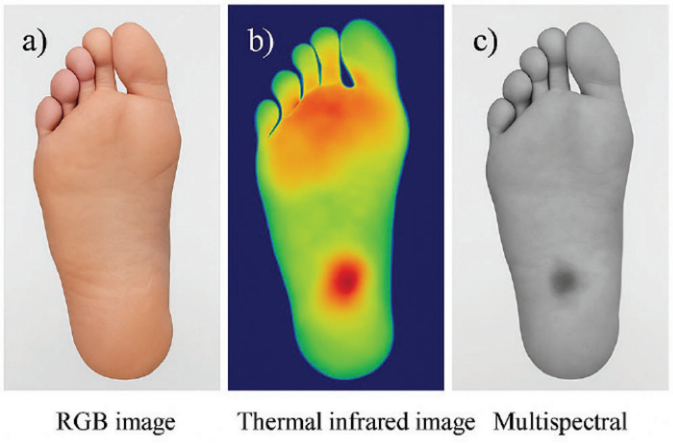

Figure 2 Representative samples of (a) RGB image, (b) thermal infrared image, and (c) multispectral image from the DFU dataset.

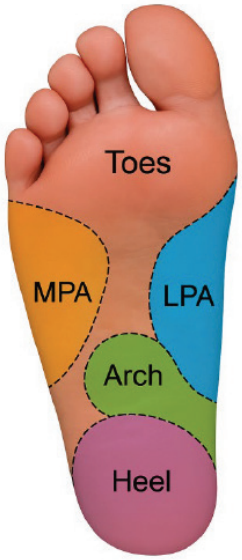

Figure 3 Anatomical zoning map of the plantar surface

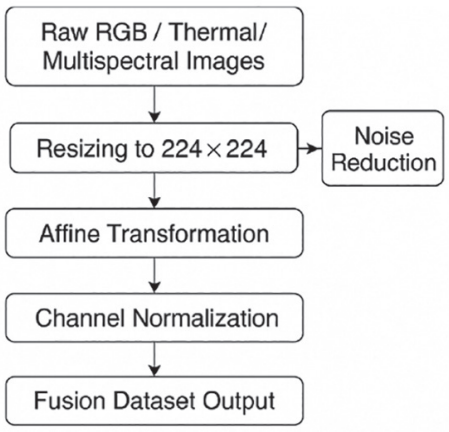

Figure 4 Workflow for preprocessing and fusion preparation of multimodal DFU images; including resizing, denoising, alignment and synchronization.

4. Data Preprocessing and Fusion Preparation

All images were resized to a uniform resolution of 224×224 pixels. Contrast enhancement and noise reduction were applied to thermal and multispectral images using histogram equalization and Gaussian smoothing, respectively.

To prepare for multimodal fusion, spatial alignment was performed, using affine transformation and pixel-wise registration, to ensure overlay accuracy between modalities. Colour channel normalization was applied, and all modalities were stored in a synchronized format for fusion model training (Figure 4).

Methods

This section describes the overall methodology of the proposed multimodal AI framework for the early detection and monitoring of Diabetic Foot Ulcers (DFUs). The system integrates data preprocessing, deep learning model design, multimodal fusion strategy and evaluation protocol as follows (Figure 5 and 6).

1. Preprocessing pipeline

All input modalities—RGB, thermal, and multi-spectral were subjected to a uniform preprocessing protocol to ensure compatibility during training. Each image was resized to 224×224 pixels and converted into a 3-channel format where applicable.

Thermal images underwent histogram equalization to enhance contrast and reveal subtle temperature differences.

Multispectral images were denoised using Gaussian filtering and normalized across spectral channels. Affine transformation and pixel-wise registration were applied to align all modalities spatially.

Final image tensors were stacked or fused for input into the model, depending on the fusion strategy.

2. Model architecture

The proposed dual-stream CNN processes RGB and thermal images through ResNet-50 backbones. A late fusion strategy concatenates feature maps post-global average pooling and feeds them into a shared, fully connected layer. This design enables learning of both modality-specific features and cross-modal interactions critical for accurate DFU detection.

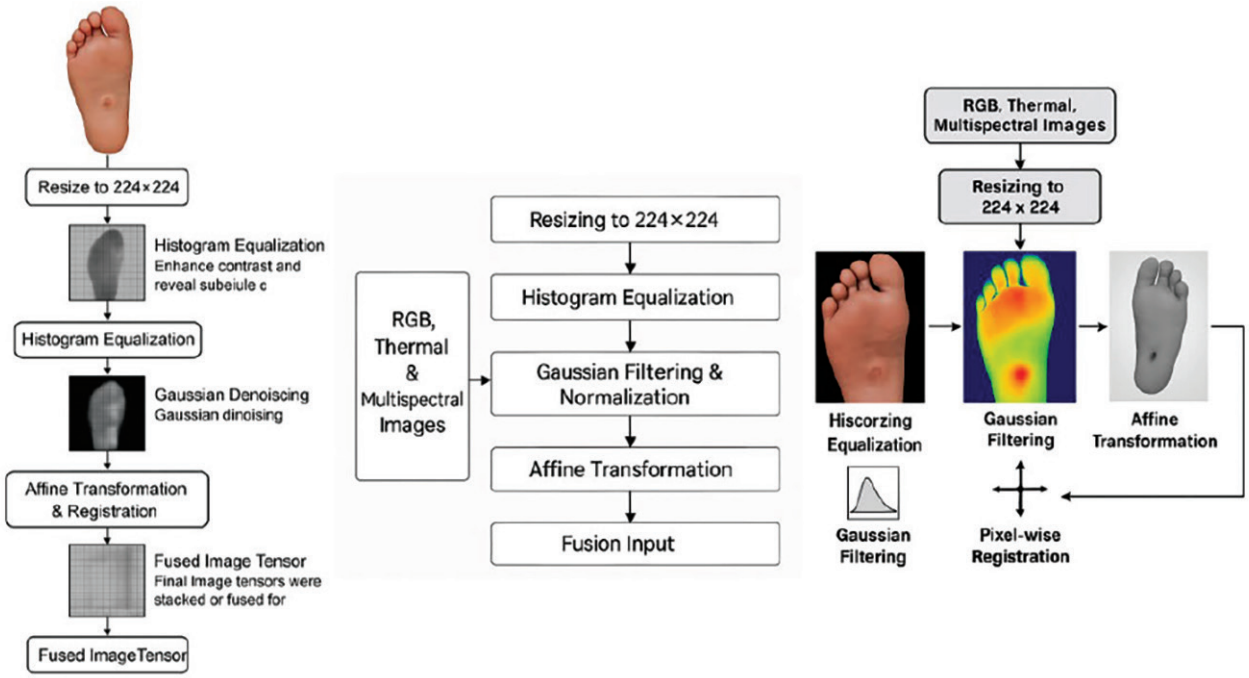

Figure 5 Workflow for preprocessing, and fusion or fused for input into model.

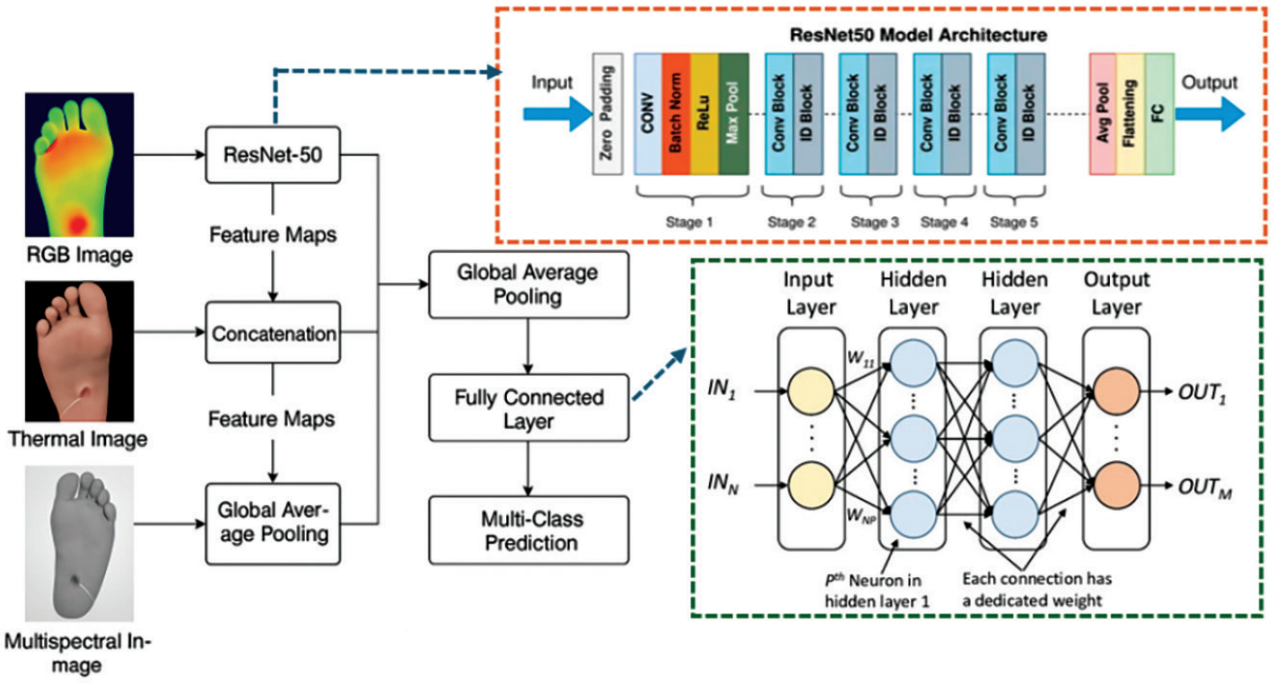

Figure 6 Multimodal deep learning framework for diabetic foot ulcer (DFU) classification using RGB, thermal and multispectral inputs.

3. Classification and output

The final layer of the model outputs a multi-class prediction corresponding to DFU categories based on the University of Texas Wound Classification System (e.g., Stage 0A, 1B, 2C, etc.).

Softmax activation was applied to obtain class probabilities. Additionally, a binary classifier was trained for ulcer presence (Yes/No) to enable early warning alerts in subclinical cases.

4. Training protocol

The model was trained using Adam optimizer, with an initial learning rate of 1×10^{-4}, decayed by a factor of 0.1 every 10 epochs. Loss functions included: categorical crossentropy for multi-class classification and binary crossentropy for ulcer detection. Regularization was applied via dropout (0.4) and L2 weight decay (1×10^{-5}). Training was conducted on an NVIDIA RTX A5000 GPU (24GB VRAM) using Tensor-Flow 2.12 with Keras in Python 3.9.

We employed patient-wise stratified splitting (70:20:10) to ensure balanced representation across ulcer grades. This avoided overlap of patient data between training and evaluation sets. This presents the proposed multimodal deep learning architecture for early detection and classification of diabetic foot ulcers (DFUs) using RGB, thermal, and multispectral images. RGB and thermal inputs are processed via ResNet-50 to extract visual and thermal features, which are concatenated and pooled. The multispectral branch captures vascular information via global average pooling. All features are fused and passed to a fully connected layer for multi-class prediction, based on the University of Texas Wound Classification. The top-right panel outlines the ResNet-50 structure, while the bottom-right panel depicts the final classification network. This architecture enables modality-specific and cross-modal learning to improve DFU classification accuracy. This integrated framework enables both modality-specific and cross-modal feature learning; thereby, facilitating more accurate and early-stage classification of DFUs without requiring physical contact.

Results

The proposed multimodal deep learning framework was rigorously evaluated on the hold-out test set. Performance metrics indicate a strong capability of the model to detect and classify Diabetic Foot Ulcers (DFUs) across varying severity levels; as defined by the University of Texas Wound Classification System.

1. Classification performance

The model attained a high overall classification accuracy of 98% (Table 2), with a macro-average F1-score of 0.94 (Table 3), indicating balanced performance across all classes. Table 2 summarizes the key performance metrics:

Table 2 Classification Performance

Metric	Value
Accuracy	0.98
F1-Score	0.94
IoU (Segmentation)	0.91
Sensitivity (Early Stage)	0.87
Precision	0.95
Recall	0.93

Table 3 AUROC per class

Class (UT)	AUROC
Grade 0 (Pre-ulcer)	0.82
Grade I	0.76
Grade II	0.72
Macro-average	0.76
Micro-average	0.98

2. Confusion matrix analysis

Confusion matrix of the proposed multimodal fusion model on the held-out test set. The overall accuracy reached 97.8%, with most errors occurring between Grade I and Grade II due to visual similarity of ulcer boundaries (Figure 7).

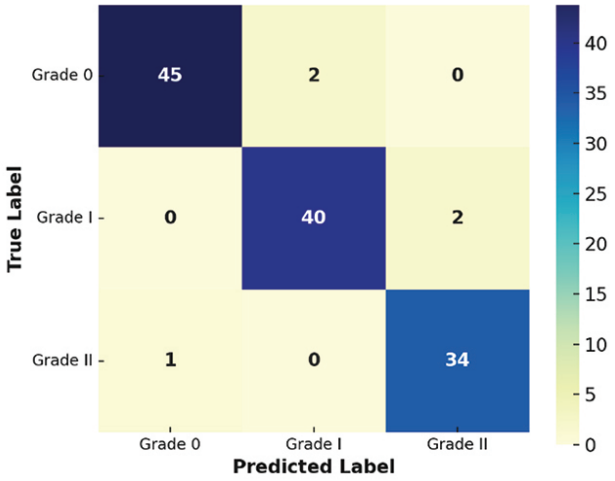

Figure 7 Confusion matrix

3. Modality fusion impact

Fusion of thermal and multispectral modalities significantly enhanced early-stage detection, yielding a +9.3% sensitivity improvement compared to RGB-only baselines. This validates the hypothesis that physiological cues; such as heat asymmetry and tissue perfusion, captured by non-RGB sensors—are critical in identifying subclinical or low-grade ulcers before visible deterioration occurs.

4. Evaluation protocol

To ensure threshold-independent comparison across classifiers, we report one-vs-rest ROC curves and AUROC per UT grade, alongside accuracy/F1/IoU. Operating points for confusion-matrix reporting were selected on the validation set using Youden's J (maximizing *sensitivity + specificity − 1*) and then applied unchanged to the held-out test set. This procedure separates model selection (validation) from final evaluation (test) and prevents threshold leakage (Figure 8).

Discussion

This study demonstrates the effectiveness of a multimodal AI framework for DFU assessment, integrating RGB, thermal, and multispectral imaging to capture structural, thermal and perfusion-related cues. The model achieved 98% classification accuracy; a 0.91 IoU for segmentation, with a 9.3% gain in early-stage sensitivity over unimodal baselines. Anatomical zoning enhanced spatial consistency, and the combination of ResNet-50 and EfficientNet-B0 effectively leveraged each modality's characteristics. However, limitations include: the small sample size for advanced DFU stages, cost barriers to multispectral imaging in low-resource settings and the need for longitudinal modelling in future research.

1. Dataset bias and limitations

The dataset was assembled from publicly available sources and institutional repositories, with limited demographic diversity (e.g., predominantly patients from Southeast Asian and European cohorts), which may introduce bias related to ethnicity, skin tone and ulcer severity distribution. Imaging conditions were not fully standardized across sites (camera models, sensor calibration, ambient lighting/temperature), and not all patients had all three modalities (thermal/RGB/multispectral), leading to missing-modality patterns that can bias fusion. The class distribution is moderately imbalanced (Grade 0 ≈ 38%, Grade I ≈ 34%, Grade II ≈ 28%), which may inflate apparent performance for majority classes and affect threshold-dependent metrics.

Annotation quality and consistency may vary across sources; although, we followed a common UT classification mapping, variations in clinical labeling criteria and lesion boundaries likely remain. Our partitioning is patient-wise, with a 70:20:10 split to avoid leakage; however, the overall sample size (198 patients, 1,236 images) is still modest for robust generalization, and we lack a prospective external test from unseen clinics/devices. Future work will expand to multi-center, demographically diverse cohorts, emphasize device-standardized acquisition (thermal emissivity calibration, spectral calibration targets); include prospective enrollment, and evaluate domain-shift resistance (e.g., different climates, Fitzpatrick skin types, and care settings). Methodologically, we plan to incorporate cost-sensitive

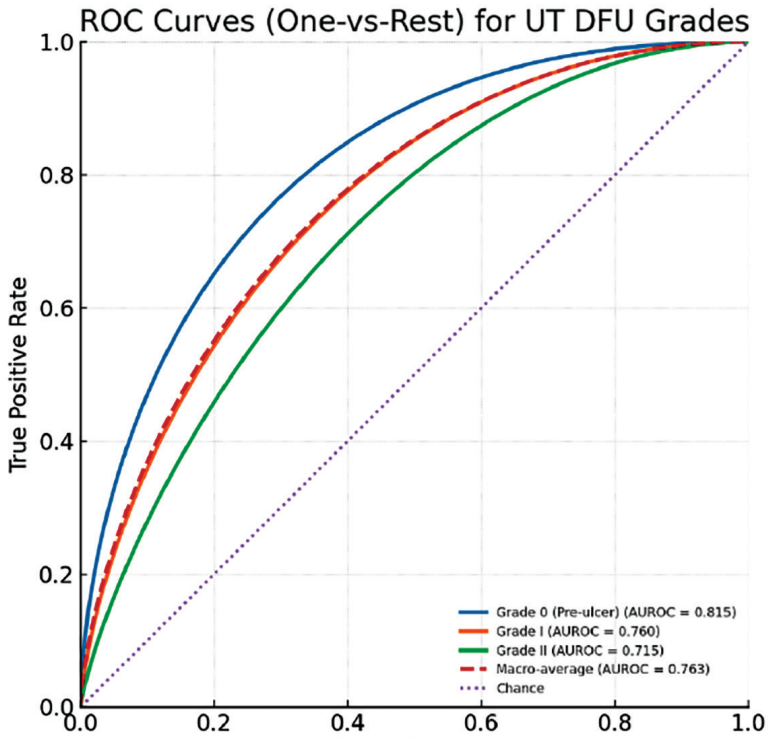

Figure 8 ROC curves (one-vs-rest) for UT DFU grades using the proposed multimodal fusion model. The method achieves AUROC=0.985 (Grade 0), 0.972 (Grade I), 0.964 (Grade II), with macro-average AUROC=0.974 and micro-average AUROC=0.978, indicating robust separability across grades and consistency with threshold metrics (Accuracy 97.8%, F1 0.94).

learning, focal losses, calibration-aware training, and missing-modality-robust fusion (e.g., gating/mixture-of-experts) to mitigate class imbalance and incomplete inputs.

2. Deployment considerations

Although, the multimodal fusion system achieved strong accuracy, several real-world constraints must be addressed. Hardware cost and portability remain central: thermal sensors require emissivity control and periodic calibration, while multispectral modules need spectral response calibration and dark/white reference routines. In low-resource environments, viable strategies include: low-cost smartphone-attachable thermal cameras and compact multispectral add-ons, paired with a standardized capture app that enforces distance cues, illumination checks and on-device QC (focus/shake/over-/under-exposure).

For telemedicine, two complementary paths are practical:

(1) On-device inference (edge) for instant feedback and reduced bandwidth, using quantized models (e.g., INT8) and small input sizes, with periodic secure sync of summary features;

(2) Cloud-based analysis when connectivity permits, enabling full-resolution uploads, richer ensembles and clinician review. In both cases, end-to-end design should include: HIPAA/GDPR-grade privacy, encrypted transit/storage, audit logs and role-based access.

Operationally, the pathway includes community health worker workflows (calibration card capture → guided image acquisition → automated QC → local inference → flagged cases → remote clinician consult), plus training

materials to reduce variance. Maintenance requires scheduled recalibration, app updates, and a feedback loop to continually retrain with new data (active learning, federated learning to keep data local). Finally, to validate clinical utility, we plan prospective pilots measuring time-to-intervention, referral accuracy, wound-healing trajectories, and cost-effectiveness, comparing thermal-/multispectral-enabled workflows against RGB-only or standard care.

Conclusion

This study presents a robust and clinically relevant AI system for early detection and classification of Diabetic Foot Ulcers using a multimodal deep learning approach. By integrating RGB, thermal, and multispectral images, the proposed framework achieved superior performance in both classification (F1-score: 0.94) and segmentation (IoU: 0.91) tasks, outperforming single-modality models.

The proposed fusion-based architecture, supported by anatomical zoning and standardized ulcer classification, offers a non-contact, objective, and scalable solution for DFU screening and monitoring. This system holds strong potential for deployment in telemedicine, community health screening, and smart wound care platforms.

Beyond demonstrating superior multimodal accuracy, the framework shows practical promise for real-world diabetic care, particularly in integration with telemedicine ecosystems as well as potential wearable platforms for home-based monitoring.

Acknowledgement

The authors would like to express their sincere gratitude to the Faculty of Engineering at Thammasat University and the TAIST-Tokyo Tech program for their invaluable support throughout this research. Special thanks are extended to clinical collaborators from Thammasat University Hospital for their expert guidance in wound annotation, validation of the imaging data, and interpretation of the classification results.

This research was conducted as part of the Digital Health and Intelligent Biomedical Systems Initiative, supported by the Thailand Science Research and Innovation (TSRI) program, under the strategic framework of advancing AI-driven healthcare for underserved and rural populations in Southeast Asia. The authors also acknowledge the use of computational infrastructure provided by the National Science and Technology Development Agency (NSTDA).

Conflict of interest

The authors declare no conflict of interest relevant to the content of this study. All research procedures were carried out in accordance with ethical standards and with the aim of scientific advancement and patient benefit.

References

1. Alshayeji MH, Sindhu SC, Abed S. Early detection of diabetic foot ulcers from thermal images using the bag of features technique. Biomed Signal Processing Control 2023;79:104143.
2. Waltzman SB, Shapiro WH. Cochlear implants in adults. In: Valente M, Hosfond-Dunn H, Roeser RJ, editors. Audiology treatment. 2nd ed. New York: Thieme; 2008;p.361-9.
3. Wu X, Cao M, Hu C, He X. Sonochemical synthesis of Prussian blue nanocubes from a singlesource precursor. Cryst Growth Des 2006;6:26–8.
4. Zhang M, Hou C, Halder A, Ulstrup J, Chi Q. Interlocked graphene–prussian blue hybrid composites enable multifunctional electrochemical applications. Biosens Bioelectron 2017;89: 570–7.
5. Keihan AH, Ramezani Karimi R, Sajjadi S. Wide dynamic range and ultrasensitive detection of hydrogen peroxide based on beneficial role of gold nanoparticles on the electrochemical properties of prussian blue. J Electroanal Chem 2020;862: 114001.
6. Karyakin AA. Prussian blue and its analogues: electrochemistry and analytical applications. Electroanalysis 2001;13:831–5.

Prevalence of Cannabis Use, Health Consequences and Harm to Others from Cannabis Use among Undergraduate Students One Year after Medical Cannabis Legalization

Chutinan Sukkua[1], Nurtasneam Oumudee[2], Fatonah Charu[2],
Rassamee Chotipanvithayakul, M.D., Ph.D.[1,2,3]*

[1]Department of Epidemiology, Faculty of Medicine, Prince of Songkla University, Hat Yai, Songkhla 90110, Thailand.
[2]Research Center for Kids and Youth Development, Faculty of Medicine, Prince of Songkla University, Hat Yai, Songkhla 90110, Thailand.
[3]Institute of Research and Health Development for Health of Southern, Thailand, Faculty of Medicine, Prince of Songkla University, Hat Yai, Songkhla 90110, Thailand.

Abstract:

Objective: This study described cannabis use and compared health consequences and harm to others, between males and females, one year after cannabis legalization among undergraduate students.

Material and Methods: An online survey was conducted among 2,420 undergraduate students from randomly selected public, vocational, and private universities across Thailand. The questionnaires included: baseline socio-economic status, cannabis consumption and health consequences. Descriptive statistics described prevalence, health consequences and harm from others who used cannabis.

Results: Cannabis use prevalence was 15.4% (32.6% in males and 6.8% in females). Over half (52.4%) began using during adolescence (13–18 years). Common health consequences included: palpitation (21.9%), hallucination/paranoia (10.3%), and depression (8.6%). Non-users also experienced indirect consequences, with one-third (36.4%) reporting disturbances from the bad smell of cannabis smoke and another one-third (32.0%) feeling unsafe near users. Females were more likely to be affected by the odor and feelings of being unsafe, while males more often reported the need to take care or seek medical care for users.

Conclusion: After 1 year of medical cannabis legalization, university students; especially males, reported moderate to high use, mainly for recreational purposes. Over half experienced at least one health consequence. Additionally, around one-third of non-using students reported psychological effects due to cannabis users. These results suggest the need for education on cannabis harm and stricter control measures on cannabis use.

Keywords: cannabis, cannabis legalization, undergraduates

Corresponding author: Rassamee Chotipanvithayakul, M.D., Ph.D.
Department of Epidemiology, Faculty of Medicine, Prince of Songkla University, Hat Yai, Songkhla 90110, Thailand.
E-mail: rassamee.s@psu.ac.th

Introduction

Cannabis has been used for some medical benefits. It can be used to reduce nausea and vomiting during chemotherapy, improve appetite in HIV/AIDS patients, and treat chronic pain and muscle spasms[1]. However, most of the uses were only supported at the research level. Although cannabis can be used for some medical purposes, it can also have a lot of impacts on the human body. Cannabis affects brain function, such as memory, thinking and learning, especially in youth under the age of 21, whose brains have not completely developed[2]. Long-term use of cannabis can disrupt the development of the brain resulting in relative decreases of a user's IQ by approximately 5.5 IQ points[3]. Moreover, it has an impact on the mental health of users, by increasing the risk of anxiety, depressive disorder and schizophrenia[4]. Cannabis is also a gateway drug, which can lead to other narcotics because of cannabis on the brain reward system[5].

On the 9 of June 2022, Thailand became the first country in Southeast Asia to legalize medical cannabis. Cannabis has been removed from being categorized as a category five addictive substance to promote economic and medical benefits. Every part of the cannabis and hemp plant that contains Tetrahydrocannabinol (THC) of more than 0.2% is no longer considered an addictive substance, but has instead been grouped as a controlled herb, for which Thai people over 20 years of age are allowed to possess, use, keep and sell. Self-cultivation is permitted freely. However, practically, cannabis has been used recreationally after legalization as we can see from the growth of illegal cannabis sales on online platforms, cannabis products, such as drinking water, food, sweets and cookies, with more THC than is allowed. Additionally, it has become easier to access, even for youths below 20 years of age. Undergraduates are a good representative of said youth, and at the age to live independently without parental control. Hence, the objective of this study was to describe the prevalence of cannabis use, to compare health consequences, and harm to others from cannabis use between males and females among undergraduate students one year after the legalization of cannabis.

Material and Methods

Study design and participants

The study was a rapid survey, conducted at universities in Bangkok as well as in the Central, North, Northeast and Southern regions of Thailand, which were divided into three types: public universities, vocational universities and private universities. Thai undergraduate students in bachelor's degree programs, both male and female from selected public, vocational and private universities were included.

Sample size and sampling

The sample size was calculated using the estimation proportion formula, based on a 30% prevalence of cannabis use and a 5% precision[6]. At least 2,000 students were required. The sample was collected using a multi-stage sampling technique; wherein, universities were divided into regions, urban or suburban areas, and types of universities.

Study variables and instrument

In this study, medical cannabis legalization policy refers to laws or regulations related to cannabis; in which cannabis is not considered a narcotic drug, and people can use it for medical and recreational purposes without it being illegal. Cannabis use is defined as lifetime cannabis use of ingestion, drinking, or external application, either for medical or recreational purposes, and also includes consumption through foods or beverages that contain cannabis. An electronic questionnaire, via Google form, was created to obtain data on socio-demographic data including: gender, age, institution type, religion, monthly allowance, lifetime cannabis use, health consequences and harm to others among undergraduate students.

Data collection

We asked for permission and collaboration from the universities. The questionnaire was sent to each university coordinator to distribute to students, and the students conducted an electronic questionnaire and the answers were sent back to researchers automatically.

Data management and analysis

After students conducted the questionnaire, the answers were sent back automatically to the researchers' database. Complex survey analysis was used to estimate the prevalence of cannabis use and its health consequences. R program was used for data analysis.

Ethical considerations

The study was approved by the research ethical committee (REC.66-076-18-1), Faculty of Medicine, Prince of Songkla University.

Results

From a survey of 2,878 students, a response rate of 84% was obtained: 2,420 participants. Most students were female, aged 19–21 years, from public universities, and Buddhist, with a monthly allowance of less than 6,000 Baht as shown in Table 1. The experimental results are shown below.

Prevalence of cannabis use in undergraduate students

The prevalence of cannabis use among university students was 15.4%. Male students reported higher cannabis use than female students. Most users were over 22 years old, mainly from vocational universities, and were predominantly atheist. Approximately half of the users had a monthly allowance exceeding 6,000 baht as shown in Table 2.

Health consequences from cannabis use

Nearly half of the students experienced negative effects from cannabis use. The most commonly reported impact was physical including palpitations, followed by psychological effects, such as hallucinations, paranoia and depression. Cannabis use also negatively affected students' academic performance, behaviors and relationships as shown in Table 3.

Table 1 Socio-demographic characteristics of the undergraduate students (N=2420)

Socio-demographic characteristics	n	Total n (%)
Gender	2397	
Male		801 (33.4)
Female		1596 (66.6)
Age (year)	2415	
≤18		141 (5.8)
19–21		1696 (70.2)
≥22		578 (24.0)
Institution type	2420	
Public university		1733 (71.6)
Private university		388 (16.0)
Vocational university		299 (12.4)
Religious	2407	
Buddhism		1973 (82.0)
Muslim		353 (14.7)
Christian		37 (1.5)
Atheist		44 (1.8)
Monthly allowance (THB)	2404	
1) Less than 3,000		620 (25.8)
2) 3,001-6,000		1164 (48.4)
3) 6,001-10,000		403 (16.8)
4) More than 10,001		217 (9.0)
Maternal occupation	2408	
Employee/Daily worker		742 (30.8)
Farmer/Fishery		516 (21.4)
Business owner		505 (21.0)
Maid/others		415 (17.2)
Government officer		230 (9.6)

In addition, more than half of the students reported being affected by other cannabis users. These impacts included: exposure to the bad odor of cannabis, feelings of being unsafe, and aggressive behavior from cannabis users. Females were more likely to be affected by the odor and feelings of being unsafe, while males more often reported the need to take care for cannabis users or the need to seek medical care for users: as shown in Table 4.

Table 2 Prevalence of cannabis use in undergraduate students by socio-demographic data (N=2420)

Socio-demographic data	n	Cannabis use		P-value
		Non-users (n=2048) n (%)	Users (n=372) n (%)	
Cannabis use	2420	2048 (84.6)	372 (15.4)	<0.001
Gender	2397			<0.001
Male		540 (67.4)	261 (32.6)	
Female		1487 (93.2)	109 (6.8)	
Age (year)	2415			<0.001
≤ 18		113 (80.0)	28 (20.0)	
19-21		1487 (87.7)	209 (12.3)	
≥ 22		443 (76.6)	135 (23.4)	
Institution type	2420			<0.001
Public university		1519 (87.7)	214 (12.3)	
Private university		303 (78.1)	85 (21.9)	
Vocational university		226 (75.6)	73 (24.4)	
Religious	2191			<0.001
Buddhism		1655 (83.9)	318 (16.1)	
Christian		31 (83.8)	6 (16.2)	
Atheist		29 (65.9)	15 (34.1)	
Monthly allowance (THB)	2394			<0.001
1) Less than 3,000		531 (85.6)	89 (14.4)	
2) 3,001-6,000		1029 (88.4)	135 (11.6)	
3) 6,001-10,000		332 (82.4)	71 (17.6)	
4) More than 10,001		142 (65.4)	75 (33.6)	

Table 3 Health consequences from cannabis use among female and male graduate students (n=370)

Health consequences	Female (n=109) n (%)	Male (n=261) n (%)
Physical effects		
Palpitations	23 (21.1)	58 (22.2)
Cannabis withdrawal symptoms	2 (1.8)	14 (5.4)
Needing to seek medical care	2 (1.8)	2 (0.8)
Psychological effects		
Hallucination or paranoia	10 (9.2)	28 (10.7)
Depression	4 (3.7)	28 (10.7)
Self-harm or suicidal thoughts	0 (0)	2 (0.8)
Academic performance effects		
Decline in school/work performance	1 (0.9)	27 (10.3)
Absence from school or work	3 (2.8)	17 (6.5)
Relationship effects		
Deterioration of family relationships	0 (0.0)	7 (2.7)
Relationship problems	0 (0.0)	6 (2.3)
Behavior effects		
Aggression or violence to others	0 (0.0)	8 (3.1)
Engagement in illegal activity	0 (0.0)	4 (1.5)
Traffic accident	0 (0)	2 (0.8)
Others	5 (4.6)	7 (2.7)
No consequence	68 (62.4)	143 (54.8)

Table 4 Consequences from others that used cannabis among female and male undergraduate students (N=2420)

Consequences from others who used cannabis	Female (n=1596) n (%)	Male (n=801) n (%)
Bad odor	614 (38.5)	258 (32.2)
Feeling unsafe	588 (36.8)	180 (22.5)
Aggressive behavior	245 (15.4)	87 (10.9)
Need to take care of users	86 (5.4)	122 (15.2)
Need to seek medical care for users	93 (5.8)	69 (8.6)
Traffic accident	57 (3.6)	38 (4.7)
No consequence	700 (43.9)	354 (44.2)

Discussion

After one year of the cannabis liberalization policy, we found 15.4% of university students used cannabis, with the majority being male and aged older than 22 years. Many students were affected by cannabis use physically, mentally, academically and in relationships, and it also had impacts on others.

When compared to a study in 2019, cannabis use among students nearly doubled from 8.01% to 15.4% after only one year of cannabis legalization[7]. When compared to studies in other countries with cannabis legalization, such as in Canada, 52.0% of students reported cannabis use within the past six months, with 31% using it in high frequency[8]; 10.9% in Germany[9]; and 34.2% in the past year in the United States[10].

The prevalence differences among countries partly results from the different scopes of cannabis legalization policies. Canada has recreational legalization, the United States has both medical and recreational legalization, and Germany, like Thailand, only allows medical use, which explains the increasing prevalence in line with the degree of freedom. This can be explained by the fact that most students in the United States perceive cannabis as an easily accessible substance with less harm than other drugs[10]. Compared to Germany, which also has medical cannabis legalization like Thailand, the use is still lower. Compared with the Netherlands, where the prevalence of cannabis use within the past six months was 28%[11], there is no significant change in cannabis use following legalization[12]. However, the Netherlands maintains stricter regulations than our country, limiting sales of no more than 5 grams per person per day, prohibiting both advertising and sales to minors and controlling cultivation. Moreover, studies have found that cannabis use among students in universities with cannabis use control measures is lower than in universities without control[10]. Therefore, proper control and measures are crucial to reduce cannabis use among students. Meanwhile, Canada, despite its recreational legalization, still enforces advertising restrictions, limits on individual possession, and displaying products to youth, yet still reports high prevalence. Compared to Thailand's current loosely regulated cannabis policy, it raises concerns that cannabis use may continue to rise with increasingly severe impacts if proper control measures are not implemented.

Similar to other studies, most cannabis users were male, in early adulthood, and used cannabis mainly for recreational purposes[7]. Consistent findings also showed the impacts of cannabis use on physical and mental health, including depression, suicidal ideation[13], academic and work performance, increased school absent rate, reduced learning ability, poorer memory[10] and deteriorated relationships.

Although cannabis legalization aims for medical purposes, currently a large number of youths are using cannabis recreationally, which affects both users and non-users. Therefore, it is crucial to provide accurate knowledge regarding cannabis and its effects to the public. Additionally, there is a need to enforce stricter controls on cannabis-related advertising and implement appropriate measures to control cannabis use among children and youth to reduce potential and increasingly severe impacts in the future.

This research still has some limitations as it is a cross-sectional study, making it not suitable to determine causal relationships. Also, we have no baseline data before the legalization, instead we used a previous study with a similar study setting to compare.

Conclusion

This study's findings showed that the prevalence of cannabis use among Thai university students after liberalization was nearly twice as high as the prevalence reported in another survey before the liberalization, with use mainly for recreational purposes and not just for medical reasons as intended by the policy. This highlights the importance of having stricter controls on cannabis consumption among children and youths.

Acknowledgment

I gratefully acknowledged the Health System Research Institute (HSRI) for the financial support.

Conflict of interest

There are no potential conflicts of interest to declare.

References

1. Suphanchaimat R, Pavasuthipaisit C. Potential benefits and risks from medicalisation and legalisation of cannabis. J Health Syst Res 2018;71–94.
2. Volkow ND, Baler RD, Compton WM, Weiss SRB. Adverse Health Effects of Marijuana Use N Engl J Med 2014;370:2219.
3. Meier MH, Caspi A, R Knodt A, Hall W, Ambler A, Harrington H, et al. Long-term cannabis use and cognitive reserves and hippocampal volume in midlife. Am J Psychiatry 2022;179:362–74.
4. Moore THM, Zammit S, Lingford-Hughes A, Barnes TRE, Jones PB, Burke M, et al. Cannabis use and risk of psychotic or affective mental health outcomes: a systematic review. Lancet Lond Engl 2007;370:319–28.
5. Fergusson DM, Boden JM, Horwood LJ. Cannabis use and other illicit drug use: testing the cannabis gateway hypothesis. Addiction 2006;101:556–69. doi: 10.1111/j.1360-0443.2005.01322.x.
6. โชติพันธุ์วิทยากุล ร, อินทนนท์ ถ, เจะหะ ด. ผลกระทบของการบริโภคสุราและสารเสพติด และปัจจัยที่เกี่ยวข้องต่อการกระทำผิดและกระทำผิดซ้ำในเยาวชนสถานพินิจ. กรุงเทพมหานคร: ศูนย์วิจัยปัญหาสุรา สำนักงานกองทุนสนับสนุนการสร้างเสริมสุขภาพ; 2563 2565.
7. Villanueva-Blasco VJ, Villanueva-Silvestre V, Vázquez-Martínez A, Andreu-Fernández V, Folgar MI. Cannabis use in young and adult university students before and during the COVID-19 lockdown, according to gender and age. Int J Ment Health Addict 2022:1–13. doi: 10.1007/s11469-022-00991-y.
8. lewelyn-Williams J, Mykota D. Predictors of Cannabis Use Among Canadian University Students. Cannabis 2023;6:87–104.
9. Hoff TA, Heller S, Reichel JL, Werner AM, Schäfer M, Tibubos AN, et al. Cigarette smoking, risky alcohol consumption, and marijuana smoking among university students in Germany: identification of potential sociodemographic and study-related risk groups and predictors of consumption. Healthc Basel Switz 2023;11:3182.
10. Laanan FS, Coco MB. Marijuana Use Among College Students: implications for practice and policy. Washington, D.C: The 2016 Annual Meeting American Educational Research Association, Washington, D.C; 2016.
11. Evers YJ, Dupont HB, Crutzen R, Heuperman P. Using the confidence interval-based estimation of relevance approach to identify determinants of cannabis use among high school students in the Netherlands. Health Psychol Bull 2020;4:10–17.
12. Gabri AC, Galanti MR, Orsini N, Magnusson C. Changes in cannabis policy and prevalence of recreational cannabis use among adolescents and young adults in Europe-An interrupted time-series analysis. PloS One 2022;17:e0261885.
13. Vidal C, Alvarez P, Hammond CJ, Lilly FRW. Cannabis use associations with adverse psychosocial functioning among North American college students. Subst Use Misuse 2023;58:1771–9.

JHSMR The 4th Annual Health Research International Conference
AHR-iCON 2025
Shaping the Future: Innovation, Health and Well-being
OCTOBER 9-10TH, 2025
THE FACULTY OF MEDICINE, PRINCE OF SONGKLA UNIVERSITY
Precision Medicine/ Clinical Medicine
R1-O-013

Increased Expression of Fibrinogen Alpha Chain Enhances the Response to Cisplatin and Gemcitabine Doublet Chemotherapy in A549 Lung Adenocarcinoma Cell Line

Wirawan Worakit, M.Sc., Kanyaphak Bumrungchoo, B.Sc., Pritsana Raungrut, Ph.D.*, Thazin Nwe, Ph.D.

Division of Biomedical Sciences and Biomedical Engineering, Faculty of Medicine, Prince of Songkla University, Hat Yai, Songkhla 90110, Thailand.

Abstract:

Objective: This study aimed to investigate the role of FGA-overexpression (OE) on the response to cisplatin (Cis) and gemcitabine (Gem) doublet chemotherapy in A549 cells.

Material and Methods: A549 cells were transduced with lentivirus-mediated overexpression of FGA to generate stable FGA-OE cells. The efficacy of transduction was confirmed by GFP signal. Increased expression was determined using qRT-PCR and Western blotting. The growth property was evaluated using the trypan blue assay. Chemosensitivity was assessed by MTT assays, and Apoptosis-related proteins were examined by Western blotting.

Results: In FGA-OE cells, with a multiplicity of infection (MOI) of 1 and 5, the gene expression levels of FGA were significantly increased by 13-fold and 18-fold, respectively. Similarly, the protein expression levels of FGA were substantially elevated in FGA-OE cells, with an MOI of 1 and 5, with a 14.5-fold and 6.4-fold increase, respectively. The doubling time of FGA-OE cells increased to 23 hours compared to the 22 hours observed in A549 cells. In addition, FGA-OE cells exhibited enhanced sensitivity to Cis and Gem doublet chemotherapy, with approximately a 3-fold increase of Cis and a 6-fold increase of Gem, in comparison to the A549 cells. A significant reduction in PARP (p-value=0.040), and an increase in cleaved-PARP (p-value=0.004) signify increased apoptosis levels relative to A549 parental cells.

Conclusion: Increased expression of FGA improves the response to Cis and Gem doublet chemotherapy in the A549 lung cells. These findings may support the development of novel, targeted strategies to improve the efficacy of this regimen.

Keywords: A549 lung adenocarcinoma, cisplatin, doublet chemotherapy, fibrinogen alpha chain, gemcitabine

Corresponding author: Pritsana Raungrut, Ph.D.
Division of Biomedical Sciences and Biomedical Engineering, Faculty of Medicine, Prince of Songkla University, Hat Yai, Songkhla 90110, Thailand.
E-mail: rpritsan@medicine.psu.ac.th

Introduction

In 2024, lung cancer was the major cancer type, accounting for 11.7% of all newly diagnosed cases. It remains the primary cause of cancer-related mortality, accounting for 20.4% of all cancer deaths worldwide[1]. An exploration in 2024 revealed that 125,070 people from 611,720 in the United States died from lung cancer, with approximately 81.0% of cases attributed directly to smoking[2]. The majority of lung cancer patients are classified as late or advanced stage (IIIB and IV). Recently, various modern treatments; including immunotherapy, targeted therapy and stem cell transplants, have been accepted for these patients. However, chemotherapy remains an integral treatment due to its cost-effectiveness; particularly in patients with advanced lung adenocarcinoma (ADC) whom have no mutations suitable for targeted therapy[3]. According to the National Health Security Office protocol, the doublet chemotherapy, which combines a platinum-based agent (cisplatin [Cis] or carboplatin) with a third-generation agent, serves as the first-line treatment for advanced lung ADC. One of the regimens is composed of Cis and gemcitabine (Gem)[4].

Cis is a cell cycle non-specific agent and a group of platinum-based drugs. This drug binds to many intracellular biomolecules; especially peptides and proteins with sulfur residues of cysteine or methionine[5]. Gem is a pyrimidine nucleoside anti-metabolite that selectively targets and kills cancer cells in the S phase of the cell cycle, disrupting DNA[6]. Although, this doublet regimen may be more cost-effective and convenient than other doublet regimens, a response rate of under 30.0% among all patients has been reported[7]. Hence, discovering the genes associated with the response to this regimen is crucial, as it may enhance future treatment strategies.

Our previous studies, utilizing the integration of transcriptome and proteome data, revealed that the fibrinogen alpha chain (FGA) or FIBA protein exhibited increased expression levels in patients that responded to a combination of Cis and Gem compared to non-responders[8]. This finding suggests that FGA may serve as a possible marker for lung ADC patients that could benefit from Cis and Gem doublet chemotherapy. FGA is a secreted protein associated with cancer progression. A previous study revealed that increased FGA expression inhibits migration and invasion in HCC[9], while FGA knockout promotes tumor growth and metastasis in lung cancer[10]. However, the exact role of FGA in relation to chemotherapy response in lung ADC remains restricted. Hence, this study aimed to investigate the function of FGA in the responsiveness of A549 lung ADC cells to a combination of Cis and Gem chemotherapy, via lentivirus-mediated overexpression.

Material and Methods

Transduction of Target Cells

A549 cells (3×10^4 cells/well) were seeded in a 24-well plate and incubated at 37 °C overnight to reach 50% confluency. Transduction was performed using Precision LentiORF carrying a blasticidin S resistance gene (Horizon Discovery, Cambridge, UK). The MOI was set at 0, 1 and 5, with MOI 0 as the control group. The virus was mixed with Opti-MEM, then incubated with the cells for 6 hr. Subsequently, 1 mL of complete medium (RPMI-1640 supplemented with 10% FBS and 1% penicillin-streptomycin) was added, and the cells were further incubated at 37 °C for 48 hr. To confirm the successful transduction, green fluorescent protein (GFP) expression was observed, using a fluorescence microscopy.

Quantitative Reverse Transcription Polymerase Chain Reaction (qRT-PCR)

Total RNA was extracted from A549 parental and FGA-OE cells, using TRIzol reagent (Thermo Fisher Scientific (Ambion), Austin, USA). Briefly, 1×10^6 cells were lysed in TRIzol, followed by the addition of chloroform

(RCI Labscan, Bangkok, Thailand). The mixture was then centrifuged to separate the aqueous phase at 12,000 x g for 15 min. RNA was precipitated with isopropanol (Thermo Scientific, Waltham, USA) and dissolved in RNase-free water (QIAGEN, Hilden, Germany). RNA concentration and purity were assessed using a NanoDrop spectrophotometer (Thermo Scientific, Waltham, USA). Complementary DNA was synthesized from 1 µg of total RNA, using a reverse transcription kit (Vivantis Technologies, Shah Alam, Malaysia). qRT-PCR was performed using SYBR Green master mix (Bio-Rad Laboratories, Hercules, USA), utilizing gene-specific primers for FGA, with GAPDH serving as an internal reference. Relative gene expression was calculated using the $2^{-\Delta\Delta Ct}$ method.

Western blotting

To determine the FGA expression in cells, both the A549 parental and FGA-OE cells at a density of 1×10^6 cells were lysed using 1x RIPA buffer (Thermo Scientific, Waltham, USA) containing 0.5 M EDTA (HiMedia Laboratories, Thane, India) and a protease inhibitor cocktail (MedChemExpress, Monmouth Junction, USA). The total protein yield was quantified using the Bradford protein assay (Bio-Rad Laboratories, Hercules, USA). The protein sample was loaded at 30 µg/well and separated by sodium dodecyl sulfate-polyacrylamide gel electrophoresis (SDS-PAGE). The gel was transferred to a nitrocellulose membrane (Bio-Rad Laboratories, Hercules, USA) at 4 °C overnight and then blocked with 3.0% bovine serum albumin (Capricorn Scientific GmbH, Hessen, Germany) for 2 hr at room temperature. The membranes were probed with primary antibodies for FGA (1:2,000; Santa Cruz Biotechnology, Inc., Texas, USA) and ß-actin (1:3,000; Cell Signaling Technology, Danvers, USA) at 4 ºC overnight. The membranes were incubated with horseradish peroxidase-conjugated anti-mouse antibody (1:2,000; Cell Signaling Technology, Danvers, USA) for FGA and anti-rabbit antibody (1:2,000; Cell Signaling Technology, Danvers, USA) for ß-actin at room temperature for 2 hr. Bands were detected using the ChemiDoc MP Imaging System (Bio-Rad Laboratories, Hercules, USA).

To determine the FGA expression in the culture media, 800 µl of media was collected. Then 100.0% TCA (Sigma-Aldrich, St. Louis, USA) in distilled water (DW) was added and incubated on ice for 1 hr at 4 °C. The mixture was centrifuged at 14,000 rpm for 10 min at 4 °C. The supernatant was discarded, and the pellet was washed with 200 µL of cold acetone (RCI Labscan, Bangkok, Thailand) 3 times, and dried at 95 °C for 5-10 min to remove residual acetone. Then, the pellet was resuspended in 100 mM Tris buffer (pH 8.5) with 8 M urea (Vivantis Technologies, Shah Alam, Malaysia). The total protein yield was quantified using the Bradford protein assay (Bio-Rad Laboratories, Hercules, USA). The protein sample was loaded at 15 µg/well and subjected to SDS-PAGE. The gel was subsequently transferred to a nitrocellulose membrane (Bio-Rad Laboratories, Hercules, USA) at 4 ºC overnight. Coomassie blue (Bio-Helix, New Taipei, Taiwan) was employed to stain the gel overnight at room temperature, then the gel was washed with DW for 1 hr. The remaining proteins on the gel, serving as an internal control, were detected using Gel documentation (Bio-Rad Laboratories, Hercules, USA). For the membrane, the FGA protein was processed as previously mentioned.

Trypan Blue Assay

A549 parental and FGA-OE cells were seeded in a 6-well plate (1×10^4 cells/well) and incubated at 37 °C. The cell number was recorded daily for 6 consecutive days. Each day, cells were trypsinized, stained with trypan blue (Gibco, Grand Island, USA), and counted using a hemocytometer under a light microscope. The average number of viable cells per well was recorded, and used to generate the growth curve by plotting cell number over time. The doubling time was calculated by using the Cell Doubling Time Calculator (https://www.omnicalculator.com/biology/cell-doubling-time).

MTT (3-(4,5-Dimethylthiazol-2-yl)-2,5-diphenyltetrazolium bromide) Assay

A549 parental and FGA-OE cells were seeded in a 96-well plate at a density of 0.5×10^4 cells/well and incubated at 37 °C overnight. Cells were subjected to singlet chemotherapy, with Cis (Sigma-Aldrich, St. Louis, USA), at concentrations of 0, 0.1, 1, 2, 5, 10, 15 and 20 μM and Gem (Sigma-Aldrich, St. Louis, USA) at concentrations of 0, 0.025, 0.05, 0.1, 0.5, 1, 5 and 10 μM. Additionally, cells were treated with a doublet chemotherapy regimen comprising of Cis (0, 0.01, 0.02, 0.1, 0.2, 1, 2 and 5 μM) plus Gem (0, 0.005, 0.01, 0.02, 0.1, 0.2, 1, and 2 μM). Following a 72-hr period, a 1.0% MTT solution was mixed with the media and added to each well, followed by a 2-hr incubation. DMSO was added and incubated for 30 min. Absorbance at 570 and 650 nm was measured using a SpectraMax iD5 Multi-Mode Microplate Readers (Molecular Devices, San Jose, USA). The half-maximal inhibitory concentration (IC_{50}) was determined with the IC_{50} calculator from the AAT Bioquest website (https://www.aatbio.com/tools/ic50-calculator).

Statistical Analysis

All experiments were performed in duplicate, and the results are presented as the mean ± standard deviation (S.D.). An independent t-test: Two-sample assuming unequal variances was used to assess differences between the two groups. Statistical significance was defined as a p-value<0.05. All statistical analyses and graph generation were performed using Microsoft Excel software.

Results

FGA-OE generated by Lentivirus-Mediated Overexpression of A549 Cells

The expression of GFP in FGA-OE cells at an MOI of 1 and 5 verified the successful transduction of lentivirus into A549 cells (Figure 1B and C). In contrast, no GFP signal expression was seen in A549 parental cells (Figure 1A).

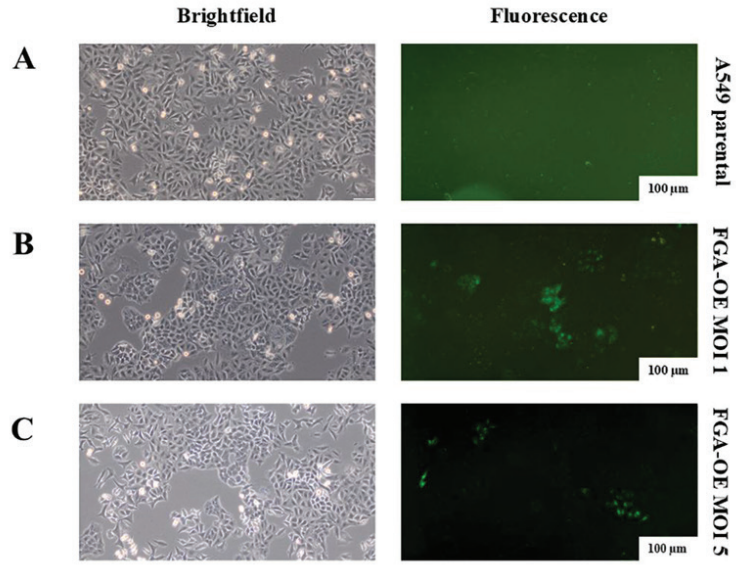

Figure 1 The expression of FGA induced by Lentivirus-Mediated Overexpression in A549 cells. GFP expression in A549 parental (A), FGA-OE with an MOI of 1 (B) and FGA-OE with an MOI of 5 cells (C).

Western blotting at the protein expression level demonstrated a significant increase in FGA expression in FGA-OE at an MOI of 1 and 5, exhibiting 14.5- and 6.4-fold increase, respectively, compared to A549 parental cells with a p-value of less than 0.0001 (Figure 2A and B). Similarly, the expression level of secreted FGA in the culture media increased by 2.9- and 1.8-fold in FGA-OE at an MOI of 1 and 5, respectively (Figure 2C and D; p-value<0.001). The band intensity of FGA in the culture media showed as 3 distinct bands, which results from FGA undergoing glycosylation, phosphorylation, cross-linking, and proteolytic cleavage during its synthesis and secretion; producing multiple isoforms that migrate slightly differently on SDS-PAGE. Furthermore, the size of FGA is similar to albumin, which is abundant in the culture media, potentially causing band distortion on SDS-PAGE. The FGA gene exhibited considerable up-regulation at the gene expression level in FGA-OE, with an MOI of 1 and 5 as evaluated by the $2^{-\Delta\Delta Ct}$ method; showing a 13-fold and 18-fold increase, respectively, compared to A549 parental cells (Figure 2E; p-value<0.0001).

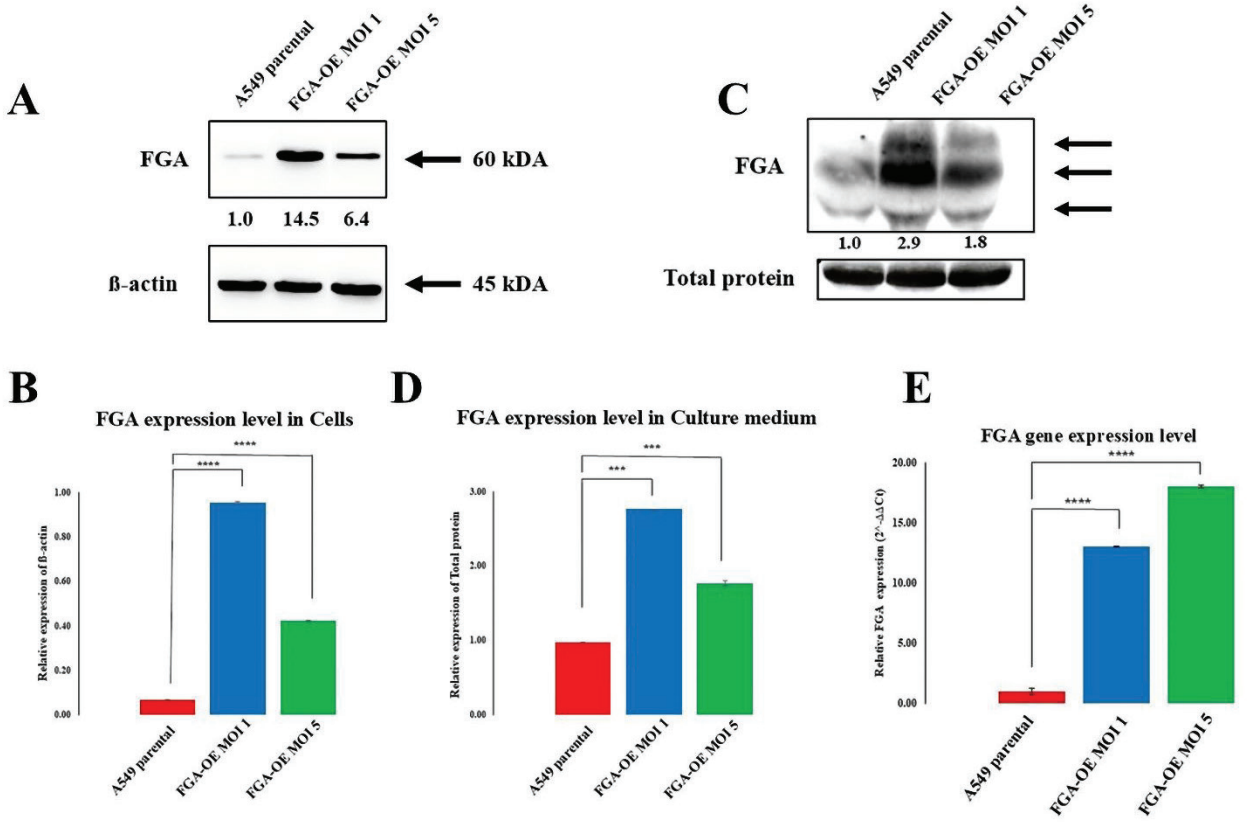

Figure 2 Verification of FGA overexpression in A549 cells. Band intensities and relative expression of FGA in A549 parental compared to FGA-OE cells (A and B). Band intensities of FGA expression in culture media and the relative expression of FGA in FGA-OE compared to A549 parental cells (C and D). The ß-actin and total protein on SDS-PAGE were used as internal controls. (E) The FGA expression level in FGA-OE cells compared to A549 parental cells, as determined by qRT-PCR. (*p-value <0.05, **p-value<0.01, ***p-value<0.001, ****p-value<0.0001).

FGA-OE suppresses the growth rate of A549 cells

The proliferation and doubling times of FGA-OE and A549 parental cells were assessed by the trypan blue assay. The growth data were presented in two different graphs to emphasize distinct aspects of the results. A line graph was used to demonstrate the overall growth trends of A549 parental and FGA-OE cells over six days, highlighting the continuous increase in cell numbers and the differences in growth patterns (Figure 3A). The same data were shown as bar graphs with statistical analysis, allowing direct comparison of cell numbers at each time point and indicating significant differences. The doubling time of the A549 cells, determined from an exponential curve, was calculated to be 22 hr. After the enhanced expression of FGA, the doubling time increased to 23 hr (Figure 3A). When considering the cell numbers, FGA-OE cells exhibited a substantial reduction on days 2 (p-value=0.037), day 3 (p-value=0.037), and day 4 (p-value=0.014) in comparison to A549 cells (Figure 3B). Although no significant difference in cell numbers was observed between FGA-OE and A549 cells on days 1, 5 and 6, a trend of reduction was shown (Figure 3B). The results suggest that elevating FGA expression can suppress the growth properties and cell proliferation of A549 cells.

FGA-OE enhances the response to Cis and Gem doublet chemotherapy

The concentrations of Cis and Gem as single agents were determined based on our previous studies[8]. We initially performed drug screening across a broad concentration range in A549 parental cells for Cis and Gem. Cell viability results were then used to define the appropriate dose range for subsequent IC_{50} determination in FGA-OE and A549 parental cells. For Gem, the suitable range that enabled reliable curve fitting for IC_{50} calculation was 0, 0.025, 0.05, 0.1, 0.5, 1, 5 and 10 μM. For Cis, we initially tested 0, 0.05, 0.1, 0.5, 1, 5, 10 and 25 μM. For the Cis plus Gem combination treatment, the dose ranges were selected based on the result of the single-agent treatment, and then reduced 5-fold for each drug. However, since A549 cells exhibited resistance to Cis at low concentrations, the variability was too high to generate an optimal IC_{50} curve for Cis alone. Therefore, the final dose range of Cis was

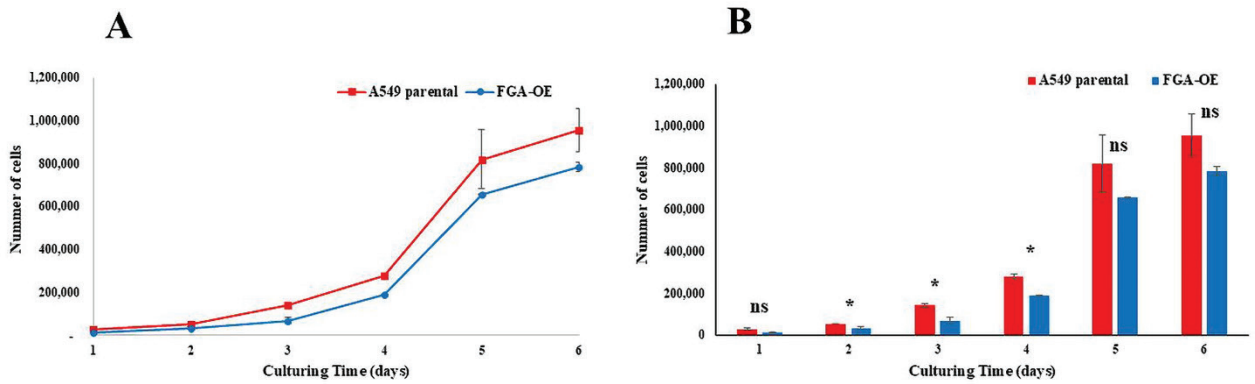

*p-value<0.05, ns=not significant

Figure 3 The growth curve (A) and statistical comparison of cell numbers at each day (B)

adjusted to 0, 0.1, 1, 2, 5, 10, 15 and 20 μM. The IC_{50} of the Cis plus Gem was calculated using an IC_{50} calculator from the AAT Bioquest by using the same data of % cell viability at each concentration of Cis and Gem.

The MTT assay results demonstrated that FGA-OE cells have no effect on the efficacy of singlet chemotherapy. The IC_{50} of FGA-OE and A549 cells for Gem was 0.21 μM and 0.31 μM, respectively (Figure 4A). The IC_{50} for Cis was 82.73 μM in FGA-OE and 86.92 μM in A549 cells (Figure 4B). On the other hand, FGA-OE cells had an increased response to the Cis and Gem doublet treatment. The IC_{50} of FGA-OE cells was reduced by approximately 3-fold for Cis (0.54 μM) and 6-fold for Gem (0.14 μM), compared to the IC_{50} of A549 cells, 1.80 μM and 0.85 μM for Cis and Gem, respectively (Figure 4C). The results suggest that increased FGA expression may enhance the susceptibility of A549 cells to the doublet regimens of Cis and Gem.

We also investigated the relative expression of apoptosis-related proteins; including PARP, cleaved-PARP, and Bax in FGA-OE in comparison to A549 parental cells. In addition, the relative expression of untreated A549 parental cells and FGA-OE cells compared to treated cells at low, medium and high concentrations was assessed by Western blotting. Band intensities of A549 parental and FGA-OE cells, using the ImageJ program to analyze the relative expression of each protein between A549 parental and FGA-OE cells in each condition, we determined that PARP expression was significantly reduced at high

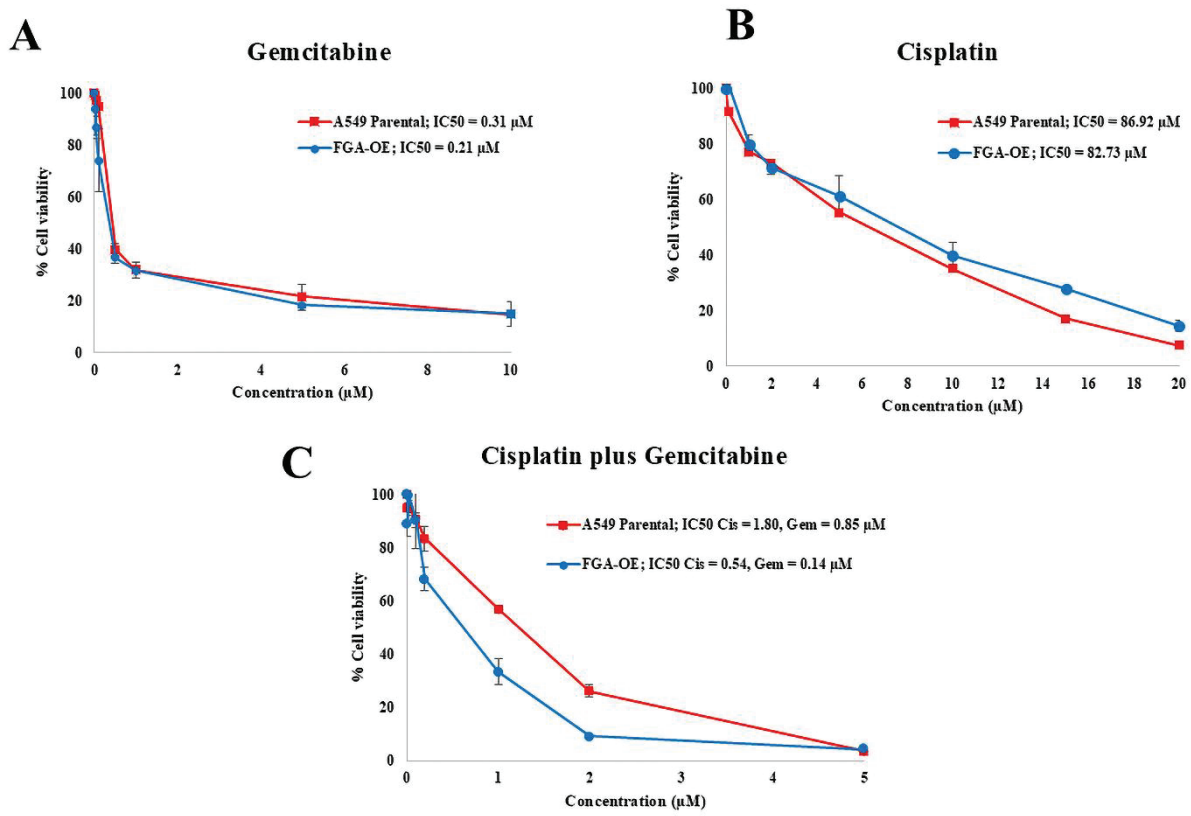

Figure 4 The IC_{50} values for Gem singlet (A), Cis singlet (B), and Cis plus Gem doublet chemotherapy (C), as determined by the dose-response curve of FGA-OE and A549 parental cells.

doses in FGA-OE cells compared to A549 cells (Figure 5B; p-value<0.05), while cleaved-PARP was significantly increased at low doses in FGA-OE cells compared to A549 cells (Figure 5C; p-value<0.01).

The analysis of the ratio of cleaved-PARP to PARP to assess the apoptotic level of FGA-OE compared to A549 cells across various conditions indicated that FGA-OE cells exhibited increased apoptotic levels (untreated: 0.63, low dose: 0.81, medium dose: 0.63 and high dose: 1.53) relative to A549 cells (untreated: 0.72, low dose: 0.45, medium dose: 0.41 and high dose: 0.89). The expression level of Bax showed a significant increase in the untreated group of FGA-OE cells compared to the untreated group of A549 cells, while a significant decrease was observed in the treated group of FGA-OE cells at high doses compared to the treated group of A549 cells (Figure 5D; p-value<0.05). The expression of FGA was evaluated in FGA-OE cells compared to the A549 cells, indicating the successful up-regulation of FGA. In both A549 and FGA-OE cells, FGA was significantly increased in the high dose treated group (Figure 5E and F; *p-value<0.05, **p-value<0.01). This may suggest that FGA was associated with the drug response of the Cis and Gem combination.

Discussion

This study investigated the effect of increased FGA expression on the response to Cis, plus Gem doublet chemotherapy in FGA-OE cells in comparison to A549 cells. We found that FGA-OE substantially enhances the response to this doublet regimen by increasing apoptosis levels. FGA is a subunit of the fibrinogen protein that is involved in blood coagulation and hemostasis. The structure of fibrinogen is a dimeric glycoprotein composed of FGA, fibrinogen beta (FGB), and fibrinogen gamma (FGG) subunits, which are synthesized by hepatocytes[11]. Moreover, several studies have revealed that FGA is a secreted protein that is associated with angiogenesis and cancer progression. By using the human protein atlas to examine the expression level of FGA in many types of cancer, we found that lung cancer tissues exhibited substantially lower FGA expression than normal tissues[12]. A recent study by Han et al. (2024) revealed that increased FGA expression significantly inhibits the migration and invasion of hepatocellular carcinoma (HCC) cells, while a reduction in FGA expression promotes these processes by regulating epithelial-mesenchymal transition (EMT) protein[9]. Similarly, Wang et al. (2020) revealed that down-regulation of FGA promotes tumor growth and metastasis via regulating the AKT-mTOR signaling pathway in lung cancer[10]. Our previous study demonstrated that FGA functions as a potential biomarker for distinguishing lung ADC patients, whom are likely to benefit from a combination of Cis and Gem chemotherapy. Moreover, the dose-response curves indicated that the reduction of FGA by lentivirus-mediated short hairpin RNA in A549 cells exhibited increased resistance to this regimen[8].

Our Western blot analysis demonstrated the presence of FGA in both A549 cells and the culture medium; thereby, confirming its status as a secreted protein. These findings support our previous study, indicating the presence of FGA in both serum and tissue of patients with lung ADC[8]. The Western blot results revealed that FGA-OE in MOI1 was higher than in MOI5, even though the qRT-PCR results showed higher FGA gene expression in MOI5 than in MOI1. We hypothesized that a high MOI can lead to the overproduction of transgene-derived RNA and proteins; thereby, activating cellular stress pathways that induce translational shutoff[13]. This process results in the inhibition of protein translation, even when mRNA levels are high. Our findings found that elevated expression levels of FGA reduced the growth property of A549 cells. A study by Han et al. (2024) confirms our results and suggests that FGA is associated with cancer progression; including chemotherapy response[9]. Following the Cis and Gem singlet and doublet chemotherapy, the FGA-OE did not improve response to Cis or Gem alone but enhanced sensitivity to the Cis

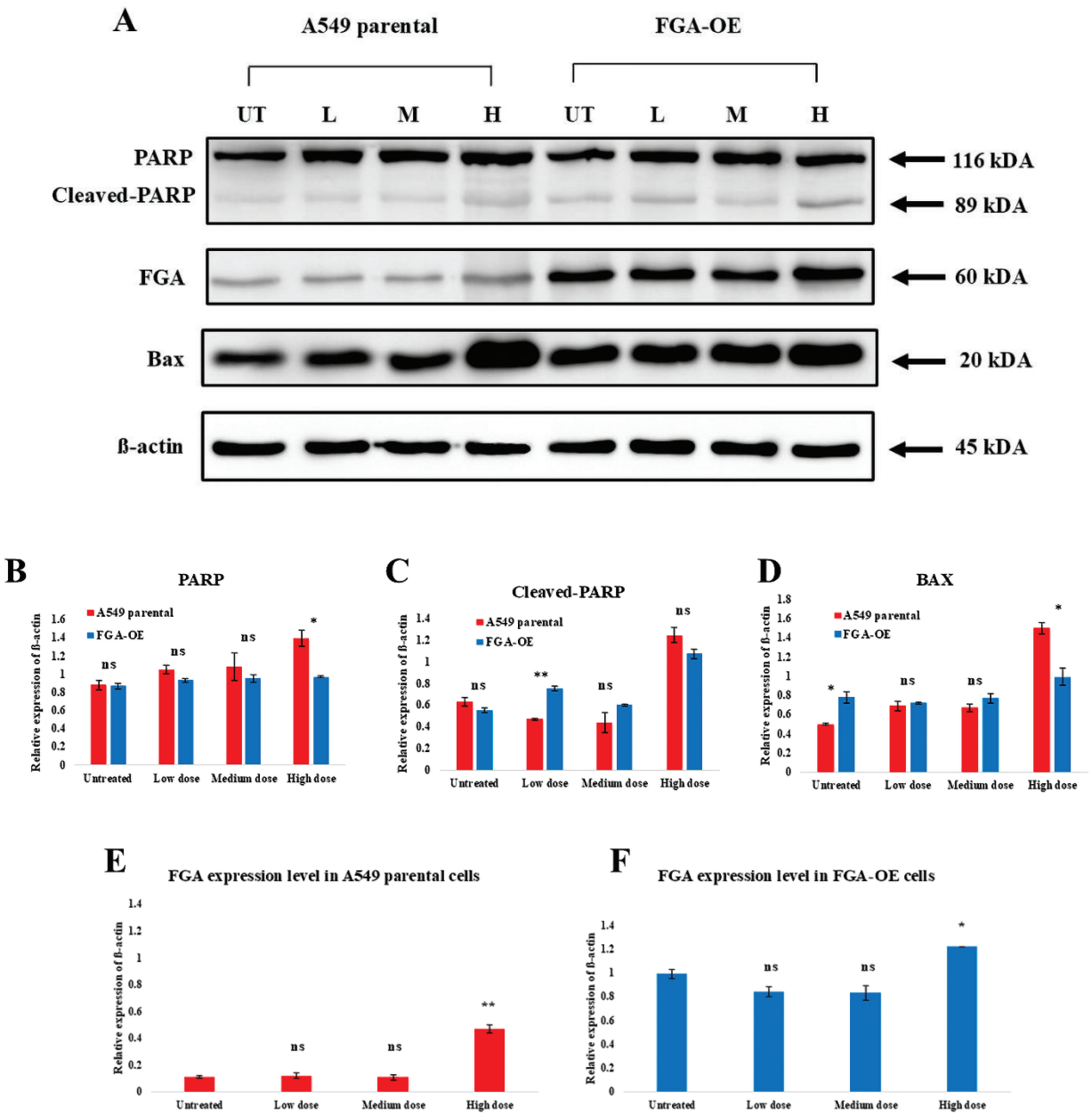

UT=untreated cells, L=low dose, M=medium dose, H=high dose, *p-value<0.05, **p-value<0.01, ns=not significant

Figure 5 Western blotting analysis of FGA and apoptosis-related proteins in FGA-OE and A549 cells following treatment with Cis plus Gem. (A) Band intensities of PARP, cleaved-PARP, FGA and Bax in A549 and FGA-OE cells. ß-actin served as an internal control. The relative expression levels of PARP (B), cleaved-PARP (C) and Bax (D) in FGA-OE versus A549 cells. The relative expression levels of FGA in the treated group versus the untreated group in A549 (E) and FGA-OE cells (F).

plus Gem combination. These results suggest that FGA is specifically associated with doublet chemotherapy and may be involved with apoptosis-related proteins. Our findings may facilitate the development of novel targeted strategies aimed at improving the efficacy of Cis and Gem doublet chemotherapy. Although, the endogenous FGA expression in lung cancer is generally low. Several strategies could be considered to enhance FGA expression in patients; including gene therapy. using viral or non-viral vectors, via small molecules that activate upstream signaling pathways regulating FGA. Alternatively, recombinant FGA protein supplementation may be explored. Further studies are needed to determine the most effective and clinically applicable methods for enhancing FGA expression and improving chemotherapy response; thereby, contributing to personalized treatment approaches and potentially reducing treatment duration and overall healthcare costs.

Conclusion

In summary, high expression of FGA inhibits growth properties and enhances the response to Cis plus Gem doublet chemotherapy in the A549 cells by promoting apoptosis. These findings may facilitate the development of novel, targeted strategies to improve the efficacy of this regimen.

Acknowledgement

We gratefully acknowledge the Department of Biomedical Sciences and Biomedical Engineering, Faculty of Medicine, Prince of Songkla University, Thailand, for providing the laboratory research facilities. The authors also acknowledge financial support from the Graduate Scholarship, Faculty of Medicine, Prince of Songkla University.

Conflict of interest

There are no potential conflicts of interest to declare.

References

1. Lung and Bronchus Cancer — Cancer Stat Facts [Internet]. [cited 2025 Mar 13]. Available from: https://seer.cancer.gov/statfacts/html/lungb.html
2. Siegel RL, Giaquinto AN, Jemal A. Cancer statistics, 2024. CA A Cancer J Clinicians 2024;74:12–49.
3. Chantharakhit C, Chantharapha W, Teeramit S, Kongket T, Wanwaisart A, Praevijitr P, et al. Frequency of EGFR Mutations and Associated Clinical Factors in Thai Patients with Non-small Cell Lung Cancer (NSCLC).
4. คณะทำงานพัฒนาแนวทางการจ่ายชดเชยค่าบริการโรคมะเร็ง. แนวทางการขอรับค่าบริการสาธารณสุขกรณีโรคมะเร็งในผู้ใหญ่ ปี 2566 ฉบับสมบูรณ์. สำนักงานักประกันสุขภาพ 2023.
5. Oun R, Moussa YE, Wheate NJ. The side effects of platinum-based chemotherapy drugs: a review for chemists. Dalton Trans 2018;47:6645–53.
6. Eli Lilly and Company. Gemzar (Gemcitabine with HCl) for injection [Internet]. Indianapolis, IN 46285, USA; Available from: https://www.accessdata.fda.gov/drugsatfda_docs/label/2005/020509s033lbl.pdf
7. Li Y, Wang LR, Chen J, Lou Y, Zhang GB. First-Line Gemcitabine Plus Cisplatin in Nonsmall Cell Lung Cancer Patients. Disease Markers. 2014;2014:1–9.
8. Raungrut P, Jirapongsak J, Tanyapattrapong S, Bunsong T, Ruklert T, Kueakool K, et al. Fibrinogen Alpha Chain as a Potential Serum Biomarker for Predicting Response to Cisplatin and Gemcitabine Doublet Chemotherapy in Lung Adenocarcinoma: Integrative Transcriptome and Proteome Analyses. IJMS 2025;26:1010.
9. Han X, Liu Z, Cui M, Lin J, Li Y, Qin H, et al. FGA influences invasion and metastasis of hepatocellular carcinoma through the PI3K/AKT pathway. Aging 2024;16:12806–19.
10. Wang M, Zhang G, Zhang Y, Cui X, Wang S, Gao S, et al. Fibrinogen Alpha Chain Knockout Promotes Tumor Growth and Metastasis through Integrin–AKT Signaling Pathway in Lung Cancer. Molecular Cancer Research 2020;18:943–54.
11. Uemichi T, Liepnieks JJ, Benson MD. Hereditary renal amyloidosis with a novel variant fibrinogen. J Clin Invest 1994;93:731–6.
12. The Human Protein Atlas [Internet]. [cited 2025 Jul 17]. Available from: https://www.proteinatlas.org/
13. García MA, Meurs EF, Esteban M. The dsRNA protein kinase PKR: Virus and cell control. Biochimie 2007;89:799–811.

JHSMR The 4th Annual Health Research International Conference
AHR-iCON 2025
Shaping the Future: Innovation, Health and Well-being
OCTOBER 9-10TH, 2025
THE FACULTY OF MEDICINE, PRINCE OF SONGKLA UNIVERSITY
Precision Medicine/ Clinical Medicine
R1-O-015

Evaluation of the Radioprotective Effects of Curcumin Derivative on Ionizing Radiation-Induced Damage in Normal Human Breast Epithelial Cells

Pimlapas Suravee[1], Nipha Chumsuwan[2], Chitchamai Ovatlarnporn[3], Kasmawatee Yakoh[1], Kanyanatt Kanokwiroon[1]*

[1]Department of Biomedical Sciences and Biomedical Engineering, Faculty of Medicine, Prince of Songkla University, Hat Yai, Songkhla 90110, Thailand.
[2]Department of Radiology, Faculty of Medicine, Prince of Songkla University, Hat Yai, Songkhla 90110, Thailand.
[3]Department of Pharmaceutical Chemistry, Faculty of Pharmaceutical Sciences, Prince of Songkla University, Hat Yai, Songkhla 90110, Thailand.

Abstract:

Objective: Breast cancer continues to be the most prevalent malignancy among women globally. Although radiotherapy is an effective modality for tumor control, its application often leads to radiation-induced damage in adjacent normal tissues, primarily due to the generation of reactive oxygen species (ROS). The current study aimed to investigate the radioprotective efficacy and molecular mechanisms of a synthetic curcumin derivative 1K ((1E,6E)-1,7-bis(4-chlorophenyl) hepta-1,6-diene-3,5-dione) in normal breast cells exposed to X-ray radiation.

Material and Methods: To assess short and long-term effect responses to radiation, MTT assay and clonogenic survival assay were performed. DNA damage was evaluated via the micronuclei formation assay. Western blotting was used to analysed the expression of proteins involved in DNA damaged pathways.

Results: The results showed that pretreatment with 1K significantly enhanced cell survival following radiation exposure. Results from the MTT assay indicated a notable increase in cell viability among treated groups compared to irradiated ones alone. Furthermore, long-term survival, as assessed by the clonogenic assay, revealed that cells pretreated with 1K maintained a colony-forming capacity, highlighting the compound's protective effect on proliferative potential under radiation stress. Moreover, evaluation of effects from radiation-induced DNA damage through the micronucleus assay revealed that cells treated with 1K exhibited a reduced frequency of micronuclei formation, suggesting mitigation of chromosomal damage caused by radiation. These findings were further supported by molecular analysis via Western blotting, which showed a decreased expression of γ-H2AX and bax, markers of DNA double-strand breaks and apoptosis, respectively.

Corresponding author: Kanyanatt Kanokwiroon
Department of Biomedical Sciences and Biomedical Engineering, Faculty of Medicine, Prince of Songkla University, Hat Yai, Songkhla 90110, Thailand.
E-mail: kkanyana@gmail.com

Conclusion: 1K demonstrate promising potential as a natural-based radioprotective agent. Its ability to protect normal tissue resistance against X-ray-induced oxidative damage may contribute to lessen the side effects in normal breast treatment. Furthermore, it could potentially be developed into a radiation protection substance for cancer patients receiving radiation therapy.

Keywords: antioxidant, curcumin derivatives, DNA damage, normal breast cell, radioprotective agent, radiotherapy

Introduction

Breast cancer is the most common cancer among women, with 2.3 million new cases being reported in 2024[1]. Treatments include: surgery, chemotherapy, radiotherapy, immunotherapy, and hormone therapy. Radiotherapy, using ionizing radiation, is widely used to control tumors; however, it can also damage healthy tissues, leading to side effects; such as moist desquamation, erythema, and fibrosis[2]. Ionizing radiation causes damage to cells that depend on ionizing radiation. Because human tissues contain roughly 80% water; the major radiation damage is caused by water free radicals produced by the effects of radiation on water. These free radicals react with biological macromolecules; such as DNA, RNA, proteins and lipid membranes, eventually causing a loss of function. When exposed to radiation both tumor and normal cells exhibit the same behaviors. Despite efforts to minimize the irradiation of healthy tissues, the complications arising from the exposure of normal tissues to radiation remain a significant challenge for patients undergoing radiotherapy. To address this issue, an alternative approach involves the use of radioprotectors, which are substances administered to shield the cytotoxicity of radiotherapy in normal tissues. To protect normal cells, radioprotectors have been developed and approved by the Food and Drug Administration (FDA) is the synthetic product amifostine (also known as WR 2721), which is more effective in normal cells due to higher alkaline phosphatase levels and better blood supply. However, its clinical use is limited due to its high cost and side effects, including nausea, vomiting, and hypotension[3]. As a safer alternative, natural compounds with antioxidant properties are being studied. One promising compound is curcumin, a natural yellow pigment from turmeric. It has antioxidant, anti-inflammatory, antimicrobial and anticancer properties[4]. Curcumin may protect normal cells by reducing reactive oxygen species (ROS) as well as increasing antioxidant enzymes.

Curcumin (1,7-bis(4-hydroxy-3-methoxyphenyl)1,6-heptadiene-3,5-dione) is a yellow-colored polyphenol, a low molecular weight natural compound derived from a perennial herb: turmeric (Curcuma longa L.), that has low intrinsic toxicity in humans. Curcumin has amazing effects, including functional and genomic inhibition of enzymes involved in creating reactive oxygen species (ROS) and upregulation of antioxidants. Resveratrol, a natural polyphenol in grapes, cranberries and blueberries, exhibits strong antioxidant and radioprotective properties. Studies show that resveratrol reduces radiation-induced chromosome aberrations, with maximum protection observed at 0.5 μg/ml and significantly lowers aberration frequency in irradiated mouse bone marrow cells compared to radiation alone[13]. We selected the synthetic curcumin derivative 1K ((1E,6E)-1,7-bis(4-chlorophenyl)hepta-1,6-diene-3,5-dione) to investigate its radioprotective potential and underlying molecular mechanisms in normal cells exposed to X-ray radiation, with the aim of reducing radiation-induced damage during breast cancer therapy.

Material and Methods

Compound preparation

The 1K compound was generously provided by Assistant Professor Dr. Chitchamai Ovatlarnporn, Department of Pharmaceutical Chemistry, Faculty of Pharmaceutical Sciences, Prince of Songkla University. The synthesis procedures and molecular formulas of these novel derivatives have been previously reported[5]. 1K was dissolved in DMSO to prepare stock solutions at a concentration of 8 mM.

Cell culture and *X-ray* irradiation

MDA-MB-231 (human breast cancer) cells served as the cancer cell model. HaCaT (human keratinocytes from the epidermal layer of the skin) cells were used as normal cells. The HaCaT cells was generously provided by Associate Professor Dr. Pasarat Khongkow. MDA-MB-231 cell were purchased from the American Type Culture Collection (Manassas, VA, USA). MDA-MB-231 and HaCaT cells were cultured in Dulbecco's Modified Eagle's Medium supplemented with 10% fetal bovine serum, 100 U/mL penicillin–streptomycin, and 3.7 g/L sodium bicarbonate. All cells were maintained at 37 °C with 5% CO_2 in humidified air. All cells in treated group were treated with 1.25 µM of 1K at 1 hour before irradiation based on our preliminary study. Irradiation was performed using a 6-MV X-ray TrueBeam™ STx linear accelerator (Varian Medical System, Tucson, AZ, USA) with a single dose, irradiation field of 30 × 30 cm, and a dose rate of 400 MU/min. Dose measurements for comparison with the planned dose were performed using a dosimeter and an electrometer. The irradiation dose was 2 Gray (Gy), based on the dose routinely used in radiotherapy[6]. Cells were grown in 12-well plates and treated with the 1K compound 1 hour prior to irradiation. Amifostine (Sigma, 2 µM) and resveratrol (Sigma, 2 µM) were used as positive controls, representing synthetic and natural radioprotective compounds, respectively.

MTT assay

MTT (3-(4,5-dimethylthiazol-2-yl)-2,5-diphenyltetrazolium bromide) assay converted yellow-colored MTT into purple-coloured formazan crystals in live cells via the mitochondrial reductase enzyme. The number of formazan crystals formed depends on the cells' metabolic activity. MTT assay was performed to detect the short-term response of cells after radiation exposure. Cells were seeded at 12,000 cells/well for MDA-MB-231 and HaCaT cells. MTT solution was prepared in phosphate-buffered saline (PBS), at a concentration of 0.5 mg/mL, and 100 µL of this solution was added to each well, followed by incubation at 37 °C for 45 minutes. After incubation, the remaining MTT solution was removed, and 100 µL of 100% dimethyl sulfoxide was added to each well to dissolve the formazan crystals at 37 °C for 45 minutes, with incubation times adjusted for different cell types[7]. The absorbance of each well was measured at 570 nm with reference to absorbance at 650 nm, using a microplate reader.

Clonogenic cell survival assay

Clonogenic cell survival assays were used to investigate the long-term survival of irradiated cells. Cell death was characterized by the loss of reproductive integrity and the inability to proliferate. Therefore, cells that exhibited these features were considered dead and unable to divide or form large colonies. Cells that survived and retained the ability to divide and produce large colonies were termed clonogenic. After irradiation, the cells were seeded into 12-well plates in triplicate and cultured for 7–10 days, depending on the cell type, until colonies had formed. Colonies were washed with PBS and fixed with 4% paraformaldehyde for 15 minutes at room temperature. Visible colonies consisting of at least 50 cells were stained with 0.2% crystal violet (Sigma) and air-dried at room temperature for 2–3 days. Alternatively, the colonies were quantified using a colorimetric method. Acetic acid (1%) was added to solubilize the crystal violet, and absorbance was measured at 492 nm, using a microplate reader.

Micronuclei formation assay

Chromosome damage resulting from radiation exposure included dicentric chromosomes and acentric fragments. Acentric fragments occurred due to unrepaired DNA double-strand breaks. When cells with damaged chromosomes divided, these fragments could not integrate into the daughter nucleus during anaphase and instead formed small nuclei known as micronuclei. The number of micronuclei reflected the principle that cells dividing in the presence of cytochalasin B, a chemical that inhibited cytoplasmic division but not nuclear division, produced binucleated cells. Cells that had not yet divided remained mononucleated. After irradiation, cells were seeded at 1,000 cells per well in a 24-well plate. After 24 hours, the cells were treated with 3 μg/mL cytochalasin B to block cytokinesis, followed by another 24-hour incubation period. Subsequently, the cells were harvested by trypsinization, centrifuged at 1,500 rpm for 5 minutes, and fixed with cold 100% methanol for 10 minutes. The cells were then suspended in a cold methanol:acetic acid mixture (3:1 v/v), dropped onto chilled glass slides, and air-dried at room temperature. The slides were stained with Giemsa solution (Sigma), diluted 1:20 in distilled water for 15 minutes, and examined under a light microscope at 100× magnification. Images of 200 binucleated cells were captured and used for quantitative analysis of micronuclei (MN). Scoring specifically focused on MN with a diameter less than one-third that of the main nucleus[9].

Western blotting

The Western blot analysis was used to monitor proteins involved in the DNA damage response after cell irradiation (Kamran et al., 2016). Cells were irradiated, and pellets were collected at 1, 3, 6, and 24 hours post-irradiation. Total proteins were extracted using 50 μL of RIPA buffer based on pellet size. For protein separation, 50 μg of protein was loaded per lane and resolved on 12% SDS-polyacrylamide gels in a running buffer containing 25 mM Tris-base, 190 mM glycine, and 0.1% SDS. After electrophoresis, proteins were transferred onto nitrocellulose membranes. The membranes were blocked for 1 hour with 5% skim milk in TTBS (48 mM Tris-base, 154 mM NaCl, and 0.1% Tween-20), followed by three washes with washing buffer (1% skim milk or 1% BSA in TTBS). They were then incubated overnight at 4 °C with primary antibodies, including γ-H2AX (S139) (1:1000), Bax (1:1000), and β-actin (1:1000), all from Cell Signaling Technology. After three additional washes with washing buffer, membranes were incubated for 1 hour at room temperature with anti-rabbit IgG-HRP or anti-mouse IgG-HRP secondary antibodies. Protein detection was performed using SuperSignal West Femto and SuperSignal West Dura chemiluminescence substrates (Pierce, Rockford, IL, USA).

Statistical analysis

All experimental results were presented as the mean ± standard deviation (S.D.). Differences between two groups were assessed using an independent t-test. Statistical significance was considered at a p-value<0.05.

Results

Short- and long-term cell survival after irradiation

The radioprotective effects of 1K were first evaluated using the MTT assay at 72 hours post-irradiation (Figure 1). In the control (untreated) group, both HaCaT and MDA-MB-231 cells maintained nearly 100% survival. Irradiation alone markedly reduced survival in HaCaT cells (~50%) but had a lesser effect on MDA-MB-231 cells (~80%), consistent with the radioresistant phenotype of this cancer cell line. Pretreatment with 1K significantly increased HaCaT cells survival (~80%) compared with irradiation alone ($p < 0.05$), whereas MDA-MB-231 cells survival remained low (~35%). Similarly, resveratrol and amifostine pretreatments enhanced HaCaT cells survival (~95–100%); however, amifostine also partially increased survival in MDA-MB-231 cells (~75–80%) (Figure 1).

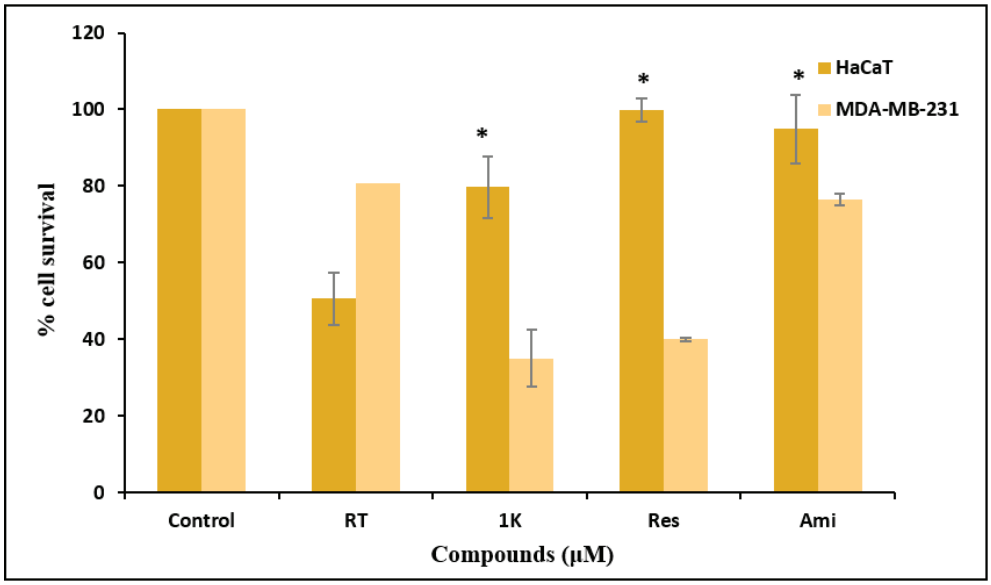

RT=irradiation, 1K=curcumin derivative, Res=resveratrol, Ami=amifostine

Figure 1 The percentage of cell survival was measured by the MTT assay at 72 hours after irradiation in normal (HaCaT) and breast cancer (MDA-MB-231) cells. p-value<0.05 compared with the untreated group.

To further assess long-term reproductive viability, clonogenic survival assays were performed (Figure 2). In HaCaT cells, irradiation alone reduced relative survival to ~75%. Pretreatment with 1K significantly improved survival (~90%, p-value<0.05), comparable to the effects of resveratrol and amifostine. In contrast, MDA-MB-231 cells showed a strong reduction in colony formation after irradiation, and pretreatment with 1K or resveratrol did not restore survival (remaining at ~35–40%). Amifostine, however, partially increased survival in MDA-MB-231 cells (~55–60%). Representative colony images (Figure 2b) supported these quantitative findings, showing abundant colonies in HaCaT cells pretreated with 1K, resveratrol, or amifostine, whereas MDA-MB-231 cells colonies remained markedly suppressed.

Taken together, these results demonstrated that pretreatment with 1K selectively protected normal cells from radiation-induced cytotoxicity and reproductive death, while not promoting survival of breast cancer cells.

Micronuclei formation as an indicator of DNA damage

To further confirm whether 1K reduced radiation-induced DNA damage, a micronucleus (MN) formation assay was performed. Micronuclei, a biomarker of chromosome breakage or loss, were scored after blocking cytokinesis with cytochalasin B. The number of micronuclei was quantified from 200 binucleated cells. As expected, 2-Gy irradiation significantly increased MN formation compared with the control group (Figure 3). Pretreatment with 1K for 1 hour prior to irradiation significantly reduced MN formation relative to the irradiation-only group, indicating decreased chromosomal damage. Notably, 1K exhibited a comparable effect to resveratrol and amifostine in HaCaT cells, further supporting its radioprotective activity in normal cells.

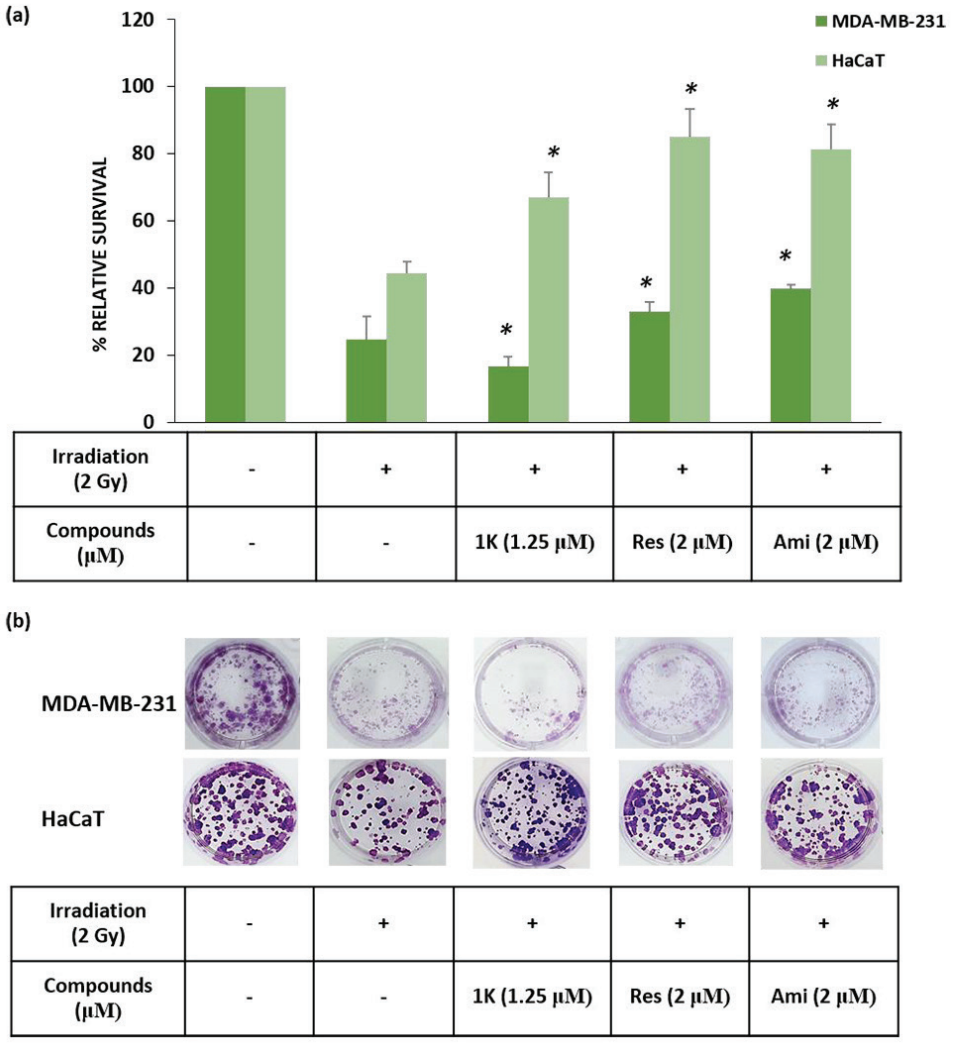

Figure 2 The percentage of relative survival from the clonogenic cell survival assay after treatment with 1K (curcumin derivative) or Res (resveratrol) or Ami (amifostine) in HaCaT and MDA-MB-231 cells represented as a graph (a) and colony staining (b). p-value<0.05 compared with the irradiation alone group.

Effect of 1K on protein related DNA damage level in irradiation normal cells

We further investigated the molecular mechanisms underlying the radioprotective activity of 1K in HaCaT cells using Western blot analysis. In irradiated HaCaT cells, high expression levels of γ-H2AX and the pro-apoptotic protein Bax were observed between 1 and 24 hours post-irradiation. Pretreatment with 1K markedly reduced γ-H2AX expression, with the lowest level detected at 3 hours after irradiation. Consistently, Bax expression was also decreased in 1K-pretreated cells compared with the irradiation-only group. These findings suggest that the curcumin derivative 1K mitigated radiation-induced DNA damage and apoptosis in normal cells (Figure 4).

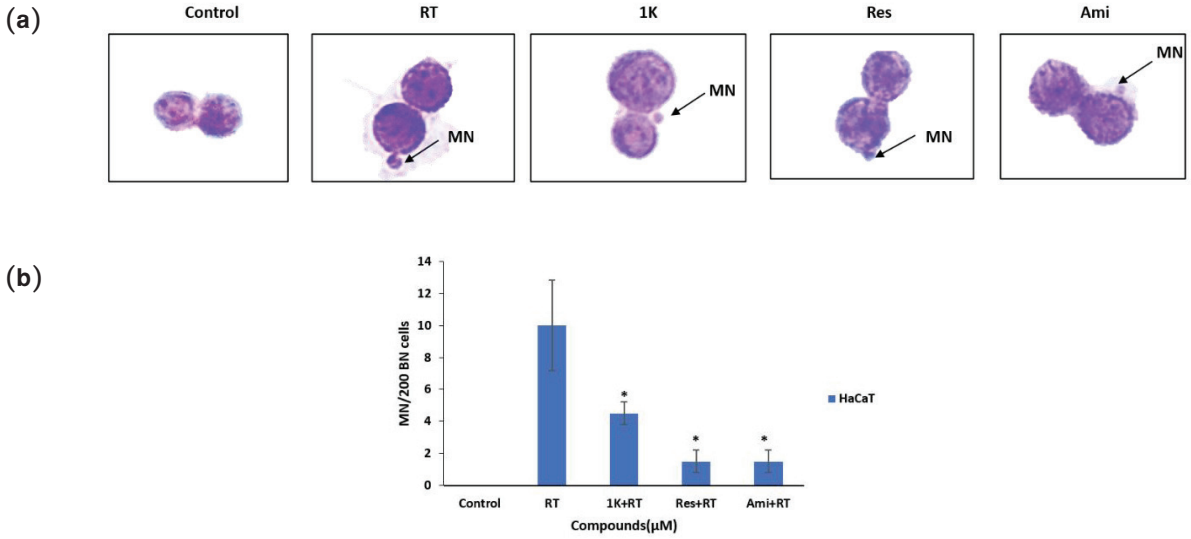

Figure 3 The micronuclei formation assay. Image showed binucleated and binucleated cells with micronuclei of non-irradiation, irradiation alone, and treated with 1K (curcumin derivative) or Res (resveratrol) or Ami (amifostine) before 2 Gy cell irradiation (a). Total number of micronuclei formation assay (b). *p-value<0.05 compared to the irradiation alone group.

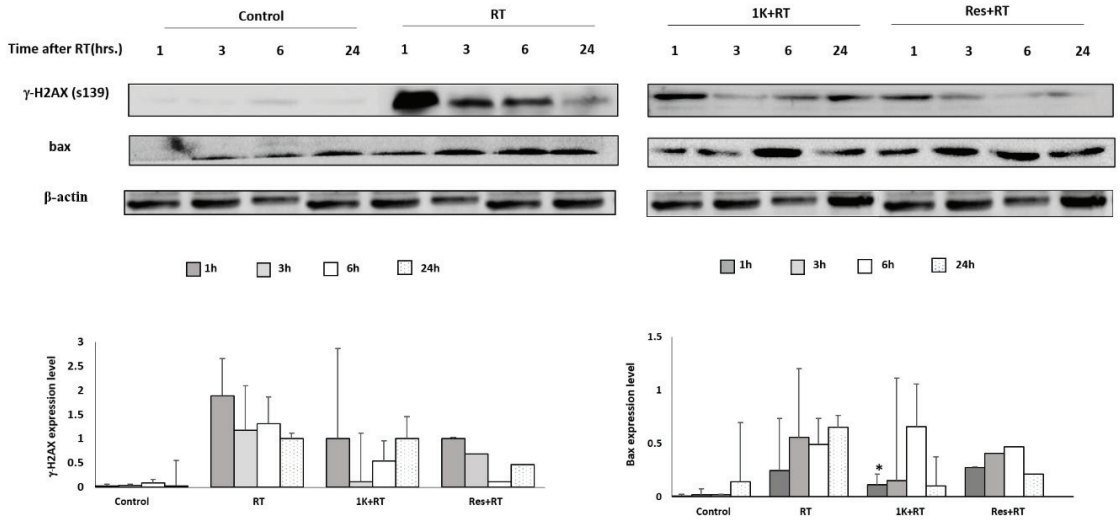

Figure 4 Representative Western blot bands of HaCaT cells under different conditions, including untreated control, irradiation alone (RT), curcumin derivative 1K pretreatment (1K+RT), and resveratrol pretreatment (Res+RT), at various incubation times after irradiation. Protein expression levels were normalized to β-actin. Data represent the mean±S.D. from three independent experiments. Statistical significance was determined using the Kruskal–Wallis test followed by Dunn's post hoc test. p-value<0.05 compared with the irradiation-only group.

Discussion

The clonogenic cell survival assay was used for the study of irradiation effects. The inability to proliferate and loss of the reproductive integrity is ones of the common manners to describe cell death[11]. 1K pretreatment increased cell survival by increasing the number of colonies after irradiation. For HaCaT cells, clonogenic cell survival assay showed significant increased of colonies after being treated with 1K when compared to cell irradiation alone. 1K are able to protect cells from radiotherapy equal to resveratrol, a positives controls. For breast cancer cells (MDA-MB-231), clonogenic cell survival assay showed insignificant increases in the number of colonies after treating cells with 1K when compared to cell irradiation alone. This result confirms that curcumin derivative did not promote breast cancer proliferation. Micronuclei formation assay (MN) occurred at post-mitosis and scored in binucleated cell post-treatment with cytochalasin B. Radioprotective agent treatment before irradiation significantly reduces radiation-induced apoptosis. Our result shown that cells treated with 1K before irradiation significantly decreased DNA damage and shown lower MN compare with cell irradiation alone. This result suggests that 1K would be able to decrease DNA damage and represent radioprotective activity. This protein related to radioprotective response identified by Western blot analysis. We found that 1K suppressed the protein level at 1 hour after irradiation and 1K also reduced DNA damage with decrease γ-H2AX at 3 hours after irradiation. Moreover, 1K pretreatment protected HaCaT cells from radiation by reducing bax, pro-apoptotic protein. Curcumin exhibits antioxidant, anti-inflammatory, antimicrobial, anticancer, and antimutagenic properties, shows strong therapeutic potential against various cancer. It regulates transcription factors, growth factors, cytokines, and enzyme to inhibit tumor growth, induce apoptosis, and suppress angiogenesis. Recent studies highlight that novel curcumin analogues, metal complexes, nanoparticles and its derivatives enhanced anticancer, anti-inflammatory and antioxidant activities compared to native-curcumin. Structural modification of curcumin enhances its pharmacological, physicochemical and pharmacokinetic properties. Derivatives with higher methoxylation, diketone unsaturation, and lower hydrogenation can improve antioxidant and anti-inflammatory activities. Many curcumin derivatives also show greater cytotoxicity against tumor cells compared to normal cells[12]. Here, curcumin derivative (1K) showed promising radioprotective activity and potential for development as radioprotectors.

Conclusion

In this study, the radioprotective activity of the curcumin derivative 1K, derived from Curcuma longa L., was investigated. Our results demonstrated that 1K selectively protected normal keratinocytes (HaCaT) without promoting the survival of breast cancer cells (MDA-MB-231) during radiotherapy. Pretreatment with 1K significantly increased clonogenic survival of HaCaT cells compared with irradiation alone. Micronucleus assays confirmed reduced chromosomal damage in 1K-pretreated cells, while Western blot analysis revealed decreased γ-H2AX and Bax expression, indicating attenuation of DNA double-strand breaks and apoptosis. These findings suggest that 1K exerted radioprotective effects through its antioxidant properties and modulation of DNA damage response pathways.

Taken together, 1K represents a promising candidate radioprotective agent for protecting normal tissues during radiotherapy. Its selective protection of normal cells, without conferring radioprotection to cancer cells, highlights its potential advantage over current agents such as amifostine. Future studies should further evaluate its pharmacological properties, delivery strategies, and potential clinical applications, including topical formulations to protect normal skin during radiation treatment.

Acknowledgement

This work was financially supported by the Research Fund of the Faculty of Medicine, Prince of Songkla University.

Conflict of interest

There are no potential conflicts of interest to declare.

References

1. Giaquinto AN, Sung H, Newman LA, Freedman RA, Smith RA, Star J, et al. Breast cancer statistics 2024. CA Cancer J Clin 2024;74:477–95.
2. Wei J, Meng L, Hou X, Qu C, Wang B, Xin Y, et al. Radiation-induced skin reactions: mechanism and treatment. Cancer Manag Res 2018;11:167–77.
3. Molkentine JM, Fujimoto TN, Horvath TD, Grossberg AJ, Garcia CJG, Deorukhkar A. Enteral activation of WR-2721 mediates radioprotection and improved survival from lethal fractionated radiation. Sci Rep 2019;9:1949.
4. Kaur K, Al-Khazaleh AK, Bhuyan DJ, Li F, Li CG. A review of recent curcumin analogues and their antioxidant, anti-inflammatory, and anticancer activities. Antioxidants (Basel) 2024;13:1092.
5. Mapoung S, Pitchakarn P, Yodkeeree S, Ovatlarnporn C, Sakorn N, Limtrakul P. Chemosensitizing effects of synthetic curcumin analogs on human multi-drug resistance leukemic cells. Chem Biol Interact 2016;244:140–8.
6. Chumsuwan N, Khongkow P, Kaewsuwan S, Kanokwiroon K. Interruptin C, A radioprotective agent, derived from cyclosorus terminans protect normal breast MCF-10A and human keratinocyte HaCaT cells against radiation-induced damage. Molecules 2022;27:3298.
7. van Meerloo J, Kaspers GJ, Cloos J. Cell sensitivity assays: the MTT assay. Methods Mol Biol 2011;731:237–45.
8. Franken NAP, Rodermond HM, Stap J, Haveman J, van Bree C. Clonogenic assay of cells in vitro. Nat Protoc 2006;1:2315–9.
9. Farabaugh CS, Doak S, Roy S, Elespuru R. In vitro micronucleus assay: method for assessment of nanomaterials using cytochalasin B. Front Toxicol 2023:5:1171960.
10. Gavini K, Parameshwaran K. Western Blot. [homepage on the Internet]. Treasure Island (FL): StatPearls Publishing; 2025. Available from: http://www.ncbi.nlm.nih.gov/books/NBK542290/
11. Munshi A, Hobbs M, Meyn RE. Clonogenic cell survival assay. Methods Mol Med 2005;110:21–8.
12. Ali NM, Yeap SK, Abu N, Lim KL, Ky H, Pauzi AZM. Synthetic curcumin derivative DK1 possessed G2/M arrest and induced apoptosis through accumulation of intracellular ROS in MCF-7 breast cancer cells. Cancer Cell Int 2017;17:30.
13. Carsten RE, Bachand AM, Bailey SM, Ullrich RL. Resveratrol reduces radiation-induced chromosome aberration frequencies in mouse bone marrow cells. Radiat Res 2008;169:633–8.

Silk Fibroin Incorporated with Disaccharide to Organize Morphological Construction of Wound Dressings; Fabrication, Characterization and Physical Performance

Nitikorn Phattanee[1], Pemikar Srifa[1,2], Kantida Juncheed[1]*

[1]Institute of Biomedical Engineering, Department of Biomedical Sciences and Biomedical Engineering, Faculty of Medicine, Prince of Songkla University, Hat Yai, Songkhla 90110, Thailand.
[2]Translational Medicine Research Center (TMRC), Department of Biomedical Sciences and Biomedical Engineering, Faculty of Medicine, Prince of Songkla University, Hat Yai, Songkhla 90110, Thailand.

Abstract:

Objective: Creating an optimal, moist environment is a critical factor in advancing wound healing outcomes. This study explores the morphological construction of advanced wound dressings designed to maintain moisture balance, while promoting tissue regeneration. This is by engineering silk firoin (SF) structures by integrated disaccharide sugar at different concentrations, via Maillard reaction. It affects moisture retention, as evaluated by morphology and drying time analyses.

Material and Methods: SF was extracted, purified, and dissolved, then combined with disaccharides (sucrose, maltose, and lactose) at 10–40% w/w ratios, and heated at 100 °C for 4 hours to induce the Maillard reaction. The resulting SF/disaccharide mixtures were dispensed into 12-well plates (5 µL per well, 1–2 mm thickness: 20 mm diameter), frozen at –80 °C for 48 hours, then lyophilized at –60 °C and 0.002 mPa for one day.

Results: The morphological and drying characteristics of SF incorporated with disaccharides were evaluated using scanning electron microscopy (SEM) and drying time analysis. SEM and drying analyses showed that incorporating disaccharides into SF enhanced interconnected porosity and reduced average pore size; with no major differences among disaccharide types or concentrations. All disaccharide-containing samples dried slower than pure SF, indicating increased water retention.

Conclusion: This study developed SF-based sheet dressings modified with disaccharides, via the Maillard reaction, to enhance moisture retention. Morphological and drying analyses showed reduced pore size and improved water retention. However, the effects of disaccharide type and concentration remains inconclusive; warranting further investigation.

Keywords: silk fibroin, disaccharide sugar, the maillard reaction, morphology characterization, drying time

Corresponding author: Kantida Juncheed
Institute of Biomedical Engineering, Department of Biomedical Sciences and Biomedical Engineering, Faculty of Medicine, Prince of Songkla University, Hat Yai, Songkhla 90110, Thailand.
E-mail: kantida.j@psu.ac.th

Introduction

Wound dressings play a critical role in modern wound management, by providing a protective barrier, promoting a moist healing environment and preventing infection[1]. A pivotal shift in modern wound care is the recognition of the importance of maintaining a moist wound environment[2]. Unlike traditional dry dressings, which can delay healing and cause pain during dressing changes, moist wound healing promotes cell migration, angiogenesis, and tissue regeneration, while reducing scab formation and minimizing scarring. Traditional wound dressings; such as gauze and cotton pads[3], are limited by their inability to retain moisture, lack of exudate management, and potential for adherence to the wound bed, leading to trauma upon removal. These modern solutions are designed to maintain optimal moisture levels and enhance patient comfort; ultimately accelerating the healing process and reducing the risk of complications.

Silk fibroin (SF) is a protein fibroin having a lot of the proper properties as a biomedical construction for wound healing; such as excellent biocompatibility, biodegradability, tailor mechanical properties and anti-inflammatory properties[4].

This study focuses on the development of wound dressing materials that investigate the effects of tailor interconnected porosity, by the combination of disaccharide sugar and SF, via the Maillard reaction, on the ability to hold moisture contents from the morphology and drying time characterization. Moreover, the drying time evaluation of different types of disaccharides was also included to determine whether which concentrations are the most effective as a retained moisture wound dressing.

Material and Methods

Preparation of SF solution

Silk cocoons from the *Bombyx mori* silkworm (Nang Noi Srisaket 1) underwent three rounds of degumming. This involved soaking the cocoon in a 0.02 M solution of Na_2CO_3 at 90 °C for 30 minutes to remove the sericin. Then, the SF fiber was dried overnight at 37 °C, and then dissolved the SF in a 9.3 M LiBr solution. The resulting solutions were dialyzed against distilled water for 72 hours. During this process, the water was changed every 6 hours to eliminate LiBr. After this, the silk solution was centrifuged at 3,000 rpm for 20 minutes[5]. The final concentration of the prepared SF was between 8–11% w/v. Then, the solution of SF was adjusted to 3%w/v, by using distilled water and the solution was stored at a temperature of 4 °C.

Preparation of SF incorporate with disaccharides via the Maillard reaction

SF solution at 3% w/v were combined with sucrose (SFS), maltose (SFM) and lactose, (SFL) at ratios 10, 20, 30 and 40% w/w. The interaction between SF and disaccharides was performed via the Maillard reaction at 100 °C for 4 hours[6].

Fabrication of soft biomaterials with freeze-drying technique

SF/disaccharide solution were dropped into 12 well-plates; at 5 µL for thickness 1–2 mm and a diameter of 20 mm freeze-dry sheets. The 12 well-plates were incubated at a temperature −80 °C for 48 hours and freeze-dried via auto mode (−60 °C, 0.002 mPa) for 1 day. Then, the lyophilized samples were stored in a desiccator at 25 °C and 65% relative humidity, before characterization[7].

Characterization of SF/disaccharides sheet

Morphology characterization

The surface morphology of the freeze-dried sheets was examined using a Scanning Electron Microscope (SEM) JSM-5800 LV, JEOL, Japan. The freeze-dries sheets were fixed on a stub, and the samples were photographed at a certain magnification (200X and 1,000X). Then, interconnect network was analyzed by image J. This was to be certain that the samples were representative for analysis: 3 samples were used to analyze pore sizes for all ratios, which were analyzed from multiple locations with each sample.

Drying time characterization

Free moisture contents (X) of all samples were detected by soaking the lyophilized sheets (M) in PBS buffer: pH 7.4 at 37 °C. Then, the wet samples were weighed (W) by doubling the weighing time until the sample was completely dry. Moreover, another condition that affected the drying of samples; such as relative humidity (%RH) and environmental temperature was attempted to be controlled at 60% and 37 °C, respectively. The free moisture content value was calculated with the equation below[8].

$$\textit{Free moisture contents (X)} = \frac{W - M}{M}$$

W=mass of wet samples

M=mass of dry samples

Statistical analysis

All experiments were performed in triplicate. The data are present as mean±standard deviation (S.D.). The independent sample t-test was applied to determine the p-value. In all cases, the difference was significant when *p-value≤0.05; with n.s. being non-significant.

Results

Morphology characterization

The effects of incorporating disaccharides into SF on the resulting material's morphology were investigated by comparing top-view images of pure SF (Figure 1) against SF reacting with different types of disaccharides, at a magnification of 200 and 1,000, respectively (Figures 2 and 3). When comparing pictures, the interconnected porosity observed in SF combined with disaccharides was notably higher than that of pure SF.

Additionally, quantitative analysis of pore sizes (Figure 4) revealed that the average pore size in SF reacting with disaccharides was significantly lower compared to pure SF. This reduction in pore size can be attributed to the presence of disaccharides acting as impurities in the aqueous SF solution, which disrupts the freezing process of water[9]. This disruption leads to the formation of smaller ice crystals during the freezing step prior to lyophilization in the disaccharide-containing SF solution. This then results in a hydrogel, with a finer pore structure after the lyophilization process compared to pure SF.

The quantitative analysis of pore sizes of SF reacting with disaccharides at each concentration (Figure 5) revealed no trend variations in the surface morphology of the lyophilized samples being observed, with increasing disaccharide concentration across the different disaccharide types.

Drying time characterization

The effects of combining disaccharides into SF on the drying time of the samples were investigated. From the results, as shown in Table 1, the drying time of SF combined with disaccharide were significantly slower than the pure SF. When comparing the drying time of SF combined with disaccharide, there were no significant differences between the samples.

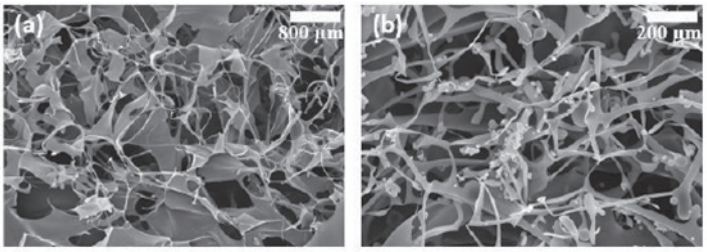

Figure 1 Scanning electron microscope (SEM) images. (a) lyophilized SF at a magnification of 200x and a scale bar at 800 µm, (b) lyophilized SF magnification: 1,000x and scale bar at 200 µm.

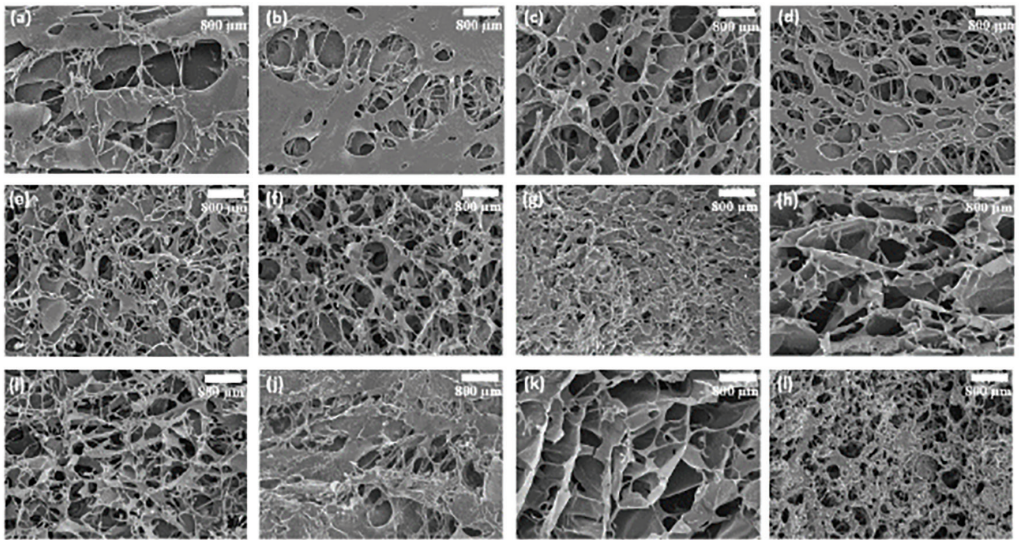

Figure 2 SEM images of SF reacting with disaccharides at a magnification of 200x and a scale bar at 800 µm. (a–d) SFM at ratios of 10, 20, 30 and 40% w/w, respectively. (e–h) SFS at ratios of 10, 20, 30 and 40% w/w, respectively. (i–l) SFL at ratios of 10, 20, 30 and 40%w/w, respectively.

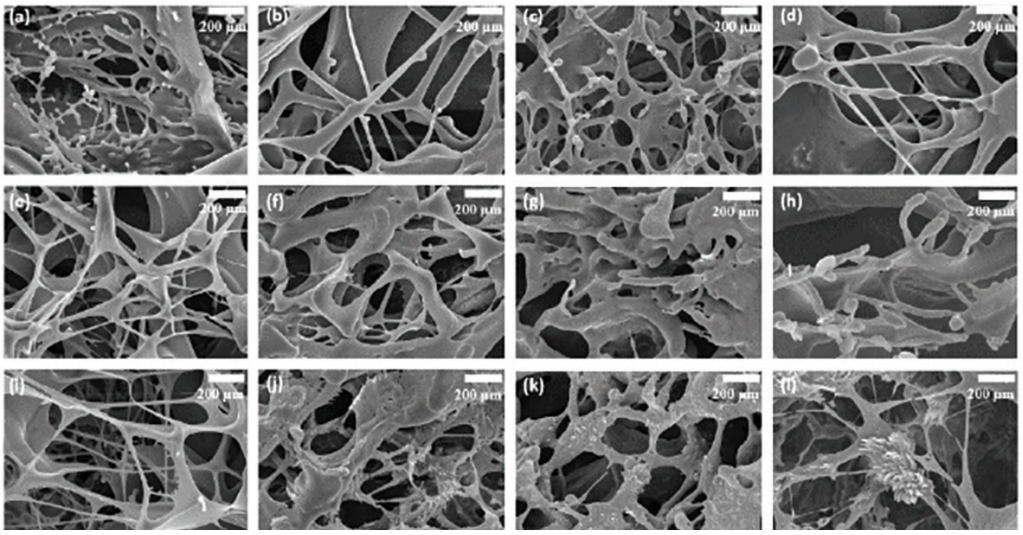

Figure 3 SEM images of SF reacting with disaccharides at a magnification of 1,000x and a scale bar at 200 µm. (a–d) SFM at ratios of 10, 20, 30 and 40% w/w, respectively. (e–h) SFS at ratios of 10, 20, 30 and 40% w/w, respectively. (i–l) SFL at concentrations of 10, 20, 30 and 40% w/w, respectively.

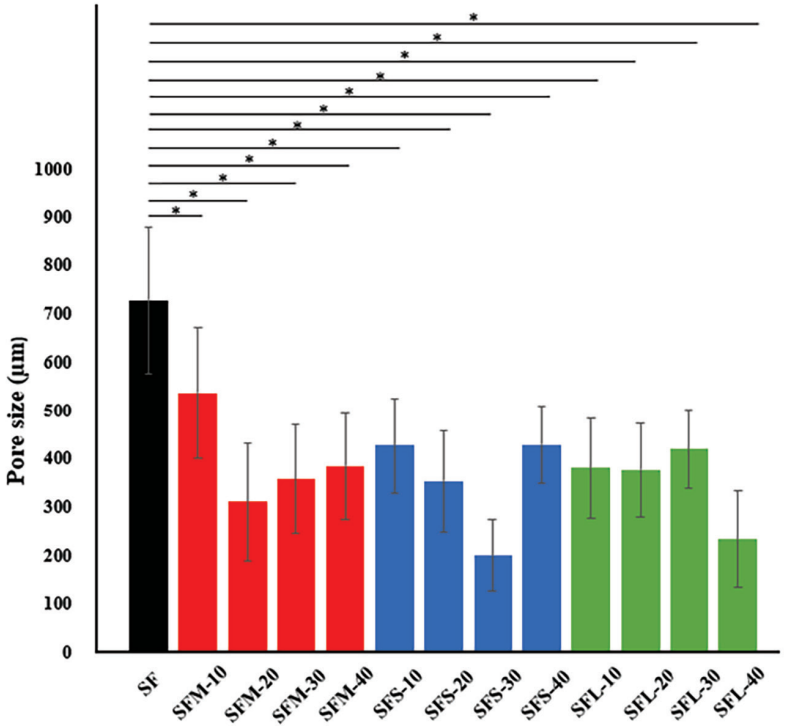

Figure 4 Average pore sizes of SF and SF reacting with disaccharides at ratios of 10, 20, 30 and 40% w/w, measured by ImageJ. Results are shown as mean±standard deviation (n=3) (*p-value≤0.05).

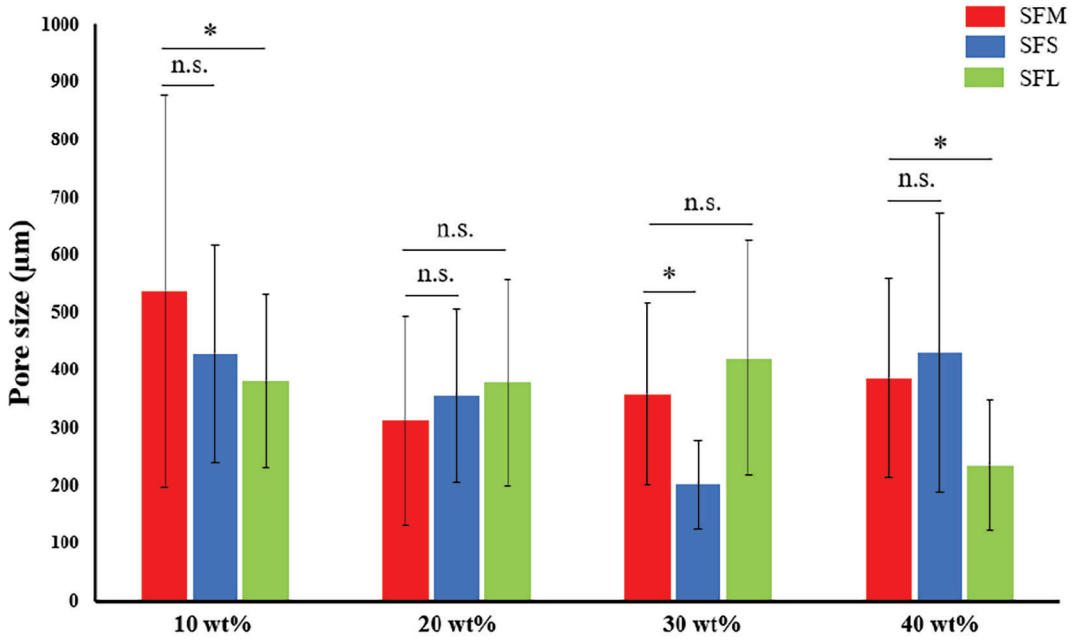

Figure 5 Statistical comparison of pore sizes of SF reacting with disaccharides at each concentration.*p-value≤0.05 (n=3). n.s. for non-significant

Table 1 The drying time of SF and SF combined with disaccharide at ratios of 10, 20, 30 and 40% w/w

Samples	Ratios of disaccharides with SF (3% w/v)	Drying time (mins)
SF	–	10.333±0.577
SFM	10 wt%	15.333±1.527*
	20 wt%	17.333±0.577*
	30 wt%	16.333±1.527*
	40 wt%	18.000±1.000*
SFS	10 wt%	15.333±0.527*
	20 wt%	16.333±0.577*
	30 wt%	17.333±1.154*
	40 wt%	16.000±1.000*
SFL	10 wt%	15.667±0.577*
	20 wt%	16.000±1.000*
	30 wt%	15.667±0.577*
	40 wt%	18.000±1.000*

*p-values were calculated from the comparison between SF and SF combined with disaccharides

Discussion

The Maillard reaction between SF and disaccharides resulted in the grafting of disaccharide molecules onto the SF backbone, leading to structural changes in the SF chains and the formation of a grafted polymer structure. However, studies comparing the morphology of conventional polymer networks with grafted polymer structures have shown that the overall network formation of grafted polymers does not differ significantly from that of normal polymer networks[10]. Some distinct features have been observed; such as slightly increased surface roughness in grafted polymers, compared to normal networks[11]. Nevertheless, morphological characterization alone provides insufficient evidence to clearly distinguish the structural differences between them.

Based on the morphology and drying time results, the larger the average porosity, the faster the drying time. This result indicates a correlation between porosity and the drying rate of liquid within a lyophilized sample. Typically, larger pore sizes lead to faster water evaporation from the sample, as the empty spaces provide additional pathways for water vapor to move through the material[12]. Therefore, the combination of SF and disaccharide via the Maillard reaction increases the interconnected porosity, resulting in a decrease in the overall pore size of the sample.

Healing occurs more quickly in a moist wound environment than in a dry one. Moisture supports faster skin cell migration (epithelialization), minimizes pain and scarring, and enhances the body's natural process of removing dead tissue (autolytic debridement)[13]. Hence, the combination of disaccharide sugar in SF structures keeps the wound in the most suitable condition for wound healing.

Conclusion

In this work, we focused on the development of a sheet dressing designed to maintain a mild environment conducive to wound healing, by tailoring the construction of the silk fibroin (SF) framework with disaccharide sugars via the Maillard reaction. Morphological and drying time characterizations show that the interaction between SF and disaccharides reduces the average pore size. As a result, SF combined with disaccharides exhibits a higher moisture retention capacity compared to pure SF. This study demonstrates the use of disaccharide sugars to engineer the silk fibroin network structure, with the aim of designing wound dressings that provide enhanced moisture retention. However, this study does not conclusively determine the effects of different types or amounts of disaccharides on the network structure and drying time of the samples. Therefore, Further investigations are necessary to be performed; such as chemical characterizations, to confirm and classify the Maillard reaction between silk fibroin and disaccharides. In addition, mechanical property testing is still required to differentiate the distinct characteristics of silk fibroin reaction with reducing sugars and non-reducing sugars for optimizing wound dressing development.

Acknowledgement

This work was supported by a PSU New Scholar Grant (MED6502043S), and partially by the Faculty of Medicine, Prince of Songkla University. Ethical approval for this research was obtained from the Human Research Ethics Unit, Faculty of Medicine, Prince of Songkla University, under project number REC. 68-128-38-2. The committee determined on 21 March, 2025, that the submitted protocol met the criteria of the Exemption Determination (according to SOP version 3, Chapter 5). Lastly, experimental costs were partially support by the Graduate School, Prince of Songkla University to Nitikorn Phattanee.

Conflict of interest

There are no potential conflicts of interest to declare.

References

1. Fahimirad S, Ajalloueian F. Naturally-derived electrospun wound dressings for target delivery of bio-active agents. International J Pharm 2019;566:307–28.
2. Rashdan HRM, El-Naggar ME. Chapter 2-Traditional and modern wound dressings—characteristics of ideal wound dressings. In: Khan R, Gowri S, editors. Developments in applied microbiology and biotechnology, antimicrobial dressings. Cambridge: Academic Press; 2023;21-42.
3. Nuutila K, Eriksson E. Moist wound healing with commonly available dressings. Adv Wound Care 2021;10:685–98.
4. Noreen A, Tabasum S, Ghaffar S, Somi T, Sultan N, Aslam N, et al. Chapter 12-Protein-based bionanocomposites. In: Zia KM, Jabeen F, Anjum MN, Ikram S, editors. Micro and nano technologies, bionanocomposites. Amsterdam: Elsevier; 2020; 267-320.
5. Huang L, Shi J, Zhou W, Zhang Q. Advances in preparation and properties of regenerated silk fibroin. IJMS 2023;24:13153.
6. Kwak HW, Park J, Yun H, Jeon K, Kang DW. Effect of crosslinkable sugar molecules on the physico-chemical and antioxidant properties of fish gelatin nanofibers. Food Hydrocoll 2021;111:106259.
7. Sangkert S, Kamonmattayakul S, Lin CW, Meesane J. Modified silk and chitosan scaffolds with collagen assembly for osteoporosis. Bioinspired Biomim Nanobiomaterials 2016;5:1–11.
8. Berk Z. Dehydration. In: Food process engineering and technology [monograph on the Internet]. Amsterdam: Elsevier; 2009 [cited 2025 Mar 10]. p.459–510. Available from: https://linkinghub.elsevier.com/retrieve/pii/B9780123736604000223
9. Raventós M, Hernández E, Auleda J, Ibarz A. Concentration of aqueous sugar solutions in a multi-plate cryoconcentrator. J Food Eng 2007;79:577–85.
10. Lim YJ, Choi YE, Lee JH, Lee GD, Komitov L, Lee SH. Effects of three-dimensional polymer networks in vertical alignment liquid crystal display controlled by in-plane field. Opt Express 2014;22:10634.
11. Barleany DR, Heriyanto H, Alwan H, Kurniawati V, Muyassaroh A, Erizal E. Effect of starch and chitosan addition on swelling properties of neutralized poly(acrylic acid)-based superabsorbent hydrogels prepared by using γ-Irradiation Technique. Atom Indo 2022;48:99.
12. Abd Al-Ghani MM, Azzam RA, Madkour TM. Design and development of enhanced antimicrobial breathable biodegradable polymeric films for food packaging applications. Polymers 2021;13:3527.
13. Field CK, Kerstein MD. Overview of wound healing in a moist environment. Am J Surg 1994;167:S2–6.

JHSMR The 4th Annual Health Research International Conference
AHR-iCON 2025
Shaping the Future: Innovation, Health and Well-being
OCTOBER 9-10TH, 2025
THE FACULTY OF MEDICINE, PRINCE OF SONGKLA UNIVERSITY
Medical Innovation
R2-O-020

Virtual Reality Intervention During Hysteroscopy: A Novel Approach to Enhancing Parasympathetic Responses

Preyahathai Aroonvanichporn[1], Thiti Chartdamring[2], Pimpun Prasanchit[2], Jittima Manomai[2], Kakanand Srungboonmee[3]*

[1]NIST International School, Bangkok 10110, Thailand.
[2]Department of Obstetrics and Gynecology, Faculty of Medicine Ramathibodi Hospital, Mahidol University, Bangkok 10400, Thailand.
[3]Center for Research Innovation and Biomedical Informatics, Faculty of Medical Technology, Mahidol University, Nakhon Pathom 73170, Thailand.

Abstract:

Objective: Pain and anxiety are barriers to patient comfort during office hysteroscopy. This study assessed whether virtual reality (VR) can modulate heart-rate variability (HRV), an objective marker of parasympathetic activity, and reduce self-reported anxiety and pain.

Material and Methods: Of 60 women recruited at Ramathibodi Hospital, 55 met the eligibility criteria and were retrospectively analysed (control, n=19; VR, n=36). All procedures used the vaginoscopic technique without anaesthesia. The control group wore a headset delivering instrumental music with eyes closed; whereas, the VR group viewed synchronized 360° nature scenes, with the same soundtrack. The VR intervention delivered an immersive environment previously shown to reduce anxiety and pain in minor procedures. Anxiety was measured with the State-Trait Anxiety Inventory (STAI-Y-1), pain with a 10-cm visual analog scale (VAS), and HRV, with a single-lead ECG recorded continuously during hysteroscopy and was analysed offline. Time-domain (RMSSD, SDNN) and frequency-domain (HF, LF) indices were evaluated.

Results: Baseline STAI-Y-1 and VAS values did not differ between groups. Post-procedure anxiety and pain remained unchanged. In contrast, RMSSD was significantly higher with VR (9.0±4.4 ms) than with control (6.8±3.7 ms; p-value= 0.03), indicating augmented parasympathetic tone; SDNN showed a borderline increase (p-value=0.05). In contrast, frequency-domain HRV metrics were not significantly different (p-value>0.05).

Conclusion: Immersive VR enhanced vagal activity during hysteroscopy, as evidenced by elevated RMSSD, despite no change in subjective anxiety or pain.

Keywords: heart-rate variability, office hysteroscopy, parasympathetic activity, virtual reality

Corresponding author: Kakanand Srungboonmee
Center for Research Innovation and Biomedical Informatics, Faculty of Medical Technology, Mahidol University, Nakhon Pathom 73170, Thailand.
E-mail: kakanand.sru@mahidol.ac.th

Introduction

Hysteroscopy can generally cause anxiety in patients. The vaginoscopic approach to office hysteroscopy has reduced reliance on anesthesia, and enabled same-day intrauterine diagnosis in ambulatory settings. Nevertheless, pain and anxiety remain barriers to patient tolerance and cooperation[1,2]. These psychological responses are multifactorial, with patients often experiencing anticipatory anxiety from prior gynecologic trauma, lack of control or fear of discovering pathology. Notably, disease-related anxiety may persist or increase following the procedure, overriding the calming effects of familiar interventions; such as music or verbal reassurance[1].

Previous studies have examined non-pharmacological interventions to modulate procedural anxiety. Among these, VR has garnered attention for its immersive, multisensory distraction effect. Trials in gynecologic care and minor surgeries have demonstrated VR's potential in reducing pain and anxiety; although, findings are not uniform across patient populations or procedures[3-6]. The immersive nature of VR generates a sense of presence in a non-threatening environment, which can divert attentional resources away from nociceptive stimuli and anticipatory worry.

Physiological indicators; such as heart-rate variability (HRV), offer valuable insight into emotional regulation during medical procedures. HRV reflects the dynamic interplay between sympathetic and parasympathetic activity. Specifically, RMSSD and SDNN are time-domain indices that capture short-term vagal tone and overall HRV. An increase in RMSSD is indicative of heightened parasympathetic modulation[7,8]. Although, frequency-domain indices; such as HF, LF and LF/HF power are also used, they require longer recordings and may be less reliable over brief time intervals, which is a recognized methodological limitation of the frequency transformation.

This retrospective observational study reviewed previously collected data from a prospective randomized controlled study aimed to determine whether VR could improve autonomic function during hysteroscopy, as measured by HRV, and whether these physiological changes correspond to reduced self-reported anxiety and pain.

Material and Methods

Study population

This retrospective observational study reviewed previously collected data from the Department of Obstetrics and Gynecology, Faculty of Medicine Ramathibodi Hospital, Mahidol University; Thailand. Clinical ECG and questionnaire recorded from 60 consecutive women (aged 18–50 years) having undergone outpatient office hysteroscopy; between February and June 2025 were screened (Figure 1). All hysteroscopies had been performed by a single gynecologist, using a TruClear™ 5C hysteroscope without anesthesia; following the vaginoscopic technique. During the procedure, patients experienced one of two pre-recorded audiovisual conditions that were identical to those validated in Sewell et al.'s randomized trial[4].

Music (control) group: patients rested with eyes closed, while listening to the instrumental-music track from that study through noise-isolating headphones.

VR (intervention) group: patients wore a Pico G2 4K headset (resolution 3840×2160; refresh rate 75 Hz; field of view 101°; weight 280 g) streaming 360° natural scenes, with synchronized instrumental music and ambient audio. This device was chosen for its high-resolution, low-latency display and comfortable lightweight design, enabling uninterrupted immersion during hysteroscopy.

Experimental protocol

The study protocol followed a standardized timeline: as indicated in Figure 2. The ECG patch was applied several minutes prior to the procedure, and continuous ECG recording was maintained throughout hysteroscopy. HRV parameters were computed offline after data collection. Pain was scored by a self-report questionnaire ("How did you rate your pain during hysteroscopy 0–10?").

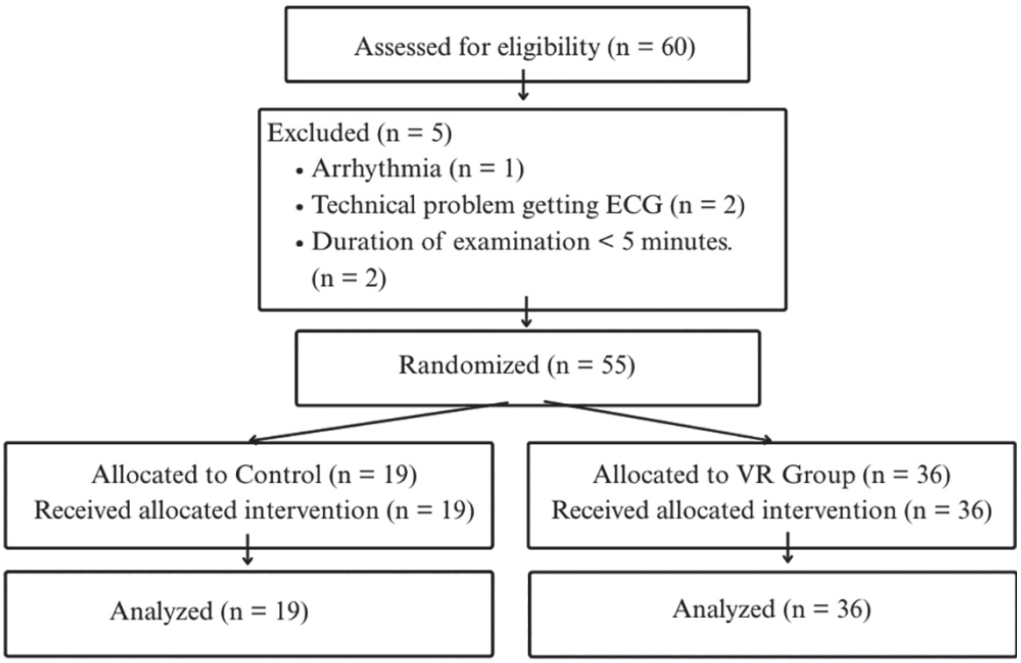

Figure 1 CONSORT flow diagram of participant recruitment

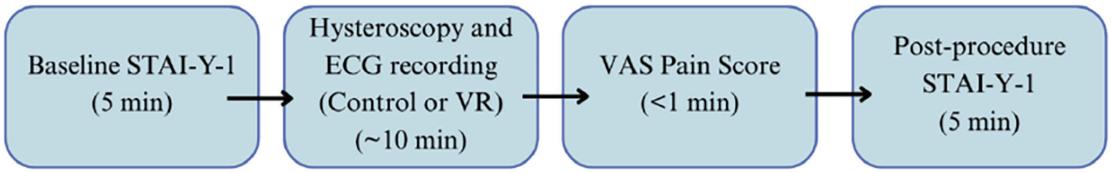

Figure 2 Experimental protocol timeline

VR design and validation

The VR module consisted of 360° high-resolution panoramic environments (forest, waterfalls and beaches) with slow camera transitions synchronized to instrumental music and ambient nature sounds. This content was intended to engage visual and auditory senses simultaneously, producing attentional redirection and promoting parasympathetic activation[3].

Immediately before and after hysteroscopy, participants completed the Thai version of the STAI-Y-1[9]. Pain intensity was recorded post-procedure on a 10-cm VAS. HRV was captured with a mobiCARE-MC100 single-lead ECG patch, with a sampling rate of 256 Hz, throughout the hysteroscopic procedure. Time-domain indices—RMSSD and SDNN—and frequency-domain indices (HF and LF power) were computed with the open-source PyHRV package[1,2], along with LF/HF; noting that frequency-domain metrics are less reliable over a brief recording interval.

Inclusion criteria for the current analysis were: (i) no prior hysteroscopy experience and (ii) complete pre- and post-procedure anxiety assessments. Exclusion criteria were: documented use of anxiolytic medication, diagnosed psychiatric or neurological disorder, cardiovascular disease or refusal/inability to wear the VR headset during the original procedure. Five datasets were excluded, owing to poor ECG

signal quality or protocol deviations; leaving 55 patients for analysis (control group=19: VR group=36)

Statistical analysis

Continuous variables were summarized as mean± standard deviation (S.D.). Group comparisons (Control vs VR) employed Mann–Whitney U tests, due to unequal samples. A two-sided p-value<0.05 denoted statistical significance. Analyses were conducted with IBM SPSS Statistics version 29.

Assessments

Anxiety levels were evaluated using the Thai version of the State-Trait Anxiety Inventory (STAI-Y-1), administered pre- and post-procedure[9]. Pain was assessed immediately after hysteroscopy, using a 10 cm Visual Analog Scale (VAS). HRV was measured using a mobiCARE-MC100 single-lead wearable ECG patch. Recordings were taken for 3 minutes post-procedure, while the patient remained seated. Time-domain parameters RMSSD and SDNN were calculated using PyHRV; an open-source Python package[1]. Frequency-domain indices HF, LF and LF/HF power were also computed, but interpreted with caution due to the short recording window.

Statistical analysis

Mann-Whitney tests were used to compare continuous variables between groups. A p-value<0.05 was considered statistically significant. Data was analyzed using SPSS version 29.

Results

Figure 3 shows RMSSD was significantly higher in the VR group (9.0±4.4 ms) compared to the control group (6.8±3.7 ms), with a p-value=0.03. SDNN values were also greater in the VR group (13.1±5.0 ms vs. 10.8±4.6 ms), with a p-value=0.05. No significant differences were found in HF or LF power (p-values=0.22 and 0.15, respectively). The LF/HF ratio did not show significant statistical difference (p-value=0.41) (Table 1).

In contrast, the mean pre-procedure STAI-Y-1 scores were 40.1±7.6 in the control group and 38.7±8.2 in the VR group (p-value=0.52). Post-procedure scores were 40.6±6.9 and 40.2±7.1, respectively (p-value=0.73), indicating no significant change in anxiety levels. Pain scores on the VAS were 4.9±2.1 in the control group and 4.7±1.9 in the VR group (p-value=0.64) (Figure 4).

Discussion

Immersive VR significantly increased RMSSD during hysteroscopy, indicating a shift toward parasympathetic dominance[7]. Although, SDNN also trended higher, the difference approached but did not reach statistical significance. These results demonstrate modulation of autonomic function even though self-reported anxiety and pain did not change. Importantly, participants were otherwise

Table 1 Comparison of heart rate (bpm) and RR intervals (ms) between the two groups

	Control group (n=19) Mean±S.D.	Intervention group (n=36) Mean±S.D.	p-value
Minimum HR	70.2±11.6	65.9±10.9	0.10
Average HR	86.2±12.0	82.9±12.4	0.18
Maximum HR	114.4±14.7	110.7±17.7	0.21
Minimum RR interval	510.5±78.5	524.2±99.3	0.29
Maximum RR interval	1032.6±254.1	1040.8±226.1	0.45

healthy gynecologic patients, with no psychiatric or cardiac disorders. This is consistent with prior literature describing anxiety in this context as a procedural response.

While subjective measures of anxiety and pain, assessed by the STAI-Y-1 and VAS, respectively, did not differ significantly between groups, this result warrants deeper interpretation. One explanation is that patients' anxiety may have been driven more by concerns over potential intrauterine pathology than by the procedure itself. This health-related anxiety might have masked any transient reductions in procedural anxiety. Prior studies have reported that the STAI can be influenced by such broader psychological factors, limiting its sensitivity in acute procedural contexts[1,2]. Furthermore, the STAI-Y-1 may not be sufficiently responsive to short-lived fluctuations in emotional state; particularly during brief, single-session interventions. These findings demonstrate that even in the absence of reduced anxiety or pain perception, VR may stabilize autonomic balance and mitigate subclinical stress responses. This physiological buffering may have downstream benefits; such as reducing vasovagal episodes, improving recovery or enhancing overall procedural tolerance.

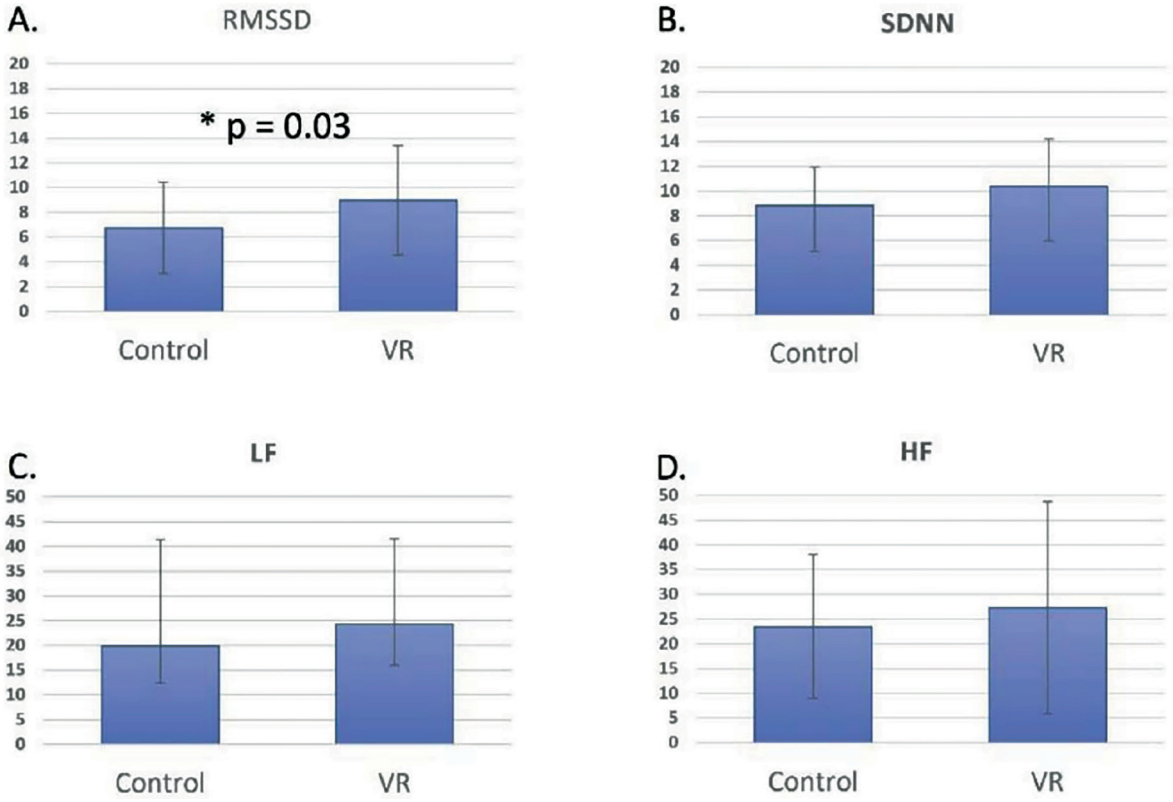

Figure 3 HRV metric comparisons between the control and VR groups

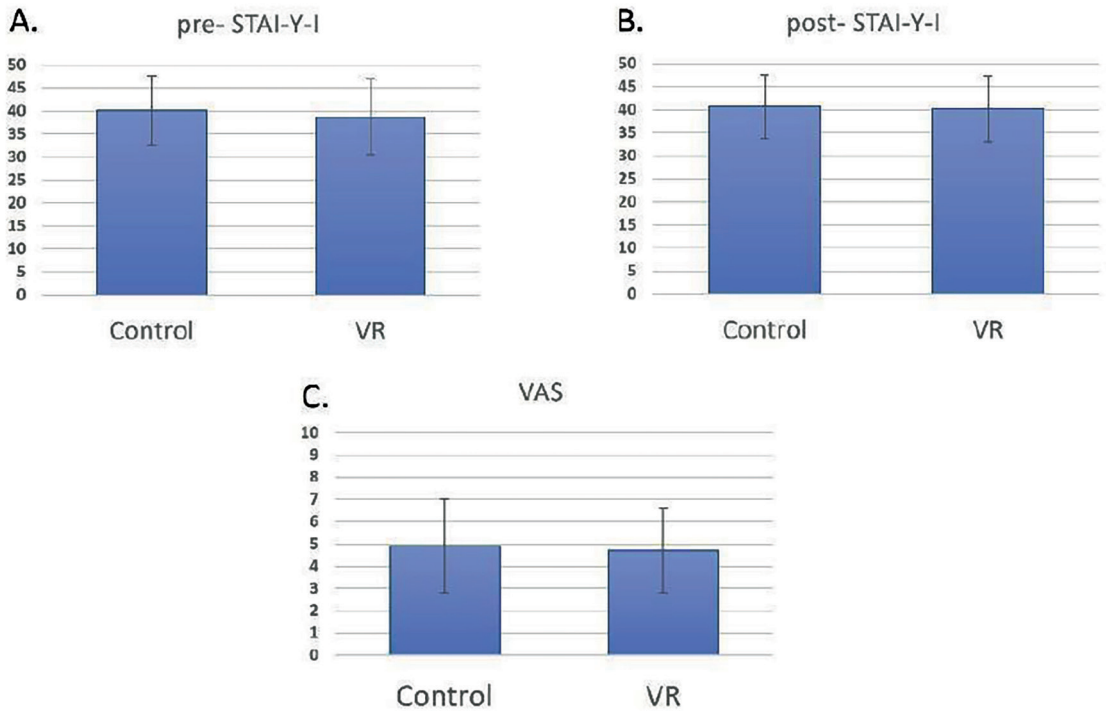

Figure 4 Anxiety before (A) and after (B) the procedures and pain perceived during hysteroscopy: as recorded by VAS (C).

The absence of a difference in VAS pain scores is consistent with the mixed findings reported in literature regarding VR's analgesic effectiveness during gynecologic procedures[3-6]. VR's pain-reducing effects may depend heavily on the nature of the content, individual pain thresholds and psychological readiness. Therefore, while VR may provide general distraction, it may not effectively override visceral discomfort for all patients.

The physiological buffering observed suggests that VR could reduce subclinical stress manifestations (e.g., vasovagal responses), support hemodynamic stability and enhance overall procedural tolerance. Rather than replacing analgesia or reassurance, VR may serve as a complementary tool that strengthens autonomic resilience. Finally, the observed increase in RMSSD adds to existing evidence that higher values reflect increased parasympathetic activity[7,8], an objective marker of physiological relaxation. Future investigations should aim to complete data collection and explore the integration of VR with other evidence-based techniques; such as guided breathing, biofeedback or cognitive behavioral therapy,to more effectively reduce both subjective and physiological markers of anxiety and pain.

Conclusion

Immersive VR significantly enhances parasympathetic activation during office hysteroscopy, as evidenced by elevated RMSSD. While self-reported anxiety and pain were unchanged, VR's physiological benefits suggest clinical value as an adjunct to existing strategies; particularly as part of multimodal approaches combining psychological and physiological interventions. Further study with longer recording time is highly recommended.

Acknowledgement

We gratefully acknowledge the Faculty of Medicine Ramathibodi Hospital for the financial support.

Conflict of interest

The authors declare no conflict of interest.

References

1. Sorrentino F, Petito A, Angioni S, D'Antonio F, Severo M, Solazzo MC, et al. Impact of anxiety levels on the perception of pain in patients undergoing office hysteroscopy. Arch Gynecol Obstet 2021;303:999–1007.
2. Gambadauro P, Navaratnarajah R, Carli V. Anxiety at outpatient hysteroscopy. Gynecol Surg 2015;12:189–96.
3. Deo N, Khan KS, Mak J, Allotey J, Gonzalez Carreras FJ, Fusari G, et al. Virtual reality for acute pain in outpatient hysteroscopy: A randomised controlled trial. BJOG 2021;128:87–95.
4. Sewell T, Fung Y, Al-Kufaishi A, Clifford K, Quinn S. Does virtual reality technology reduce pain and anxiety during outpatient hysteroscopy? A randomised controlled trial. BJOG 2023;130:1466–72.
5. Cohen N, Nasra LA, Paz M, Kaufman Y, Lavie O, Zilberlicht A. Pain and anxiety management with virtual reality for office hysteroscopy: systematic review and meta-analysis. Arch Gynecol Obstet 2024;309:1127–34.
6. Eijlers R, Utens EMWJ, Staals LM, et al. Systematic review and meta-analysis of virtual reality in pediatrics: Effects on pain and anxiety. Anesth Analg 2019;129:1344–53.
7. Shaffer F, Ginsberg JP. An overview of heart rate variability metrics and norms. Front Public Health 2017;5:258.
8. Kim HG, Cheon EJ, Bai DS, Hwan Lee Y, Koo BH. Stress and heart rate variability: a meta-analysis and review. Psychiatry Investig 2018;15:235–45.
9. Techakomol P. Manual for the Thai version of the State-Trait Anxiety Inventory. Bangkok: Thai Health Promotion Foundation; 1998.

Phloretin Inhibits Glucose Uptake in HepG2 Cells: *In Vitro* and Docking Insights

Worarat Boonpech[1], Pemikar Srifa, Ph.D.[1,2], Kantida Juncheed, Ph.D.[1]*

[1]Institute of Biomedical Engineering, Department of Biomedical Sciences and Biomedical Engineering, Faculty of Medicine, Prince of Songkla University, Hat Yai, Songkhla 90110, Thailand.
[2]Translational Medicine Research Center (TMRC), Department of Biomedical Sciences and Biomedical Engineering, Faculty of Medicine, Prince of Songkla University, Hat Yai, Songkhla 90110, Thailand.

Abstract:

Objective: Hepatocellular carcinoma (HCC), one of the leading causes of cancer-related deaths worldwide, is strongly associated with enhanced glycolysis and glucose dependence. This metabolic reprogramming is often driven by overexpression of glucose transporters; including GLUT-2, which facilitate rapid glucose uptake to support tumour growth. Targeting these transporters has therefore emerged as a promising therapeutic strategy. To evaluate the therapeutic potential of phloretin, a natural GLUT-2 inhibitor, this study investigated its effect on glucose uptake in HepG2 cells. Additionally, it explored its binding interactions and inhibitory mechanism with GLUT-2 using molecular docking analysis.

Material and Methods: Glucose uptake was quantified using the 2-NBDG fluorescence assay, following 24-hour treatment with phloretin at a half-maximal inhibitory concentration (150 µM) and full IC_{50} (300 µM). In parallel, molecular docking simulations were conducted using a homology model of human GLUT-2, so as to compare the binding affinity and interaction profiles of phloretin and glucose.

Results: Phloretin significantly reduced glucose uptake in HepG2 cells in a dose-dependent manner. Fluorescence microscopy confirmed a decreased 2-NBDG signal in treated cells. Docking analysis showed that phloretin binds to GLUT-2 with a higher predicted affinity (-7.08 kcal/mol) than glucose (-4.31 kcal/mol), engaging key binding residues. This suggests a competitive inhibition mechanism.

Conclusion: Phloretin effectively inhibits GLUT-2-mediated glucose uptake in HepG2 cells, and demonstrates strong molecular interactions at the transporter site. These findings support its potential as a metabolic inhibitor, and provide a basis for further development of GLUT-2-targeted therapies for liver cancer.

Keywords: GLUT-2, glucose uptake, HepG2 cells, molecular docking, phloretin

Corresponding author: Kantida Juncheed, Ph.D.
Institute of Biomedical Engineering, Department of Biomedical Sciences and Biomedical Engineering, Faculty of Medicine, Prince of Songkla University, Hat Yai, Songkhla 90110, Thailand.
E-mail: kantida.j@psu.ac.th

Introduction

Hepatocellular carcinoma (HCC), the most common liver cancer and a major cause of cancer deaths globally[1], is characterized by a metabolic shift called: 'the Warburg effect'; wherein, cancer cells preferentially use aerobic glycolysis for energy[2]. This increased glycolytic activity is fuelled by a significant rise in glucose uptake; often facilitated by the overexpression of glucose transporters (GLUTs) on the cell surface[3]. In HCC, the upregulation of glucose transporter type 2 (GLUT-2) directly contributes to elevated glucose uptake, providing the necessary metabolic fuel for tumour growth and survival. This makes GLUT-2 a key player in the disease's metabolic pathology[4]. Therefore, inhibiting GLUT-2 could provide a therapeutic strategy for HCC. By reducing glucose uptake in HCC cells, it could starve tumour cells of their primary energy source; thereby, diminishing cell proliferation and inducing apoptosis[5].

Numerous GLUT inhibitors are derived from either synthetic or naturally extracted sources. Among these is phloretin, which is a natural dihydrochalcone polyphenol (Figure 1) abundant in fruits; such as apples, pears and strawberries[6]. It possesses a wide range of pharmacological activities; including antioxidants[7], anti-inflammatory[8], and anti-cancer properties[8,9]. Notably, accumulating evidence has revealed that phloretin effectively inhibits class I facilitative glucose transporters; particularly GLUT-2, which is frequently overexpressed in hepatic and malignant tissues[4,10]. This dual functionality, general anti-cancer effect combined with selective inhibition of glucose metabolism highlights phloretin's potential as a promising candidate for targeted cancer therapy[11,12]. However, despite the established biological activity of phloretin, the precise mechanism by which it inhibits GLUT-2 in liver cancer remains inadequately understood; especially with respect to its transporter specific binding interactions.

Hence, this work aimed to investigate phloretin's effect on glucose uptake in the HepG2 cell line, a cellular model for HCC. To further understand its mechanism, *in silico* molecular docking was employed to model interactions between phloretin, glucose, and the GLUT-2 transporter. This combined approach provides a comprehensive understanding of phloretin's potential as a therapeutic agent targeting glucose metabolism in HCC.

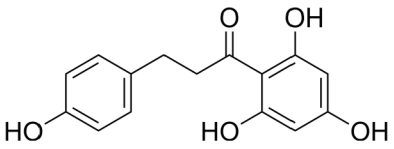

Figure 1 Chemical structure of phloretin (2′,4,4′,6′-tetrahydroxydihydrochalcone)[6]

Material and Methods

Materials

In vitro experiments

Phloretin (≥98.0% purity; Sigma-Aldrich, USA) and glutor (SML-2765; Sigma-Aldrich, USA). Stock solutions of both compounds were prepared in dimethyl sulfoxide (DMSO; Merck, Germany). The fluorescent glucose analog 2-NBDG (2-(N-(7-nitrobenz-2-oxa-1,3-diazol-4-yl)amino)-2-deoxyglucose) was obtained from Thermo Fisher Scientific (USA). Cell culture reagents; including Dulbecco's Modified Eagle Medium (DMEM), fetal bovine serum (FBS), L-glutamine; penicillin-streptomycin and phosphate-buffered saline (PBS), were purchased from Gibco (USA). All reagents and solvents used were of analytical grade. The human hepatocellular carcinoma cell line (HepG2) was obtained from Associate Professor Dr. Potchanapond Graidist, Biological Activity Testing Center, Faculty of Medicine, Prince of Songkla University; Thailand. Fluorescence intensity measurements were performed using a Synergy HTX microplate reader (BioTek, USA), and fluorescence imaging was acquired with a Lionheart FX automated fluorescence microscope (Agilent BioTek, USA).

***In vitro* glucose uptake assay by using 2-NBDG**

Glucose uptake was measured using a modified 2-NBDG assay. based on Hassanein et al.[13], with optimized incubation times. HepG2 cells (3×10^4/well) were seeded in 96-well plates and treated with phloretin at half IC_{50} (150 µM) and IC_{50} (300 µM) for 24 hr, based on prior MTT cytotoxicity result. After treatment, cells were washed and incubated with 100 µM 2-NBDG in glucose-free DMEM (supplemented with 2 mM L-glutamine, 10.0% FBS, and 1.0% penicillin–streptomycin) for 30, 45, 60, or 120 min at 37 °C to determine the optimal incubation time. Cells were then washed, centrifuged and incubated briefly with glucose-free medium to remove unphosphorylated dye before final PBS washing. Fluorescence was measured at 465/540 nm, and glucose uptake was quantified by comparing fluorescence intensity between treated and control groups.

Molecular docking simulation

The three-dimensional structure of human GLUT-2 (UniProtKB ID: P11168-1, 524 amino acids) was modelled for molecular docking using SWISS-MODEL (ExPASy, Switzerland) with the 4zwc.1.A. A template (90.0% query coverage), achieving GMEQ and QMEAN scores of 0.73 and 4.05[14]. The original 3D structure of phloretin (PubChem CID: 4788) was sourced from PubChem (NCBI), and subsequently optimized via a hybrid b3lyp/6-31g (d,p) calculation in Gaussian 09 software[15,16].

Molecular docking simulations were performed using AutoDock 4.2 (Scripps Research, USA)[17,18]. The ligand compound and the receptor were saved into the PDB format through the BIOVIA discovery studio visualizer[19]. Subsequently, the compound and the receptor were converted into PDBQT files using the AutoDockTool (ADT) package[17]. Molecular docking was performed using 50 GA runs, with a population size of 200. The grid size was set to 120 x 120 x 120 Å, with other parameters set to their default values. The binding affinity was evaluated based on the predicted relative binding energy (ΔGbind). Structures with lower ΔGbind values than glucose were considered potential candidates; whereas, those with higher ΔGbind values were excluded from further analysis. Molecular visualization tools; such as VMD (Visual Molecular Dynamics) ang Discovery Studio[19], were used to explore and analyse the docking poses and interactions.

Statistical analysis

All quantitative data are presented as mean ± standard deviation (S.D.), from at least three independent experiments. Statistical significance was determined using one-way analysis of variance (ANOVA), followed by Tukey's post hoc test for multiple comparisons. A p-value of less than 0.05 (p-value<0.05) was considered statistically significant. GraphPad Prism (version 10.4.2; GraphPad Software, USA) was used for data analysis and graphical representation.

Results

Incubation time optimization for 2-NBDG glucose uptake assay

To determine the optimal 2-NBDG incubation time in HepG2 cells, a time-course experiment was performed with untreated cells. After incubation with 100 µM of 2-NBDG in glucose-free medium for 30, 45, 60, and 120 minutes, fluorescence intensity (FI) was measured. 2-NBDG uptake progressively increased over time, reaching a peak at 120 minutes. A 45-minute incubation was selected as optimal for subsequent experiments (Figure 2). This duration balanced sufficient fluorescence signal with maintained cell adherence and monolayer integrity. Incubation beyond 60 minutes led to significant cell detachment and increased variability in fluorescence intensity; as indicated by wider standard deviation ranges.

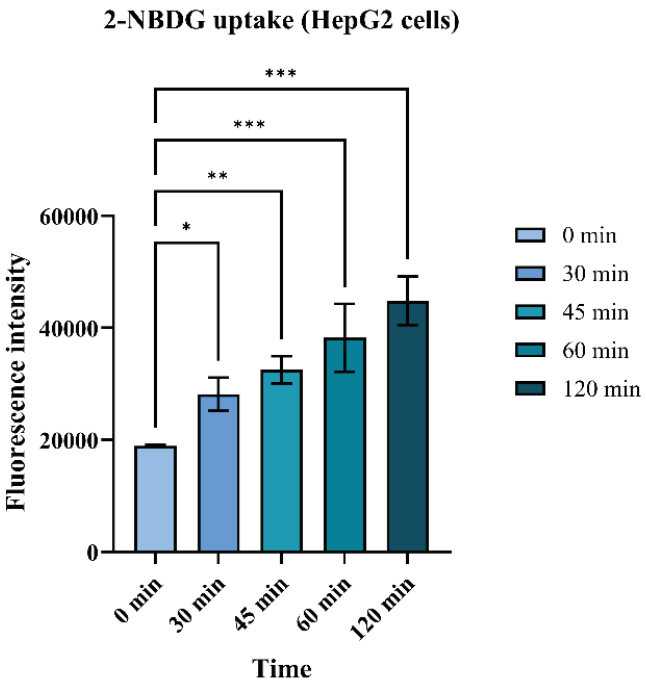

Figure 2 Time-dependent 2-NBDG uptake was assessed in HepG2 cells to optimize glucose uptake detection. Data (mean±S.D., n=3) were analyzed by one-way ANOVA and Dunnett's multiple comparison test (vs. 0 minute). **p-value<0.01.

Inhibitory effect of phloretin on glucose uptake in HepG2 cells

In previous experiments, cell viability was assessed in parallel by MTT under conditions identical to the glucose uptake assay. Regarding the cytotoxic results, at 150 µM and 300 µM phloretin (24 h), HepG2 cells retained ≥70.0% viability; whereas, higher concentrations induced clear dose- and time-dependent cytotoxicity. Therefore, to assess phloretin's inhibitory effect on glucose uptake in HepG2 cells, treatments were conducted at half IC_{50} (150 µM) and full IC_{50} (300 µM) of phloretin concentrations for 24 hours. Subsequently, cells were incubated with 100 µM 2-NBDG for 45 minutes under glucose-free conditions before measuring fluorescence intensity (FI). The results (Figure 3) demonstrated a dose-dependent reduction in glucose uptake, with significant inhibition observed at the IC_{50} concentration. This inhibitory effect was further confirmed by capturing fluorescence intensity images, which revealed strong green fluorescence in untreated controls, markedly diminished signals in IC_{50} treated cells, and intermediate fluorescence intensity with half IC_{50} phloretin. These findings confirm phloretin's dose-dependent impairment of glucose uptake in HepG2 cells.

GLUT-2 docking with phloretin and glucose

Molecular docking simulations were performed using a human GLUT-2 homology model as the main receptor. The protein model was built from the template of human GLUT-3 crystal structure (PDB ID: 4ZWC.1.A), using SWISS-MODEL[14]. The structure of GLUT-3 has 90.0%

sequence similarity as compared to GLUT-2; especially within the transmembrane helices. The model was validated for structural reliability with GMQE and QMEAN scores of 0.73 and 4.05, respectively. From the negative docking results, it showed that phloretin had a more favourable binding energy (-7.08 kcal/mol) than glucose (-4.31 kcal/mol), suggesting a stronger predicted binding affinity. This supports the hypothesis that phloretin competitively inhibits glucose by occupying its native binding site (Figure 4).

Two-dimensional (2D) ligand–receptor interaction diagrams (Figure 5) revealed that both glucose and phloretin shared common interacting residues within the GLUT-2 binding pockets; including GLN193, GLN314, GLN315, GLU412, ASN443, ASN447, ILE196, ILE200, ILE319, PHE323; PHE411, TRP420, VAL197, ASN349 and GLY416. These overlapping contacts support direct competition. Lastly, phloretin exhibited additional π–π T-shaped and π–alkyl interactions with PHE24, TRP444, and ILE28; which were not present in the glucose-bound complex. These distinct aromatic and hydrophobic interactions likely contribute to the stabilization of phloretin within the binding site; henceforth, confirming its potential as an inhibitor of GLUT-2.

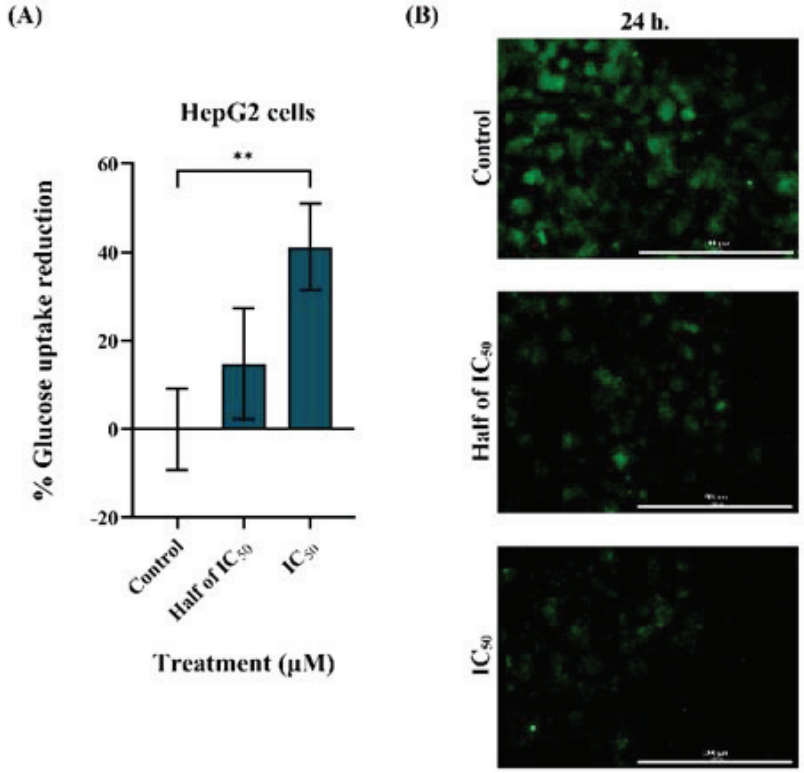

Figure 3 Phloretin inhibits glucose uptake in HepG2 cells after 24 hr. (A) Bar graph shows 2-NBDG fluorescence intensity in HepG2 cells treated with control, phloretin concentration of half of IC_{50} and IC_{50}, respectively. (B) Representative fluorescence images of 2-NBDG uptake (green) in HepG2 cells under each treatment condition (Scale bar=1000 µm). Data are mean±S.D. (n= 3). **p-value<0.01 vs. Control (one-way ANOVA, Dunnett's test).

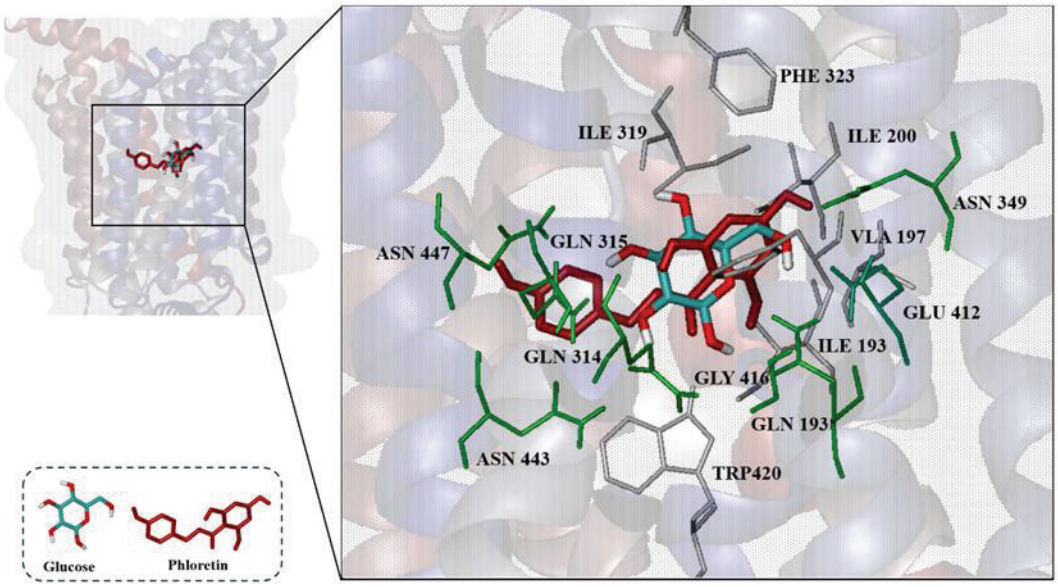

Figure 4 Predicted binding interactions of phloretin and glucose within the GLUT–2 binding pocket. The docking poses of phloretin (red) and glucose (cyan) are shown in the GLUT–2 substrate–binding site. The inset shows ligand positioning within the transmembrane region of GLUT–2. Structural models were prepared using VMD.

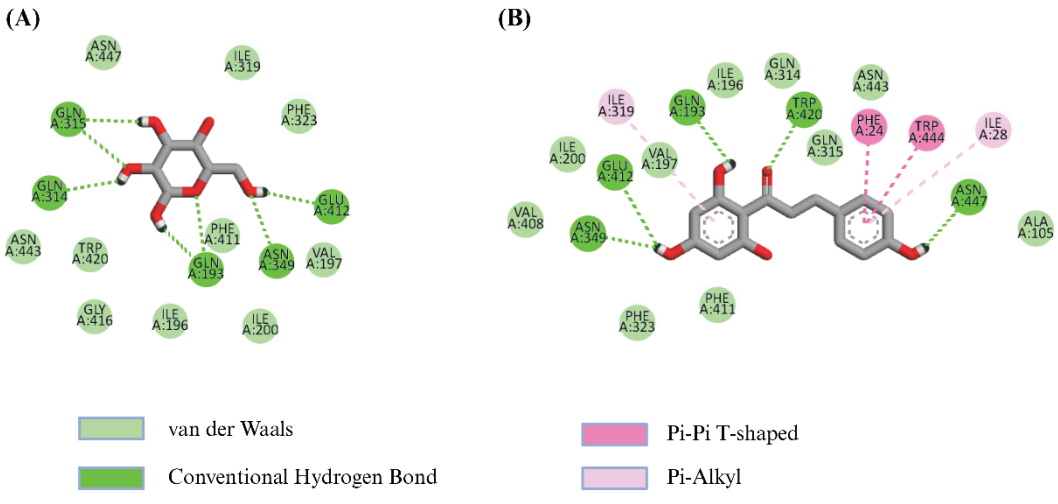

Figure 5 2D interaction diagrams of GLUT–2 with glucose (A) and phloretin (B), generated using Discovery Studio.

Discussion

Cancer's rapid growth and survival depend on its ability to reprogram its metabolism. A key change is the Warburg effect; wherein, cancer cells switch from efficient oxidative phosphorylation to less efficient aerobic glycolysis[20]. This shift significantly increases glucose uptake, leading to the frequent overexpression of Class I glucose transporters (GLUTs) in many cancers[21]. For example, GLUT-1 is often overexpressed in breast[22], lung and colorectal[23], while GLUT-2 is notably increased in liver and colorectal cancer[3,4]. In HCC specifically, GLUT-2 is crucial for hepatic glucose transport and is frequently overexpressed to meet the high metabolic demands of malignant cells[4]. These findings highlight GLUT inhibitors as promising targeted metabolic treatments. While a lot of research focuses on developing inhibitors for Class I GLUTs; particularly GLUT-1 and GLUT-3, there is limited information on GLUT-2 inhibitors. This is despite their potential in targeted metabolic therapies. Among known inhibitors, phloretin, a natural dihydrochalcone, has shown broad inhibitory effects on glucose uptake in various cancer cell lines; including breast (MDA-MB-231), colon (COLO 205) and gastric (AGS) cells[24-26]. This metabolic interference aligns with emerging therapeutic strategies that aim to selectively deprive tumor cells of glucose; thereby, disrupting their energy supply and impeding growth. Hence, a mandatory next step is to assess phloretin's inhibitory effect on glucose uptake in HCC cellular models like HepG2: specifically to confirm its potential in blocking glucose uptake and verify its efficacy in HCC treatment.

To evaluate phloretin's inhibitory effect on glucose transport in HepG2 cell line, a 2-NBDG fluorescence assay was employed. 2-NBDG is a non-metabolizable fluorescent analog of glucose that enters cells via facilitative GLUTs, allowing for real-time assessment of glucose uptake[13]. Since optimal 2-NBDG incubation times vary by cell types, assay conditions were first optimized for HepG2 cells. Previous studies in other cancer models; such as MDA-MB-231, COLO 205 and HCT116, have used incubation times ranging from 30 to 60 minutes[27-29]. In our study, HepG2 cells responded best to a 45-minute incubation, which provided strong, reproducible fluorescence signals, while preserving cell morphology. Longer incubations (>60 minutes) resulted in increased cell detachment and variability. These findings emphasize the necessity of cell-specific optimization in metabolic assays.

Under these optimized conditions, 24-hour treatment with phloretin induced a clear dose-dependent reduction in glucose uptake, with the strongest inhibition observed at the IC_{50} concentration (300 µM). Importantly, parallel cytotoxicity data from MTT assays demonstrated that cell viability under these conditions remained above ~70.0%, confirming that the decreased 2-NBDG signal reflects inhibition of glucose transport rather than loss of viable cells. Our results align with previous reports demonstrating that phloretin can inhibit glucose transport in various cancer cell types by targeting class I GLUTs; including GLUT-2[26,30,31]. The observed suppression of glucose uptake supports the hypothesis that phloretin disrupts metabolic activity in HCC cells by selectively inhibiting GLUT-2, offering a potential strategy for targeted cancer therapy.

To further elucidate the mechanism of GLUT-2 inhibition, molecular docking analysis was conducted. Using a validated homology model of human GLUT-2, phloretin exhibited a higher predicted binding affinity (-7.08 kcal/mol) than glucose (-4.31 kcal/mol), suggesting its potential role as a competitive inhibitor. Both ligands shared interactions with critical substrate binding residues GLN193, GLN315 and TRP420, which have been previously identified as essential for GLUT-2 transport function[10,32,33]. Additionally, phloretin formed unique stabilizing interactions not observed in the glucose-bound complex; including π–π stacking with PHE24 and TRP444, and hydrophobic contacts with ILE28. This likely enhanced its binding stability and inhibitory persistence: as shown in Figure 5. These findings support a competitive inhibition model, and provide a molecular rationale for the observed biological effects.

To this end, this study demonstrated that phloretin effectively inhibits GLUT-2 glucose uptake in HepG2 cells through a competitive binding mechanism. By integrating optimized *in vitro* glucose uptake analysis with mechanistic *in silico* modeling, our findings provide compelling evidence of phloretin's specificity for GLUT-2. These results highlight phloretin's potential as a lead compound for the development of targeted metabolic therapies in HCC. This study offers sufficient proof of phloretin's inhibitory effect on the uptake of glucose in HepG2 cells; nevertheless, additional research is necessary; especially in normal hepatocytes, to evaluate selectivity and safety. For further study, molecular dynamics (MD) simulations are required to assess the stability and conformational behavior of the phloretin GLUT-2 complex under physiological conditions.

Conclusion

The combination of *in vitro* and *in silico* results supports the hypothesis that phloretin functions as a competitive inhibitor of GLUT-2, preferentially obstructing glucose uptake in HCC cells compared to glucose. This dual validation strongly confirms phloretin's potential as a metabolic inhibitor and underlines the necessity for further exploration of its structure-activity relationship.

Acknowledgement

This work was supported by a PSU New Scholar Grant (MED6502043S) and partially by Faculty of Medicine, Prince of Songkla University funding (REC.65-241-38-2) to Kantida Juncheed. The study has received ethical approval from the Human Research Ethics Unit, Faculty of Medicine, Prince of Songkla University, under project number REC.66-412-38-1. Lastly, experimental cost was partially support by the Graduate School, Prince of Songkla University to Worarat Boonpech.

Conflict of interest

There are no potential conflicts of interest to declare.

References

1. Villanueva A. Hepatocellular Carcinoma. Longo DL, editor. N Engl J Med 2019;380:1450–62.
2. Ganapathy V, Thangaraju M, Prasad PD. Nutrient transporters in cancer: relevance to Warburg hypothesis and beyond. Pharmacol Ther 2009;121:29–40.
3. Pliszka M, Szablewski L. Glucose transporters as a target for anticancer therapy. Cancers 2021;13:4184.
4. Kim YH, Jeong DC, Pak K, Han ME, Kim JY, Liangwen L, et al. SLC2A2 (GLUT2) as a novel prognostic factor for hepatocellular carcinoma. Oncotarget 2017;8:68381–92.
5. Sooksawat D, Boonpech W, Tipmanee V, Churuangsuk C, Srifa P, Juncheed K. Warburg effect and type II glucose transporter inhibitors as a potential targeted therapy for liver cancer: a review. Trends in Sciences 2024;21:8309.
6. Picinelli A, Dapena E, Mangas JJ. Polyphenolic pattern in apple tree leaves in relation to scab resistance. A preliminary study. J Agric Food Chem 1995;43:2273–8.
7. Commisso M, Bianconi M, Poletti S, Negri S, Munari F, Ceoldo S, et al. Metabolomic profiling and antioxidant activity of fruits representing diverse apple and pear cultivars. Biology 2021;10:380.
8. Hytti M, Ruuth J, Kanerva I, Bhattarai N, Pedersen ML, Nielsen CU, et al. Phloretin inhibits glucose transport and reduces inflammation in human retinal pigment epithelial cells. Mol Cell Biochem 2023;478:215–27.
9. Hsiao YH, Hsieh MJ, Yang SF, Chen SP, Tsai WC, Chen PN. Phloretin suppresses metastasis by targeting protease and inhibits cancer stemness and angiogenesis in human cervical cancer cells. Phytomedicine 2019;62:152964.
10. Schmidl S, Ursu O, Iancu CV, Oreb M, Oprea TI, Choe J yong. Identification of new GLUT2-selective inhibitors through *in silico* ligand screening and validation in eukaryotic expression systems. Sci Rep 2021;11.
11. Tuli HS, Rath P, Chauhan A, Ramniwas S, Vashishth K, Varol M, et al. Phloretin, as a potent anticancer compound: from chemistry to cellular interactions. Molecules 2022;27:8819.
12. Choi BY. Biochemical basis of anti-cancer-effects of phloretin—a natural dihydrochalcone. Molecules 2019;24:278.
13. Hassanein M, Weidow B, Koehler E, Bakane N, Garbett S, Shyr Y, et al. Development of high-throughput quantitative assays for glucose uptake in cancer cell lines. Mol Imaging Biol 2011;13:840–52.

14. Waterhouse A, Bertoni M, Bienert S, Studer G, Tauriello G, Gumienny R, et al. SWISS-MODEL: homology modelling of protein structures and complexes. Nucleic Acids Res 2018;46:W296–303.
15. Frisch MJ, Trucks GW, Schlegel HB, Scuseria GE, Robb MA, Cheeseman JR, et al. Gaussian 09, Revision D.01 [Internet]. Wallingford, CT: Gaussian, Inc.; 2009. Available from: https://gaussian.com/g09citation/
16. Tirado-Rives J, Jorgensen WL. Performance of B3LYP density functional methods for a large set of organic molecules. J Chem Theory Comput 2008;4:297–306.
17. Morris GM, Huey R, Lindstrom W, Sanner MF, Belew RK, Goodsell DS, et al. AutoDock4 and AutoDockTools4: Automated docking with selective receptor flexibility. J Comput Chem 2009;30:2785–91.
18. Cosconati S, Forli S, Perryman AL, Harris R, Goodsell DS, Olson AJ. Virtual screening with AutoDock: theory and practice. Expert Opin Drug Discov 2010;5:597–607.
19. BIOVIA DS. Discovery Studio Visualizer [Internet]. San Diego; 2020. Available from: https://www.3ds.com/products/biovia/discovery-studio/visualization
20. Soga T. Cancer metabolism: Key players in metabolic reprogramming. Cancer Sci 2013;104:275–81.
21. Kim SH, Baek KH. Regulation of cancer metabolism by deubiquitinating enzymes: The Warburg effect. Int J Mol Sci 2021;22:6173.
22. Suteau V, Bukasa-Kakamba J, Virjogh-Cenciu B, Adenis A, Sabbah N, Drak Alsibai K. Pathological significance of GLUT-1 expression in breast cancer cells in diabetic and obese patients: the french Guiana study. Cancers 2022;14:437.
23. Kokeza J, Strikic A, Ogorevc M, Kelam N, Vukoja M, Dilber I, et al. The effect of GLUT1 and HIF-1α expressions on glucose uptake and patient survival in non-small-cell lung carcinoma. Int J Mol Sci 2023;24:10575.
24. Liou CJ, Wu SJ, Shen SC, Chen LC, Chen YL, Huang WC. Phloretin ameliorates hepatic steatosis through regulation of lipogenesis and Sirt1/AMPK signaling in obese mice. Cell Biosci 2020;10:114.
25. Wu KH, Ho CT, Chen ZF, Chen LC, Whang-Peng J, Lin TN, et al. The apple polyphenol phloretin inhibits breast cancer cell migration and proliferation via inhibition of signals by type 2 glucose transporter. J Food Drug Anal 2018;26:221–31.
26. Yang K, Tsai C, Wang Y, Wei P, Lee C, Chen J, et al. Apple polyphenol phloretin potentiates the anticancer actions of paclitaxel through induction of apoptosis in human hep G2 cells. Mol Carcinog 2009;48:420–31.
27. Abruscato G, Tarantino R, Mauro M, Chiarelli R, Vizzini A, Arizza V, et al. Glucose consumption and uptake in HepG2 cells is improved by aqueous extracts from leaves, but not rhizomes, of *Posidonia oceanica* (L.) Delile via GLUT-4 upregulation. Protoplasma 2025.
28. Hassanein M, Weidow B, Koehler E, Bakane N, Garbett S, Shyr Y, et al. Development of high-throughput quantitative assays for glucose uptake in cancer cell lines. Mol Imaging Biol 2011;13:840–52.
29. Hung HC, Li LC, Guh JH, Kung FL, Hsu LC. Discovery of new glucose uptake inhibitors as potential anticancer agents by non-radioactive cell-based assays. Molecules 2022;27:8106.
30. Kapoor S, Padwad YS. Phloretin induces G2/M arrest and apoptosis by suppressing the β-catenin signaling pathway in colorectal carcinoma cells. Apoptosis 2023;28:810–29.
31. Wu C, Ho Y, Tsai C, Wang Y, Tseng H, Wei P, et al. *In vitro* and *in vivo* study of phloretin-induced apoptosis in human liver cancer cells involving inhibition of type II glucose transporter. Int J Cancer 2009;124:2210–9.
32. Hensley MS, Hutchings D, Ismail A, Tanasova M. Turn-on fluorescent glucose transport bioprobe enables wash-free real-time monitoring of glucose uptake activity in live cells and small organisms. RSC Chem Biol 2025;6:987–95.
33. Enogieru OJ, Ung PMU, Yee SW, Schlessinger A, Giacomini KM. Functional and structural analysis of rare *SLC2A2* variants associated with Fanconi-Bickel syndrome and metabolic traits. Hum Mutat 2019;40:983–95.

Closing Message

Asst. Prof. Kittipong Riabroi, M.D., M.Sc.

Dean, Faculty of Medicine, Prince of Songkla University

October 10, 2025

The 4th Annual Health Research International Conference (AHR-iCON 2025), under the theme *"Shaping the Future: Innovation, Health, and Well-being,"* was successfully held during October 9–10, 2025, at the Medical Research, Innovation, and Technology Transfer Building, Faculty of Medicine, Prince of Songkla University.

This achievement was made possible through the collective efforts and active participation of all sectors, including researchers, faculty members, physicians, nurses, public health professionals, students, as well as representatives from various organizations. Their valuable contributions in sharing knowledge and presenting research have played a vital role in advancing health research and innovation, ensuring their practical application at the community, national, and international levels, and ultimately leading to more effective medical services aligned with the needs of society.

On behalf of the organizing committee, we sincerely apologize for any limitations or shortcomings that may have occurred during the organization of this event. We humbly welcome suggestions and recommendations from all participants in order to further improve and enhance the quality of future conferences.

Finally, the organizing committee would like to extend our heartfelt appreciation to all participants for your support and contributions to the success of this conference. We truly hope to have the honor of welcoming you again at future AHR-iCON conferences as we continue to foster impactful research and innovations for the benefit of the nation and society at large.

Asst. Prof. Kittipong Riabroi, M.D., M.Sc.

Dean of Faculty of Medicine, Prince of Songkla University

Journal of Health Science and Medical Research (JHSMR)

The journal's former title: Songklanagarind Medical Journal

Owner: Prince of Songkla University

Aims and scope: Journal of Health Science and Medical Research (JHSMR) offers an interdisciplinary forum for basic or applied medical and health sciences research, evidence-based and scientifically written articles. Our content focuses on, but is not limited to, these areas of medicine and health science;

- -Clinical medicine
- -Biomedical science and biomedical engineering
- -Public health research
- -Data science in medicine and health care

Language: Fulltext and Abstract in English

Abstracting and Indexing Information: Scopus, Thai-Journal Citation Index (TCI), Asean Citation Index (ACI), Google Scholar, Crossref, Directory of Open Access Journals (DOAJ), and EuroPub

Frequency: 6 issues per year (January-February, March-April, May-June, July-August, September-October and November-December)

Editorial office: Songklanagarind Medical Journal Office, Faculty of Medicine, Prince of Songkla University, Hat Yai, Songkhla 90110, Thailand.
Tel: +66 7445 1159 Fax: +66 7428 1103
E-mail: manager@jhsmr.org
Website: http://www.jhsmr.org

Polathep Vichitkunakorn	Prince of Sonkla University	Thailand
Pornprot Limprasert	Prince of Songkla University	Thailand
Potchanapond Graidist	Prince of Songkla University	Thailand
Prasit Wuthisuthimethawee	Prince of Songkla University	Thailand
Pritsana Raungrut	Prince of Songkla University	Thailand
Quazi Monirul Islam	Liverpool School of Tropical Medicine	UK
Raphatphorn Navakanitworakul	Prince of Songkla University	Thailand
Rasmon Kalayasiri	Chulalongkorn University	Thailand
Rungsun Bhurayanontachai	Prince of Songkla University	Thailand
Sally Chan	Tung Wah College	Hong Kong
Saranyou Suwanugsorn	Prince of Songkla University	Thailand
Sirawee Chaovalit	Prince of Songkla University	Thailand
Sitthichok Chaichulee	Prince of Songkla University	Thailand
Somchit Jaruratanasirikul	Prince of Songkla University	Thailand
Somkiat Sunpaweravong	Prince of Songkla University	Thailand
Sun Jing	Inner Mongolia Medical University	China
Sunisa Chatmongkolchart	Prince of Songkla University	Thailand
Supamai Soonthornpun	Prince of Songkla University	Thailand
Suwanna Setthawatcharawanich	Prince of Songkla University	Thailand
Thanarpan Peerawong	Prince of Songkla University	Thailand
Tang Xianyan	Guangxi Medical University	China
Thirachit Chotsampancharoen	Prince of Songkla University	Thailand
Tippawan Kaewmanee	Prince of Songkla University	Thailand
Tippawan Liabsuetrakul	Prince of Songkla University	Thailand
Varah Yuenyongviwat	Prince of Songkla University	Thailand
Verapol Chandeying	Princess of Naradhiwas University	Thailand
Viranuj Sueblinvong	Emory University	USA
Virat Kirtseesakul	Prince of Songkla University	Thailand
Volker Winkler	University of Heidelberg	Germany
Vorapong Phupong	Chulalongkorn University	Thailand
Warut Aunjitsakul	Prince of Songkla University	Thailand
Weeranan Yaemrattanakul	Prince of Songkla University	Thailand
Weerawat Kiddee	Prince of Songkla University	Thailand
Wit Wichaidit	Prince of Songkla University	Thailand
Yong Poovorawan	Chulalongkorn University	Thailand

Advisor of Editor-in-Chief

Puttisak Puttawibul	Prince of Songkla University	Thailand
Kittipong Riabroi	Prince of Songkla University	Thailand

Manager

Kamolthip Suwanthavee

Assistant Manager

Sarinthra Khunsiri

Supanich Lertjettanakul

Nutchada Binlateh

Tarathep Boonpipat

Guide for Authors

Journal of Health Science and Medical Research (JHSMR)

Condition

Manuscript language

Only manuscripts written in English are considered. For non-native speaking countries, the manuscript should be edited in English, by a native English speaker and be accompanied with an English language approval letter, before being submitted. If the manuscript does not have an English language approval letter, please contact our editorial office via: at manager@jhsmr.org.

Publication charges

There are no page charges for submission or publication.

Ethics approval of research

JHSMR requires the copy of Ethics approval of research for all investigations involving humans. For Original articles and Case reports, details of ethical approval of research should be stated in the Material and Methods section.

Acknowledgement

If authors receive assistance for research or manuscript writing, authors should clearly describe in the: "Acknowledgment section"; after the main body and before the Funding sources section.

Funding sources

If authors receive financial support or sponsorship for the study research, Authors must give full details about the funding of any research relevant to their study; including: sponsor names and explanations of the roles of these sources in the funding sources section, before the conflict of interest section.

Conflict of interest

Authors must declare whether their articles have or do not have any potential, or existing, conflicts of interest either; after the main body or in the Acknowledgement section, before the references section. These declarations should include; but are not limited to: relationships with pharmaceutical and biotechnology companies, device manufacturers, or other commercial entities, whose products or services are related to the subject matter of the manuscript submission. If the manuscript has no conflicts of interest, authors should state: "There are no potential conflicts of interest to declare."

Review process

Primary review

After submission, manuscripts are first reviewed by journal manager and editor-in-chief. All manuscripts are screened using the 'Turnitin' (please see the details of plagiarism on the Publication Ethicts page). Manuscripts with incorrect formatting, unacceptable language or style will be returned to authors for correction before transference to the section editor.

Peer-review

JHSMR is a quarterly peer-reviewed scientific journal, which uses the double-blinded peer-review process. The careful selection of relevant experts as reviewers will facilitate and speed up the review process. Therefore, our section editors will select at least 3 potential reviewers, who have been published or have areas of expertise relating to the submitted manuscript. However, JHSMR does not select reviewers from within the author's institutions, especially for international authors, wherein it avoids only local reviewers. Acceptable manuscripts are

those that have been accepted by 2 of the 3 reviewers, upon which, the editor-in-chief will examine and determine if the manuscript is suitable for publication, or requires further revisions. Requested revisions, by the section editors or the editor-in-chief to the author, may be requested during the revision process.

Manuscript types

JHSMR now welcomes 4 types of Manuscripts.

1. Selected editorials: These are invited by the editor-in-chief of JHSMR, and should be both written in English and structured as follows: Introduction, Main text, Conclusion, and References. Editorials should not be less than 1,000 words, but cannot exceed 1,500 words in total. (Counting from Introduction to Conclusion) They should also keep cited references to a minimum.

2. Original articles or Systematic reviews

2.1 Original articles: These form the largest majority of papers published by JHSMR. These should consist of 3,500 words, with no more than a total of 8 tables and/or figures, and limited to 40 references. Additionally, all efforts should be undertaken to keep the manuscripts as succinct as possible. Full reports should include separate sections entitled: Abstract, Introduction, Material and Methods, Results, Discussion, Conclusion, Acknowledgements, Funding sources and Conflicts of interests. Abstracts should contain no more than 250 words. The following sections should be included after the text: Acknowledgement, Funding sources, and Disclosures regarding real or perceived conflicts of interest

2.2 Systematic reviews: This format can be used for a review of a clearly formulated question, that uses systematic and reproducible methods to identify, select and critically appraise all relevant research, so as to collect and analyst data from the studies that are included in the review. The scope of study is focused on medical and health science research. These should contain: 6,000 words, with 8 tables and/or figures limit. The abstract should contain no more than 250 words, however, there is no limit on the amount of references

3. Case reports: This format can be used for submission of: important, preliminary observations, technique modifications, or data that do not warrant publication as a full paper. Short reports should contain no sub-headings, and be no more than 2,000 words in length, with no more than 250 words in the abstract, 2 tables and/or figures, and 15 references.

4. Review articles: JHSMR will consider reviews on relevant topics in medicine, medical education, medical innovation and related areas. Typically reviews will be submitted by leading authorities in such relevant fields. We encourage mini-reviews, providing concise reviews of focused topics containing no more than 4,000 words, 8 tables and/or figures, with no limit of references. Abstracts should contain no more than 250 words. In so saying, larger reviews will be considered.

Manuscript preparation

Prepare your manuscript using a word processing program, saved as a .doc file, using Microsoft Word. For items that accompany text (letters, figures, copyright forms, and so forth.), you may upload the following file types: .jpg, .jpeg, .tif

Cover letter and signatures: All manuscripts should be accompanied by a cover letter containing the following information:

1. The title of the paper

-A brief description of the significance of the paper to the readers of JHSMR

-A statement confirming that the material is original, has not already been published, and has not, nor will not, be submitted for publication elsewhere, so long as it is under consideration by JHSMR

-Written disclosure of any relationships or support, which might be perceived as constituting a conflict of interest

-Name and signature of corresponding author(s)

2. Authorship

There is no limit to the number of authors that may be listed. Howbeit, the corresponding author should confirm that the authorship of research publications accurately reflect all authors' contributions to the work and reporting. All sources of funding along with any conflicts of interest must also be disclosed.

Manuscript formatting

1. Title page: This should include, in the following sequence: the title, a list of all authors with their degrees, the authors institutions- identified by superscripts in Arabic numerals. The corresponding author should be denoted by an asterisk, with address, e-mail and phone number in a footnote. The running title should be limited to 40 characters and contain at least 6 keywords.

2. Title: The manuscript title should be as succinct as possible. Titles should generally not include abbreviations, and not be longer than 60 characters (including spaces).

3. Abstract: The abstracts of original articles or systematic reviews must have a structured abstract that states the purpose, basic procedures, main findings and principal conclusions of the study. Divide the abstract with the headings Objective, Material and Methods, Results, and Conclusion. Case reports or review articles should have an unstructured abstract.

4. Spacing: The text should be 12 point type, fully double-spaced, leaving a margin of 1 inch on all sides. Continuous line numbers (NOT restarting with each page) should be included throughout the manuscript, and pages should be numbered consecutively.

5. Abbreviations: Abbreviations are commonly overused, compromising the clarity of manuscripts. Authors are advised to keep abbreviations to a minimum, using them only when they are clearer than their long/full terminology (For example: PCR, DNA), however they should be avoided whenever possible, or when they are non-standard and idiosyncratic. Terms should be written out in full upon first usage, in both the abstract and text, with the abbreviation following in parentheses. After this first usage, the abbreviation must be used consistently. Plurals of abbreviations do not require apostrophes.

6. Keywords: Keywords must be listed after the abstract section, and should be between 3-6 words.

7. Drug names: Proprietary names of drugs may not appear in the title, but may be used in conjunction with the generic name when the drug is first mentioned in the abstract, and again when first mentioned in the text. Thereafter, use only the generic name.

8. Names of organisms: Genus and species should be italicized. After the first usage the genus should be abbreviated with a single letter (For example: *E. coli*). For different species, within a genus, the genus should be fully written out upon first usage of each.

9. Figures: Figures should be numbered in Arabic numerals, and cited in the text. It should be noted that: a fee is required for color illustrations in print, however authors can select a black & white in print, without an attached fee. All figures should contain a brief legend, with the size being 5x7 inches, and of at least of 300 dpi.

10. Tables: Tables should be serially numbered in Arabic numerals, and cited in the text. Each table should be placed on a separate page, at the appropriate point in the text, or at the end of the manuscript.

11. References: References should be from published manuscripts, or manuscripts that have either been accepted or are pending publication (in press), these should be cited in the reference list. The reference formatting of JHSMR uses the: Vancouver style. All references

should be cited by consecutive numbers in the text. The numbers should appear in superscripts, that appear after closing punctuation.

In the reference list, the first 6 authors should be listed. If there are more than 6 authors followed by "et al." The journal names, which appear in the reference list, should use the abbreviate journal, as in PubMed.

Examples of references

1. Journal

- Hanprasertpong J, Geater A, Jiamset I, Padungkul L, Hirunkajonpan P, Songhong N. Fear of cancer recurrence and its predictors among cervical cancer survivors. J Gynecol Oncol 2017;28:e72.
- Rujirojindakul P, Liabsuetrakul T, McNeil E, Chanchayanon T, Wasinwong W, Oofuvong M, et al. Safety and efficacy of intensive intra-operative glycaemic control in cardio-pulmonary bypass surgery: a randomised trial. Acta Anaesthesiol Scand 2014;58:588-96.

2. Supplement

- Lofwall MR, Strain EC, Brooner RK, Kindbom KA, Bigelow GE. Characteristics of older metha-done maintenance (MM) atients [abstract]. Drug Alcohol Depend 2002;66(Suppl 1):S105.

3. Book

- Fealy S, Sperliny JW, Warren RF, Craig EV. Shoulder anthroplasty: complex issues in the primary and revision setting. New York: Thieme; 2008.

4. Chapter

- Waltzman SB, Shapiro WH. Cochlear implants in adults. In: Valente M, Hosfond-Dunn H, Roeser RJ, editors. Audiology treatment. 2nd ed. New York: Thieme; 2008;p.361-9.

5. Patent

- Tintara H, inventor; Prince of Songkla University, assignee. Amniotomy training model. Thai petty patent 7488. September 18, 2012.

6. Journal article on the Internet

- Sanders GD, Bayoumi AM, Holodniy M, Owens DK. Cost-effectiveness of HIV screening in patients older than 55 year of age. Ann Intern Med [serial on the Internet]. 2008 Jun [cited 2008 Oct 7]; 148(12). Available from: http://www.annals.org/cgi/reprint/148/12/889.pdf

7. Monograph on the Internet

- Field MJ, Behrman RE. Where children die: improving palliative and end-of-life case for children and their families [monograph on the Internet]. Washington: National Academy Press; 2003 [cited 2008 Sep 26]. Available from: http://nap.edu/openbookphp?record_id=10390&page=1

8. Homepage/Website

- Cancer-Pain.org [homepage on the Internet]. New York: Association of Cancer Online Resources, Inc.; c2000-01 [cited 2008 Oct 3]. Available from: http://www.cancer-pain.org/

Contact

E-mail: manager@jhsmr.org

Other websites

Thai Journals Online: https://www.tci-thaijo.org/index.php/jhsmr

Faculty of Medicine, Prince of Songkla University
15 Karnjanavanich Road, Hat Yai
Songkhla 90110, Thailand
Tel: 074-451129
E-mail: medpsuresearch@gmail.com